DOCTOR OF PHILOSOPHY

Probing the assembly of the Bacillus subtilis flagellum and its role in signal transduction.

Cairns, Lynne S.

Award date:
2014

DOCTOR OF PHILOSOPHY

Probing the assembly of the Bacillus subtilis flagellum and its role in signal transduction.

Lynne Cairns

2014

University of Dundee

Probing the assembly of the *Bacillus subtilis* flagellum and its role in signal transduction

Lynne S. Cairns

Division of Molecular Microbiology

College of Life Sciences

University of Dundee

2014

A thesis submitted in partial fulfilment of the requirements for the degree of Doctor of Philosophy

Table of Contents

List of Figures

List of Tables

Abbreviations

amp	ampicillin
APS	ammonium persulphate
ATP	adenosine-5’-triphosphate
ATPase	adenosine-5’-triphosphatase
AU	arbitrary units
BSA	bovine serum albumin
Bs-FlgN	*B. subtilis* FlgN
BY-kinase	bacterial tyrosine kinase
c-di-GMP	bis-(3'-5')-cyclic dimeric guanosine monophosphate
cDNA	complementary DNA
cml	chloramphenicol
ddH_2O	double distilled water
DIC	differential interference contrast
DNA	deoxyribonucleic acid
DNase	deoxyribonuclease
dNTP	deoxyribonucleotide triphosphate
DR	direct repeat
e.g.	*exempli gratia* (for example)
ECF	extracytoplasmic function sigma factor
ECL	enhanced chemiluminescence
ECM	extracellular matrix
EGTA	ethylene glycol tetraacetic acid
EPS	exopolysaccharide
et al.	*et alii* (and others)
gDNA	genomic DNA
GFP	green fluorescent protein
GTE	glucose tris EDTA
HBB	hook-basal body
HK	histidine kinase
IPTG	isopropyl-β-D-1-thiogalactopyranoside
IR	Indirect repeat
kan	kanamycin
kDa	kilo Dalton

LB	lysogeny broth or Luria-Bertani media
MLS	macrolide-lincosamide-streptogramin
OD_{600}	optical density measured at wavelength 600 nm
ONPG	ortho-Nitrophenyl-β-galactoside
PAGE	polyacrylamide electrophoresis
PBS	phosphate buffered saline
PCR	polymerase chain reaction
PFA	paraformaldehyde
γ-PGA	γ-poly-$_{D\text{-}L}$-glutamic acid
Phr	phosphatase regulator
PVDF	polyvinylidene fluoride
RNA	ribonucleic acid
rRNA	ribosomal RNA
RNase	ribonuclease
RR	response regulator
RT-PCR	reverse transcription polymerase chain reaction
SDS	sodium dodecyl sulphate
SEM	standard error of the mean
spc	spectinomycin
*S*T-FlgN	S. Typhimurium FlgN
T3SS	type 3 secretion system
TAE	tris acetate EDTA
tet	tetracycline
TET	tris EDTA triton
TBS	tris buffere saline
TBST	tris buffere saline tween
TEMED	N, N, N', N'-tetramethylethylenediamine
U	units
UV	ultra violet
v/v	volume per volume
w/v	weight per volume
WT	wild-type
YFP	yellow fluorescent protein

Acknowledgements

The work presented in this thesis wouldn't have been possible without my supervisor, Nick. My biggest and best thanks go to you; I've had such a great time in your lab! Thank you so much for giving me a great project and for your support, patience, guidance, advice and enthusiasm. Whether it's been about science, running, driving lessons or even the dreaded career chats, you've been nothing but encouraging and have given me a little push when I've needed it most. I hope I didn't spend too long on the worry list along the way! Thank you for all of the opportunities I've had. I really couldn't have asked for more.

I owe a lot to members of Team NSW past and present. Thanks to Amy for being my office buddy for 3 years, for putting up with my bad singing and loud laugh, for all of the gossip and chat we've shared and for always being honest with me, even if that meant telling me I was being stupid! Thanks also to Victoria who had the onerous task of teaching me the basics of microbiology in my rotation and who also became my running buddy in sun, rain, hail and snow. I'm really grateful to Laura for all of her help (wisdom!) and advice throughout, and also more recently to Rachel and Sofia. Emma and Jess also deserve a huge thank you for being so much fun to supervise and work with, and for keeping me laughing (loudly) along the way.

MMB is the best division in CLS and I am so grateful to everyone who works here and who has been a source of knowledge, wisdom, chat, laughs and cake over the course of my PhD. CLS itself has been a great place to work and I appreciate all of the resources and opportunities that I've had from carrying out my PhD here. I am very grateful to the Wellcome Trust for funding and to everyone involved in running the PhD programme here in Dundee.

My time in Dundee would not have been the same without all of the brilliant friends I've made along the way. All of the brunch dates, gym sessions, bottles of wine, road trips, runs, parties, shots of tequila (T-time!) and Firbush and Crieff x 4 have made this experience even better. Thanks especially to my rotation cohort – Anna, Dun Jack, Kat and Jens – for being great fun and for always encouraging me to try new things, to my gym buddies for keeping me fit and to Debbie and Sianadh for all of the chat and aforementioned T-times. I also need to thank my non-science pals David, Isla and Geraldine for pretending to understand what I do ("how are the bugs doing today, pal?"), for always being there when I needed a chat or a distraction and for sharing a lot of fun and laughter with me.

Finally thanks to my family, especially my mum and dad, for their never-ending love and support. You brought me up to do what I enjoy, to pursue knowledge and to work hard and do my best, and I wouldn't have gotten to this stage without those values. I may have doubted myself along the way but you always believed I could achieve whatever I set out to do. I can't ever thank you enough for everything you've done for me, but I hope this is a good start.

Publications

Primary publications generated during the course of this work:

Cairns, L.S., Marlow, V.L., Kiley, T.B., Birchall, C., Ostrowski, A., Aldridge, P.A., and Stanley-Wall, N.R. Defining the role of FlgN in flagellum-based motility in *Bacillus subtilis*. (**2014**) *Journal of Bacteriology.* **196(12)**: 2216-2226.

Marlow, V.L., Cianfanelli, F.R., Porter, M., **Cairns, L.S.,** Dale, J.K., and Stanley-Wall, N.R. (**2014**). The prevalence and origin of exoprotease-producing cells in the *Bacillus subtilis* biofilm. *Microbiology.* **160(1)**: 56-66.

Cairns, L.S., Marlow, V.L., Bissett, E., Ostrowski, A., and Stanley-Wall, NR. (**2013**) A mechanical signal transmitted by the flagellum controls signalling in *Bacillus subtilis*. *Molecular Microbiology.* **90(1)**: 6-21.

Review article generated during the course of this work:

Cairns, L.S., Hobley, L., and Stanley-Wall, N.R. (**2014**) Biofilm formation by *Bacillus subtilis*: new insights into regulatory strategies and assembly mechanisms. *Molecular Microbiology.* **93(4):** 587-98.

Declaration

I declare that I am the author of the thesis; that, unless otherwise stated, all references cited have been consulted by myself; that the work of which the thesis is a record has been done by myself, and that it has not been previously accepted for a higher degree: where thesis is based upon joint research, the nature and extent of my individual contribution is defined.

Lynne Cairns

September 2014

Summary

Microbes live in diverse, challenging and competitive environments. To survive and propagate microbes must be able to sense and respond to environmental fluctuations, such as changes in pH, nutrient status or temperature. As such, bacteria have a number of signal transduction mechanisms at their disposal that allow them to detect a range of different stimuli, integrate different signals and react to them appropriately. The work presented in this thesis aimed to understand more about the signalling cascades that the Gram positive soil-dwelling bacterium *Bacillus subtilis* uses to mediate its transition from a motile lifestyle that requires rotating helical flagella, to a sessile lifestyle called the biofilm, where cells adhere to a surface and are encased in a self-produced extracellular polymeric matrix.

Bacterial tyrosine phosphorylation is required for *B. subtilis* biofilm formation and has been suggested to also play a role in regulating the putative motility protein, YvyG. This led to the hypothesis that tyrosine phosphorylation might play a role in both motility and biofilm formation. The first part of this thesis investigates this hypothesis and successfully ascribes a function to YvyG as an orthologue of a flagellar type 3 secretion system chaperone that is essential for flagellar assembly. Crucially this work provides further evidence that the *B. subtilis* flagellum is regulated by both conserved and species-specific means. These experiments led to YvyG being re-named as FlgN. Despite previous work suggesting that phosphorylation of YvyG was important for protein function and localisation, the data presented here found no evidence of this, and therefore indicate that the impact of bacterial tyrosine phosphorylation must be assessed *in vivo* before any significance can be drawn from the identification of such modifications by *in vitro* approaches.

The second part of this study examines the role of the DegS-DegU two component signal transduction system in mediating the transition from motility to biofilm formation. DegS-DegU is required for both motility and biofilm formation, and previous work indicated that DegS-DegU may sense flagellar assembly. The data presented show that upon an inhibition of flagellar rotation DegU~P levels are increased, as inferred from accepted proxies. This could conceivably be the first step in biofilm formation to allow cells to sense and respond to a surface and change their gene expression profile. The *B. subtilis* flagellum therefore acts as a mechanosensor to control the DegS-DegU two component system. Collectively, the work presented here contributes to our understanding of how *B. subtilis* regulates flagellar assembly, and further enhances our knowledge of how bacteria are able to use their flagella not only as devices for propulsion, but also to sample changes in the extracellular environment.

1
Introduction

1.1 Sensing and responding to the environment

Bacteria live in diverse, challenging and competitive environments. To survive and propagate bacteria must be able to adapt to their surroundings quickly and effectively. For this reason bacteria have evolved a number of strategies that allow them to sense and respond to a wide range of extracellular stimuli. Such signals include, but are not limited to: pH, temperature, nutrient and iron availability, reactive oxygen species and cell density.

1.1.1 Bacterial signal transduction

Signal transduction pathways are used by bacteria to sense and react to changes in the extracellular environment. The signal transduction mechanisms used can be as diverse as the environmental signals that they detect. Two component signal transduction pathways represent the prototypical signalling cascade that bacteria use to react to external signals (Nixon *et al.*, 1986). Canonical two component signal transduction systems (**Figure 1-1A**) are comprised of a histidine sensor kinase (HK), which senses a signal via an input domain, and a response regulator (RR), which controls the output. Information is passed from the HK to the RR by phosphotransfer between histidine and aspartate residues (Laub & Goulian, 2007). The phosphorylated RR most commonly elicits downstream effects by binding to DNA and altering gene expression. Bacteria use a number of mechanisms to ensure that distinct pathways are insulated from inappropriate cross-talk with other pathways (Podgornaia & Laub, 2013). Such specificity in the response may be engineered by additional proteins or solely by the HK and RR themselves, for example an HK is likely to have a higher affinity for its cognate RR than for any other RR in the cell (Laub & Goulian, 2007). Typically the input and output domains of HKs and RRs, respectively, show conservation at the amino acid sequence or structural level (Laub & Goulian, 2007). Indeed such domains have also been found to be fused in a single protein, producing a one-component regulator that directly couples signal perception to the output (Ulrich *et al.*, 2005).

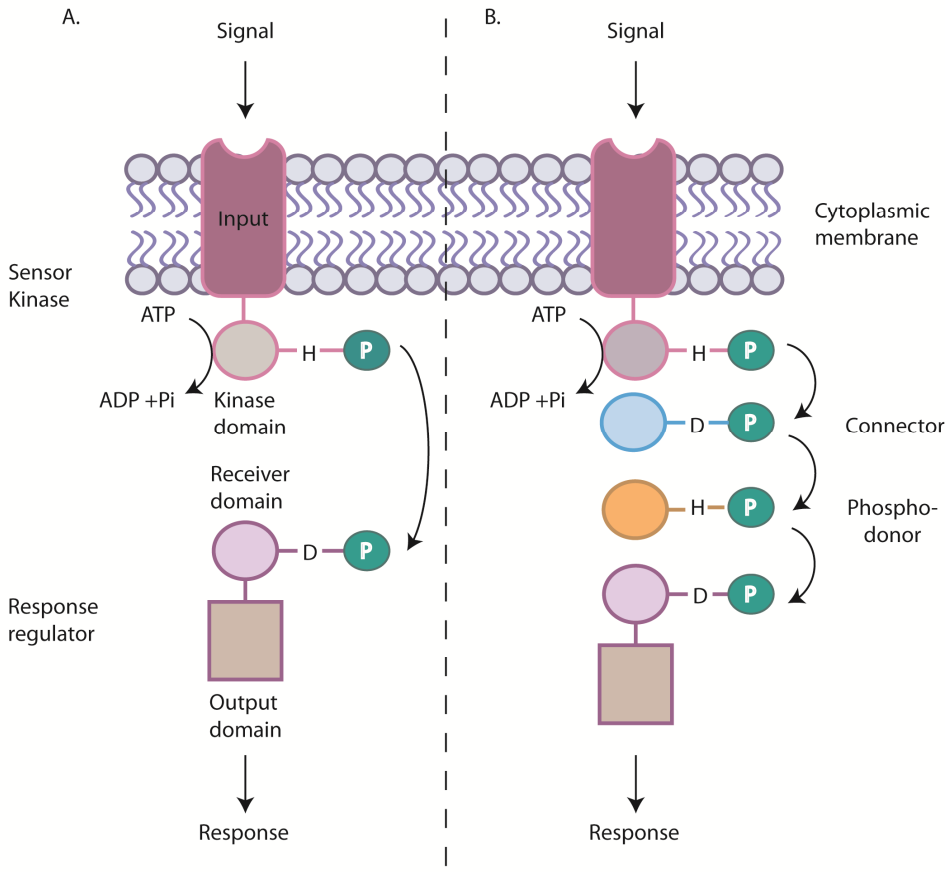

Figure 1-1 Prototypical two component signal transduction and phosphorelay pathways. (A) Schematic diagram of a prototypical two component signal transduction system, where a membrane bound kinase senses an extracellular signal and autophosphorylates at a conserved histidine residue. The phosphoryl group is then transferred to a conserved aspartic acid residue on the receiver domain of the cytosolic response regulator. P in a green circle denotes a phosphoryl group with the arrow between circles denoting phospho-transfer. **(B)** Schematic of a phosphorelay where the phosphoryl group is passed first to a connector protein and then to a phospho-donor before being accepted by the response regulator.

Conversely, extensions of two component signalling systems are also useful to allow for cross-talk and integration of multiple signals (Buelow & Raivio, 2010). Such pathways are called phosphorelays and see the phosphoryl group moved between several proteins before transfer to the terminal RR (**Figure 1-1**).

Bacteria also use serine, threonine and tyrosine phosphorylation to relay information. While histidine and aspartate phosphorylation have long been known to play crucial roles in bacterial signal transduction, the role of serine, threonine and tyrosine phosphorylation in bacteria has been comparatively underappreciated. In eukaryotes the impact of serine, threonine and

tyrosine phosphorylation has been widely studied and is recognised to be crucial in a multitude of cellular processes (Pawson & Scott, 2005). Eukaryotic kinases and phosphatases are tightly controlled and often highly specific for their target proteins. In contrast, in bacteria each serine, threonine and tyrosine kinase has multiple substrates (Cousin *et al.*, 2013). Bacterial and eukaryotic serine and threonine kinases share a degree of similarity, but bacterial tyrosine kinases (BY-kinases) are distinct from their eukaryotic counterparts, with structural differences even being apparent between Gram-negative and Gram-positive bacterial species (Grangeasse *et al.*, 2012). Serine, threonine and tyrosine kinases are essential for many cellular processes, but the upstream signals that regulate their activity are, as yet, largely unknown. Proteomic studies have also shown that proteins can be arginine phosphorylated, identifying a further role for post-translational modifications in bacterial physiology (Elsholz *et al.*, 2012).

Bacterial signal transduction does not always rely on post-translational modifications. For example, bacteria also harness extracytoplasmic function σ factors (ECFs) to detect and react to stimuli. ECFs respond to the external environment by binding to RNA polymerase and targeting specific promoters to activate gene transcription (Mascher, 2013). ECFs are typically bound and held inactive by their cognate membrane-spanning anti-σ factor. When activated by an appropriate signal the anti-σ factor releases the ECF, permitting the expression of target genes (Mascher, 2013). One example in *Bacillus subtilis* is σ^X, which is controlled by its anti-σ factor YpuN, and plays a role in indirectly activating biofilm formation (Murray *et al.*, 2009).

Crucially, cross-talk can occur between these multiple mechanisms of signal perception and response output, allowing communication between signalling pathways and the integration of multiple stimuli. For example histidine sensor kinases may be additionally phosphorylated on serine, as occurs for the DegS-DegU two component regulatory system in *B. subtilis* (Jers *et al.*, 2011) (see section 1.3.1). Two component pathways and ECFs can also communicate by σ factor mimicry. In the general stress response exhibited by α-proteobacteria the PhyR RR has an N-terminal ECF-like domain and a C-terminal receiver domain. Upon phosphorylation of the

RR, the ECF-like domain is released, allowing it to bind to the anti-σ factor NepR, and hence allow release of the true ECF (EcfG) to promote gene transcription (Francez-Charlot *et al.*, 2009).

1.1.2 Bacterial stress responses

Upon perception of an external signal, an appropriate physiological response must be elicited to allow survival of the cell, or indeed of the population. Bacterial stress responses are varied and dependent on the signal perceived, but share the common theme of promoting survival. Such survival processes may encompass strategies such as cell movement, surface colonisation, cooperation with other members of the community or secretion of an array of proteins and virulence factors as a means of protection from neighbouring cells.

To move to a better niche, bacteria can use flagellar-based motility. The direction of movement is regulated by the chemotaxis phosphorelay, where cells undertake a "biased random walk" to allow them to sense gradients of nutrients and change their trajectory as necessary (Porter *et al.*, 2011). Under nutrient-limiting conditions bacteria may instead adhere to a surface and form a biofilm; a community of cells encased in a self-produced exopolymeric matrix (Flemming & Wingender, 2010). In doing so, bacteria are able to share resources amongst members of the community and protect themselves from physical or chemical stress. Alternatively, to survive within the host bacteria also use virulence factors, for example *Listeria monocytogenes* produces a large repertoire of virulence factors upon activation of the transcription factor PrfA, which responds to temperature (Johansson *et al.*, 2002). Moreover, bacteria employ secretion systems to aid their survival, not only to evade a eukaryotic host, but also to compete in a polymicrobial environment. Using the Type VI secretion system bacteria export effector proteins to kill competitor bacteria (Russell *et al.*, 2014). Such effectors can target the peptidoglycan layer, cell membrane or nucleic acids of neighbouring cells. Each effector is encoded alongside an immunity protein, ensuring that the bacterium

does not show toxicity towards itself (Russell *et al.*, 2014). Therefore this secretion system is likely to play an important role in polymicrobial infections and symbiosis. Secretion systems are also crucial in mediating bacterial phytopathogenesis (Feng & Zhou, 2012). Using the type III secretion system the plant pathogen, *Pseuodomonas syringae* injects a tyrosine phosphatase effector protein, HopA01, into the host to dampen the immune response of the plant by dephosphorylating a pattern recognition receptor (Macho *et al.*, 2014). This process aids in the colonisation of the plant by the bacterium.

Bacteria also respond to cell density. Indeed the ability to sense other cells is essential for many processes. Cells can sense each other and communicate in a process called quorum sensing, which allows the population to coordinate their response and cooperate to enable their survival (Ng & Bassler, 2009). Quorum sensing pathways can control intra-species and inter-species communication. Essentially, cells synthesise chemical signals called auto-inducers that may be sensed by neighbouring bacteria of the same or different species when cell density increases. In Gram-negative species these signals are often sensed by two component signalling pathways, whereas in some Gram-positive bacteria such signals diffuse into the cytoplasm where they interact with transcription factors to directly alter gene expression (Ng & Bassler, 2009). In fact many processes including competence, biofilm formation, sporulation and virulence can be regulated in this manner (Ng & Bassler, 2009).

The Gram-positive bacterium *Bacillus subtilis* uses several of the signalling mechanisms outlined here to regulate a range of cellular processes and stress responses. The work presented in this thesis aimed to investigate the regulation of flagellar motility and the link between the flagellum and biofilm formation in *B. subtilis*.

1.2 *Bacillus subtilis*

Bacillus subtilis is a Gram-positive, rod-shaped, soil-dwelling, motile bacterium that is able to sense and respond to its environment. In its natural habitat *B. subtilis* acts as biocontrol agent to promote plant growth and protect the host plant from other bacterial pathogens (Nagorska *et al.*, 2007). Furthermore *B. subtilis* is related to the pathogenic species *Bacillus cereus* and *Bacillus anthracis.* Until recently, genetic information in *B. subtilis* was thought to be carried by a single 4.2 Mbp chromosome. However, the ancestral strain NCIB3610 (used throughout this study) also carries a large 80 kb plasmid, although the majority of proteins encoded by the plasmid remain uncharacterised (McLoon *et al.*, 2011, Konkol *et al.*, 2013).

The *B. subtilis* NCIB3610 strain is a model organism for the study of bacterial multicellularity. Multicellular behaviours are defined as processes that require the cooperation of a group of cells to work together to perform a task that is beneficial for the population (Shapiro, 1998). These processes cannot be carried out by single cells alone. Such behaviours include genetic competence (Hamoen *et al.*, 2000), swarming motility where groups of cells move over a surface powered by flagella (*B. subtilis* has been reported to synthesise 26 flagella per cell which are arranged peritrichously under growth in liquid culture (Guttenplan *et al.*, 2013)) (Kearns *et al.*, 2004), biofilm formation (Branda *et al.*, 2001, Hamon & Lazazzera, 2001) and sporulation where cells become metabolically inert to ensure their survival under nutrient-limiting conditions (Higgins & Dworkin, 2012). *B. subtilis* also secretes the polymer γ-poly-$_{D\text{-}L}$-glutamic acid (γ-PGA) (Stanley & Lazazzera, 2005) and enzymes such as proteases (Veening *et al.*, 2008), which benefit the population and allow *B. subtilis* to adapt to the surrounding environment. Multicellularity was only proposed as a general bacterial trait in 1988 (Shapiro, 1988). However, multicellular aggregates of *B. subtilis* cells were discovered and depicted by Ferdinand Cohn as far back as the 19th century. Despite this *B. subtilis* biofilms were only reported again in 2001 (Branda *et al.*, 2001, Hamon & Lazazzera, 2001). The study of

multicellular behaviours has been enhanced by the recognition that strains that have been extensively propagated, or mutated to select for favourable attributes such as competence, have also lost their multicellular traits (Branda *et al.*, 2001). The *B. subtilis* 168 laboratory strain carries several point mutations that limit its ability to perform many processes, including swarming motility and biofilm formation (Branda *et al.*, 2001, Kearns *et al.*, 2004, Stanley & Lazazzera, 2005). For this reason the ancestral NCIB3610 strain, which 168 is thought to originate from, is used to investigate multicellular behaviours.

In *B. subtilis* several multicellular traits are regulated by the DegS-DegU two component signal transduction system (Kobayashi, 2007, Verhamme *et al.*, 2007). Interestingly, both flagellar motility and biofilm formation are linked by DegS-DegU. This is of note because these are apparently opposing behaviours in that they cannot take place in the same cell at the same time. Flagella have however been implicated in biofilm formation in a range of different bacterial species. Details on this signalling pathway, flagellar motility and biofilm formation are now further discussed.

1.3 Two component signal transduction systems

Two component signal transduction systems are used by bacteria to sense and respond to environmental stimuli (Laub & Goulian, 2007). The stimuli that activate two component systems are often unknown but include cell shape (Callewaert *et al.,* 2009), temperature (Aguilar *et al.,* 2001), osmolarity (Igo *et al.,* 1989), cellular redox state (Georgellis *et al.,* 2001, Malpica *et al.,* 2004) and quorum signals (Neiditch *et al.,* 2006). Signals are perceived by the HK and the response elicited by the cognate RR. HKs are composed of an N-terminal input domain that senses a signal and a C-terminal histidine kinase domain (**Figure 1-1A**). The majority of HKs are integral membrane proteins that sample the extracellular environment, although some are fully cytoplasmic (Cheung & Hendrickson, 2010). Upon receipt of an appropriate stimulus, the HK dimerises and autophosphorylates at a conserved histidine

residue in the kinase domain. The phosphoryl group is then transferred to the N-terminal receiver domain of the cognate RR, leading to conformational changes within the output domain of the RR (Bourret, 2010). This typically alters the DNA binding activity of the RR such that the transcription of downstream target genes is up or down-regulated. Alternatively, phosphorylation of the RR may stimulate enzymatic activity or allow interaction with RNA or different protein partners (Gao *et al.*, 2007).

Two component signal transduction systems and phosphorelays are exquisitely regulated by a suite of auxiliary proteins and phosphatases (Buelow & Raivio, 2010). For example, many HKs also act as phosphatases to prevent non-specific phosphorylation of their cognate RRs. The activity of HKs may additionally be adjusted by interaction with proteins that modulate auto-kinase activity, stimulate phosphoryl transfer to the RR, or sense extracellular signals (Buelow & Raivio, 2010). In this way the two component signal transduction pathways and phosphorelays are able to assimilate multiple stimuli to orchestrate a response that alters cellular physiological processes.

1.3.1 The DegS-DegU two component signal transduction system

DegU is a response regulator that is phosphorylated by its cognate sensor histidine kinase, DegS (Msadek *et al.*, 1990, Dahl *et al.*, 1991) (**Figure 1-2**). DegS is predicted to be a cytoplasmic protein that carries an N-terminal coiled-coil input domain that bears no homology to other sensor kinases (**Figure 1-2**). As for most sensor kinases DegS displays dual kinase and phosphatase activities (Tanaka *et al.*, 1991). Upon sensing an appropriate stimulus, DegS autophosphorylates at histidine 189 and subsequently transfers its phosphoryl group to DegU (Dahl *et al.*, 1991). Phosphotransfer is aided by the small protein, DegQ, which has been reported to act by stabilising phosphorylated DegS (Kobayashi, 2007, Do *et al.*, 2011). The DegU protein consists of an N-terminal receiver domain, which contains the phosphorylation site at aspartate 56, and a C-terminal LuxR-like helix-turn-helix DNA binding domain (Shimane

& Ogura, 2004) (**Figure 1-2**). DegU is thought to bind to DNA as a dimer and recognises AT rich sequences arranged in different orientations (Sanchez & Olmos, 2004, Shimane & Ogura, 2004).

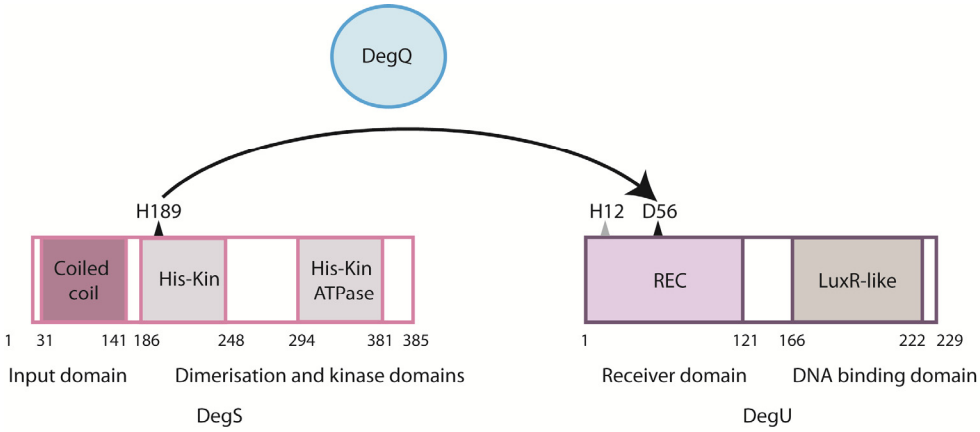

Figure 1-2 Domain organisation of the *B. subtilis* DegS-DegU two component signal transduction system. Schematic diagram indicating functional domains of the DegS and DegU proteins. Black triangles denote the histidine and aspartate phosphorylation sites on DegS and DegU, respectively, with the black arrow indicating phospho-transfer between the two sites. DegQ is indicated in aiding the phosphor-transfer reaction. The grey triangle indicates the DegU H12 amino acid that can be mutated to yield a highly active variant of DegU~P. Numbers below rectangles indicate the amino acid number of each protein.

DegU is a pleiotropic regulator that promotes or represses transcription of target genes depending on the level of phosphorylated DegU (DegU~P) within the cell (Kobayashi, 2007, Verhamme *et al.*, 2007). DegU has a plethora of targets, with genome-wide microarray analyses identifying over 120 members of the DegU regulon (Ogura *et al.*, 2001, Mader *et al.*, 2002), although it is likely that DegU regulates many of these genes indirectly. Regulatory activity is exhibited by DegU in both its unphosphorylated and phosphorylated states, leading to a model whereby DegU acts as a rheostat to integrate a variety of environmental signals to control several physiological processes (Verhamme *et al.*, 2007) (summarised in **Figure 1-3**).

To manipulate DegU~P levels within the cell many studies have harnessed a number of different genetic mutations in *degS* and *degU*. The *degU146* allele produces a protein variant of DegU that cannot be phosphorylated due to mutation of aspartic acid 56 to asparagine

(Dahl *et al.*, 1991, Dahl *et al.*, 1992). To increase the level of DegU~P in the cell mutations in *degS* and *degU* have been used. The most commonly used allele, *degU32hy*, encodes a DegU protein variant where histidine at position 12 is mutated to leucine (DegU $H^{12}L$), resulting in DegU~P being dephosphorylated at a rate seven times slower than the wild-type (Henner *et al.*, 1988, Dahl *et al.*, 1992) (site of mutation indicated in **Figure 1-2**). Using these alleles it has been possible to tune the level of DegU~P to test the effects on gene transcription (summarised in (**Figure 1-3**). Unphosphorylated DegU is required for genetic competence; DegU binds directly to the *comK* promoter to activate transcription and also recruits the transcription factor ComK to the promoter, which activates the expression of genes for DNA binding and uptake and allows establishment of a positive autoregulatory loop (Hamoen *et al.*, 2000). Low levels of DegU~P permit swarming motility by enhancing transcription of the *fla/che* operon, which is required for flagellar biosynthesis (section 1.4.1), while mid-levels of DegU~P promote biofilm formation by indirectly increasing transcription from the *bslA* promoter (Kobayashi, 2007, Verhamme *et al.*, 2007) (discussed in section 1.5.4). High levels of DegU~P directly activate transcription of several promoters, including those of *aprE* and *bpr*, which encode the exoproteases subtilisin and bacillopeptidase F, respectively (Tanaka *et al.*, 1991, Dahl *et al.*, 1992, Ogura *et al.*, 2001), and *sacB* which encodes the levansucrase enzyme (Ogura *et al.*, 2001). Transcription of the *pgsB* operon, which encodes proteins for the biosynthesis of the exopolymer γ-PGA, also requires high DegU~P (Stanley & Lazazzera, 2005, Ohsawa *et al.*, 2009). Conversely, high levels of DegU~P abrogate motility by repressing transcription of the *fla/che* operon (Amati *et al.*, 2004) and also inhibit competence and biofilm formation (Dahl *et al.*, 1992, Verhamme *et al.*, 2007, Marlow *et al.*, 2014b). Therefore, the level of DegU~P within the cell must be tightly controlled to allow for the appropriate cellular response.

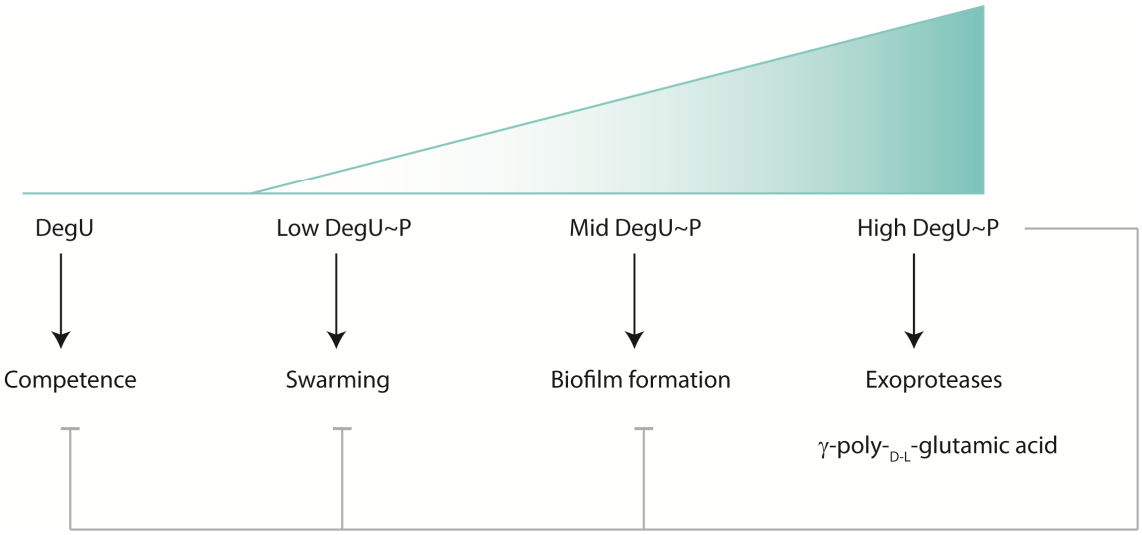

Figure 1-3 The effects of increasing levels of DegU~P on cellular processes. Schematic diagram to indicate that increasing levels of DegU~P can activate or repress different processes. Increasing DegU~P is indicated by an increase in both the size of the triangle and an increasing intensity of colour. Black arrows indicate activation of a process while grey T-bars indicate repression by high levels of DegU~P.

1.3.1.1 *The DegU consensus sequence*

The ability of DegU to modulate such a myriad of processes is likely underpinned by a variation in promoter affinities or consensus sequences. The consensus sequence for DegU binding was identified for the *comK* promoter as an inverted repeat (IR) of an AT-rich sequence (G-N2-ATTTA-N7-TAAAT-N2-C), and for the *aprE* promoter as direct repeats (DR) of an AT-rich sequence (TAAAT) (Shimane & Ogura, 2004). These findings led the authors to hypothesise that unphosphorylated and phosphorylated DegU bind to different arrangements of the consensus sequence, i.e unphosphorylated DegU preferentially binds IRs while DegU~P binds DRs. In support of this theory, the binding site of DegU at the *fla/che* operon was also mapped to an IR sequence, while DegU~P binds a DR sequence in both the *bpr* and *sacB* promoters (Tsukahara & Ogura, 2008b, Tsukahara & Ogura, 2008a). Moreover, mutation of the *sacB* DR sequence to an IR sequence enabled binding of unphosphorylated DegU, as investigated by both *in vitro* gel shift assays and *in vivo* transcriptional analysis (Tsukahara & Ogura, 2008b).

Whether other DegU and DegU~P targets are defined by the arrangement of their consensus sequences remains to be determined.

1.3.1.2 *Transcriptional regulation of degS and degU*

Several studies have identified means by which the DegS-DegU signalling pathway might be regulated. Firstly, the *degS* and *degU* genes are under strict transcriptional regulation. Three promoters control the expression of *degU*: the first promoter (P1) is upstream of *degS* and allows co-transcription of both genes (Msadek *et al.*, 1990), the second (P2) resides within the *degS* coding sequence (Msadek *et al.*, 1990, Yasumura *et al.*, 2008), while the third (P3) solely governs transcription of *degU* and is found in the intergenic region between *degS* and *degU* (Yasumura *et al.*, 2008) (see **Figure 1-4**). Transcription from P1 is activated at the onset of stationary phase, is driven by the major sigma factor σ^A, and results in homogeneous expression of *degS* and *degU* throughout the population (Msadek *et al.*, 1990, Veening *et al.*, 2008). The P2 promoter is activated under conditions of nitrogen limitation (Yasumura *et al.*, 2008), while expression from P3 is increased by DegU~P itself, allowing a positive feedback loop to be established (Kobayashi, 2007, Veening *et al.*, 2008, Yasumura *et al.*, 2008) (**Figure 1-4**). Expression from only P1 and P2 does not appear to be sufficient to allow high levels of DegU~P to accumulate. Thus activation of P3 is required to regulate gene transcription controlled by high levels of DegU~P (Yasumura *et al.*, 2008). The *degQ* gene, which encodes the DegQ protein that is thought to increase phospho-transfer from DegS to DegU (Kobayashi, 2007, Do *et al.*, 2011), is also regulated by several means. The ComA-ComP two component system, which responds to cell density signals, activates transcription of *degQ*, thereby ensuring that DegU~P levels rise as growth approaches stationary phase (Msadek *et al.*, 1991). Transcription of *degQ* is also increased by expression of the *degS* and *degU* genes and by nitrogen limitation, alongside other nutritional signals (Msadek *et al.*, 1990, Msadek *et al.*, 1991).

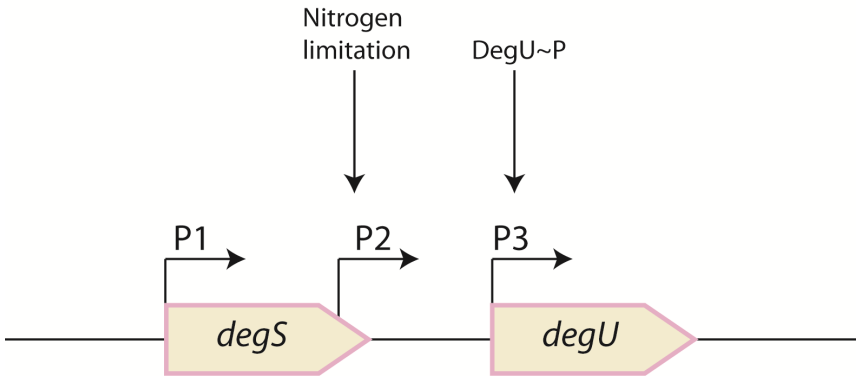

Figure 1-4 Organisation of the *degS-degU* operon. Schematic diagram representing the organisation of the *degS* and *degU* genes on the chromosome. Open reading frames are indicated by coloured block arrows, black arrows indicate activation and bent arrows represent promoter regions. P1, P2 and P3 denote promoters 1, 2 and 3.

1.3.1.3 *Regulation of DegU phosphorylation and activity*

The DegS-DegU two component signal transduction pathway is also tightly controlled at the post-translational level. In addition to being autophosphorylated at histidine 189, DegS can also be phosphorylated at serine 76 by at least two Hanks-like kinases (Macek *et al.*, 2007, Jers *et al.*, 2011). It is hypothesised that serine phosphorylation might promote phospho-transfer to DegU, increasing DegU~P in the cell (Jers *et al.*, 2011). However, this work did not present kinetic data to test if the catalytic properties of DegS were altered upon serine phosphorylation. The upstream signal that triggers phosphorylation of DegS on serine is also unknown.

DegS activity is also controlled by interaction with the bacterial kleisin protein, ScpA (Dervyn *et al.*, 2004). The structural maintenance of chromosome (SMC) protein forms a complex with ScpA and ScpB and is essential for chromosome partitioning and DNA repair (Soppa *et al.*, 2002, Dervyn *et al.*, 2004). Deletion of *scpA*, *scpB* or *smc* resulted in increased production of levansucrase, increased exoprotease production and decreased motility, which were all

dependent on DegU~P (Dervyn *et al.*, 2004). These findings led to the suggestion that DegS kinase activity might be under the negative control of the SMC-ScpA-ScpB complex.

DegU~P itself is regulated by proteolysis (Ogura *et al.*, 2003). The AAA+ protease ClpP, in combination with the ATPase subunit ClpC, degrades DegU~P. Mutation of amino acids in the N-terminal region of DegU increased the stability of the DegU~P (Ogura *et al.*, 2003), raising DegU~P to a level sufficient to activate transcription from the *degU* P3 promoter, but not to a level where transcription from *aprE* could be activated. This indicates that DegU~P is still degraded, or that protection of DegU~P from proteolysis alone is not sufficient to raise DegU~P to a high level. How ClpCP specifically recognises DegU~P over DegU is unknown. Subsequent work suggested that glucose may act as an upstream signal to regulate *clpC*, and therefore DegU~P (Ishii *et al.*, 2013).

DegU~P is further regulated by the RapG-PhrG system (Ogura *et al.*, 2003). Rap proteins are aspartyl proteases that are inhibited by phosphatase regulator (Phr) pentapeptides. RapG and PhrG affect *aprE* expression. Surprisingly, RapG does not decrease *aprE* transcription by dephosphorylation of DegU~P but rather interferes with the binding of DegU to the *aprE* promoter. This effect can be reversed by addition of PhrG (Ogura *et al.*, 2003). The same effect was observed when the *comK* promoter region was used in similar experiments. The *phrG* gene is under the control of σ^H (a sigma factor that controls expression of genes in stationary phase), so is likely to account for the increase in DegU~P observed during stationary growth. However, these experiments used DegU instead of DegU~P, and so there could be slight differences in how DegU~P binding to DNA is regulated by RapG.

While many aspects of DegU activation and regulation are understood the signal sensed by DegS to trigger phosphorylation of DegU has remained somewhat elusive. Signals such as osmolarity and nitrogen depletion have been suggested (Ruzal & Sanchez-Rivas, 1998, Yasumura *et al.*, 2008). Recent work also indicated that the completion status of the flagellar

basal body (Hsueh *et al.*, 2011) could be important with respect to DegU~P levels. Experiments presented in Chapter 4 uncovered a link between the flagellum and activation of DegU~P regulated processes.

1.4 Flagellar motility

Bacteria use a range of motility strategies to escape from harsh conditions and to explore new environments. Several of these mechanisms involve different surface appendages (Jarrell & McBride, 2008). Type IV pili are used by many bacteria for gliding (smooth movement over a surface) or twitching (an irregular movement over a surface) motility (McBride, 2001, Mattick, 2002). The pilus extends, attaches to a surface and retracts to propel the cell forward. Several species also show gliding motility in the absence of Type IV pili. For example, in addition to twitching motility *Myxococcus xanthus* also glides using a system that does not require pili but that has been proposed to rely on a proton-motive force driven motor that transduces mechanical energy to a protein complex, propelling the cell forward when it comes into contact with an appropriate surface (Jarrell & McBride, 2008).

The best studied motility structure is the flagellum. The bacterial flagellum is powered by a gradient of H^+ or Na^+ ions and rotates to propel the cell forward. Flagella are needed for both swimming, where cells move through liquid, and swarming, where cells move over a solid surface in groups (Kearns, 2010). Flagella also have roles in surface adhesion and biofilm formation (O'Toole & Kolter, 1998, Watnick & Kolter, 1999, Guttenplan & Kearns, 2013, Serra *et al.*, 2013). Most bacteria display flagella on the cell surface; this might be as a single polar flagellum, as a group of lateral flagella, or around the entire cell (peritrichously). Curiously, the spirochaetes have periplasmic flagella that are located at the cell poles and wrap around the cell (Jarrell & McBride, 2008). Their rotation drives the cell forward, either by rotating the inner and outer membranes in opposite direction or by bending the cell to trigger movement. The flagellin protein (the major component of the flagellum) is extremely antigenic and is

sensed by the host to activate signalling pathways for innate immunity. For this reason some bacteria, e.g. *Listeria monocytogenes* down-regulate flagellar biosynthesis at physiological temperatures to avoid detection (Peel *et al.*, 1988). The flagellum has also been shown to mediate symbiosis (Shimoyama *et al.*, 2009).

The majority of experiments on flagellar motility have been carried out in Gram-negative bacterial species, such as *Salmonella enterica* serovar Typhimurium, *Escherichia coli* and *Rhodobacter sphaeroides* (Chevance & Hughes, 2008), but increasing details on the Gram-positive flagellum are emerging and suggest that flagellar biosynthesis in *B. subtilis* is regulated by both conserved and species-specific mechanisms (Blair *et al.*, 2008, Hsueh *et al.*, 2011, Guttenplan *et al.*, 2013). The subsequent section will describe the current knowledge on flagellar biosynthesis, its regulation and role in biofilm formation.

1.4.1 Transcriptional regulation of flagellar biosynthesis

The flagellum is organised into three main structural components: the basal body, hook and filament (Chevance & Hughes, 2008). The basal body consists of the flagellar motor, which is required to power rotation of the flagellum, and a type III secretion system that permits the export of proteins required for the biosynthesis of the hook and filament. The hook is a flexible joint that permits a change in the angle of rotation of the flagellum, while the filament acts as a propeller to drive movement.

To ensure proper assembly of the flagellum, its biosynthesis is tightly regulated at the transcriptional level (Chevance & Hughes, 2008). In Gram-negative bacteria the flagellar genes are organised hierarchically and regulated by three different promoters: class I, class II and class III. In *Salmonella* flagellar genes are organised as follows: the master operon *flhDC* is controlled by a class I promoter, the genes required for assembly for the HBB are regulated by class II promoters (driven by the housekeeping sigma factor σ^{70}), and the genes needed for the flagellar filament and motor proteins are under the control of class III promoters (driven by the

alternative sigma factor σ^{28}). Briefly, once *flhDC* is transcribed the FlhD and FlhC proteins form a complex that acts to inhibit their own transcription and promote transcription from the class II promoters to synthesise the hook basal-body (HBB). Upon completion of the HBB, there is a secretion specificity switch. The FliT regulator is usually bound in the cytoplasm by its inhibitor, FliD. Similarly, σ^{28} is held inactive by the anti-sigma factor, FlgM (Chadsey *et al.*, 1998). When the HBB is completed FlgM is secreted (Hughes *et al.*, 1993, Karlinsey *et al.*, 2000b). This results in activation of class III promoters by σ^{28}, allowing transcription of flagellar filament and motor genes. Additionally, FliD is secreted, releasing FliT. FliT can then prevent FlhDC from inhibiting its own transcription. This re-sets the transcriptional programme, allowing transcription of class I promoters and flagellar gene transcription to begin again (Chevance & Hughes, 2008). The net result of this regulatory cascade is that transcription is temporally ordered such that the HBB genes are expressed before the filament genes (Chevance & Hughes, 2008).

In *Bacillus subtilis*, the flagellar genes are organised in a slightly different manner. The proteins needed for the HBB are transcribed in the 31 gene *fla/che* operon (Marquez-Magana & Chamberlin, 1994, West *et al.*, 2000) (**Figure 1-5**). This operon also encodes proteins required for the chemotaxis pathway, for flagellar type III secretion and to regulate the placement of flagella around the cell. The penultimate gene of this operon, *sigD*, encodes the sigma factor σ^{D}, a homologue of σ^{28} (Helmann *et al.*, 1988, Chen & Helmann, 1992), that activates transcription of the late flagellar genes: the flagellar filament gene, *hag*; the flagellar stator genes, *motA* and *motB*; the anti-sigma factor, *flgM*; the hook-filament junction genes, *flgK* and *flgL* (Mirel *et al.*, 1994) and the autolysins, which are needed for cell separation (Marquez *et al.*, 1990). Three promoters control expression of this operon: (i) the strong *fla/che* promoter located upstream of the first gene in the operon, *flgB*, that is driven by the housekeeping sigma factor, σ^{A}, (ii) P_{D-3} that is activated by σ^{D} but only appears to play a minor role (Estacio *et*

al., 1998, West *et al.*, 2000) and (iii) P_{ylxF3}, an internal promoter that responds to σ^D and may increase transcription of *sigD* (Cozy & Kearns, 2010) (**Figure 1-5**)

.

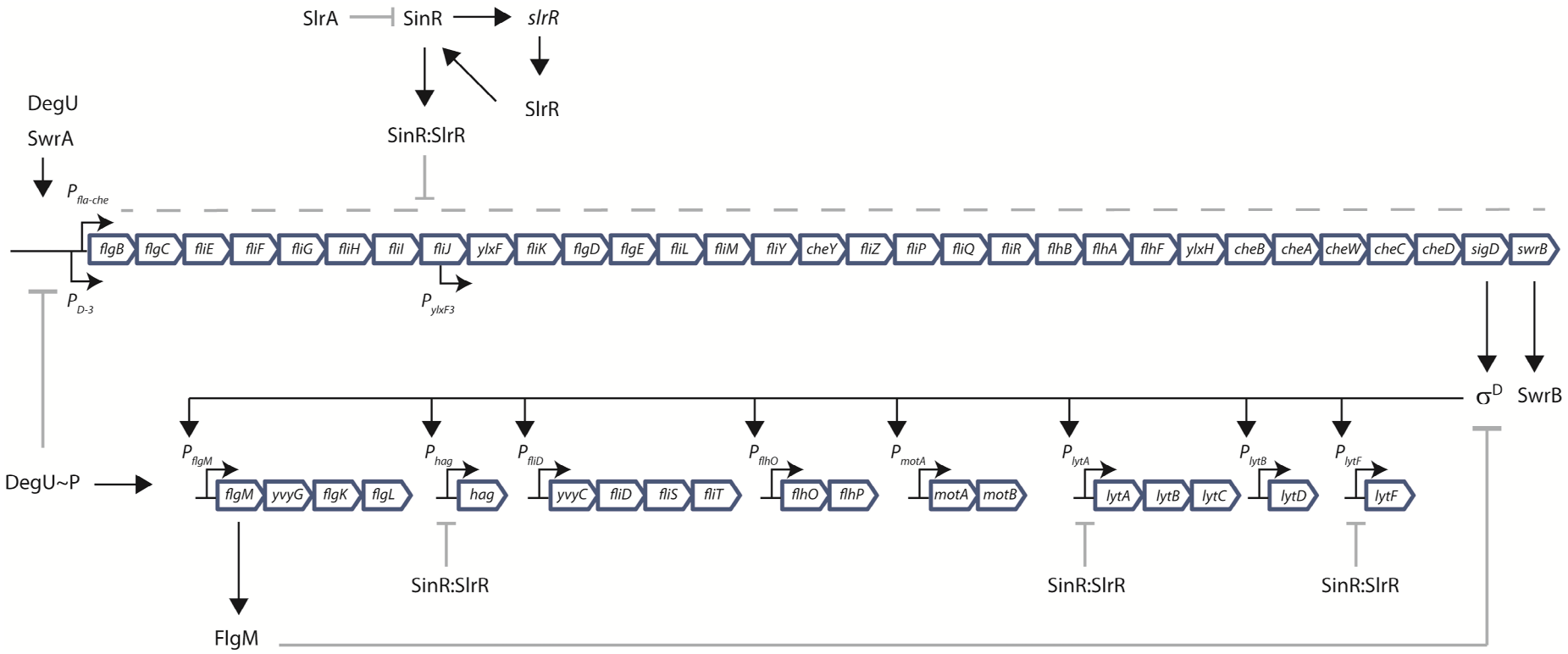

Figure 1-5 Organisation and regulation of flagellar gene transcription in *B. subtilis*. Blue open arrows represent open reading frames, bent arrows indicate promoter regions, black arrows represent a positive genetic interaction, grey T-bars indicate repression, the dashed grey line indicates the *fla/che* operon. Gene number annotations can be found on the Subtilist website.

Motility is a bimodal trait in *B. subtilis* and the proportion of motile cells likely varies depending on the environmental conditions and specific strain studied (Kearns & Losick, 2005). When the NCIB3610 strain is grown under standard conditions in rich media, the majority of cells are motile while a small population grow as non-motile chains (Kearns & Losick, 2005). These phenotypes are explained by the presence or absence of σ^D, respectively. While the *fla/che* operon is transcribed in all cells, σ^D-regulated operons are only transcribed in a sub-population (Kearns & Losick, 2005). This is due to tight regulation of σ^D at the level of transcription and also at the level of activity (Kearns & Losick, 2005, Cozy & Kearns, 2010). A threshold level of σ^D is required to activate transcription of target genes. The location of *sigD* at the end of the *fla/che* operon means it is less likely to be transcribed. Indeed, in experiments where *sigD* was moved closer to the promoter region, *sigD* transcription was increased along with transcription of σ^D target genes (Cozy & Kearns, 2010). These experiments also allowed the discovery of a σ^D-regulated promoter, P_{ylxF3}, that resides within the *fla/che* operon (**Figure 1-5**). Activation of this promoter may increase the likelihood of *sigD* transcription reaching a threshold level and could also stabilise *sigD* transcription to allow continued expression of flagellar genes (Cozy & Kearns, 2010). The activity of σ^D is further controlled by the anti-sigma factor, FlgM (Cozy & Kearns, 2010) (**Figure 1-5**). However, the exact role of FlgM in flagellar biosynthesis by *B. subtilis* has not been determined so it is unclear if, as in *S.* Typhimurium, FlgM is secreted upon HBB completion to allow σ^D to activate transcription of its target genes.

The SwrA protein promotes expression of the *fla/che* operon and has been defined as the master regulator for flagellar biosynthesis in *B. subtilis* (Calvio *et al.*, 2005, Kearns & Losick, 2005) (**Figure 1-5**). Cells are able to swim in the absence of *swrA* but cannot swarm. The *swrA* gene is transcribed from two promoters: the σ^A promoter is activated during swarming motility, while the σ^D promoter is active in swimming and swarming cells (Calvio *et al.*, 2005). Consistent with an important role in swarming motility, one of the mutations in the *B. subtilis*

168 domesticated strain that ablates swarming motility resides within the *swrA* coding region (Kearns *et al.*, 2004). Furthermore, over-expression of *swrA* is sufficient to overcome the lag phase that is observed when cells begin to swarm (Kearns & Losick, 2005). SwrA increases the probability that the *fla/che* operon will be transcribed in full, and therefore that σ^D will reach a threshold to activate expression of target genes (Cozy & Kearns, 2010). In a population where *swrA* is deleted the number of non-motile, chaining cells greatly increases, indicating that the σ^D regulon is not transcribed (Kearns & Losick, 2005, Cozy & Kearns, 2010). Further work has shown that SwrA controls the number of flagella (as inferred from the number of basal bodies that are assembled) that are constructed per cell (Guttenplan *et al.*, 2013). A second gene called *swrB* also plays a role in controlling σ^D directed transcription, but only seems to play a prominent role when *swrA* is absent (Kearns & Losick, 2005).

To further investigate why σ^D regulated genes are not transcribed in a sub-population of cells, Kearns and colleagues used transposon mutagenesis in a strain lacking both *swrA* and *swrB* to mimic the non-motile sub-population (Hsueh *et al.*, 2011, Cozy *et al.*, 2012). Using this approach it was shown that the SlrA protein represses transcription of the *fla/che* operon in a manner that is dependent on the distance of a given gene from the promoter (Cozy *et al.*, 2012) (**Figure 1-5**). SlrA is an antagonist of the transcriptional repressor SinR (Kobayashi, 2008, Chai *et al.*, 2009) (see section 1.5.1 and **Figure 1-10**). It is hypothesised that SlrA prevents the association of SinR with its target DNA, allowing SinR to form a complex with the SlrR protein (Chu *et al.*, 2008, Kobayashi, 2008, Chai *et al.*, 2009, Cozy *et al.*, 2012). It is thought that the SinR:SlrR heterodimer may inhibit expression of the *fla/che* operon (Cozy *et al.*, 2012), as the SinR:SlrR complex has previously been shown to inhibit transcription of the *hag* gene and the autolysins (Chai *et al.*, 2010) (**Figure 1-5**). Using a similar transposon mutagenesis approach, it was also found that DegU~P activates transcription of the anti-sigma factor, *flgM*, by binding upstream from the *flgM* promoter (Hsueh *et al.*, 2011) (**Figure 1-5**). This in turn ablates σ^D

activity. Therefore, in non-motile, chaining cells SlrA and DegU both contribute to inhibition of σ^D activity.

The DegS-DegU two component system also confers further regulation of flagellar gene transcription. DegU is not essential for swimming motility, but is required for swarming motility (Verhamme *et al.*, 2007). More specifically, low levels of DegU~P are needed for increased transcription of the *fla/che* operon (Kobayashi, 2007, Verhamme *et al.*, 2007) (**Figure 1-5**). Conversely, high levels of DegU~P repress transcription of the *fla/che* operon (Amati *et al.*, 2004, Kobayashi, 2007, Verhamme *et al.*, 2007) (**Figure 1-5**). Moreover, the role of DegU~P at the *flgM* promoter is not only relevant in the absence of *swrA*, but also in genetic backgrounds that perturb HBB synthesis, suggesting a role for DegU~P in sensing flagellar biosynthesis (Hsueh *et al.*, 2011). Thus, the DegS-DegU two component system plays multiple roles in flagellar gene regulation.

Given that flagellar biosynthesis is energetically expensive it is unsurprising that several mechanisms exist to regulate flagellar gene transcription. These methods allow for temporal regulation and ensure that the flagellum is properly assembled. Bimodality of flagellar gene expression might also be important to allow cells to quickly respond to their dynamic surroundings. As well as being controlled at the transcriptional level flagellar biosynthesis is further regulated post-transcriptionally and during assembly.

1.4.2 Post-transcriptional regulation of the flagellar filament protein, Hag

In *B. subtilis* the global regulator CsrA represses translation of *hag* mRNA by binding directly to the *hag* transcript and preventing association of the ribosome (Yakhnin *et al.*, 2007). In Gram-negative bacteria CsrA activity is typically regulated by small RNAs (sRNAs). However, in *B. subtilis* CsrA is antagonised by the FliW protein (Mukherjee *et al.*, 2011). When Hag protein accumulates in the cytoplasm before secretion, FliW is bound by Hag to prevent its association with CsrA. Thus, *hag* translation is inhibited. When Hag is secreted (following completion of

the HBB, discussed in section 1.4.3.1) FliW is released and is able to bind to CsrA, sequestering it from the *hag* mRNA leader sequence (Mukherjee *et al.*, 2011). This allows *hag* translation and secretion to occur in parallel. Therefore, Hag can homeostatically regulate itself.

1.4.3 Structure and assembly of the flagellum

Regulation at the transcriptional level ensures that the flagellum is assembled in a strict order: the basal body is inserted into the membrane first and acts to anchor the hook and filament, the proteins for which are secreted through the basal body using a specialised type III secretion system (T3SS). Flagellar assembly is best characterised for *S.* Typhimurium, although many proteins are conserved in *B. subtilis* and have been identified as being flagellar components by proteomics and electron microscopy approaches (Kubori *et al.*, 1997) (**Figure 1-6**).

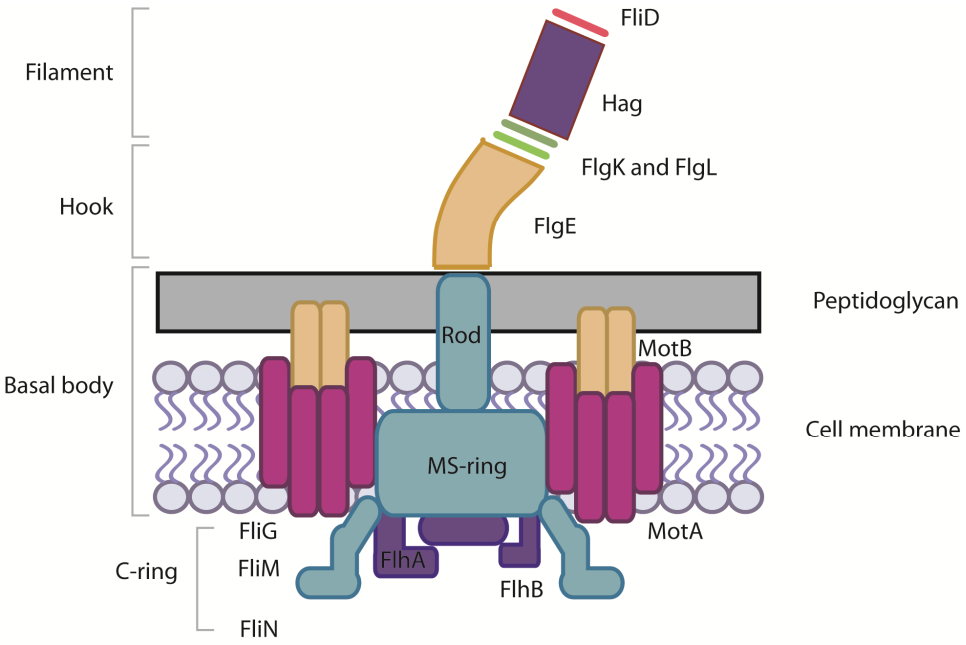

Figure 1-6 Schematic diagram of the predicted organisation of the *B. subtilis* flagellum. The basal body, hook and filament regions are indicated. Major components of the flagellum are labelled. Few flagellar components have been studied at a functional level in *B. subtilis*.

1.4.3.1 *Flagellar assembly*

The basal body is assembled by the formation of an integral-membrane structure called the MS-ring, which is composed of multiple copies of the FliF protein. The C-ring, which comprises the rotor proteins, FliG, FliM and FliN, is attached to the MS ring (Khan *et al.*, 1992). In Gram-negative bacteria the P and L-rings form at the peptidoglycan layer and outer membrane, respectively, with their components secreted by the Sec pathway. The components comprising the rod, hook and filament require the flagellar type III secretion system for their export and assembly. The rod is constructed from FlgB, FlgC, FlgF and FlgG. Notably, homologues of the *flgF* and *flgG* genes are not found on the *B. subtilis* chromosome, suggesting that the *B. subtilis* rod is either shorter than that of *S.* Typhimurium, or that other proteins make up the distal rod, for example FlhO and FlhP, as recently hypothesised (Courtney *et al.*, 2012). After assembly of the basal body, the hook capping protein, FlgD, is secreted followed by the major hook protein, FlgE, which is polymerised and inserted below FlgD. The length of the hook is controlled by FliK. After completion of the hook, a checkpoint is activated such that FlgM is secreted and late flagellar genes are transcribed (Hughes *et al.*, 1993). At this point a secretion-specificity switch is also triggered permitting the export of late flagellar proteins required for assembly of the hook and filament (**Figure 1-7**). This switch is mediated by FlhB (part of the export machinery) and FliK. The hook-filament junction proteins, FlgK and FlgL are secreted and replace FlgD at the end of the hook and are followed by the filament cap protein, FliD. The flagellar filament protein (FliC in *S.* Typhimurium or Hag in *B. subtilis*) is secreted and polymerised via a mechanism where subunits are linked in a chain that pulls them through the transit channel (Evans *et al.*, 2013) and are then arranged beneath FliD. Due their regulation by FlgM and σ^{28}/σ^{D}, the flagellar stator proteins, MotA and MotB, can be assembled in the membrane after HBB construction.

1.4.3.2 *Flagellar type III secretion*

The late flagellar proteins require chaperones for export via the T3SS. Regulation at this level has been described most extensively in *S.* Typhimurium (Minamino, 2013), with little known about the function of chaperones in Gram-positive bacterial species (Titz *et al.*, 2006, Mukherjee *et al.*, 2013). T3SS chaperones are small proteins comprised of an N-terminal domain that mediates homodimerisation and a C-terminal domain that interacts with the substrate. Chaperones bind to their cognate substrate(s) in the cytoplasm, protecting the substrate from degradation and/or preventing aggregation (Bennett & Hughes, 2000, Aldridge *et al.*, 2003). The N-terminal region of the substrate determines whether the protein is a late class substrate while the C-terminus mediates binding to the chaperone (Fraser & Hughes, 1999, Bennett & Hughes, 2000, Minamino, 2013). Chaperones therefore expedite transport of the substrate to the export machinery. A schematic diagram of late flagellar protein secretion is presented in **Figure 1-7**.

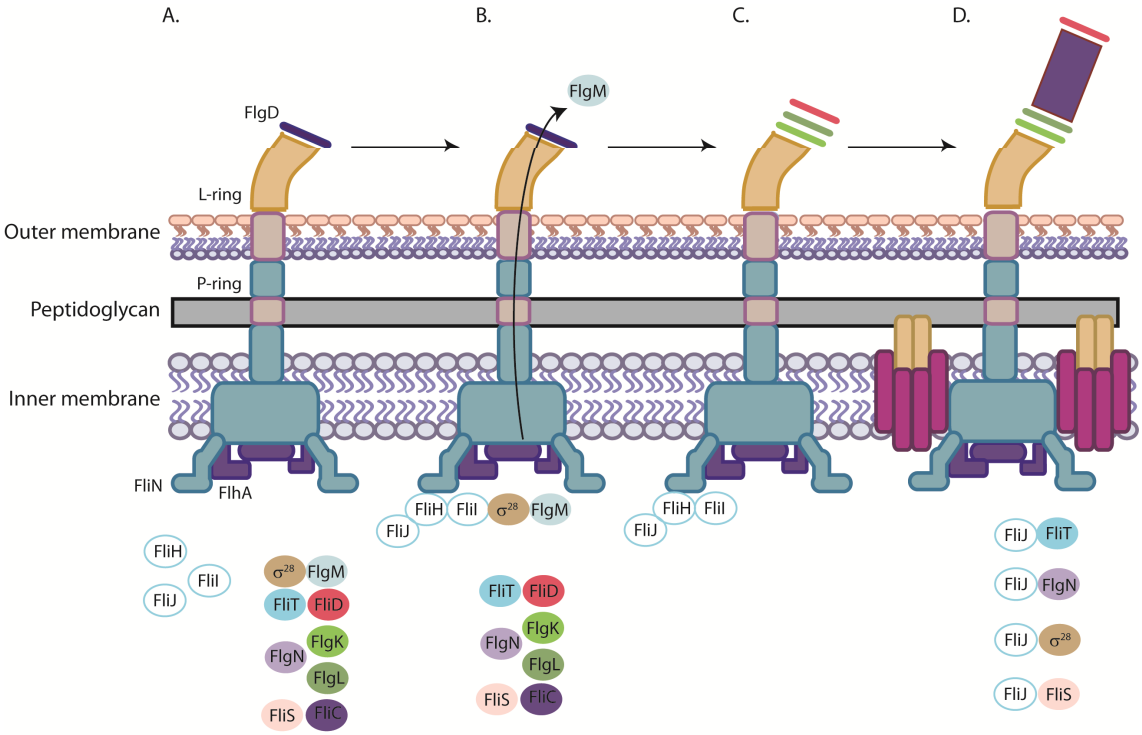

Figure 1-7 Schematic diagram of secretion of late flagellar proteins by the type III secretion system in *S.* Typhimurium. (A) Hook assembly is completed and late flagellar secretion substrate proteins are bound by their cognate chaperones in the cytoplasm. **(B)** The FliH-FliI complex binds to the chaperone-substrate pair and localises the proteins to the membrane. The complex initially binds to the C-ring via an interaction with FliN. Upon FliJ binding FliH releases FliI, allowing relief of inhibition of its ATPase activity. This causes the chaperone-substrate pair to dissociate, allowing interaction with FlhA. FlgM is secreted first, thereby allowing transcription of late class genes to occur. The black arrow through the flagellum represents secretion through the structure. **(C)** The hook cap protein, FlgD is lost and FlgK, FlgL and FliD are secreted and assembled. **(D)** FliC is also secreted and assembled. The flagellar motor is also assembled in the membrane and FliJ recycles empty chaperones. Figure adapted from Chevance and Hughes (2008).

The T3SS export machinery in *S.* Typhimurium comprises 6 integral membrane proteins: FlhA, FlhB, FliO, FliP, FliQ and FliR that form an export gate complex at the base of the MS ring, and 3 soluble proteins: FliH, FliI and FliJ (Minamino & Macnab, 1999, Minamino & MacNab, 2000b). Chaperone-substrate complexes form in the cytoplasm and reach the secretion apparatus with the aid of FliI and FliH (Thomas *et al.*, 2004) (**Figure 1-7B**). FliI is an ATPase that associates with the inner membrane and binds to chaperone-substrate complexes, resulting in their recruitment to the membrane (Auvray *et al.*, 2002). FliH binds directly to FliI to inhibit its

ATPase activity (Minamino & MacNab, 2000a, Auvray *et al.*, 2002, Gonzalez-Pedrajo *et al.*, 2002), and together these proteins initially bind to the C-ring (Gonzalez-Pedrajo *et al.*, 2006), along with an interacting chaperone-substrate pair, and subsequently dock at the membrane associated export machinery (Bange *et al.*, 2010) (**Figure 1-7**). Interactions between FliH, FliI and the FliJ protein allow a conformational change to occur that activates the ATPase activity of FliI and triggers release of the chaperone and substrate (Kazetani *et al.*, 2009). Following dissociation from FliI, the chaperone-substrate complex interacts with the C-terminal cytoplasmic domain of the integral membrane protein, FlhA, and a series of conformational changes and protein-protein interactions facilitate the entry of the substrate protein into the export gate (Minamino & MacNab, 2000b, Bange *et al.*, 2010, Morimoto *et al.*, 2010, Minamino *et al.*, 2012). Proteins are transported in an unfolded state and secretion is driven by proton-motive force (Minamino & Namba, 2008, Paul *et al.*, 2008). In *S.* Typhimurium, σ^{28} is a chaperone for FlgM (Aldridge *et al.*, 2006), FliS is a specific chaperone for flagellin (Ozin *et al.*, 2003), FliT is specific for the FliD filament cap protein, and FlgN is specific for the hook-filament junction proteins, FlgK and FlgL (Fraser *et al.*, 1999, Bennett *et al.*, 2001) (**Figure 1-7**). Export of FlgM allows free σ^{28} to activate transcription of class III promoters. FliT-FliD and FlgN-FlgK complexes have a higher binding affinity for FlhA, which may aid in their export before filament formation (Kinoshita *et al.*, 2013). FliJ, which binds to FliH and to the C-ring, docks at the export machinery and binds to and recycles empty chaperones, increasing the efficiency of export (Evans *et al.*, 2006).

Recently, it has been shown that FliS is required for Hag (flagellin) secretion in *B. subtilis* (Titz *et al.*, 2006, Mukherjee *et al.*, 2013). In addition, *in silico* analysis has suggested that YvyG of *B. subtilis* is an orthologue of the *S.* Typhimurium protein FlgN (Pallen *et al.*, 2005). However, a defined function for YvyG has not yet been determined experimentally (see Chapter 3).

1.4.4 The flagellar motor

The flagellum is powered by a rotary motor that comprises stator and rotor protein complexes, and can be driven by sodium or proton-motive force (Manson *et al.*, 1977, Chernyak *et al.*, 1983). Torque is generated by specific interactions between the rotor and stator components (Zhou *et al.*, 1998a). As for studies of flagellar secretion and assembly, most work on the flagellar motor has been carried out in Gram-negative bacterial species. The rotor is comprised of the cytoplasmic C-ring proteins, FliG, FliM and FliN, which are attached to the MS-ring (Khan *et al.*, 1992). The stator complex, which for proton-driven motors studied in *Escherichia coli* comprises a complex of four MotA proteins and two MotB proteins, forms two proton channels (Kojima & Blair, 2004). Species which use Na^+ ions to power rotation, such as *Vibrio* species and alkaliphilic bacteria, have specific stator components that respond to Na^+, but they are thought to function in a similar manner to MotA and MotB. Several bacterial species contain both proton and sodium-driven motors. Indeed, the *B. subtilis* chromosome encodes for the MotA and MotB proteins as well as their sodium-driven counterparts, MotP and MotS, which only play a role when grown in sodium-rich conditions (Ito *et al.*, 2004, Ito *et al.*, 2005). Recent work has illustrated that "hybrid fuel" motors may be assembled by bacteria that express both H^+ and Na^+ stators to allow them to acutely respond to external conditions (Sowa *et al.*, 2014).

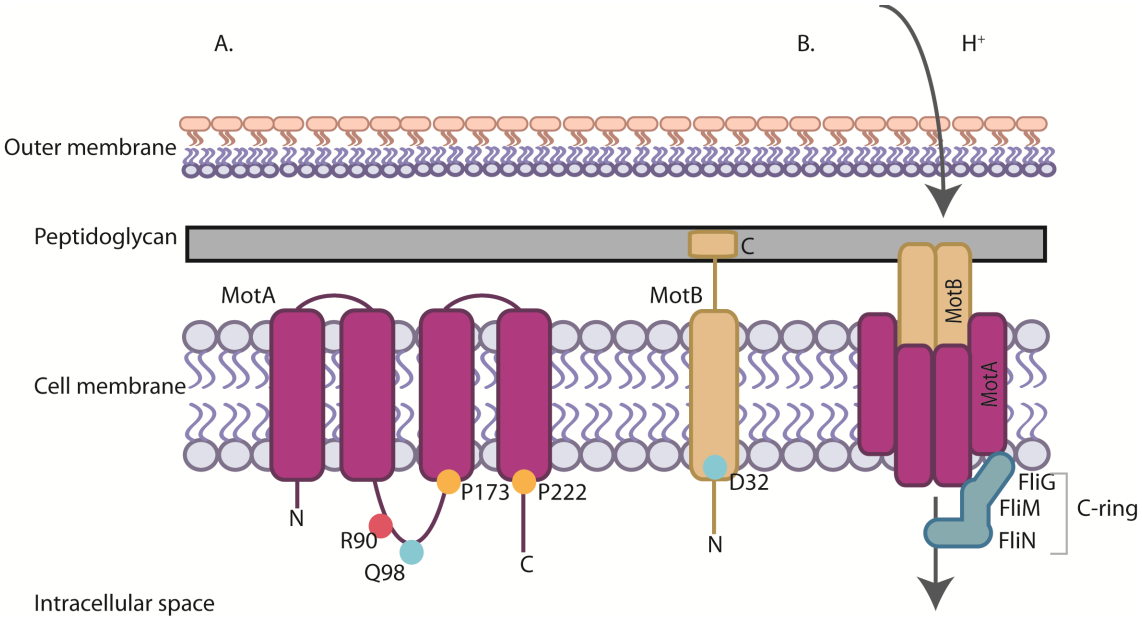

Figure 1-8 The flagellar stator proteins, MotA and MotB, and their assembly with the C-ring in *E. coli*. **(A)** Membrane organisation of MotA and MotB. Transmembrane domains, N and C-termini are indicated. Amino acids that are important for the functioning of each protein are indicated by filled circles. A red circle denotes a positively charged residue, a blue circle denotes a negatively charged residue and yellow circles denote proline residues. **(B)** Arrangement of MotA and MotB upon interacting to form a proton channel. Proton flux through the channel causes a conformational change between MotA and FliG of the C-ring to generate torque. Partially adapted from Chan *et al* (2014).

The MotA protein is comprised of four transmembrane domains and two cytoplasmic domains (Zhou *et al.*, 1995) (**Figure 1-8A**). Charged residues within the cytoplasmic domains of MotA (Arg 90 and Glu 98) enable interaction with charged residues of FliG (Arg 281, Arg 288 and Arg 289) (Zhou *et al.*, 1998a). These interactions are essential for motility. Two proline residues in MotA (Pro 173 and Pro 222) are important for torque generation (Zhou *et al.*, 1998b). MotB is comprised of a short N-terminal cytoplasmic region, a single transmembrane helix and a periplasmic region (**Figure 1-8A**). A charged aspartate residue (Asp 32 in *E. coli*) within the transmembrane domain of MotB binds to protons passing through the MotAB channel (Zhou *et al.*, 1998b). Upon protonation of this residue there is a conformational change such that the interaction of MotA with FliG is altered, allowing torque to be generated (Zhou *et al.*, 1998b, Kojima & Blair, 2001). MotB also contains a peptidoglycan binding domain which is essential for function and anchors the stator to the cell wall (De Mot & Vanderleyden, 1994). The MotA and MotB proteins are each thought to dimerise in the membrane before interacting to form

the proton channel (Braun *et al.*, 2004). The assembled channel then interacts with the rotor elements to drive torque (Zhou *et al.*, 1998a). A short 14 amino acid region of MotB acts as a plug to prevent protons from flowing through the channel prematurely (Hosking *et al.*, 2006). Deletion of this segment causes proton leakage and inhibits cell growth (Hosking *et al.*, 2006). Crucially, flagella are still assembled in the absence of *motA* or *motB.* These proteins are therefore not required for flagellar biosynthesis *per se*.

The MotA and MotB proteins are very dynamic in that they are able to rapidly diffuse in and out of functional motors. Evidence for this comes from studies where the *mot* genes were expressed from an inducible promoter, resulting in discrete, step-wise increments in speed as new stators were incorporated (Blair & Berg, 1988). Fluorescence recovery after photobleaching experiments have also shown that stators exchange quickly and that each is only associated with the motor for a short time before being replaced (Leake *et al.*, 2006). Ion availability has been shown to impact stator assembly at the motor for the sodium-driven stators in *Vibrio alginolyticus*, with Na^+ binding required for placement at the motor (Fukuoka *et al.*, 2009). However, disruption of proton-motive force did not prevent localisation of the *Salmonella* proton-driven stator at the motor (Morimoto *et al.*, 2010), although in the absence of proton-motive force, the stator elements have been shown to dissociate from the *E. coli* motor (Tipping *et al.*, 2013b). Indeed, it has been shown that assembly of the *E. coli* stator is dependent on the external load that is applied, with a higher load associated with increased numbers of stators being incorporated into the motor (Lele *et al.*, 2013, Tipping *et al.*, 2013a). This work has further suggested that it is not rotation that is needed for assembly, but rather torque (Tipping *et al.*, 2013a). Collectively, these studies highlight the complexity of stator assembly and may indicate hitherto unidentified species-specific mechanisms.

1.4.4.1 *Chemotaxis and changing direction*

Flagellar motility allows a cell to escape unfavourable environments and explore new niches. To do this, cells must be able to sense chemical gradients in their surroundings and respond by changing their direction of movement. The chemotaxis pathway mediates this process by modulating the frequency of straight runs (associated with counter-clockwise rotation) and re-orientating tumbles (clockwise rotation) (Porter *et al.*, 2011). Motile cells undertake a biased random walk, where they intersperse periods of straight swimming with brief tumbles, to allow their constant sampling of the external environment. When cells sense attractants they will not change their direction of movement, but will tumble and change their trajectory upon sensing repellents. In *B. subtilis* when cells sense attractants the membrane-spanning receptors are activated. The signal is transmitted to the CheA kinase, which autophosphorylates and is then able to transfer its phosphoryl group to the response regulator, CheY. Phosphorylated CheY (CheY~P) binds to FliM and FliN (components of the flagellar rotor C-ring) and causes counter-clockwise rotation of the motor (Bischoff & Ordal, 1991). Therefore in the absence of attractant the flagella rotate clockwise and tumble. This is in contrast to the system in *E. coli* where it is the presence of a repellent that activates the system and allows CheY~P to accumulate. CheY~P then binds to the rotor to promote clockwise rotation (Welch *et al.*, 1993, Dyer *et al.*, 2009). The pathway is regulated extensively by an array of accessory proteins, phosphatases, a methyltransferase and a methylesterase, which in combination ensure that the cell can adapt quickly and effectively (Rao *et al.*, 2008, Porter *et al.*, 2011).

1.4.5 Stopping motility: the transition to a sessile lifestyle

Further to its role in motility, the flagellum is also required for biofilm formation in several bacterial species. The attachment of bacteria to a surface is generally accepted as the first step in the formation of a biofilm, where initial adhesion is often mediated by flagella or pili

(O'Toole & Kolter, 1998, Pratt & Kolter, 1998, Watnick & Kolter, 1999). Indeed, several studies have identified flagella, or flagellar motility, as a key aspect of biofilm development or biofilm microanatomy (Vlamakis *et al.*, 2008, Serra *et al.*, 2013).

Bacteria must ensure that the transition from motility to biofilm formation can occur quickly upon a change in the external environment. For this to occur the flagellar motor must stop. To facilitate this several species use specific proteins to inhibit flagellar rotation that act by interacting with motor components. Depending on their mechanism of action, these proteins are termed as either flagellar brakes or clutches. For example, in *R. sphaeroides* rotation stops when (in the absence of a chemoattractant) CheY~P binds to the rotor (Pilizota *et al.*, 2009). This was shown to be analogous to a brake mechanism by experiments where the angle of the cell body was measured when cells were tethered by their flagella, external torque applied and the chemoattractant removed. Under such conditions the cell body was held at a specific angle, indicative of the motor locking (Pilizota *et al.*, 2009). In *E. coli* and *S.* Typhimurium the cyclic di-GMP (bis-(3'-5')-cyclic dimeric guanosine monophosphate) effector protein, YcgR, acts as a brake to inhibit motility (Boehm *et al.*, 2010, Paul *et al.*, 2010). Cyclic di-GMP is a second messenger that regulates both motility and biofilm formation in a range of bacterial species. Typically low levels of cyclic di-GMP support motility while high levels support biofilm formation. When cyclic di-GMP levels rise in *E. coli*, the YcgR protein responds by binding to components of the flagellar motor and as a result perturbs flagellar rotation (Boehm *et al.*, 2010, Paul *et al.*, 2010).

In *B. subtilis* the EpsE protein functions as a clutch to disengage the flagellar motor from the stator and inhibit motility (Blair *et al.*, 2008, Guttenplan *et al.*, 2010). EpsE is encoded by the 15 gene *epsA-O* operon (hereafter the *eps* operon) that is required for the synthesis of the exopolysaccharide (EPS) component of the biofilm matrix (section 1.5.4). EpsE is thought to function by directly interacting with a number of surface exposed residues on FliG (Blair *et al.*, 2008), as depicted in **Figure 1-9B**. EpsE has been defined as a clutch; upon tethering of cells by

their flagella the cell body rotates in line with what would be expected from movement driven by Brownian motion (Blair *et al.*, 2008). Further to its role as a flagellar clutch, EpsE also acts as a glycosyltransferase enzyme to promote biofilm formation (Blair *et al.*, 2008, Guttenplan *et al.*, 2010). These functions are genetically separable; mutations in residues required for interaction with FliG do not perturb biofilm morphology, while mutation of the glycosyltransferase active site does not interfere with the ability of EpsE to abrogate motility (Guttenplan *et al.*, 2010). The clutch activity of EpsE likely allows the cell to inhibit motility quickly and efficiently and synergises with glycosyltransferase activity, which catalyses synthesis of the exopolysaccharide, to promote biofilm formation (Blair *et al.*, 2008, Guttenplan *et al.*, 2010) (**Figure 1-9**).

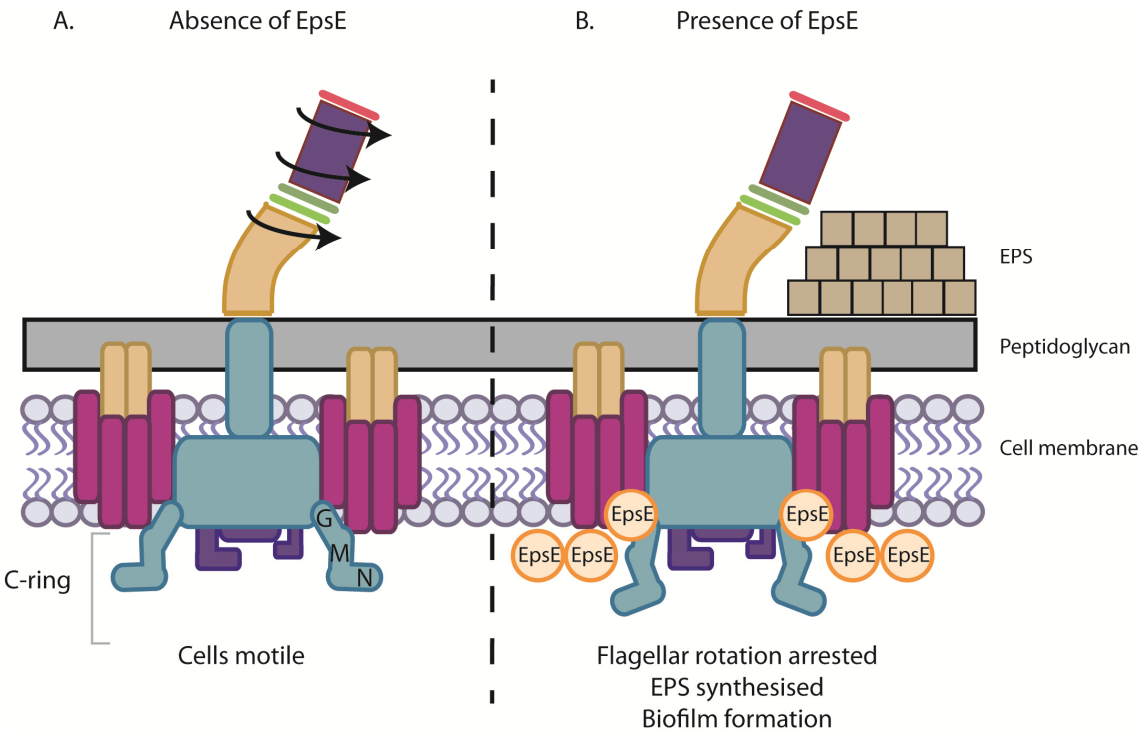

Figure 1-9 The role of the flagellar clutch protein, EpsE, in *B. subtilis*. Schematic diagram of the *B. subtilis* flagellum. **(A)** In the absence of EpsE the flagellum is free to rotate and cells are motile. **(B)** When EpsE protein is made cells are non-motile as flagellar rotation is blocked due to the interaction of EpsE with FliG. EpsE is also involved in the production of the EPS and so drives the cell towards matrix production and a sessile state. G indicates FliG, M indicates FliM and N indicates FliN; together all three comprise the C-ring. Diagram adapted from Guttenplan *et al* (2010).

Bacteria also use polysaccharides to achieve the transition from motility to permanent adhesion. In *E. coli* a second c-di-GMP effector protein BcsA indirectly inhibits flagellar rotation

(Zorraquino *et al.*, 2013). BcsA is needed for the biosynthesis of cellulose, which perturbs the flagellum by means of steric hindrance (Zorraquino *et al.*, 2013). Cellulose is a crucial component of the *E. coli* biofilm and as such this mechanism provides a means by which motility can be abrogated and biosynthesis of the matrix activated concomitantly (Zorraquino *et al.*, 2013). In *Caulobacter crescentus*, the swarmer cell requires the cooperation of its pili and flagellum for initial surface adhesion (Li *et al.*, 2012). Upon reaching a surface the flagellum arrests its rotation in a pili-dependent manner (Li *et al.*, 2012). This allows differentiation of the swarmer cell into a stalked cell that synthesises an adhesive polysaccharide holdfast, which mediates irreversible attachment to the surface. Therefore, the flagellum is crucial in biofilm formation due to its role in surface-sensing.

The flagellum can also be considered as a critical structural component of the biofilm for some bacterial species. Flagella or cells expressing flagellar genes have been identified within biofilms grown under diverse conditions and data also indicate that flagella may be important throughout the development of the biofilm (Domka *et al.*, 2007, Vlamakis *et al.*, 2008, Serra *et al.*, 2013). The *B. subtilis* biofilm shows spatial and temporal organisation with regard to gene expression, where cells expressing flagellar genes are detectable in the early stages of biofilm formation at the agar interface (Vlamakis *et al.*, 2008). When grown on an agar surface the *E. coli* biofilm also shows spatial organisation. Scanning electron microscopy studies revealed that cells at the agar surface and at the edge of the macrocolony are entangled in their flagella (Serra *et al.*, 2013). Flagellar rotation is required for this phenotype as cells that lack the flagellar stator genes show less tangling. Overall, the biofilm is less stable in the absence of rotating flagella, suggesting that flagella may provide structural integrity (Serra *et al.*, 2013). Furthermore, motile *Bacillus thuringienis* can construct dynamic channels within the biofilm that allow transport of macromolecules through the structure (Houry *et al.*, 2012). In this way Bacilli were able to penetrate biofilms constructed by a number of different bacterial species,

enabling the delivery of nutrients to promote growth, or of disinfectants to kill bacteria residing within the biofilm (Houry *et al.*, 2012).

Collectively, these studies infer that flagella are not only crucial for motility in liquid environments, but also play roles in the initial stages of surface-sensing and in the structural integrity and development of the biofilm. Retaining a motile population, or indeed a group of cells that bear immobilised flagella, within the biofilm therefore confers a number of advantages to the sessile community and may aid escape from the biofilm upon a change in external conditions.

1.5 Biofilms

It is now well recognised that for the most part bacteria live as part of complex communities of cells called biofilms. In the biofilm bacteria are held together and protected by a self-produced exopolymeric matrix, commonly comprised of polysaccharides, proteins and DNA (Flemming & Wingender, 2010). For bacteria this confers several advantages, for example biofilms can provide cells with access to nutrients and provide protection from environmental forces. Indeed, biofilms can also be harnessed in industrial settings for bioremediation purposes or for use as biocontrol agents. Of course, biofilms also present problems with regard to public health, mainly due to their roles in chronic infection, but also in industry where their formation in cooling towers, for example, can have serious implications (Liu *et al.*, 2009).

While most biofilms are polymicrobial in nature, a great deal has been learnt from the study of single-species biofilms. *Bacillus subtilis* has been used as a model organism for biofilm formation since the discovery that ancestral (or non-domesticated) strains are able to form fruiting body structures (Branda *et al.*, 2001). In the laboratory, *B. subtilis* biofilms are studied as pellicles, where communities form at the liquid-air interface, and as complex colonies, where communities form at the agar-air interface (Branda *et al.*, 2001). Given the role of *B. subtilis* as a biocontrol agent, an increasing number of studies have also focussed on the

formation of biofilms on plant roots (Chen *et al.*, 2012, Chen *et al.*, 2013). The *B. subtilis* biofilm comprises an amyloid-like protein called TasA (Branda *et al.*, 2006, Chu *et al.*, 2006), which is encoded by the *tapA-sipW-tasA* operon, an exopolysaccharide, synthesised by protein components encoded by the 15 gene *epsA-O* operon (Branda *et al.*, 2001, Branda *et al.*, 2004) and the bacterial hydrophobin, BslA, encoded by the monocistronic gene of the same name (Kobayashi, 2007). BslA is made by all cells (Hobley *et al.*, 2013), whereas TasA and the EPS are synthesised by a sub-population which shares the components amongst the entire community (Chai *et al.*, 2008, Vlamakis *et al.*, 2008). As well as matrix producing cells, several other cell types exist within the biofilm including motile cells, protease producers and spores (Vlamakis *et al.*, 2008, Marlow *et al.*, 2014a, Marlow *et al.*, 2014b). The differentiation and specialisation of cells for function is elegantly controlled by the integration of multiple signalling cascades.

The DegS-DegU two component signal transduction system and the Spo0A pathway are chiefly responsible for triggering the production of the biofilm matrix and for the differentiation of cells residing within the biofilm (Hamon & Lazazzera, 2001, Stanley & Lazazzera, 2005, Verhamme *et al.*, 2007, Chai *et al.*, 2008, Vlamakis *et al.*, 2008). Each transcription factor must be finely tuned to ensure that cells can respond to environmental stimuli to initiate biofilm formation and to promote maturation of the cells residing within the biofilm. This section will describe the main components of the *B. subtilis* biofilm and demonstrate the critical roles of Spo0A and DegS-DegU.

1.5.1 Transcriptional regulation during biofilm formation

1.5.1.1 *The Spo0A phosphorelay*

The Spo0A pathway is a multicomponent phosphorelay that promotes the expression of several genes involved in both biofilm formation and sporulation. The Spo0A pathway begins with five sensor kinases: KinA, KinB, KinC, KinD and KinE, which phosphorylate Spo0F (Burbulys *et al.*, 1991). The phosphoryl group is then passed to Spo0B before being transferred to the

terminal RR, Spo0A (Burbulys *et al.*, 1991). The level of phosphorylated Spo0A (Spo0A~P) within a cell dictates which process will be activated or inhibited (Fujita *et al.*, 2005). Low levels of Spo0A~P are associated with biofilm gene expression, whereas high levels of Spo0A~P are required for the terminal developmental process of sporulation (Fujita *et al.*, 2005). KinA and KinB have been shown to allow the accumulation of high levels of Spo0A~P and therefore likely respond to sporulation-specific signals such as nutrient limitation, whereas KinC and KinD have been associated with lower levels of Spo0A~P that are compatible with matrix synthesis (Lopez *et al.*, 2009).

Several signals that may activate KinC and KinD, and therefore regulate biofilm formation, have been identified and include: surfactin, potassium leakage, L-malic acid, glycerol, pyruvate and acetate (Lopez *et al.*, 2009, Chen *et al.*, 2012, Lundberg *et al.*, 2013, Wu *et al.*, 2013). The level of Spo0A~P can also be modulated by several auxiliary proteins and phosphatases that tune the activity of intermediate components of the phosphorelay (Veening *et al.*, 2005, Carabetta *et al.*, 2013, Parashar *et al.*, 2013).

Low levels of Spo0A~P promote biofilm formation by two means: (i) by activating transcription of *sinI* and *abbA*, which encode anti-repressors for the transcriptional repressors SinR and AbrB, respectively (Chai *et al.*, 2008, Chai *et al.*, 2009), and (ii) by directly repressing transcription of *abrB* (Strauch *et al.*, 1990) (summarised in **Figure 1-10**).

1.5.1.2 *The biofilm repressor SinR*

SinR is described as the master regulator for *B. subtilis* biofilm formation due to its ability to directly inhibit transcription of the *eps* and *tapA* operons (Kearns *et al.*, 2005, Chu *et al.*, 2008) and indirectly inhibit transcription of *bslA* (Verhamme *et al.*, 2009). SinR also represses transcription of *slrR*, which encodes a biofilm activating protein that promotes transcription of the *tapA* and *eps* operons (Chu *et al.*, 2008, Kobayashi, 2008, Murray *et al.*, 2009). Furthermore, SinR can form a complex with SlrR, resulting in its repurposing such that the

SinR:SlrR complex restricts motility. Therefore, SlrR can concomitantly repress motility and activate biofilm formation (Chai *et al.*, 2010) (discussed in section 1.4.1 and shown in **Figure 1-10**).

The repressive effect of SinR is alleviated by the anti-repressor protein, SinI, which directly binds to SinR by forming a heterodimer, leaving SinR unable to occlude target promoters and therefore allowing transcription of target genes (Bai *et al.*, 1993, Lewis *et al.*, 1998, Scott *et al.*, 1999). The assembly of the SinR:SinI complex is tight and essentially irreversible (Newman *et al.*, 2013). Interestingly, whereas *sinR* is expressed throughout the population, *sinI* is only transcribed by a small sub-population (Chai *et al.*, 2008). Only when a threshold level of SinI is reached can SinR be inhibited, allowing bimodal transcription of the *eps* and *tapA* operons (Chai *et al.*, 2008). These findings support a model where only a sub-population of cells synthesise the matrix, which can then be shared with the entire community. A second anti-repressor, SlrA, which is under the control of the YwcC TetR-like repressor protein, has also been identified (Kobayashi, 2008, Chai *et al.*, 2009, Newman & Lewis, 2013). The ability of both SinI and SlrA to act as anti-repressors for SinR might allow the integration of different signals to initiate biofilm formation (Newman & Lewis, 2013).

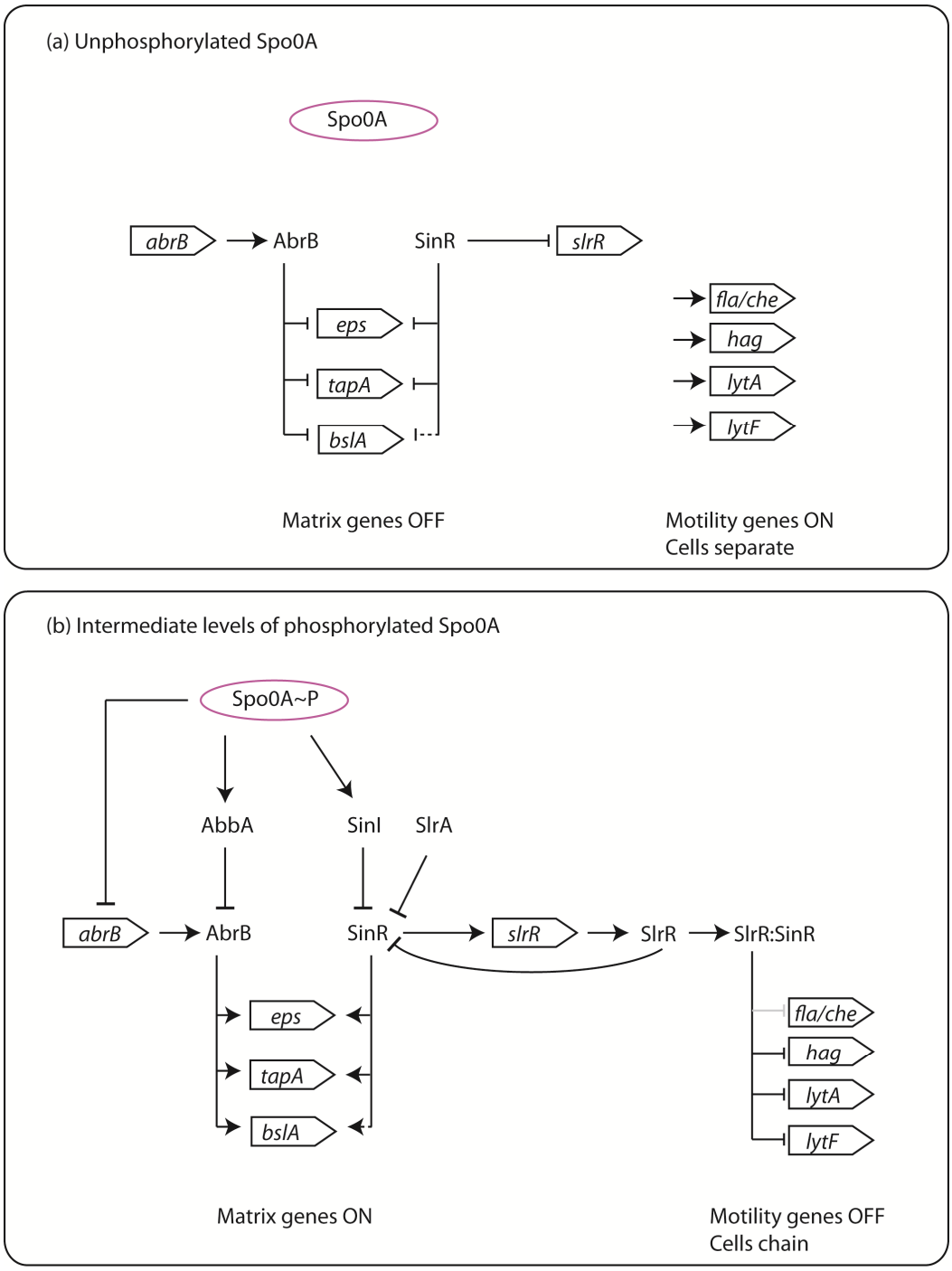

Figure 1-10 Two pathways of anti-repression govern matrix gene transcription in *B. subtilis*. The phosphorylation state of Spo0A dictates whether cells will transcribe matrix genes or not. **(A)** In conditions where Spo0A is not phosphorylated matrix genes are not transcribed due to repression by AbrB and SinR. Genes associated with flagellar motility and cell separation are transcribed. **(B)** When Spo0A is phosphorylated at an intermediate level matrix gene transcription is switched on as parallel pathways of anti-repression are evoked. Motility and autolysin genes are inhibited due to repression by the SinR:SlrR complex leading to a non-motile, cell chaining, biofilm state. Open triangles represent open reading frames, arrows indicate activation, black T-bars direct repression, a grey T-bar indicates hypothesised repression. Dashed arrows or T-bars indicate indirect activation or repression, respectively. SlrR:SinR indicates a complex between the two proteins.

1.5.1.3 *The transition state regulator AbrB*

The transition state regulator, AbrB, also functions to regulate biofilm formation. AbrB directly binds to DNA to repress transcription from promoters involved in a plethora of cellular processes, including those needed for biofilm formation: *eps*, *tapA*, *bslA* and *slrR* (Hamon *et al.*, 2004, Banse *et al.*, 2008, Chu *et al.*, 2008, Kobayashi, 2008, Chumsakul *et al.*, 2011). AbrB target genes are repressed during exponential growth, but are transcribed when AbrB levels fall upon the transition to stationary phase (Strauch *et al.*, 1990). This shift in gene transcription allows *B. subtilis* to adapt to its changing growth state. By directly inhibiting *abrB* transcription (Strauch *et al.*, 1990) and promoting the expression of the AbrB DNA mimic anti-repressor, *abbA* (Banse *et al.*, 2008, Tucker *et al.*, 2014), Spo0A~P causes a fall in AbrB protein levels and activity, culminating in increased transcription of the biofilm matrix genes (**Figure 1-10**).

1.5.2 Tyrosine phosphorylation in the biofilm

In addition to regulation at the transcriptional level, biofilm formation is also controlled post-translationally by tyrosine phosphorylation (Kiley & Stanley-Wall, 2010, Gerwig *et al.*, 2014). The *B. subtilis* chromosome encodes two tyrosine kinases, PtkA and EpsB, which are regulated by the predicted membrane-bound modulator proteins, TkmA and EpsA, respectively (Mijakovic *et al.*, 2003, Gerwig *et al.*, 2014). It is thought that upon sensing an environmental signal the modulator interacts with the cytosolic kinase to stimulate kinase activity (Grangeasse *et al.*, 2012). Proteomic approaches in combination with *in vitro* experiments have identified over 20 tyrosine phosphorylated proteins (Mijakovic *et al.*, 2003, Levine *et al.*, 2006, Macek *et al.*, 2007, Jers *et al.*, 2010), suggesting that PtkA and EpsB act in a promiscuous manner. One of these protein targets is the putative flagellar motility protein, YvyG, presenting the possibility that BY-kinases may function in two opposing behaviours: motility and biofilm

formation. The functional role of this protein and the impact of phosphorylation on its function are explored in Chapter 3.

With respect to biofilm formation, deletion of *ptkA* or *epsB* reduces the complexity of the biofilm architecture. Interestingly, deletion of *ptkA* in a ∆*epsB* strain exacerbates this defect and appears to completely ablate biofilm formation (Kiley & Stanley-Wall, 2010, Gerwig *et al.*, 2014). These experiments indicate that PtkA and EpsB cooperate to allow wild-type biofilm development. By testing the effects of mutation of amino acids required for ATP binding it was deduced that the kinase activity of PtkA is required for its activity with respect to biofilm formation (Kiley & Stanley-Wall, 2010). It is likely that PtkA and EpsB mediate their effects by phosphorylation of downstream proteins. These targets remain to be elucidated but could provide new insights into how the matrix components are regulated.

1.5.3 Cell differentiation within the biofilm.

Multiple cell types exist within the biofilm, and it has been suggested that individual cells follow a developmental programme where a motile cell becomes a matrix producer which differentiates into a spore forming cell (Vlamakis *et al.*, 2008). Indeed, all three cell types can be visualised within the biofilm at distinct locations, suggesting a level of spatial regulation (Vlamakis *et al.*, 2008). At early stages of development motile cells expressing flagella are detectable. As the biofilm matures, the number of cells transcribing genes required for biofilm matrix synthesis increases and the motile population declines. Eventually, matrix producing cells differentiate into spores. This differentiation is controlled by the Spo0A pathway (Vlamakis *et al.*, 2008, Aguilar *et al.*, 2010). Cells that are deficient for matrix production are unable to proceed to sporulation, indicating that both cell processes are tightly linked and that matrix production engenders sporulation (Vlamakis *et al.*, 2008, Aguilar *et al.*, 2010). The KinD sensor kinase is thought to act as a checkpoint protein that only allows a high level of Spo0A~P

to accumulate once the matrix has been synthesised, allowing activation of sporulation genes (Aguilar *et al.*, 2010).

DegU~P also coordinates cell differentiation (**Figure 1-11**). In addition to its role in indirectly promoting transcription of the *bslA* gene (Kobayashi, 2007, Ostrowski *et al.*, 2011), DegU also impacts the expression of other genes that are important for the biofilm. However, under conditions where DegU~P levels are high, biofilm formation is inhibited due to a lack of transcription from the *eps* and *tapA* operons (Verhamme *et al.*, 2007, Marlow *et al.*, 2014b) (**Figure 1-11**). A higher number of spores could also be detected in the presence of high levels of DegU~P. These effects were predicted to be due to increased levels of Spo0A~P in the population (Marlow *et al.*, 2014b). Thus, DegU is able to coordinate cell fate decisions depending on its phosphorylation. Furthermore, DegU~P plays an additional role in the biofilm by directly activating transcription of the exoprotease genes, *aprE* and *bpr* (Ogura *et al.*, 2001, Mader *et al.*, 2002), which are expressed heterogeneously throughout the population (Veening *et al.*, 2008) (**Figure 1-11**). Spo0A~P is also needed for expression of the exoprotease genes (due to its ability to de-repress AbrB and SinR) (Veening *et al.*, 2008), again demonstrating that interplay between the Spo0A and DegU pathways is essential for the expression of genes involved in biofilm formation. Protease producers can arise from cells that transcribe matrix genes and indeed both cell states can co-exist (Marlow *et al.*, 2014a). These findings infer that protease production may present an additional step in cell differentiation during biofilm maturation (Marlow *et al.*, 2014a).

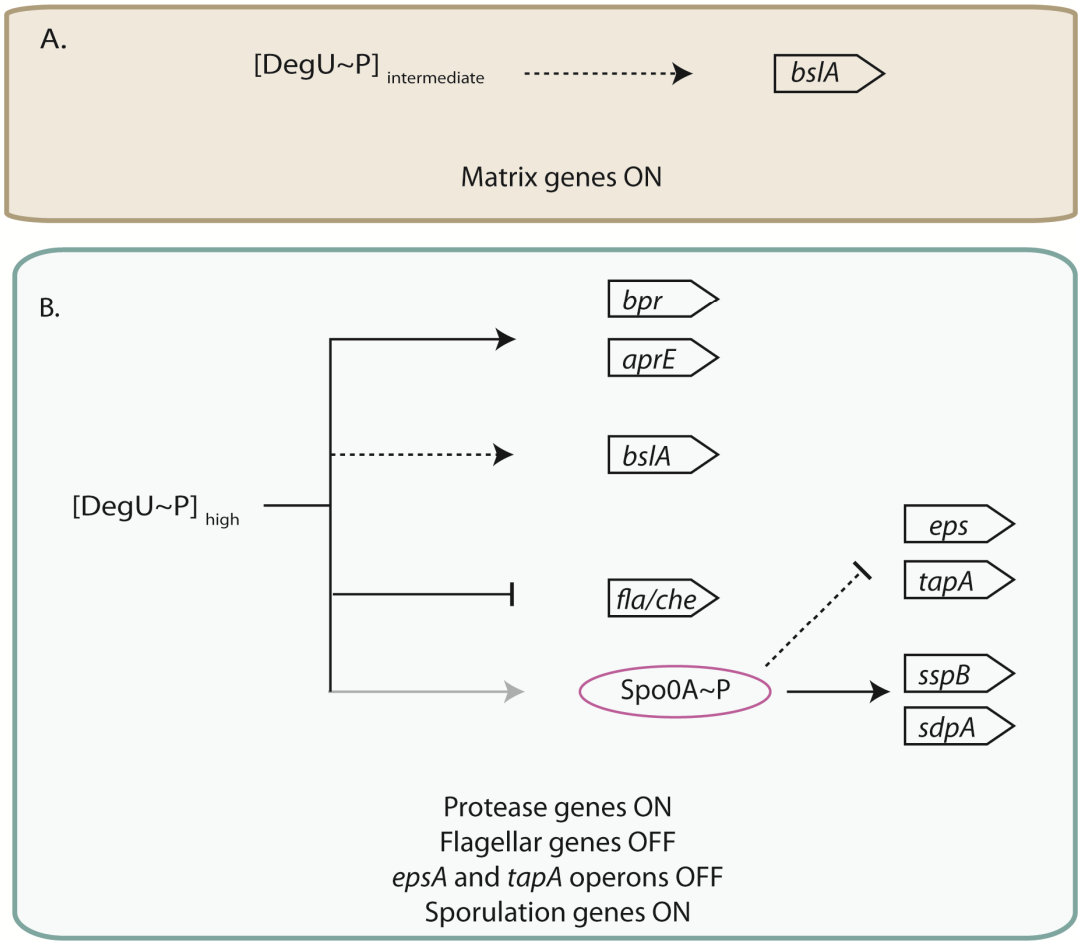

Figure 1-11 The role of the DegS-DegU two component signal transduction pathway in *B. subtilis* biofilm formation. (A) When DegU is phosphorylated at an intermediate level transcription of *bslA* is activated indirectly. **(B)** High levels of DegU~P promote cell differentiation within the biofilm. DegU~P activates protease genes, indirectly promotes *bslA* transcription, inhibits transcription of the *fla/che* operon and inhibits transcription of the *eps* and *tapA* operons while activating transcription of the sporulation genes *sspB* and *sdpA*, likely through the activity of Spo0A~P. This leads to an inhibition of motility and matrix production and drives the cell towards protease production or sporulation. Dashed arrows represent indirect activation, black arrows represent direct activation, a grey arrow indicates a hypothesised route of activation. A black T-bar denotes inhibition while a dashed T-bar indicates indirect repression. Open triangles represent open reading frames.

1.5.4 Components of the *B. subtilis* biofilm

The *B. subtilis* biofilm extracellular matrix (ECM) is comprised of three main components: the proteins BslA and TasA and the exopolysaccharide (EPS) (Branda *et al.*, 2004, Branda *et al.*, 2006, Kobayashi, 2007). All three are communal resources shared by the community (Branda *et al.*, 2006, Ostrowski *et al.*, 2011). In certain isolates of *B. subtilis*, such as the environmental strain R0-FF-1, the exopolymer γ-PGA is also a principle component of the ECM (Stanley & Lazazzera, 2005). γ–PGA is comprised of glutamic acid residues linked by γ-amino bonds. In *Bacillus anthracis* γ–PGA is anchored to the cell, is the main component of the capsule and is correlated with virulence, whereas in *B. subtilis* γ–PGA is secreted and likely enhances cell-surface interactions (Stanley & Lazazzera, 2005, Candela & Fouet, 2006). In *B. subtilis* γ–PGA production is governed by the *pgs* operon which expresses genes required for the synthesis, elongation and transport of γ–PGA, while the *pgdS* gene, under control of σ^D, encodes a γ–glutamyl-$_D$-$_L$-hydrolase that is responsible for the disassembly of γ–PGA (Candela & Fouet, 2006). The NCIB3610 strain has the genetic capability to synthesise and secrete γ-PGA but the polymer is not required for biofilm formation under laboratory conditions (Branda *et al.*, 2006). However, it is possible that γ-PGA may be important for biofilm formation by the NCIB3610 isolate in the environment, for example on plant roots.

The 15 gene *epsA-O* operon encodes the proteins required to synthesise and secrete the EPS component, and is essential for wild-type biofilm morphology (Branda *et al.*, 2001, Branda *et al.*, 2004). In addition to its role in the biofilm, the EPS can also modulate the host immune response to enteric pathogens (Jones & Knight, 2012, Jones *et al.*, 2014). As well as being under the control of the SinR and AbrB regulatory pathways, the *eps* operon is under the additional control of a cis-acting RNA element (eps-associated RNA or EAR element) that is required to allow transcription of the operon to complete (Irnov & Winkler, 2010). The chemical composition of the exopolysaccharide component of the biofilm remains to be fully

established. Monosaccharide analysis of *B. subtilis* grown in glycerol based media identified galactose, glucose and N-acetyl-galactose (GalNAc) as components of the EPS (Chai *et al.*, 2012). However, upon growth in an LB based medium the principal monosaccharide identified was mannose (Jones *et al.*, 2014). In both studies the *eps* operon was required for the synthesis of the identified EPS components. Additionally, pellicles grown in sucrose-containing media were found to contain levan as an exopolysaccharide component, but its synthesis does not appear to require the *eps* genes (Dogsa *et al.*, 2013). Therefore, it is likely that the growth conditions and media composition used are able to dictate which monosaccharides are synthesised. To date, only a subset of proteins encoded by the *eps* operon in biofilm formation has been studied: the tyrosine kinase modulator and tyrosine kinase, EpsA and EpsB (Gerwig *et al.*, 2014) (section 1.5.2), and the bi-functional glycosyltransferase/flagellar clutch, EpsE (Blair *et al.*, 2008) (section 1.4.5).

The protein component of the ECM is comprised of the amyloid-like protein, TasA and the hydrophobin, BslA (Branda *et al.*, 2006, Romero *et al.*, 2010, Hobley *et al.*, 2013). Deletion of *tasA* from the chromosome produces a smooth pellicle phenotype and cells show reduced chaining (Branda *et al.*, 2006). The contribution of TasA to the matrix is unique to that of the exopolysaccharide, as deletion of both *tasA* and the *eps* operons resulted in a pellicle phenotype distinctive from single mutations in each gene (Branda *et al.*, 2006). Moreover, co-culture of a Δ*tasA* strain with a Δ*eps* strain produced a wild-type pellicle morphology, indicating that the components of the matrix can be effectively shared by the population (Branda *et al.*, 2006). TasA is localised to the biofilm matrix, with its export from the cell dependent on the SipW peptidase. Using electron microscopy TasA was found to produce amyloid fibres, with further experiments showing that TasA could polymerise *in vitro* (Romero *et al.*, 2010). The TapA protein is a minor component of the TasA fibres, is required for their assembly and has also been suggested to stabilise the TasA protein (Romero *et al.*, 2011).

The third critical component of the *B. subtilis* biofilm is the secreted bacterial hydrophobin BslA, which acts synergistically alongside TasA and the EPS (Kobayashi, 2007, Ostrowski *et al.*, 2011, Hobley *et al.*, 2013). The *bslA* gene is transcribed by all cells in a population and is regulated by the transcription factor Rok, AbrB and DegU~P (Kobayashi, 2007, Verhamme *et al.*, 2009, Kovacs & Kuipers, 2011, Hobley *et al.*, 2013). Expression of *bslA* requires mid-levels of DegU~P and is the main target of DegU~P during biofilm formation, although its regulation by DegU~P is indirect (Kobayashi, 2007, Ostrowski *et al.*, 2011). The hydrophobic properties of the biofilm are conferred by BslA and EPS (Epstein *et al.*, 2011, Kobayashi & Iwano, 2012, Hobley *et al.*, 2013). During growth as a complex colony on an agar surface BslA forms a hydrophobic layer around the biofilm, while during pellicle formation it can be visualised as a protein raft below the cells (Kobayashi & Iwano, 2012, Hobley *et al.*, 2013). The structure of BslA has been determined and has provided much insight into the function of the protein. BslA consists of an Ig-like domain and a β-sheet rich hydrophobic "cap" (Hobley *et al.*, 2013). It is this unique hydrophobic cap that is essential for the surface-activity of BslA and that primarily confers the hydrophobic properties of the biofilm (Hobley *et al.*, 2013).

1.6 Overall aims of this study

Flagellar motility and biofilm formation are two apparently opposing bacterial processes. However, both must be intimately linked to allow for the transition from a motile lifestyle to a sessile state to occur. This requires the cell to couple changes in the external environment to changes in physiology. As such, it is reasonable to suggest that signal transduction pathways will play a prominent role in the switch between motility and biofilm formation.

When this study began a novel role for tyrosine phosphorylation in biofilm formation had only just been recognised (Kiley & Stanley-Wall, 2010). At the same time, a putative motility protein called YvyG was shown to be phosphorylated by both *in vitro* experiments and global proteomic studies (Macek *et al.*, 2007, Jers *et al.*, 2010). In combination these studies

suggested that tyrosine phosphorylation, in particular of YvyG, may play a role in both flagellar motility and biofilm formation. The work presented in Chapter 3 aimed to define the function of YvyG and to ascertain if phosphorylation of YvyG impacted its function. These data have been published (see Appendix B).

The *B. subtilis* DegS-DegU two component signal transduction system has been known to play a role in both motility and biofilm formation for several years. However, recent work from our group suggested that DegS-DegU may "sense" the completion status of the flagellum. Preliminary data from the Kearns group supported this hypothesis (Hsueh *et al.*, 2011). The experiments presented in Chapter 4 aimed to investigate the role of the flagellum in the activation of the DegS-DegU two component signal transduction system. This study has been published (see Appendix B).

2
Materials and methods

2.1 Oligonucleotides, plasmids and bacterial strains

Escherichia coli strain MC1061 [*F'lacIQ lacZM15 Tn10* (*tet*)] was used for the routine construction and maintenance of plasmids. DNA constructs were initially integrated into *Bacillus subtilis* chromosome using the genetically competent laboratory strains, 168 and JH642. Genetic information was transferred from the laboratory strain to the ancestral strain, NCIB3610, via phage-mediated transduction. All experiments concerning the physiology and molecular biology of *Bacillus subtilis* were performed with the NCIB3610 isolate. Strains, plasmids and primers used in this work are listed in Tables 2-1, 2-2 and 2-3, respectively.

2.2 Media and reagents

2.2.1 Growth media and growth conditions

Escherichia coli and *Bacillus subtilis* strains were routinely grown in Luria-Bertani media (LB) (10 g L^{-1} NaCl, 5 g L^{-1} yeast extract, 10 g L^{-1} tryptone) or on LB plates supplemented with 1.5 % agar (hereafter LB agar) at 37 °C unless otherwise stated. To ensure uniform growth of *B. subtilis* cells prior to either stocking of strains or growth in liquid LB over time, strains were grown as lawns. Briefly, a single colony of the required strain was inoculated into and mixed with 100 µl of LB. The cell suspension was then spread on an LB plate and incubated at either 30 °C (for stocking strains) or 20 °C (when cells were to be diluted into LB and grown in liquid) overnight.

B. subtilis cells to be used for phage-mediated transduction were grown in TY media (LB supplemented with 10 mM $MgSO_4$ and 1 µM $MnSO_4$). Transduced cells were selected on TY media solidified with 1.5 % agar, supplemented with 10 mM sodium citrate and appropriate antibiotic(s).

2.2.2 Media supplements

Media for growth and selection of *E. coli* strains were supplemented with the following antibiotics as required: ampicillin (100 μg ml^{-1}) and kanamycin (50 μg ml^{-1}). Media for growth and selection of *B. subtilis* strains were supplemented with the following antibiotics as required: kanamycin (10 μg ml^{-1}), chloramphenicol (5 μg ml^{-1}), spectinomycin (100 μg ml^{-1}), erythromycin (1 μg ml^{-1}) and lincomycin (25 μg ml^{-1}). To check for integration of constructs at the non-essential *amyE* locus on the *B. subtilis* chromosome, colonies were patched onto LB plates containing 1 % soluble starch.

2.2.3 Reagents

All chemicals used in this study were of analytical grade and were purchased from Sigma Aldrich, Merck, Melford Laboratories Ltd, VWR and Fisher Scientific. Buffers and solutions used in this study are presented in Table 2-4.

Table 2-1 *Bacillus subtilis* strains used in this study.

Strain	Relevant Genotype[a]	Source[b]
NCIB 3610	Prototroph	B.G.S.C.
168	*trpC2*	B.G.S.C.
JH642	*trpC2 pheA1*	(Perego & Hoch, 1988)
RL2420	PY79 pIC333	(Kearns *et al.*, 2004)
DS1677	3610 Δ*hag*	Kind gift D. Kearns
BAL1151	JH642 *pgdS::pBL141(cml)*	(Stanley & Lazazzera, 2005)
BAL1811	JH642 *pgsB::spc*	(Stanley & Lazazzera, 2005)
NRS1136	JH642 *degS::cml*	(Verhamme *et al.*, 2007)
NRS1314	3610 *degU::pBL204 (cml)*	(Verhamme *et al.*, 2007)
NRS1325	3610 *degU::pBL204 (cml) amyE::*$P_{hy\text{-}spank}$*-degU32-hy-lacI (spc)*	(Verhamme *et al.*, 2007)
NRS1467	3610 *amyE::Phy-spank-gfp-lacI (spc)*	(Verhamme *et al.*, 2007)
NRS1534	168 *thrC::*P_{aprE}*-lacZ (mls)*	(Verhamme *et al.*, 2007)
NRS1561	3610 *thrC::*P_{aprE}*-lacZ (mls)*	(Verhamme *et al.*, 2007)
NRS2051	JH642 *thrC::*P_{bslA}*-lacZ (mls)*	(Verhamme *et al.*, 2009)
NRS2052	3610 *thrC::*P_{bslA}*-lacZ (mls)*	(Verhamme *et al.*, 2009)
NRS2544	3610 *ΔptkA*	(Kiley & Stanley-Wall, 2010)
NRS3070	168 *sacA::*P_{hag}*-yfp (kan)*	Constructed by N.R. Stanley-Wall pNW546 →168
NRS3076	3610 *sacA::*P_{hag}*-yfp (kan)*	Constructed by N.R. Stanley-Wall SPP1 NRS3070 →3610
NRS3256	168 *amyE::*$P_{hy\text{-}spank}$*-flgN-lacI (spc)*	pNW380 →3610
NRS3347	3610 *pgdS::cml*	SPP1 BAL1151→NCIB3610
NRS3348	3610 Δ*motB* + *pgdS::cml*	SPP1 BAL1151→NRS3494
NRS3374	168 *degU::*pNW703 *(kan)*	Constructed by N.R. Stanley-Wall pNW703 →168
NRS3433	3610 *pgsB::spc*	SPP1 BAL1811 →NCIB3610
NRS3434	3610 Δ*motB* + *pgsB::spc*	SPP1 BAL1811 →NRS3494
NRS3494	3610 Δ*motB*	Constructed by A. Ostrowski pNW654 → NCIB3610
NRS3514	168 *amyE::*$P_{hy\text{-}spank}$*-motB-lacI (spc)*	Constructed by A. Ostrowski pNW680 → 168
NRS3570	3610 *ΔflgN*	Constructed by T. Kiley pNW399 →3610
NRS3571	3610 *flgN* $Y^{49}A$	Constructed by T. Kiley pNW801 →3610
NRS3578	3610 *ΔflgN+ amyE::*$P_{hy\text{-}spank}$*-flgN-lacI (spc)*	Constructed by T. Kiley SPP1 NRS3256 →NRS3570
NRS3708	3610 *ΔflgN + sacA::*P_{hag}*-yfp (kan)*	SPP1 NRS3070 →NRS3570
NRS3713	3610 *ΔflgN + sacA::*P_{hag}*-yfp (kan) + amyE::*$P_{hy\text{-}spank}$*-flgN-lacI (spc)*	SPP1 NRS3256 →NRS3708
NRS3718	3610 *ΔflgN hag* $T^{209}C$	pNW1010 →NRS3570

Strain	Relevant Genotype[a]	Source[b]
NRS3719	3610 *hag* $T^{209}C$	pNW1010 →3610
NRS3724	3610 *flgN* $Y^{49}E$	pNW1012 →3610
NRS3735	168 *amyE::*$P_{hy\text{-}spank}$*-flgK-flgL-lacI (spc)*	pNW1017 →168
NRS3744	3610 Δ*motAB*	pNW1021→ NCIB3610
NRS3764	3610 *pgsB::spc* + *degU::kan*	SPP1 NRS3374 →NRS3433
NRS3769	168 *amyE::*$P_{hy\text{-}spank}$*-motAB-lacI (spc)*	pNW1029 → 168
NRS3770	3610 *pgsB::spc* + *degU::kan amyE::*$P_{hy\text{-}spank}$*-degU32-hy-lacI (cml)*	SPP1 NRS1268 →NRS3764
NRS3775	3610 Δ*motB* + $P_{hy\text{-}spank}$*-motB-lacI (spc)*	Constructed by A. Ostrowski SPP1 NRS3514 →NRS3494
NRS3866	168 $P_{hy\text{-}spank}$*-motB*$D^{24}A$*-lacI (spc)*	pNW1051→168
NRS3867	3610 Δ*motB* + *amyE::*$P_{hy\text{-}spank}$*-motB*$D^{24}A$*-lacI (spc)*	SPP1 NRS3866 →NRS3494
NRS3868	3610 *amyE*:: $P_{hy\text{-}spank}$*-motB*$D^{24}A$*-lacI (spc)*	SPP1 NRS3866 →NCIB3610
NRS3870	3610 Δ*motB* + *amyE::*$P_{hy\text{-}spank}$*-motB*-$D^{24}A$*-lacI (spc) thrC::*P_{aprE}*-lacZ (mls)*	SPP1 NRS1534 →NRS3867
NRS4017	3610 *flgN* $R^{60}E$	pNW1028 →3610
NRS4041	3610 Δ*fliD*	pNW1034 →3610
NRS4042	3610 Δ*flgE*	pNW1036 →3610
NRS4043	3610 *ΔflgN + amyE::*$P_{hy\text{-}spank}$*-flgK-flgL-lacI (spc)*	SPP1 NRS3735 →NRS3570
NRS4060	3610 *ΔflgK-flgL*	pNW1042 →3610
NRS4063	3610 *flgN* $R^{60}A$	pNW1027 →3610
NRS4064	3610 *ΔflgK-flgL + amyE::*$P_{hy\text{-}spank}$*-flgK-flgL-lacI (spc)*	SPP1 3735 → NRS4060
NRS4071	3610 *ΔflgK-flgL+ sacA::*P_{hag}*-yfp (kan)*	pNW1042 →NRS4060
NRS4078	3610 *ΔflgK-flgL + sacA::*P_{hag}*-yfp (kan) + amyE::*$P_{hy\text{-}spank}$*-flgK-flgL-lacI (spc)*	SPP1 3735 → NRS4078
NRS4083	168 *amyE::*$P_{hy\text{-}spank}$*-epsE-lacI (spc)*	pNW1044 →168
NRS4084	168 *thrC::*P_{degU}*-lacZ (mls)*	pNW1045 →168
NRS4085	3610 *amyE::*$P_{hy\text{-}spank}$*-epsE-lacI (spc)*	SPP1 NRS4083 →NCIB3610
NRS4093	3610 Δ*motAB* + *thrC::*P_{aprE}*-lacZ (mls)*	SPP1 NRS1534 →NRS3744
NRS4345	3610 *amyE::*$P_{hy\text{-}spank}$*-epsE-lacI (spc) thrC::*P_{aprE}*-lacZ (mls)*	SPP1 NRS1534 →NRS4085
NRS4351	3610 *thrC::*P_{degU}*-lacZ (mls)*	SPP1 NRS4084 →NCIB3610
NRS4353	3610 Δ*motB* + *thrC::*P_{degU}*-lacZ (mls)*	SPP1 NRS4084 →NRS3494
NRS4354	3610 Δ*motAB thrC::*P_{degU}*-lacZ (mls)*	SPP1 NRS4084 →NRS3744
NRS4373	3610 *degU::cml* + *thrC::*P_{degU}*-lacZ (mls)*	SPP1 NRS4084 →NRS1314
NRS4374	3610 *amyE::*$P_{hy\text{-}spank}$*-epsE-lacI (spc) thrC::*P_{degU}*-lacZ (mls)*	SPP1 NRS4084 →NRS4085
NRS4385	168 *amyE::*$P_{hy\text{-}spank}$*-epsE*-$K^{106}E$*-lacI (spc)*	pNW1048 →168
NRS4386	168 *amyE::*$P_{hy\text{-}spank}$*-epsE*-$D^{94}A$*-lacI (spc)*	pNW1047 →168
NRS4387	3610 Δ*motAB* + *amyE::*$P_{hy\text{-}spank}$*-motAB-lacI (spc)*	SPP1 NRS3469 →NRS3744

Strain	Relevant Genotype[a]	Source[b]
NRS4388	3610 *amyE::*$P_{hy\text{-}spank}$*-epsE*-D^{94}A-*lacI (spc)*	SPP1 NRS4386 →NCIB3610
NRS4389	3610 *amyE::*$P_{hy\text{-}spank}$*-epsE*-K^{106}E-*lacI (spc)*	SPP1 NRS4385 →NCIB3610
NRS4392	3610 *amyE::*$P_{hy\text{-}spank}$*-epsE*-D^{94}A-*lacI (spc)* + *thrC::*P_{degU}*-lacZ (mls)*	SPP1 NRS4084 →NRS4388
NRS4393	3610 *amyE::*$P_{hy\text{-}spank}$*-epsE*-D^{94}A-*lacI (spc)* + *thrC::*P_{aprE}*-lacZ (mls)*	SPP1 NRS1534 →NRS4388
NRS4394	3610 *amyE::*$P_{hy\text{-}spank}$*-epsE*-K106E-*lacI (spc)* + *thrC::*P_{degU}*-lacZ (mls)*	SPP1 NRS4084 →NRS4389
NRS4395	3610 *amyE::*$P_{hy\text{-}spank}$*-epsE*-K106E-*lacI (spc)* *thrC::*P_{aprE}*-lacZ (mls)*	SPP1 NRS1534 →NRS4389
NRS4396	3610 Δ*motB* + *thrC::*P_{degU}*-lacZ (mls)* *amyE::*$P_{hy\text{-}spank}$*-motB-lacI (spc)*	SPP1 NRS3514 →NRS4353
NRS4397	3610 Δ*motB* + *thrC::*P_{degU}*-lacZ (mls)* *amyE::*$P_{hy\text{-}spank}$*-motB-*D^{24}*A-lacI (spc)*	SPP1 NRS3866 →NRS4353
NRS4398	3610 Δ*motB* + *degS::cml*	SPP1 NRS1136 →NRS3494
NRS4399	3610 *amyE::*$P_{hy\text{-}spank}$*-epsE-lacI (spc)* + *thrC::*P_{aprE}*-lacZ (mls)*	SPP1 NRS1136 →NRS4345
NRS4400	3610 *amyE::*$P_{hy\text{-}spank}$*-epsE*-D^{94}A-*lacI (spc)* + *thrC::*P_{aprE}*-lacZ (mls)*	SPP1 NRS1136 →NRS4393
NRS4401	3610 *amyE::*$P_{hy\text{-}spank}$*-epsE*-K106E-*lacI (spc)* + *thrC::*P_{degU}*-lacZ (mls)*	SPP1 NRS1136 →NRS4395
NRS4405	3610 *amyE::*$P_{hy\text{-}spank}$*-epsE-lacI (spc)* + *thrC::*P_{bslA}*-lacZ (mls)*	SPP1 NRS2051→NRS4345
NRS4406	3610 *amyE::*$P_{hy\text{-}spank}$*-epsE*-D^{94}A-*lacI (spc)* + *thrC::*P_{bslA}*-lacZ (mls)*	SPP1 NRS2051→NRS4393
NRS4407	3610 *amyE::*$P_{hy\text{-}spank}$*-epsE*-K106E-*lacI (spc)* + *thrC::*P_{bslA}*-lacZ (mls)*	SPP1 NRS2051→NRS4395
NRS4419	D*degSU::spc* + *amyE::*P_{spac}*-degU32hy-lacI (cml)*	SPP1 NRS1268→NRS1499
NRS4794	168 *amyE::*P_{hag}*-lacZ* translational *(cml)*	pNW1069 →168
NRS4795	3610 *amyE::*P_{hag}*-lacZ* translational *(cml)*	SPP1 NRS4794 →3610
NRS4796	3610 *ΔflgN + amyE::*P_{hag}*-lacZ* translational *(cml)*	SPP1 NRS4794 →NRS3570
NRS4798	3610 *ΔflgE + amyE::*P_{hag}*-lacZ* translational *(cml)*	SPP1 NRS4794 →NRS4042
NRS4799	3610 *ΔflgKL + amyE::*P_{hag}*-lacZ* translational *(cml)*	SPP1 NRS4794 →NRS4060
NRS4801	3610 *His-flgK*	pNW1063 →NRS3610
NRS4812	3610 *flgK-His*	pNW1065 →NRS3610

[a] Drug resistance cassettes are indicated as follows: *kan*, kanamycin resistance; *mls*, lincomycin/erythromycin resistance; *cml*, chloramphenicol resistance and *spc*, spectinomycin resistance.
[b] The direction of strain construction is indicated with DNA or phage (SPP1) (→) recipient strain.
B.G.S.C. is the *Bacillus* genetic stock centre.

Table 2-2 Plasmids used in this study.

Plasmid	Relevant Genotype [a]	Source
pDR111	*amyE* integration plasmid *(spc)*	(Britton *et al.*, 2002)
pMAD	In-frame markerless deletion plasmid	(Arnaud *et al.*, 2004)
pDG1663	*lacZ* reporter fusion plasmid, *thrC* integration	(Guerout-Fleury *et al.*, 1996)
pUC19	Cloning plasmid	(Vieira & Messing, 1982)
pBL204	pUC19 containing a *cmI* resistance cassette	(Stanley & Lazazzera, 2005)
pBL132	cmI^R cassette in pUC19	(Stanley *et al.*, 2003)
pBL165	*amyE* integration plasmid $P_{spac\text{-}hy}$-*gfp mut2*	(Stanley *et al.*, 2003)
pDR183	*lacA integration plasmid*	(Stanley *et al.*, 2003)
pKM3a	*yfp amyE* integration plasmid	Kind gift D. Rudner
pSAC-KAN	*sacA* integration plasmid	(Middleton & Hofmeister, 2004)
pEHISGFPTEV	Protein expression vector	(Liu & Naismith, 2009)
pDG1728	*lacZ* reporter fusion plasmid, *amyE* integration	(Guerout-Fleury *et al.*, 1996)
pNW380	*flgN* coding region in pDR111	Constructed by T. Kiley
pNW398	*flgN* in pUC19	Constructed by T. Kiley
pNW399	Δ*flgN* in pMAD	Constructed by T. Kiley
pNW546	P_{hag}-*yfp* in pSAC-KAN	Constructed by N.R. Stanley-Wall
pNW651	Region upstream of *motB* in pUC19	Constructed by A. Ostrowski
pNW652	Region downstream of *motB* in pUC19	Constructed by A. Ostrowski
pNW653	Δ*motB* in pUC19	Constructed by A. Ostrowski
pNW654	Δ*motB* in pMAD	Constructed by A. Ostrowski
pNW680	*motB* in pDR111	This study
pNW700a	P_{hag} in pKM3a	Constructed by A. Ostrowski
pNW701	pUC19 containing internal region of *degU*	(Marlow *et al.*, 2014b)
pNW703	Kanamycin resistance cassette and an internal region of *degU* coding region	(Marlow *et al.*, 2014b)
pNW800	*flgN* $Y^{49}A$ in pUC19	Constructed by T. Kiley
pNW801	*flgN* $Y^{49}A$ in pMAD	Constructed by T. Kiley
pNW1006	*hag* in pBL132	This study
pNW1009	*hag* $T^{209}C$ in pBL132	This study
pNW1010	*hag* $T^{209}C$ in pMAD	This study
pNW1011	*flgN* $Y^{49}E$ in pUC19	This study
pNW1012	*flgN* $Y^{49}E$ in pMAD	This study
pNW1017	*flgK-flgL* coding region in pDR111	This study
pNW1019	Δ*motAB* in pUC19	This study

pNW1021	Δ*motAB* in pMAD	This study
pNW1025	*flgN* $R^{60}A$ in pUC19	This study
pNW1026	*flgN* $R^{60}E$ in pUC19	This study
pNW1027	*flgN* $R^{60}A$ in pMAD	This study
pNW1028	*flgN* $R^{60}E$ in pMAD	This study
pNW1029	*motAB* in pDR111	This study
pNW1034	Δ*fliD* in pMAD	This study
pNW1036	Δ*flgE* in pMAD	This study
pNW1042	Δ*flgK-flgL* in pMAD	This study
pNW1044	*epsE* in pDR111	This study
pNW1045	P_{degU} in pDG1663	This study
pNW1047	*epsE* $D^{94}A$ in pDR111	This study
pNW1048	*epsE* $K^{106}E$ in pDR111	This study
pNW1058	*motB* in pUC19	This study
pNW1059	*motB* $D^{24}A$ in pUC19	This study
pNW1060	*motB* $D^{24}A$ in pDR111	This study
pNW1063	His-flgK in pMAD	This study
pNW1065	*flgK*-His in pMAD	This study
pNW1069	P_{hag} in pDG1728	This study

[a] Drug resistance cassettes are indicated as follows: *cml*, chloramphenicol resistance; *kan*, kanamycin resistance, and *spc*, spectinomycin resistance.

Table 2-3 Primers used in this study.

Primer	Target	Sequence [a]	Position [b]
DEN5	*rRNA*	TCACGRCACGAGCTGACGAC	Internal 16S rRNA
DEN7	*rRNA*	ACTCCTACGGGAGGCAGC	Internal 16S rRNA
NSW12	*amyE*	CGATTCAAAACCTCTTTACTG	+13 → +33
NSW13	*amyE*	GCTTAAGCCCGAGTC	1965 → +1951
NSW207	*sacA*	CATGACCAGGAGCTTCGT	10 → 28
NSW208	*sacA*	CGCACTGGCTGTTACTTC	1398→ 1381
NSW404	*degU*	GCATGAATTCGGCCTGATTCCAACTTTAA	-487→-468
NSW405	*degU*	GCATAAGCTTCTGATGGTCGTCGATAAT	+26→+39
NSW652	*hag*	CCGGAATTCGAATTGACGCCCCAAAGCATATTG	-272→-248
NSW653	*hag*	GGCAAGCTTCTGAATATGTTGTTAAGGCACGTC	-38→-14
NSW872	*pDR111*	AGGTGTGGCATAATGTGTGTAATTGTGAGC	$P_{hy\text{-}spank}$
NSW873	*pDR111*	TGAACAATCACGAAACAATAATTGGTACGTACG	*lacI* region
NSW817	*pMAD*	CGTCATCTACCTGCCTGGA	Preceding MCS
NSW818	*pMAD*	CGTAGGATCGATCCGACCT	Following MCS
NSW860	*sigA*	GCATCCATGGCTGATAAACAAACCCACG	+5→+22
NSW861	*sigA*	GCATCTCGAGTTATTCAAGGAAATCTTTC	+1095→+1116
NSW874	*motB*	GTACGGATCCATTGAGGATGTAGATGATGC	-480→-460
NSW875	*motB*	ATGCTCTAGAGTACAGCACAATAAACAATGC	+77→+98
NSW876	*motB*	GCATTCTAGAGTTGAAGTTCTCATTTTGCCG	+700→+721
NSW877	*motB*	GCATGTCGACCATCGCTCCAACATACACC	+1500→+1519
NSW936	*flgN*	GCATGGATCCATC AGG CAG AAG CGA ATT CAG	-588→-558
NSW937	*flgN*	GCATTCTAGATAATTGCCTTCGCTGACATGG	+92→+123
NSW938	*flgN*	GCATTCTAGACTGTTTGAT TCAAAAGCTTAGCAGAAAG	+453→+490
NSW939	*flgN*	GCATGTCGACCAACACAGTTGTATTTAGCT TGC	+1104→1137
NSW940	*flgN*	GCAT GTCGACAAGCAATAAAAAAGGAGAAAGCCC	-34→-1
NSW941	*flgN*	GCATGCATGCAATTCCTTTCTGCTAAGCTTTTGAATC	+469→+505
NSW942	*flgN*	ACAAAAGAGCAAAAA**GCA**ATTCAAGCAATCACG	+130→+162
NSW943	*flgN*	CGTGATTGCTTGAAT**TGC**TTTTTGCTCTTTTGT	+130→+162
NSW965	*motA*	GCTAGGATCCTTGAGGATGAAATGACCGATCTGC	-479→-156
NSW966	*motA*	GCTATCAGACGAAGTTTTATCCATAGTTTTCACC	-10→+16
NSW969	*motA*	GCTAGTCGACAGACAAGCTAGTAAAAAAGGATTTGG	-66→-9
NSW1011	*motB*	TCATGGCTCGTTCCTTACGCCG**C**CATCCTTACTCTTCTC CTG	+49→+91
NSW1012	*motB*	CAGGAGAAGAGTAAGGATG**G**CGGCGTAAGGAACGA GCCATGA	+49→+91
NSW1312	*motB*	GCATAAGCTTGCAGAACAAGGAGAGGCGCAAAAT	-30→-6
NSW1313	*motB*	GCATGCATGCCTATTTTTCATTTGTTTCCGCTGCGC	+880→+904
NSW1401	*hag*	GCATGGATCCGCGATCTCTGAAAA	+39→+52
NSW1402	*hag*	CGATGGATCCTCGTTTATATCGACTAAGT	+1103→1121

NSW1403	*hag*	GCAGATAATGCAGCAGAT**TG**TGCTGATATCGGTTTCG ATGC	+107→+147
NSW1404	*hag*	GCATCGAAACCGATATCAGC**AC**AATCTGCTGCATTAT CTGC	+107→+147
NSW1436	*flgN*	ACAAAAGAGCAAAAA**GAA**ATTCAAGCAATCACG	+130→+162
NSW1437	*flgN*	CGTGATTGCTTGAAT**TTC**TTTTTGCTCTTTTGT	+130→+162
NSW1438	*yvyF*	GAAAACCGGCAATCAACTTTGAGC	+133→+156
NSW1439	*yvyF*	CTCGTGGTTCAAATGATCCATTTGATC	+322→+348
NSW1440	*flgM*	ATCAATCAATTTGGAACACAATCCG	+7→+31
NSW1441	*flgM*	GTCTACTTTGTATGACCCGTTTTC	+196→+216
NSW1442	*flgN*	GCC GGC AAAACAAAAGAGCTTTCT	+97→+120
NSW1443	*flgN*	TCCGAGAACTTGAGAAAGAGATTCGTA	+283→+309
NSW1444	*flgK*	TACAACAAATCAGGCGGGAATGCA	+682→+705
NSW1445	*flgK*	AGACTCTATAAACCCTAAAAGGGATCCC	+894→+921
NSW1446	*flgL*	CAAGCGATTGGCGTAGAGGTAAA	+322→+344
NSW1447	*flgL*	GCCTCCAAAAGCTGACTTTGGATC	+526→+549
NSW1459	*yviE*	CTGCTCATTTTTAAGCTGGC	+64→+83
NSW1462	*flgK*	GCATGTCGACTTAGCAGAAAGGAATT	-22→-6
NSW1463	*flgL*	GACTGCATGCTTACTTTAAAAAGTCAAT	+880→+897
NSW1464	*flgN*	CAGACAGAAGATGAC**GCG**ATCAAAACAACTTCG	+163→+193
NSW1465	*flgN*	CGAAGTTGTTTTGAT**CGC**GTCATCTTCTGTCTG	+163→+193
NSW1466	*flgN*	CAGACAGAAGATGAC**GAG**ATCAAAACAACTTCG	+163→+193
NSW1467	*flgN*	CGAAGTTGTTTTGAT**CTC**GTCATCTTCTGTCTG	+163→+193
NSW1474	*pgsB*	CTGTTAACCCAGATTATCAAATC	+331→+354
NSW1475	*pgsB*	CTGCGCGGCAGTTCATGATGAT	+889→+868
NSW1486	*flgE*	CCAAGATCCGTTTACAACG	-214→-195
NSW1487	*flgE*	CCGGTTCCTCTATTCCTT	+1028→+1046
NSW1490	*fliD*	CTGAAATGGTGGGGGAA	-225→-208
NSW1491	*fliD*	GCTGATAGGCTGTATATGG	+1534→1553
NSW1600	*flgK*	GACAAGAGACGCGCTGCAAT	-237→-217
NSW1601	*flgL*	CTGCTCCATTTTTAAGCTGGC	+1007→1028
NSW1602	*epsE*	AGGAGGTCGACAAAGGAGAAAAGCGTATGAACTCAG	-16→-1
NSW1603	*epsE*	CTCCTGCATGCTGGCTGCTATTCATGCTTGACAAG	+820→+843
NSW1604	*pgdS*	GGAGACGGCCAAATGGTTC	+370→+388
NSW1605	*pgdS*	GCAAGCCGGTCAGAAAAAG	+778→+796
NSW1608	*epsE*	CGCACGTCAG**G**CCGGAGATGACCTTTCG	+270→+298
NSW1609	*epsE*	CGAAAGGTCATCTCCG**G**CCTGACGTGCG	+270→+298
NSW1610	*epsE*	CCGCGCCGTCTGGAA**G**AGCAGGTCGCGTTTTTA	+301→+333
NSW1611	*epsE*	TAAAAACGCGACCTTCT**C**TTCCAGACGGCGCGG	+301→+333
NSW1670	*hag*	GCAGGATCCAAGAAGAACAAATCATTCTTTTTGAAAG	-766→-727
NSW1671	*hag*	TTGCGGTCGACGTGGTTAATTCTCATTGTTTTGTTCCT	-12→+25

[a] Underlined sequences indicate endonuclease restriction cut sites. Bold sequences represent base pairs mutated by site-directed mutagenesis.
[b] Position of primer is indicated in relation to the translational start site (noted as +1) of the named gene.

Table 2-4 Buffers and solutions used in this study.

Buffer/Solution	Components
Bacillus subtilis competent cells and their transformation	
SpC	1 X T-Base 1 mM MgSO4 0.5 % Glucose
SpII	1 X T-Base 35 mM MgSO4 0.5 % Glucose 0.1 % Yeast extract 0.01 % Casamino Acids 40 µg ml^{-1} Tryptophan
Wash buffer	1 X T-Base 1 mM Mg_2SO_4
Transformation buffer	1 X T-Base 2 mM EDTA
Molecular Biology	
TAE	40 mM Tris 1.142 % Acetate 1 mM EDTA
DNA loading dye	0.025 % (w/v) Bromophenol Blue 30 % (v/v) Glycerol
B. subtilis cell lysis buffer	100 mM NaCl 50 mM EDTA
Separation of proteins by SDS-PAGE gel electrophoresis	
SDS-PAGE loading dye	60 mM Tris-HCl (pH 8.8) 4% (v/v) β-Mercaptoethanol 2% (w/v) SDS 10% Glycerol 0.04% Bromophenol Blue
SDS Running Buffer	25 mM Tris 192 mM Glycine 0.1 % (v/v) SDS
Coomassie protein stain	50 % (v/v) Ethanol 7.5 % (v/v) Acetic acid 0.1 % (w/v) Coomassie brilliant blue
De-staining solution	50 % (v/v) Methanol 10 % (v/v) Acetic acid
Western Blotting	
Western transfer buffer	25 mM Tris 192 mM Glycine 0.2% (v/v) Tween-20 20% (v/v) Methanol
Tris Buffered Saline Tween (TBST)	20 mM Tris-HCl, pH 8.0

	150 mM NaCl 0.05 % Tween
ECL 1	100 mM Tris –HCl (pH 8.5) 2.5 mM Luminol in DMSO 0.4 mM p-Coumaric acid in DMSO
ECL 2	100 mM Tris-HCl (pH 8.5) 0.064% (v/v) H_2O_2
Enrichment of hook-basal bodies	
Sucrose Solution	0.5 M Sucrose 0.15 M Tris, pH not adjusted
Alkaline Solution	100 mM KCl-KOH 500 mM Sucrose 0.1 % Triton X-100 pH 11
TET Buffer	10 mM Tris-HCl, pH 8 5 mM EDTA 0.1% Triton X-100 pH 8
Acidic Solution	50 mM Glycine-Hydrochloride 0.1 % Triton X-100 pH 3
Miscellaneous	
T-Base	40 mM Tris-acetate 1 mM EDTA
GTE	15 mM $(NH_4)2SO_4$ 80 mM K_2HPO_4 44 mM KH_2PO_4 3.4 mM Sodium citrate
Z buffer	60 mM $Na_2HPO_4.7H_2O$ 40 mM $NaH_2PO_4.H_2O$ 10 mM KCl 1 mM $MgSO_4.7H_2O$ pH 7 50 mM β-mercaptoethanol*
Phosphate buffered saline (PBS)	0.137M NaCl 2.68 mM KCl 10.436 mM $NaHPO_4$ 1.764 mM KH_2PO_4

* β-mercaptoethanol was added immediately before use.

2.3 General molecular biology methods

2.3.1 Molecular cloning techniques

2.3.1.1 *Generation of competent* E. coli *cells and transformation*

Genetically competent *E. coli* cells were prepared using calcium chloride solution, as previously described (Sambrook & Russell, 2001). *E. coli* strain MC1061 [*F'lacIQ lacZM15 Tn10* (*tet*)] was grown overnight in LB media and diluted 1 in 1000 into 200 ml of fresh LB media. The cells were grown with aeration at 37 °C until the OD_{600} reached approximately 0.3 and chilled on ice for 30 min. Cells were harvested by centrifugation at 3000 x *g* for 10 min and the resulting cell pellet re-suspended in 20 ml sterile, ice-cold 0.1 M $CaCl_2$. The cells were harvested as previously and re-suspended in 8 ml sterile, ice-cold 0.1 M $CaCl_2$. Cells were incubated on ice at 4 °C overnight. Glycerol was added to a final concentration of 10 % and cells aliquoted and stored at -80 °C until required for use.

2.3.1.2 *Plasmid purification from* E. coli *cells*

Plasmids were purified from *E. coli* MC1061 cells using the QIAprep Spin Miniprep Kit (Qiagen), according to manufacturer's instructions. This method is based on the alkaline lysis procedure (Birnboim & Doly, 1979). Briefly, 1.5 ml of cells from an overnight culture grown in appropriate antibiotics was harvested by centrifugation at 17,000 x *g*. Cells were re-suspended in lysis buffer containing RNAse A and the cell debris removed by centrifugation at 17,000 x *g* for 10 min. The supernatant, in a high salt buffer, was applied to a column containing a silica membrane to allow binding of DNA. Endonucleases were removed by a brief wash step with a buffer containing guanidine hydrochloride and isopropanol. Salts were removed by a subsequent wash step with a low salt buffer and the DNA eluted in 30-50 µl ddH_2O.

2.3.1.3 *Polymerase chain reaction (PCR)*

During cloning procedures DNA was amplified with Phusion Polymerase (Finnzymes) according to manufacturer's instructions. Reactions were prepared as follows: 200 µM dNTPs, 0.5 µM forward primer, 0.5 µM reverse primer, 1 U Phusion Polymerase, 0.5 µl template DNA with

reaction buffer diluted to 1X in a total volume of 50 µl. PCR reactions were performed in a thermocycler and cycling conditions consisted of denaturation, annealing and extension steps and are presented in Table 2-5.

Table 2-5 PCR cycling conditions for Phusion polymerase

PCR Step	Temperature	Time (min:sec)
Initial denaturation	98 °C	00:30
Denaturation Annealing Extension	98 °C 3 °C above T_m of primers 72 °C	00:15 00:15 00:15 per kb DNA
Number of cycles	25-35	
Final extension	72 °C	10:00

For the purposes of screening potential clones, screening for integration of DNA into the *B. subtilis* chromosome and RT-PCR analyses, DNA was amplified using Taq polymerase (Qiagen), according to manufacturer's instructions. Reactions were prepared as follows: 200 µM dNTPs, 0.5 µM forward primer, 0.5 µM reverse primer, 1.5 mM $MgCl_2$, 5 U Taq polymerase with Q solution and PCR buffer both diluted to 1X with ddH_2O in a total volume of 20 µl. Typically 1 µl of gDNA or 2.5 µl of cDNA was used as a template. For colony PCR with *E. coli*, a single colony was inoculated into the reaction as a template. For colony PCR with *B. subtilis*, a single colony was inoculated into 25 µl of ddH_2O, vortexed and incubated at -80°C for 10 min, before incubation at 95 °C for 5 min. Debris was collected by centrifugation at 17,000 x *g* for 5 min and 7.6 µl of the supernatant containing DNA used as template in a PCR reaction. PCR reactions were performed in a thermocycler and cycling conditions consisted of denaturation, annealing and extension steps and are presented in Table 2-6.

Table 2-6 PCR cycling conditions for Taq polymerase

PCR Step	Temperature	Time (min:sec)
Initial denaturation	95 °C	02:00
Denaturation Annealing Extension	95 °C 5 °C below T_m of primers 72 °C	00:30 00:30 01:00 per kb DNA
Number of cycles	25-35	
Final extension	72 °C	10:00

2.3.1.4 *Site-directed mutagenesis*

Single amino acid substitutions were introduced to plasmids using PCR site-directed mutagenesis with KOD Hotstart polymerase (Novagen), with the appropriate primer pairs from Table 2-3. Reactions were prepared as follows: 0.2 mM dNTPs, 1 mM $MgSO_4$, 0.3 µM forward primer, 0.3 µM reverse primer, 60 ng template, 1 U KOD Hotstart polymerase in PCR buffer diluted to 1X in a total volume of 50 µl. Cycling conditions consisted of denaturation, annealing and extension steps and are presented in Table 2-7.

Table 2-7 PCR cycling conditions for site-directed mutagenesis with KOD Hotstart polymerase.

PCR Step	Temperature	Time (min:sec)
Initial denaturation	95 °C	02:00
Denaturation Annealing Extension	95 °C 55 °C 68 °C	00:30 00:30 05:30
Number of cycles	18	
Final extension	68 °C	05:00

The PCR reaction was then incubated with 1 µl DpnI to digest methylated (i.e. original template) DNA. 1.5 µl of the reaction was transformed into 200 µl of competent *E. coli* cells (section 2.3.1.10).

2.3.1.5 *Restriction digest*

To excise inserts or PCR products for cloning restriction digests were designed. Each reaction typically consisted of 1 µl of each appropriate restriction enzyme (NEB), 5 µl of the recommended buffer, with 40 µl of purified PCR product or 15 µl of plasmid DNA with ddH_2O in a total volume of 50 µl. For restriction digests performed to confirm the size and

authenticity of cloned vectors a reaction volume of 20 µl was used. Reactions were incubated at the recommended temperature for each enzyme (most commonly 37 °C) for 3-5 hours.

2.3.1.6 *Phosphatase treatment of digested plasmids*

When required digested plasmids for use in downstream cloning applications were dephosphorylated using calf intestinal alkaline phosphatase (CIP) (NEB). This enzyme removes the 5' phosphate group from DNA and therefore prevents re-ligation of the plasmid. 40 µl of digested plasmid which had been purified (section 2.3.1.8) was incubated with 0.5 U of CIP and NEB buffer 3 diluted to 1X in a total reaction volume of 50 µl. The enzyme was heat-inactivated by incubation at 65 °C for 15 min and purified as detailed in section 2.3.1.8.

2.3.1.7 *Agarose gel electrophoresis*

Following all enzymatic reactions, DNA products ranging from 100 bp to 10kb in size were resolved by agarose gel electrophoresis using horizontal agarose gels. Briefly, DNA samples were prepared with 6X loading dye (Table 2-4) and 1-2 % agarose gels were prepared in 1X TAE buffer (Table 2-4). 3 µl of a DNA ladder (NEB) was loaded alongside the samples. Electrophoresis was performed in 1X TAE buffer under constant voltage at 100-120 V for 30-60 minutes and gels post-stained in ethidium bromide. Alternatively, 1-2 % agarose gels were prepared in 1X TAE buffer with 1X GelRed nucleic acid stain (Biotium) in place of post-staining with ethidium bromide. Nucleic acids were either imaged by exposure to UV light, or images were documented using the Gel-Doc XR system (BioRad).

2.3.1.8 *Purification of DNA after enzymatic reactions*

Purification of DNA after separation by agarose gel electrophoresis was performed using the QIAQuick Gel Extraction Kit (Qiagen), according to manufacturer's instructions. Essentially, gel slices were dissolved in QG buffer (a high salt buffer containing guanidine thiocyanate and a pH indicator) at 50 °C with agitation and the resulting sample applied to a column containing a silica membrane to allow binding of DNA. Contaminating salts were washed through the column using a buffer containing ethanol and DNA eluted from the column in ddH_2O. A similar procedure was also followed to purify enzymatic reactions when gel electrophoresis was not

required, where 500 µl of buffer QG was added to the reaction and the protocol followed as outlined.

2.3.1.9 *Ligation*

Purified DNA fragments were ligated into linearised plasmids using T4 DNA ligase (NEB). Reactions were typically prepared as follows: 400 U T4 DNA ligase, 1X T4 DNA ligase buffer with varying volumes of plasmid and insert (typically a 1:2 ratio), with ddH_2O in a total reaction volume of 20 µl. Reactions were incubated at room temperature for a minimum of 1 hour and the entire reaction transformed into competent *E. coli* cells (section 2.3.1.10).

2.3.1.10 *Transformation into competent* E. coli

Prior to transformation competent MC1061 *E. coli* cells were thawed on ice. 1 µl of plasmid DNA or 20 µl of a ligation reaction was incubated with 200 µl of cells, incubated on ice for 30 min and heat-shocked for 90 s at 42 °C. For plasmids carrying ampicillin resistance cassettes, cells were chilled on ice for 5 min and colonies selected on LB agar supplemented with ampicillin and incubation at 37 °C overnight. For plasmids carrying kanamycin resistance cassettes, cells were incubated with 1 ml LB and incubated with aeration for 1 hour at 37 °C. Cells were recovered by centrifugation at 17,000 x *g* and colonies selected on LB agar supplemented with kanamycin and incubation at 37 °C overnight.

2.3.1.11 *DNA sequencing*

DNA sequencing was performed to ensure that any plasmids cloned were free from unwanted mutations. Additionally, gDNA harvested from *B. subtilis* strains was sequenced to ensure that any mutations introduced to the chromosome were as expected. All sequencing was performed by the DNA sequencing service at the University of Dundee (http://www.dnaseq.co.uk). Raw nucleotide sequencing data was analysed using Chromas Lite v2.01 (Technelysium Pty Ltd). BLAST was used to compare query nucleotide sequences to databases of known sequences (http://blast.ncbi.nlm.nih.gov/Blast.cgi). CLC Main Workbench was used for generating and annotating electronic sequences.

2.3.2 Generation of *Bacillus subtilis* strains

2.3.2.1 *Extraction of genomic DNA from* B. subtilis

Genomic DNA was harvested from *B. subtilis* using phenol/chloroform extraction (Sambrook & Russell, 2001). 3 ml of *B. subtilis* cells grown to exponential phase were harvested by centrifugation at 17,000 x *g* and the pellet resuspended in 500 µl lysis buffer (Table 2-4). Digestion of the peptidoglycan layer was aided by addition of lysozyme to the cell lysate at a final concentration of 1.2 mg ml^{-1} and the reaction incubated at 37 °C for 30 min or until lysis had occurred. The detergent sarkosyl was added to a final concentration of 0.76 % (w/v) and mixed on ice until the lysate had cleared, indicating disruption of cell membranes. Proteins in the lysate were precipitated by addition of a 1:1 ratio of Tris-buffered phenol, pH 6.6 (Fisher Scientific): a 24:1 mixture of chloroform/isoamyl alcohol. The reaction was subsequently vortexed and the organic layer separated from the aqueous layer by centrifugation at 17,000 x *g* for 5 min. The aqueous layer was removed and combined with 500 µl of the 1:1 mix of Tris-buffered Phenol: chloroform/isoamyl alcohol (24:1). The reaction was vortexed and centrifuged as before. The aqueous layer was then removed and combined with 200 µl 3 M sodium acetate and 100 % ethanol was to a total volume of 1.5 ml. The DNA was precipitated by gentle inversion and then centrifuged at 17,000 x *g* for 3 min. The DNA pellet was washed with 70 % ethanol and dried before resuspension in 200 µl ddH_2O and storage at -20°C.

2.3.2.2 *Generation of competent* B. subtilis *168 cells*

To generate derivatives of the NCIB3610 strain, DNA constructs were initially integrated into *Bacillus subtilis* chromosome using the genetically competent laboratory strains, 168 and JH642 (both strains are genetically competent due to loss of the pBS32 plasmid that is found in NCIB3610 (Konkol *et al.*, 2013)). To prepare genetically competent cells the following protocol was used. An overnight lawn of cells (see 2.2.1) grown to exponential phase was collected using wash buffer (Table 2-4), the OD_{600} measured and the cell suspension diluted to OD_{600} = 0.01 in SpC medium (Table 2-4). Cells were incubated with aeration at 37 °C for 5 hours. Cells

were subsequently diluted 1:10 into SPII medium (Table 2-4) and incubated with aeration at 37 °C for 90 min. Cells were harvested by centrifugation at 3000 x *g* and concentrated 10-fold by re-suspension in SPII supernatant. Sterile glycerol was added to a final concentration of 10 % and cells were aliquoted and stored at -80 °C.

2.3.2.3 *Transformation of competent* B. subtilis *cells*

Transformation of either competent *B. subtilis* 168 cells or competent *B. subtilis* JH642 cells with genetic material was carried out based on the method described by Harwood and Cutting (Harwood & Cutting, 1990). Briefly, 100 µl of competent cells, 100 µl of transformation buffer (Table 2-4) and 5-30 µl of DNA were incubated with aeration at 37 °C for 20 min. Transformed cells were selected on LB agar containing the appropriate antibiotic(s) and incubated at 37 °C overnight.

2.3.2.4 *Phage-mediated transduction of* B. subtilis *NCIB3610*

SPP1 phage-mediated transduction was used to transfer genetic information from *B. subtilis* 168 and JH462 strains to the NCIB3610 ancestral strain (Yasbin & Young, 1974). To generate phage carrying genetic information from the appropriate laboratory ("donor") strain, the donor strain was grown in TY medium to stationary phase. 0.2 ml of donor cells were infected with 1 µl of SPP1 phage and incubated at 37 °C for 15 min. The cells were then mixed with 3 ml of TY top agar (molten TY medium supplemented with 0.7 % (w/v) agar). This mixture was then plated on to TY medium solidified with 1.5 % (w/v) agar and incubated for approximately 3 h at 37 °C or at room temperature overnight, until plaques were visible. The top agar layer containing lysed cells and phage was harvested from the plate, vortexed and cells separated from phage by centrifugation at 3000 x *g* for 10 min. The supernatant containing phage was passed through a 0.22 µm syringe filter and stored at 4 °C until required.

To transduce the donor phage into the recipient strain, 900 µl of cells from the recipient strain grown to stationary phase and 60 µl of phage generated from the donor strain were incubated under static conditions for 30 min at 37 °C. Cells were harvested by centrifugation at 3000 x *g*

for 10 min, resuspended in 100 µl of the supernatant and selected on TY medium solidified with 1.5 % agar supplemented with 10 mM sodium citrate and appropriate antibiotic(s) and incubated at 37 °C overnight. Resulting colonies were streak-purified on LB plates containing the appropriate antibiotic(s).

2.3.2.5 *Screening for double crossovers at the* amyE *and* thrC *loci*

To ensure that the genetic region of interest was stably integrated into the chromosome, potential clones were screened by PCR. To check for integration at the *amyE* (which encodes the amylase enzymes) locus, colonies were replica patched onto LB plates containing 1 % soluble starch. Candidates which were unable to digest starch, as assessed by staining with Lugol solution, were taken forward for further screening by colony PCR (section 2.3.1.3) with primers NSW12 and NSW13 (Table 2-3). Genomic DNA was extracted (section 2.3.2.1) from candidate mutants and integration at *amyE* was again checked for by PCR with primers NSW12 and NSW13. Integration at the *thrC* locus was checked by antibiotic resistance. The pDG1663 plasmid (Table 2-2) carries an MLS resistance cassette between the *thrC* integration sites and a spectinomycin resistance cassette elsewhere on the plasmid. Therefore, if a genetic region has integrated as a double crossover, the strain is resistant to MLS but sensitive to spectinomycin.

2.3.2.6 *Generation of in-frame marker-less deletion strains by allelic replacement*

In-frame markerless deletion strains of *B. subtilis* were constructed using an allelic exchange method similar to that detailed by Arnaud *et al*. (Arnaud *et al.*, 2004) using the pMAD plasmid. Essentially, upstream and downstream flanking regions of the target gene were amplified by PCR (primers detailed in Table 2-3) or generated by gene synthesis (sequences detailed in Appendix A) and cloned into a pUC-derived cloning plasmid using restriction sites engineered into the gene fragment to generate an in-frame deletion construct. The region of DNA required to construct the mutation was then excised from the pUC plasmid by restriction digest and ligated into the pMAD vector. pMAD derived plasmids (Table 2-2) were transformed into competent cells generated from the *B. subtilis* 168 strain (section 2.3.2.3) with incubation at 30°C for 1 hour. At 30 °C the temperature sensitive origin of replication present on the pMAD

plasmid allows replication of the plasmid. Colonies were selected for resistance to erythromycin and lincomycin, antibiotics which belong to the macrolide-lincosaminde-streptogramin (MLS) group. Several transformants were collected and used to inoculate 5 ml TY media supplemented with MLS antibiotics. The culture was grown with aeration at 30 °C for 16 h and used to generate phage containing the pMAD derived plasmid, which was transduced into the *B. subtilis* NCIB3610 ancestral strain (section 2.3.2.4) by incubation of the phage with target cells for 1 h at 30 °C. Transduced colonies were selected by growth on TY media solidified with 1.5 % agar supplemented with 10 mM sodium citrate and MLS antibiotics and incubated for 48 h at 30 °C. Next, a pool of NCIB3610 transduced colonies were collected and used to inoculate LB medium supplemented with MLS. The culture was grown at 37 °C for 16 hours with agitation. Growth of the cells at 37 °C prevents initiation from the temperature sensitive origin of replication, and so in the presence of antibiotics maintenance of the resistance cassette requires integration of the plasmid into the chromosome. Post-integration colonies were selected for on LB plates supplemented with MLS. Subsequently, a pool of MLS-resistant colonies were collected and inoculated into 5 ml of LB medium. The culture was grown under static conditions for 16 h at 30 °C, after which the culture was incubated with aeration for at 30 °C for 4 h. Growth at 30 °C in the absence of antibiotics permits eviction of the plasmid from the chromosome. Colonies were selected by growth on LB agar and then replica patched on LB agar and LB agar supplemented with MLS. MLS-sensitive colonies were taken forward for further screening by colony PCR. Genomic DNA was extracted (section 2.3.2.1) from candidate mutants and the absence of the target gene checked by PCR with the following primer pairs: *flgE* (NSW1486 and NSW1487), *fliD* (NSW1490 and NSW1491), *flgK-flgL* (NSW1600 and NSW1601) and *motA-motB* (NSW969 and NSW1313).

2.3.2.7 *Introduction of site-specific mutations to the chromosome by allelic replacement*

To construct site-specific mutations to the *B. subtilis* chromosome the allelic exchange method with the pMAD plasmid outlined in section 2.3.2.6 was used. Firstly, pMAD-derived plasmids

were generated as follows. The target gene was amplified by PCR (primers detailed in Table 2-3) and cloned into a pUC-based plasmid using restriction enzymes engineered into the primers. Site-directed mutagenesis was used to introduce specific point mutations to the target gene (section 2.3.1.4) and the resulting plasmid sequenced (section 2.3.1.11) to ensure the correct mutation was introduced. The target gene was excised from the pUC plasmid and ligated into pMAD using restriction sites engineered into the original primers. The pMAD-derived plasmid was introduced to the *B. subtilis* chromosome (section 2.3.2.6) and candidate mutants checked by sequencing of genomic DNA.

For the generation of strains NRS4801 and NRS4812 gene fragments comprising the *flgK* gene fused to DNA encoding the Histidine epitope tag were constructed by gene synthesis and cloned into a pUC-derived plasmid (GenScript, sequences detailed in Appendix A). The target gene was then excised from the pUC plasmid using engineered restriction sites and ligated into pMAD.

2.4 RNA methods

2.4.1 Extraction of RNA

RNA extraction was performed with the RiboPure Bacteria RNA Isolation kit (Ambion, Life Technologies). This method combines disruption of bacterial cell walls with phenol extraction and glass-fibre filter purification of RNA and is outlined in the following sections.

2.4.1.1 *Cell disruption and initial DNA purification*

Briefly, cells for RNA isolation were harvested from an overnight lawn plate and diluted into 25 ml of LB medium at an OD_{600} of 0.01. Cultures were grown to mid-exponential phase and 2 aliquots of cells, each 5 ml in volume, were harvested by centrifugation at 3000 x *g* for 10 min. Each cell pellet was re-suspended in 350 µl of the phenol-based RNAwiz reagent and mixed by vortexing. The sample was then applied to a tube containing Zirconia beads and vortexed horizontally (vortex adaptor Ambion, Life Technologies) to disrupt cells. Centrifugation for 5 min at 17,000 x *g* at 4 °C allowed separation of the lysate from the Zirconia beads. Both lysates for each strain were combined at this point and chloroform added and the lysate centrifuged. This resulted in the formation of an upper aqueous phase of RNA, a semi-solid interphase of DNA and an organic phase containing proteins and other cell debris.

2.4.1.2 *Final RNA purification*

The aqueous phase obtained in section 2.4.1.1 was combined with 0.5 ml volumes of ethanol to precipitate residual DNA, applied to a glass-fibre filter cartridge and centrifuged. The filter was washed with a wash solution provided by the manufacturer that contains guanidium thiocyanate to denature proteins. The filter was washed twice more with a second wash buffer containing ethanol to remove contaminants and eluted in a low ionic strength solution.

2.4.1.3 *DNAse treatment*

To remove trace gDNA from the eluted RNA, the RNA sample was diluted 1 in 2 with RNAse-free water, 1 U of DNAse I in a 1X solution of DNAse buffer (Ambion, Life Technologies) and

incubated at 37 °C for 30 min. The reaction was inactivated with DNAse inactivation reagent and the RNA harvested by centrifugation at 17,000 x *g* for 2 min at 4 °C.

2.4.2 Reverse transcription of RNA to cDNA

RNA samples were reverse-transcribed to cDNA for use in PCR reactions. Reactions were prepared as follows: 0.5 µM random hexameric primers, 200 µM dNTPs, 300 ng of RNA and RNAse-free water were combined in a total reaction volume of 12 µl and incubated at 65 °C for 5 min and 4 °C for 1 min. The following components were then added to each sample: First strand buffer to a final concentration of 1X, 5 mM DTT, 4 U RNAse out (Life Technologies), 200 U Superscript III (Life Technologies) and RNAse-free water to a total volume of 20 µl. Control reactions without Superscript III were also prepared. Reactions were incubated at 25 °C for 5 min, 50 °C for 60 min and 70 °C for 15 min. Samples were then treated with 1 µl of RNAse H (NEB) by incubation at 37 °C for 20 min and diluted in RNAse-free water to a total volume of 100 µl for use in later PCR reactions.

To assess transcription of *pgsB*, *pgdS* or rRNA the following primer pairs were used: DEN5 and DEN7 (rRNA), NSW1474 and NSW1475 (*pgsB*) and NSW1604 and NSW1605 (*pgdS*). Primer sequences are detailed in Table 2-3.

To validate the co-transcription of the *flgM*, *flgN*, *flgK* and *flgL* genes a cDNA was synthesised using the *yviE* gene-specific primer NSW1459 instead of random hexamers. To amplify internal gene products, the following primer pairs were used: NSW1446 and NSW1447 (*flgL*), NSW1444 and NSW1445 (*flgK*), NSW1442 and NSW1443 (*flgN*) and NSW1440 and NSW1441 (*flgM*). Primer sequences are detailed in Table 2-3.

2.5 Bacteriology techniques

2.5.1 Swimming and swarming assays

Swimming and swarming analyses were conducted using low-salt LB medium (5 g L^{-1} NaCl, 5 g L^{-1} yeast extract, 10 g L^{-1} tryptone) supplemented with 0.3 % (w/v) or 0.7 % (w/v) agar (Invitrogen, Life Technologies), respectively (Kearns & Losick, 2003). For swarming assays, cultures were grown in 3 ml LB medium at 37 °C, with aeration, until the OD_{600} was approximately 1.0. The cultures were then concentrated to an OD_{600} of 10, and 10 µl of culture was spotted onto the swarming media. Swarming media plates were freshly prepared. Plates were poured under laminar flow, and dried for 20 min prior to spotting. The inoculated plates were then dried for a further 10 min and incubated at 37 °C. For swimming assays, media was prepared prior to use and the swimming plates were not dried. Cell material was picked using a sterile pipette tip and inoculated into the centre of a swimming plate. Plates were incubated at 37 °C. The extent of swimming or swarming noted at defined time-points; the area of the plate where cells were initially spotted was marked and migration measured in millimetres over time. Plates were photographed at the end of each experiment.

2.5.2 Assaying γ-poly-$_{D\text{-}L}$-glutamic acid production

2.5.2.1 *γ-poly-$_{D\text{-}L}$-glutamic acid colony morphology*

γ-poly-$_{D\text{-}L}$-glutamic acid (γ-PGA) production was first assessed by a mucoid colony morphology as compared to that of the wild-type strain, NCIB3610. Cells were streaked to single colonies on an LB agar plate and incubated at 37 °C overnight prior to photography the following morning.

2.5.2.2 *γ-poly-$_{D\text{-}L}$-glutamic acid extraction from liquid media*

The method used for γ-PGA isolation was adapted from Stanley and Lazazzera (2005). Briefly, cells were grown overnight on LB lawn plates, collected in 5 ml LB and diluted to an OD_{600} of 0.01. Cells were grown to stationary phase in 25 ml LB and harvested by centrifugation. A total

of 10 ml of the culture supernatant was retained and the cell pellet suspended in 2.5 ml of 0.14 mM NaCl. The cells were again harvested by centrifugation and the supernatant from the wash added to the previously collected supernatant. The combined supernatants were brought to pH 2.0 with concentrated sulphuric acid and incubated at 4 °C overnight. To precipitate γ-PGA, 40 ml 100 % ethanol was added to the supernatant and the sample incubated at -20 °C for a minimum of 10 min. The γ-PGA was harvested by centrifugation and the resulting pellet suspended in 1 ml 10 mM Tris-HCl pH 8.0 and concentrated in a vacuum concentrator. The resulting γ-PGA pellet was suspended in 200 µl 10 mM Tris-HCl pH 8.0 and analysed by SDS-PAGE (section 2.8.3.2).

2.5.3 Inhibition of flagellar rotation with a Hag specific antibody

The *B. subtilis* flagella were tangled using a Hag-specific antibody as carried out previously for *E. coli* (Meister *et al.*, 1987). A wild-type strain carrying the P_{degU}-*lacZ* transcriptional reporter fusion (NRS4351) was grown to OD_{600} of 0.4 in LB prior to addition of a 1 in 20 dilution of Hag antibody (Prof. Kursad Turgay) or pre-immune sera. To check the motility of the cells, a small sample of each culture was imaged by phase contrast microscopy at each time-point. A thin channel was generated between a glass slide and the coverslip using double sided sticky tape. Cells were injected into the viewing chamber and visualised using a Zeiss Axio10 Imager.M10 under a Zeiss 40x EC Plan-NEO FLUAR objective and recorded using the high speed digital recorder function in the Zen lite software (Zeiss). Stills from these movies are presented in Chapter 4. Additionally, 0.5 ml samples were collected by centrifugation over the course of the experiment, frozen at -20 °C and later analysed by β-galactosidase assay (section 2.6.1) to ascertain the effect on activity of the *degU* promoter. At the end of the time-course samples were also collected for later analysis of secreted protease activity (section 2.6.2).

2.6 Enzymatic assays

2.6.1 β-galactosidase assays

Samples for measurement of β-galactosidase activity at specific growth stages and time-points were prepared as follows: cells were harvested from overnight lawn plates and diluted into 25 ml LB to an OD_{600} of 0.01 and grown at 37 °C with aeration. When required the OD_{600} was reached, 0.5 ml samples were harvested by centrifugation at 17,000 x *g* for 1 min and the cell pellet stored at -20 °C for later analysis.

For measurement of β-galactosidase activity, a method based on that described by Miller was used (Miller, 1972). The cell pellet was re-suspended in 1 ml Z buffer (see Table 2-4) and cells permeabilised by drop-wise addition of toluene and vortexing. The reaction was started by addition of 200 µl of 4 µg ml^{-1} of the substrate, o-nitrophenyl β-galactoside (ONPG). The cleavage of ONPG by β-galactosidase results in the production of galactose and o-nitrophenol, which is evidenced by a colorimetric change. Upon observation of this colour change, the reaction was stopped by the addition of 0.5 ml 1 M $NaCo_3$ and debris removed by centrifugation at 17,000 x *g* for 5 min. The absorbance at 420 nm was measured using a spectrophotometer and activity calculated as Miller Units using the following formula, where t = time of the reaction in minutes and v= volume of cells assayed (Miller, 1972).

$$\text{Specific activity} = (1000(OD_{420})/(t * v * OD_{600}))$$

2.6.2 Secreted protease activity

To measure the activity of secreted proteases an azocasein assay was performed based on the method detailed by Braun & Schmitz (Braun & Schmitz, 1980). Cells were harvested from an overnight lawn plate and diluted in 25 ml LB to an OD_{600} of 0.01. Cultures were grown with aeration at 37 °C to stationary phase. Culture samples were collected by centrifugation

(17,000 x *g* for 5 min) after which the cell pellet was stored at -20 °C prior to quantification of total protein (section 2.8.2) and the supernatant removed and stored at -20 °C until use.

To measure secreted protease activity, a 150 µl aliquot of thawed supernatant was mixed with 500 µl of 2 % w/v azocasein (Sigma), along with 100 µl of 1 M Tris-HCl (pH 8.0) and 650 µl of ddH_2O. A blank sample was prepared containing ddH_2O in the place of the supernatant and a media only control sample containing LB in the place of the supernatant was also prepared. The samples were incubated for 1 hour at 30 °C, after which 375 µl of 14 % v/v perchloric acid was added to stop each reaction. The samples were centrifuged (17,000 *x g* for 5 min) and 750 µl of the supernatant was mixed directly in a cuvette with 75 µl of 10 M NaOH and the absorbance at 436 nm was measured using a spectrophotometer. The background activity of the medium-only control was subtracted and activity was calculated as ΔA_{436} h^{-1} ml^{-1} per mg of total protein.

2.7 Single-cell analyses

2.7.1 Flow cytometry

For flow cytometry analysis strains were harvested from overnight lawn plates, diluted to an OD_{600} of 0.01 in 25 ml LB and grown at 37 °C with aeration to mid-exponential phase. Cells were collected by centrifugation at 17,000 x *g* for 2 min and re-suspended in 500 µl 1 X sterile PBS. The resulting cell suspension was fixed with 4 % paraformaldehyde (PFA) in PBS for 7 minutes. The cells were collected by centrifugation (17,000 x *g* for 1 min) and washed with 1 ml of PBS. The cells were again collected by centrifugation and re-suspended in 500 µl Glycine-Tris-EDTA (GTE) buffer (Table 2-4). 1 µl of the cell suspension was added to 1 ml of PBS with 1% (w/v) of Bovine Serum Albumin (BSA)(VWR). Single cell fluorescence was directly measured on a BD FACS Calibur (BD Biosciences). Single cells were identified on the basis of side scatter, while GFP or YFP fluorescence was analysed using 488 nm excitation with detection at

530±30nm. Data were captured using Cell Quest™ Pro (BD Biosciences) and further analysed using FlowJo software version 4.3.

2.7.2 Fluorescence microscopy

2.7.2.1 *Staining flagella and fluorescence microscopy*

To stain flagella, strains were constructed where the *hag* gene was mutated such that the protein variant produced carried an amino acid change of threonine to cysteine at position 209. This enabled labelling with a thiol-reactive maleimide dye. Cells carrying the Hag $T^{209}C$ point mutation were harvested from overnight lawn plates, diluted to an OD_{600} of 0.01 in 25 ml LB and grown at 37 °C with aeration to mid-exponential phase. 0.5 ml of culture was collected and cells harvested by centrifugation at 4,000 *x g*. Cells were washed once with 1 X T-Base (Table 2-4), pelleted and re-suspended in 50 µl T-base containing 5 µg/ml Alexa Fluor 488 C_5 maleimide dye (Molecular Probes, Life Technologies) and incubated for 5 min at room temperature. Cells were washed three times with 500 µl 1 X T-Base and suspended in 50 µl 1 X PBS. 2 µl of the cell suspension was spotted onto a thin matrix of 1.5 % (w/v) agarose (Ultrapure agarose, Life Technologies) in water contained in a 1.7 X 2.8 cm Gene Frame (AB-0578; ABgene House, Epsom, Surrey, United Kingdom) and mounted on a standard microscope slide (VWR superpremium). Each slide was prepared as follows: the gene frame was filled with molten 1.5 % agarose and covered firmly with a standard microscope slide to flatten the agarose surface. Following solidification of the agarose the slide was carefully removed and the cell suspension added. Once the cell suspension was dry the gene frame was sealed with a coverslip (thickness No 1.5; VWR) and images immediately acquired. Imaging was performed using a DeltaVision Core wide-field microscope (Applied Precision) mounted on an Olympus lX71 inverted stand with an Olympus 100X 1.4 NA lens and CoolSNAPHQ camera (Photometrics) with Differential Interference Contrast (DIC) and fluorescence optics. GFP was imaged using a 100 W Mercury lamp and a FITC filter set (EX 490/20; EM528/38) with an exposure time of 200 ms. DIC images were illuminated with an LED Transmitted light source.

To monitor P_{hag}-*yfp* expression, cells were grown at 37 °C in LB to an OD_{600} of 1.0, 0.5 ml of the culture was harvested, washed and suspended in 1 x PBS. The cell suspension was prepared for microscopy and imaged as described above. YFP fluorescence was imaged using a 100 W Mercury lamp and a FITC filter set (EX 490/20; EM 528/38) with an exposure time of 50 ms. The threshold used to define activation of the transcriptional reporter P_{hag} was set as a YFP fluorescence intensity value greater than 2 standard deviations above the mean background fluorescence. All images were rendered and analysed post-acquisition using OMERO software (www.openmicroscopy.org)(Allan *et al.*, 2012).

2.8 Protein methods

2.8.1 Harvesting proteins from liquid cultures

2.8.1.1 *Extraction of proteins from cellular fractions*

Proteins were extracted from whole cell lysates to allow quantification for the calculation of total protease activity per mg protein (section 2.6.2) or for downstream analysis by SDS-PAGE. For whole cell lysates, 1-2 ml of liquid culture was collected and cells harvested at the indicated stage of growth by centrifugation at 17,000 x *g* for 2-5 min. For extracts where intact flagella were to be isolated along with the cellular fraction, 7 ml of liquid culture was collected and cells harvested by centrifugation at 7,000 x *g* for 3 min. Cell pellets were stored at -20 °C until required and supernatants collected and processed immediately as outlined in section 2.8.1.2. To extract proteins, cell pellets collected from 1-2 ml of liquid culture were re-suspended in 300 µl Bugbuster Protein Extraction Reagent (Novagen), which contains a mixture of non-ionic detergents to allow gentle disruption of the cell wall. The lysate was rotated end-over-end for 20 min. To separate the soluble fraction from the insoluble material, the lysate was centrifuged at 17,000 x *g* for 10 min at 4 °C. The supernatant fraction containing soluble protein was collected and stored at -20 °C until required.

2.8.1.2 *Extraction of proteins from the extracellular milieu*

To extract secreted proteins from the extracellular milieu, a method based on that used by Karlinsey *et al.* was used (Karlinsey *et al.*, 2000a). Supernatant fractions were collected (section

2.8.1.1) and all subsequent steps carried out on ice. Briefly, the supernatant was filtered through a 0.2 µm acrodisc 13 mm syringe filter (Nalgene) into a fresh tube. Cellulose nitrate membrane filters (pore size 0.45 µm; Whatman, GE Healthcare) were prepared by wetting in ddH_2O and assembled into syringe filter holders (Sartorius). Supernatants were passed through filters using a 1.5 ml syringe and the flow-through discarded. Filters were subsequently placed in 1.5 ml microfuge tubes with 50 µl 4 X SDS loading dye (Table 2-4), vortexed and incubated at 70 °C with agitation for 30 min, with vortexing every 10 min. Proteins were recovered in the SDS loading dye (Table 2-4) and were boiled for 5 min prior to analysis by SDS-PAGE (2.8.3.1).

2.8.2 Quantification of protein concentration

The protein concentration of whole cell lysates and cellular samples was measured using the DC Protein Assay (BioRad), a colourimetric assay based on the Lowry method, according to manufacturer's instructions.

2.8.3 Sodium Dodecyl Sulphate-Polyacrylamide Gel Electrophoresis (SDS-PAGE)

2.8.3.1 *Separation of proteins by SDS-PAGE*

Gel electrophoresis of proteins was performed using SDS-polyacrylamide gels according to a method published previously (Laemmli, 1970), using the Mini-Protean system (BioRad). The resolving gels for SDS-PAGE were prepared as follows: 375 mM Tris-HCl (pH 8.8), 0.1 % (w/v) SDS, 0.1 % (w/v) APS, 0.1 % (v/v) TEMED. Polyacrylamide was added to reach a final concentration of either 10 or 12 % (v/v). The stacking gels for SDS-PAGE contained the following: 125 mM Tris-HCl (pH 6.8), 0.1 % (w/v) SDS, 0.1 % (w/v) APS, 0.1 % (v/v) TEMED and 6 % (v/v) polyacrylamide. Typically 7-10 µg of protein (or in the case of supernatant samples, 10-15 µl) was analysed. Protein samples were mixed with the appropriate volume of SDS-PAGE loading dye boiled for 5 min and the insoluble material removed by centrifugation at 17,000 x *g.* Samples were loaded into the wells of the stacking gel alongside the pre-stained molecular weight protein marker, SeeBlue®Plus2 (Invitrogen). Electrophoresis was performed in SDS running buffer (Table 2-4) at 200 V (constant voltage) for approximately 1 h, or until the

sample buffer dye front reached the edge of the resolving gel. To visualise all proteins, gels were stained with Coomassie Brilliant Blue (Table 2-4) with agitation for 30 min and unbound dye removed by incubation with de-staining solution (Table 2-4) for 1 hour before incubation in ddH_2O prior to photography.

2.8.3.2 *Separation of γ-PGA by SDS-PAGE*

SDS-PAGE analysis of γ-PGA was performed essentially as for proteins (section 2.8.3.1), but with the following exceptions. The gels were not comprised of resolving and stacking gels; rather the entire gel was comprised of stacking solution. Samples were prepared by mixing with SDS-loading dye, without β-mercaptoethanol, and samples were loaded without boiling and centrifugation. 20 µl of each sample was resolved and the gel subsequently stained in 0.5 % methylene blue in 3 % acetic acid for 30 min and de-stained in ddH_2O.

2.8.4 Western blotting

Samples to be analysed by Western blotting were firstly separated by SDS-PAGE gel electrophoresis (section 2.8.3.1). Resolved proteins were transferred to polyvinylidene difluoride (PVDF; Millipore) membranes by electroblotting using the Mini-Protean blotting cassettes (BioRad) in Tris-glycine transfer buffer (Table 2-4) at a constant current of 100 mA for 90-120 min. To prevent non-specific binding of antibodies, membranes were then incubated in blocking solution (5 % (w/v) non-fat dry milk in 1 X TBST (Table 2-4)), for 1 h at room temperature or overnight at 4 °C, with agitation. Membranes were then incubated with primary antibody at the appropriate dilution (see Table 2-8) in blocking solution for 1 h at room temperature or overnight at 4 °C, with agitation. Membranes were washed 3 times for 5 min in 1X TBST with agitation to remove unbound antibody before incubation with the required species-specific secondary HRP-conjugated antibody (Pierce) for 1 h at room temperature with agitation. Membranes were again washed 3 times in 1X TBST, developed

with Enhanced Chemiluminescence (ECL) reagents (Table 2-4) and exposed to X-ray film (Konica). Films were developed with the Medical Film Processor SRX-101A (Konica).

Table 2-8 Primary antibodies used in this study.

Protein antibody raised against	Species raised in	Dilution	Source
FlgE (*B. subtilis*)	Rabbit	1:20,000	D. Kearns
Hag (*B. subtilis*)	Rabbit	1:40,000	K. Turgay
SigA (*B. subtilis*)	Rabbit	1:500	NSW Lab
AtpB (*E. coli*)	Mouse	1:1000	Abcam
GFP	Mouse	1:1000	Roche

2.8.5 Whole cell analysis of Hag

Cells were harvested from overnight lawn plates and diluted to an OD_{600} of 0.01 in 25 ml LB and grown at 37 °C with aeration to mid-exponential phase. Cells were harvested by centrifugation at 7,000 x *g* and protein extracted as in section 2.8.1.1. 7 µg of proteins were resolved by SDS-PAGE and stained with Coomassie Brilliant Blue (section 2.8.3.1). Hag was identified by comparison with the Δ*hag* strain (DS1677) and confirmed by mass spectrometry (FingerPrints Proteomics and Mass Spectrometry Facility, University of Dundee).

2.8.6 Enrichment of flagellar hook-basal bodies

The flagellar HBB fraction of NCIB3610 was enriched for as described previously (Aizawa *et al.*, 1985, Kubori *et al.*, 1997). Essentially, 1 L of cells were grown to early exponential phase and harvested by centrifugation at 6000 x *g*, 45 minutes, 4 °C. The cell pellet was resuspended in 100 ml sucrose solution (Table 2-4) with a protease inhibitor tablet (Roche) and cells homogenised with a loose pestle on ice. To lyse cells and allow spheroplast formation, lysozyme was added to the cell suspension at a final concentration of 0.1 mg ml^{-1} and incubated at 4 °C with stirring for 40 minutes. Spheroplasts were lysed by addition of Triton X100 to a final concentration of 1 % and viscosity decreased by stirring at room temperature for 30 minutes, allowing endogenous DNAses to degrade cellular DNA. Unlysed cells were

removed by centrifugation at 4000 x *g* for 10 min and EDTA added to the suspension at a final concentration of 10 mM. To aid removal of contaminating membrane proteins, the pH of the lysate was raised to 10 by addition of NaOH. The lysate then underwent high speed centrifugation (60,000 x *g*, 60 minutes) and the pellets were resuspended in alkaline solution (Table 2-4) and centrifuged again. The pellet was then resuspended in 90 ml TET buffer (Table 2-4) and a 36 % CsCl gradient established. The solution was centrifuged using a Beckman SW41Ti swinging bucket rotor at 55,000 x *g* for 16 h at 15 °C. The flagellar fraction was visible as a band approximately 2 cm from the bottom of the tube and was collected with a Pasteur pipette and dialysed against TET buffer. In an attempt to dissociate the flagellar filaments the flagellar fraction was suspended in acidic solution (Table 2-4) for 1 h and HBB complexes collected by centrifugation at 100,000 x *g* for 1 h. HBBs were resuspended in TET buffer and analysed by SDS-PAGE and mass spectrometry.

2.8.7 Protein identification by mass spectrometry

To identify proteins found in the enriched HBB fractions or to prove the identity of the Hag protein found by SDS-PAGE analyses, mass spectrometry analyses were used and the results searched against the *Bacillus subtilis* Mascot database. Mass spectrometry analyses were carried out by the FingerPrints Proteomics and Mass Spectrometry Facility, University of Dundee.

2.9 Primary sequence and secondary structure prediction.

Primary protein sequences of *S.* Typhimurium FlgN, *B. subtilis* FlgN, FlgK and FlgL were obtained from GenoList (http://genodb.pasteur.fr/cgi-bin/WebObjects/GenoList) and aligned using Clustal Omega (http://www.ebi.ac.uk/Tools/msa/clustalo/) (Sievers *et al.*, 2011). The secondary structures of *S.* Typhimurium FlgN and *B. subtilis* FlgN were predicted using PsiPred (http://bioinf.cs.ucl.ac.uk/psipred/) and manually aligned against the primary sequence of the proteins (McGuffin *et al.*, 2000, Buchan *et al.*, 2013).

3

Defining the role of FlgN in flagellar motility in *B. subtilis*

3.1 Experimental aims and objectives

Post-translational modifications allow the cell to finely tune the activity, localisation or interactions of proteins (Pawson & Scott, 2005). Tyrosine kinases are used by bacteria to sense external signals and phosphorylate, and thereby regulate, target proteins to ensure that an appropriate response is elicited. The signals that activate or repress the activity of such kinases are largely unknown, but global proteomic studies have identified a number of protein targets of BY-kinases (Macek *et al.*, 2007, Macek *et al.*, 2008). However, the functional consequences of these modifications have only been assessed for a handful of proteins in a few bacterial species.

One such phosphorylated protein in *B. subtilis* is YvyG. YvyG has been shown to be phosphorylated on tyrosine 49 by studies using both proteomic strategies and *in vitro* kinase experiments (Macek *et al.*, 2007, Jers *et al.*, 2010). When this study began YvyG was predicted to be involved in flagellar motility (Pallen *et al.*, 2005). In *B. subtilis* the tyrosine kinases PtkA and EpsB are both essential for biofilm formation (Kiley & Stanley-Wall, 2010, Gerwig *et al.*, 2014). Flagellar motility and biofilm formation are incompatible behaviours, but the potential involvement of tyrosine phosphorylation in both processes led to the hypothesis that BY-kinases may present a means by which cells coordinate the transition from a motile lifestyle to a sessile state. To begin to investigate this possibility, the function of YvyG had to be established and the effect of tyrosine phosphorylation on its function ascertained. The work presented in this chapter began with these aims. While this work was being undertaken an additional proteomic screen identified YvyG as a substrate of an arginine kinase (Elsholz *et al.*, 2012). The impact of arginine phosphorylation on YvyG function was therefore also assessed.

3.2 YvyG of *Bacillus subtilis* shares secondary structure homology with the *Salmonella Typhimurium* protein, FlgN.

Previous bioinformatic analysis postulated that YvyG of *B. subtilis* was an orthologue of the flagellar chaperone protein, FlgN (Pallen *et al.*, 2005). The assembly of the bacterial flagellum is exquisitely controlled and construction is underpinned by a specialised T3SS that allows export of proteins from the cytoplasm to the nascent structure. Late flagellar proteins must be bound by their cognate chaperone to allow their transit to the export machinery and subsequent secretion (Bennett & Hughes, 2000). FlgN is a flagellar T3SS chaperone and is an essential component of the flagellar biosynthesis machinery (Kutsukake *et al.*, 1994, Gygi *et al.*, 1997, Fraser *et al.*, 1999). FlgN has been most extensively studied in *S.* Typhimurium (Kutsukake *et al.*, 1994, Fraser *et al.*, 1999), but homologues have been recognised in a number of different bacterial species (Gygi *et al.*, 1997, Pallen *et al.*, 2005). Three criteria were employed by Pallen *et al.* (2005) to identify FlgN homologues in a broad range of bacterial species: (i) the protein must be encoded by a gene adjacent to a *flgM* homologue (**Figure 3-1A** and **C**), (ii) the gene should be of a similar length to *flgN* of Salmonella (**Figure 3-1C**) and (iii) the protein must be recognisable (however distantly) by PSI-BLAST analysis as FlgN-like. These criteria were set as the primary amino acid sequence of FlgN is highly variable (Pallen *et al.*, 2005). To confirm that YvyG is likely to be an orthologue of FlgN, the amino acid sequence of YvyG was compared with that of *S.* Typhimurium FlgN. As expected, there was little primary sequence homology (**Figure 3-1C**). However, upon comparison of the predicted secondary structures of YvyG and FlgN a high degree of similarity was clearly apparent (**Figure 3-1C**). Thus, YvyG was re-named as FlgN and its function in motility in *B. subtilis* further investigated.

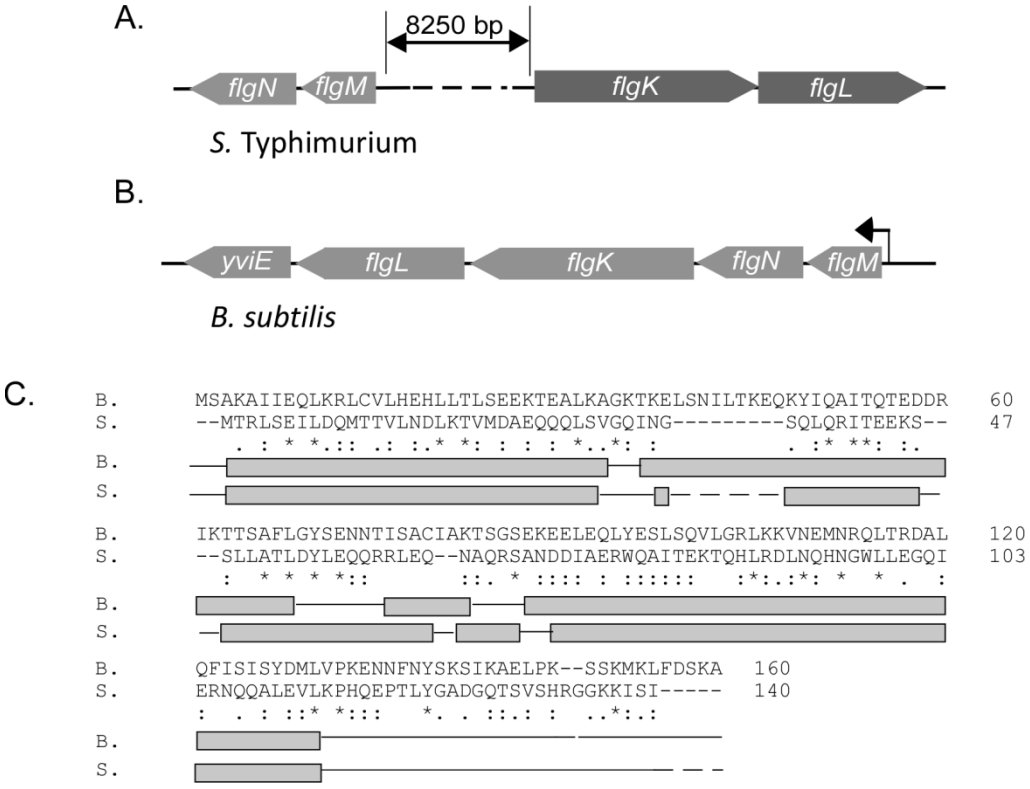

Figure 3-1 Primary sequence and secondary structure comparison of *B. subtilis* FlgN with *S.* Typhimurium FlgN. Schematic representation of the chromosomal regions surrounding **(A)** *S.* Typhimurium *flgN* and **(B)** *B. subtilis flgN*. Arrows represent open reading frames (ORF), with the direction of the arrow indicating the direction of the ORF. The bent arrow represents the promoter located before the *flgM* coding region. **(C)** Primary sequence and secondary structure alignments of *Bs*-FlgN and *S*T-FlgN. B. represents *B. subtilis* and S. represents *S.* Typhimurium. For primary sequence alignments an asterisk indicates a fully conserved amino acid, a colon indicates a highly conserved amino acid and a full stop indicates a weakly conserved amino acid. Gaps indicate no homology. Dashed lines indicate a break in the sequence. For secondary structure alignments light grey boxes indicate α-helices, solid lines indicate coiled coils and dashed lines indicate a break in the sequence.

On the *B. subtilis* chromosome the *flgM, flgN*, *flgK* and *flgL* coding regions are adjacent (**Figure 3-1B**). To ascertain whether all four genes were encoded as part of the same operon in the NCIB3610 strain reverse transcription-PCR (RT-PCR) analysis was used. RNA was extracted from wild-type *B. subtilis* and cDNA synthesised using a primer specific to *yviE*, the gene proximal to *flgL* at the 3' end (**Figure 3-1B**). The cDNA generated was used as a template for PCR with primer pairs specific to the internal coding regions of *flgM*, *flgN*, *flgK* and *flgL*. Regions of DNA internal to the coding regions of *flgM*, *flgN*, *flgK* and *flgL* could each be amplified from cDNA

generated using a primer at the 3' end of *flgL* (just beyond the termination codon) (**Figure 3-2**), demonstrating that all four genes are co-transcribed.

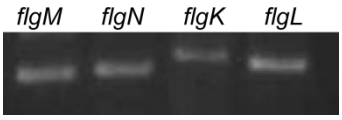

Figure 3-2 RT-PCR analysis of co-transcription of *flgM*, *flgN*, *flgK* and *flgL*. Regions of DNA internal to *flgM*, *flgN*, *flgK* and *flgL* were amplified from cDNA generated using a primer specific to the gene 3' proximal to *flgL,* using RNA from the wild-type strain (NCIB3610). Primers used are indicated in **Table 2-3**.

3.3 FlgN is essential for motility

The *flgN* gene is located in a region of the chromosome known to be required for motility (Mirel *et al.*, 1994). To test if *flgN* is required for motility, a *B. subtilis* strain carrying an in-frame deletion of *flgN* was constructed and its phenotype assessed in swimming and swarming assays. A strain containing a deletion in the *hag* gene (DS1677) was used as a non-motile control. While the wild-type strain was able to both swim and swarm efficiently, this behaviour was lost in the Δ*flgN* strain (NRS3570) (**Figure 3-3A**, **C** and **E**). It was confirmed that transcription of the other genes in the operon was not impacted by the *flgN* deletion using RT-PCR (**Figure 3-3F**). To further ensure that this loss of motility was specific to the deletion of *flgN*, the motility of a strain where the coding region of *flgN* was re-introduced at the *amyE* locus under the control of an IPTG inducible promoter ($P_{hy\text{-}spank}$) was also assessed. Both the swimming (**Figure 3-3B**) and swarming (**Figure 3-3D** and **E**) phenotypes of Δ*flgN* could be restored by the re-introduction of *flgN* on the chromosome upon induction with IPTG. These data demonstrate for the first time *in vivo* that the product of the *flgN* gene is required for both swimming and swarming motility. It is notable that higher levels of *flgN* transcription are required to complement the swarming defect presented by the Δ*flgN* strain than the swimming defect (compare **Figure 3-3B** with **Figure 3-3D**). This is most likely attributable to a higher demand on flagella biosynthesis in swarming when compared to swimming motility (Fraser & Hughes, 1999).

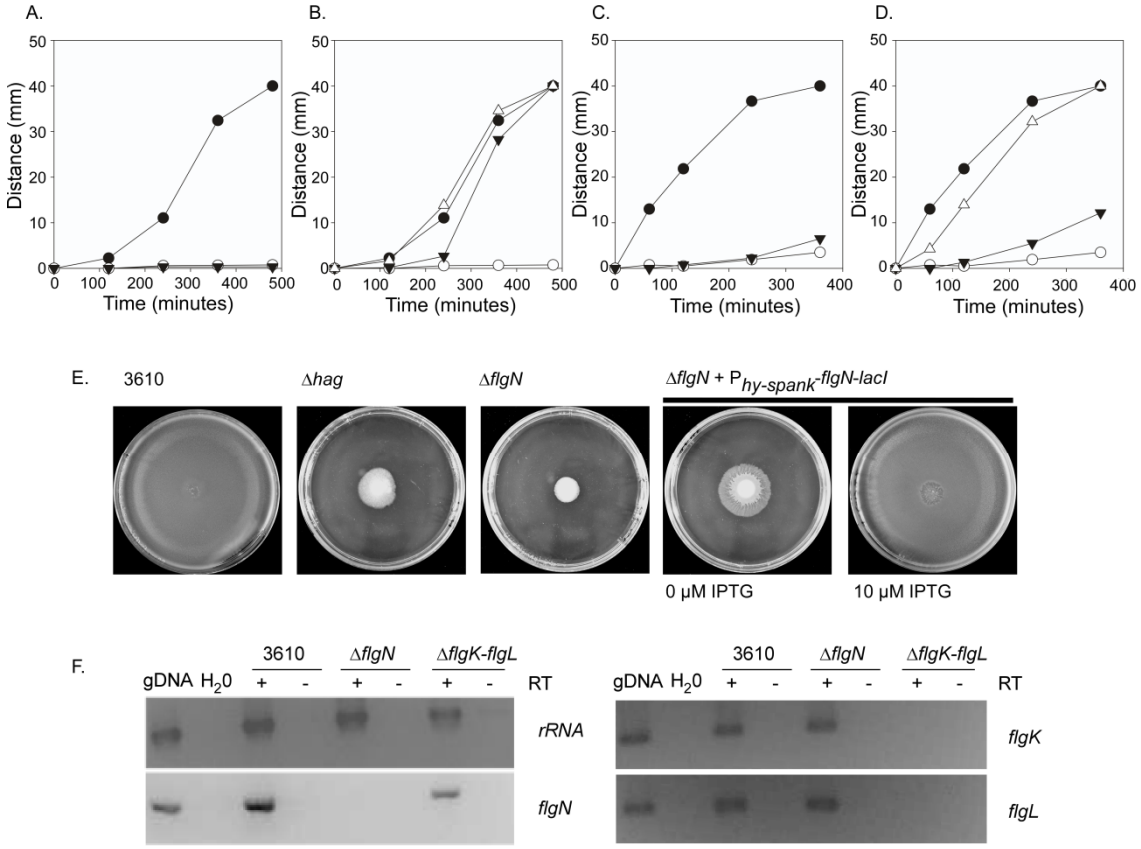

Figure 3-3 Motility analysis of the Δ*flgN* strain. Swim expansion assays **(A and B)** and swarm expansion assays **(C and D)**. Wild-type (3610; filled circle), Δ*hag* (DS1677; filled triangle), Δ*flgN* (NRS3570; hollow circle) for A and C. Wild-type (3610; filled circle), Δ*flgN* (NRS3570; hollow circle) and Δ*flgN* + $P_{hy\text{-}spank}$-*flgN-lacI* (NRS3578) without (filled triangle) and with 10 μM IPTG induction (hollow triangle) for B and D. Each graph is representative of three independent biological replicates. **(E)** Photographs of swarm expansion plates taken at the end of the assay, after 6 hours incubation at 37 °C. **(F)** RT-PCR analysis of transcription of *flgN*, *flgK* and *flgL* in wild-type (NCIB3610), Δ*flgN* (NRS3570) and Δ*flgK-flgL* (NRS4060) strains. gDNA and H_20 are shown as positive and negative controls for amplification, respectively. rRNA was amplified as an internal control. The + and – symbols indicate reactions incubated with or without reverse-transcriptase (RT).

3.4 Deletion of *flgN* allows transcription of *hag* in all cells

To dissect the role of *flgN* in motility, the effect of deletion of *flgN* on the transcription of the flagellar filament gene *hag* was tested. The *hag* gene is under the control of a promoter driven by the alternative sigma factor σ^D (encoded by the penultimate gene of the *fla/che* operon, *sigD*) (Marquez *et al.*, 1990). In wild-type *B. subtilis* only a sub-population of cells express flagella as *sigD* is not transcribed in all cells and so as a result transcription of *hag* is bimodal (Kearns & Losick, 2005, Cozy & Kearns, 2010). Due to this heterogeneity, single cell techniques are ideally suited for analysis. To this end, a P_{hag}-*yfp* transcriptional reporter was integrated at a heterologous location on the chromosome. Flow cytometry and single cell microscopy were used to assess the transcriptional profile using the fluorescence generated by YFP as a reporter. In the wild-type strain the bimodality of *hag* transcription in the cell population is clearly evident (**Figure 3-4A** and **Figure 3-4C**). Strikingly, upon deletion of *flgN* bimodality is lost as *hag* transcription was observed for all cells within the population, albeit at a lower level than in the wild-type (**Figure 3-4A** and **Figure 3-4C**). The alteration in the *hag* transcriptional profile can be complemented upon re-introduction of *flgN* under the control of an IPTG inducible promoter at the heterologous *amyE* locus, confirming the requirement of *flgN* for bimodal *hag* transcription (**Figure 3-4B**). However, as the *hag* gene is still transcribed in the absence of *flgN*, these findings indicate that lack of motility in the Δ*flgN* strain is not due to a lack of *hag* transcription.

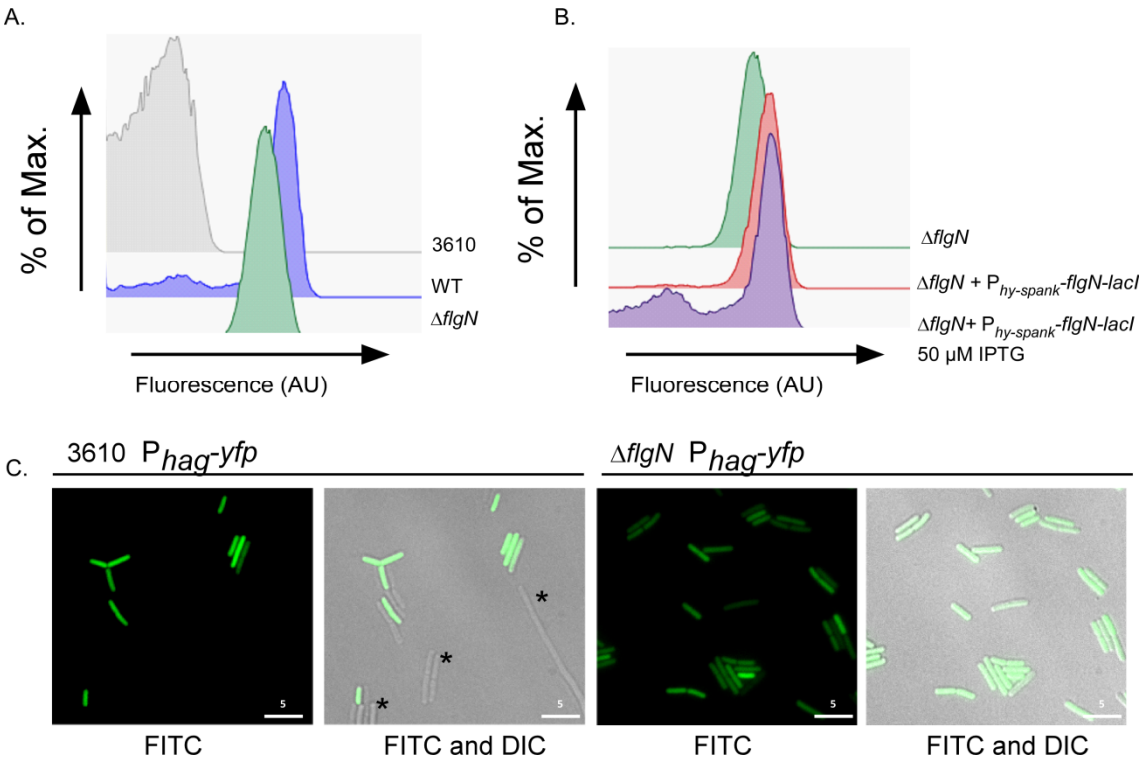

Figure 3-4 Single-cell analyses of *hag* transcription in a Δ*flgN* strain. (A and B) Flow cytometry analysis of *hag* transcription in strains carrying the P_{hag}-*yfp* transcriptional reporter fusion. 3610 was used as a non-fluorescent control. Strains shown are: WT (NRS3076), Δ*flgN* (NRS3708) and Δ*flgN* + $P_{hy\text{-}spank}$-*flgN-lacI* (NRS3713) without and with induction with 50 µM IPTG. **(C)** Fluorescence microscopy analysis of the WT (NRS3076) and Δ*flgN* (NRS3708) strains carrying the P_{hag}-*yfp* transcriptional reporter (false-coloured green). Scale bars represent 5 µm. An asterisk indicates examples of cells that do not transcribe *hag*. Data are representative of at least 3 independent experiments. *Fluorescence microscopy was performed in collaboration with Dr. Victoria Marlow.*

3.5 Loss of *flgN* is associated with a defect in flagellar biosynthesis

3.5.1 Translation of *hag* is decreased in the absence of *flgN*

As the *hag* coding region is transcribed (**Figure 3-4**), a lack of motility in the absence of *flgN* could arise from lack of translation of the *hag* transcript. To assess *hag* translation a P_{hag}*'-'lacZ* translational reporter fusion (under the control of the *hag* promoter, the *hag* leader region, Shine-Dalgarno sequence and start codon) was constructed and introduced into *B. subtilis* at the *amyE* locus. When the β-galactosidase activity levels in the *flgN* mutant were compared with the wild-type, Hag translation was found to be 2-fold lower (**Figure 3-5**). However, a strain carrying an in-frame deletion of *flgE*, which encodes the main protein component of the

flagellar hook, showed a 100-fold decrease in Hag translation (**Figure 3-5**) (Mukherjee *et al.*, 2011).

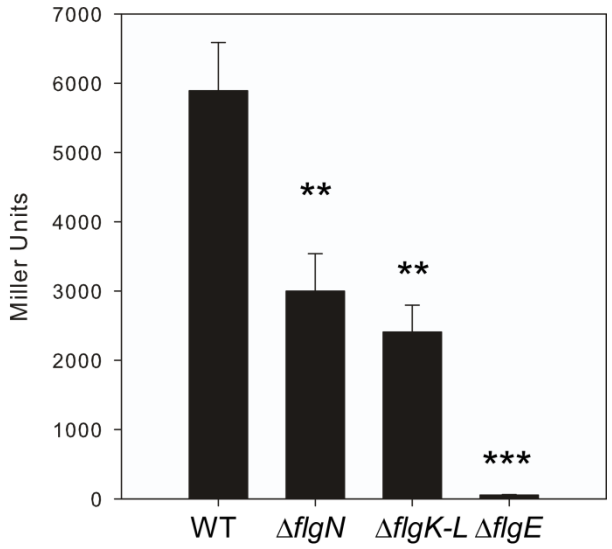

Figure 3-5 Quantification of *hag* translation in Δ*flgN* and Δ*flgK-flgL* strains. β-galactosidase assays of strains carrying the P*hag'-'lacZ* translational reporter fusion. Strains shown are WT (NRS4795), Δ*flgN* (NRS4796), Δ*flgK-flgL* (NRS4799) and Δ*flgE* (NRS4798). Data are plotted as the average of at least 3 independent replicates. Error bars represent standard error of the mean. An asterisk denotes significance as calculated by the Student's t-test where ** represents $P<0.01$ and *** $P<0.001$.

It is likely that the observed decrease in the translation of *hag* in the Δ*flgN* mutant strain is a result of *hag* being transcribed at a lower level in all cells compared to wild-type (**Figure 3-4**). Alternatively, it is technically possible that translation itself may be regulated, as occurs in the absence of *flgE* (see Discussion) (Mukherjee *et al.*, 2011).

3.5.2 Hag is secreted in the Δ*flgN* strain

While there is a statistically significant ($P=0.01$) decrease in Hag translation in the absence of *flgN* it did not appear to be sufficient to account for the complete lack of motility demonstrated in **Figure 3-3** (i.e. the severity of the motility defect does not match the small decrease in translation of Hag). A lack of motility in the presence of *hag* transcription and translation could be due to a lack of Hag polymerisation (Mukherjee *et al.*, 2013). To test if Hag was secreted but not assembled in the Δ*flgN* strain proteins were extracted from the cellular

and supernatant fractions of cells grown to mid-exponential phase. The presence or absence of Hag was detected by Western blot analysis, with the cytoplasmic sigma factor, SigA, used as a loading and fractionation control. For the wild-type strain Hag is seen in the cellular fraction (which includes assembled flagella) and in the supernatant fraction (including unassembled and sheared flagella) (**Figure 3-6**). However, for the Δ*flgN* strain Hag is only detected in the supernatant fraction at a lower molecular weight (**Figure 3-6**). This is likely to be unpolymerised Hag or the products of proteolytic degradation resulting from the action of the extracellular proteases (Mukherjee *et al.*, 2013). As a positive control for Hag secretion, a strain carrying an in-frame deletion of *fliD*, which encodes the filament cap protein, was also assessed. This strain phenocopies the Hag secretion profile seen in Δ*flgN,* thus supporting the conclusion that deletion of *flgN* is associated with a lack of filament polymerisation.

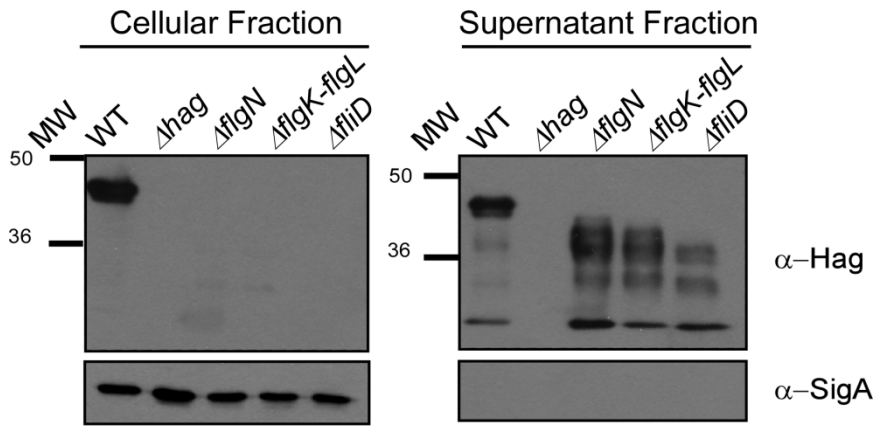

Figure 3-6 Western blot analysis of Hag secretion and polymerisation. Western blot analysis of whole cell proteins (including assembled flagella) and supernatant fractions (including sheared and unassembled flagella) of the wild-type (3610), Δ*hag* (DS1677), Δ*flgN* (NRS3570), Δ*flgK-flgL* (NRS4060) and Δ*fliD* (NRS4041) strains, separately probed with α-Hag and α-SigA primary antibodies. MW represents molecular weight (kDa).

3.5.3 The flagellar filament is not assembled in the absence of *flgN*

Loss of filament polymerisation in Δ*flgN* was confirmed by single cell fluorescence microscopy of strains where the codon for threonine at position 209 of the *hag* gene was mutated to cysteine to enable labelling with an alexa-fluor 488 C_5 cysteine maleimide dye (Blair *et al.*,

2008). In the wild-type background (NRS3719) the flagellar filaments are clearly visible (**Figure 3-7**). However, upon deletion of *flgN* no signal was detected (**Figure 3-7**).

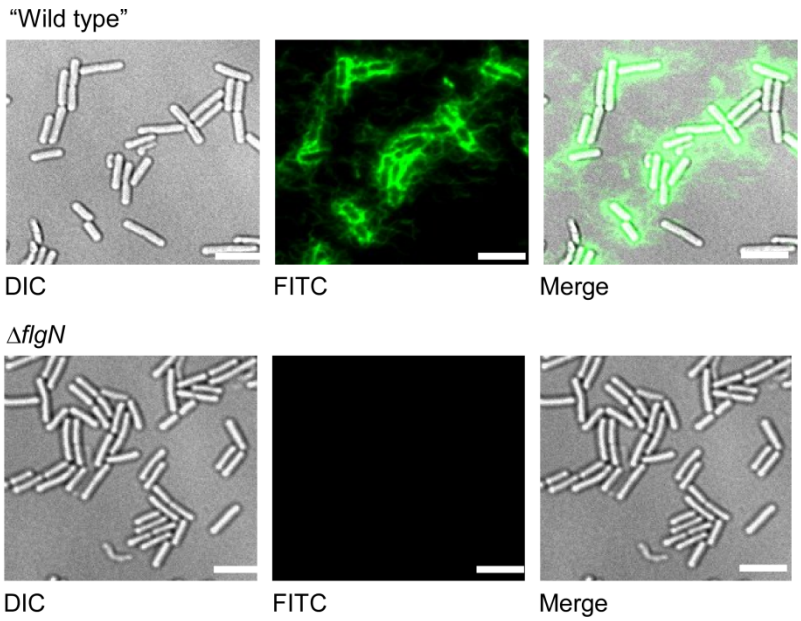

Figure 3-7 Detection of flagellar filament assembly by fluorescence microscopy. Fluorescence micrographs of strains carrying the Hag $T^{209}C$ point mutation labelled with Alexa fluor 488 maleimide (false-coloured green). Shown are the wild-type (NRS3719) and Δ*flgN* (NRS3718) strains. Scale bars represent 5 μm.

Collectively, these data show that the Δ*flgN* strain is non-motile due to both a small decrease in translation of Hag and a block in filament assembly, which results in the accumulation of unpolymerised Hag in the extracellular milieu. Together these data prove that the lack of motility exhibited by the *flgN* mutant is due to a lack of flagellar filament assembly.

3.6 Deletion of *flgK* and *flgL* phenocopies deletion of *flgN*

A lack of filament polymerisation in the absence of *flgN* is consistent with the hypothesis that *B. subtilis*-FlgN (*Bs*-FlgN) is an orthologue of *S.* Typhimurium (*S*T-FlgN); i.e. if FlgK and FlgL are not properly localised to hook-filament junction, the flagellar filament cannot be assembled (Gygi *et al.*, 1997, Fraser *et al.*, 1999). It was therefore postulated that if *Bs*-FlgN were an orthologue of *S*T-FlgN, then a strain mutated for *flgK* and *flgL* may phenocopy the Δ*flgN* strain. A strain carrying an in-frame deletion of *flgK-flgL* was constructed and found to be unable to

swarm (**Figure 3-8**). This effect was specific to deletion of *flgK* and *flgL* as the mutant strain could be complemented upon re-introduction of *flgK-flgL* to the chromosome under the control of the IPTG-inducible promoter, $P_{hy\text{-}spank}$.

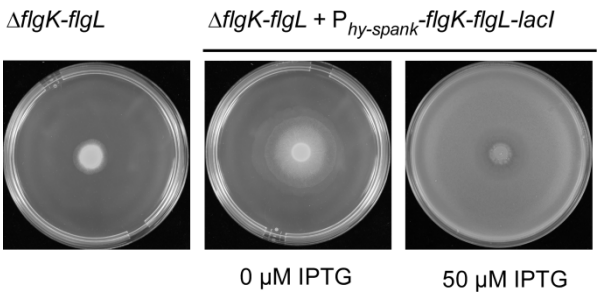

Figure 3-8 Swarm expansion assay of the Δ*flgK-flgL* strain. Photographs of swarm expansion plates taken after 6 hours incubation at 37 °C. Strains shown are wild-type (3610), Δ*flgK-flgL* (NRS4060) and Δ*flgK-flgL* + $P_{hy\text{-}spank}$-*flgK-flgL-lacI* (NRS 4064) without and with induction with 50 µM IPTG.

To test if transcription of *hag* was also altered upon deletion of *flgK-flgL* the P_{hag}-*yfp* transcriptional reporter was integrated to the Δ*flgK-flgL* strain and single cell analyses employed. Flow cytometry and microscopy revealed a loss of bimodality with respect to transcription of the σ^D-regulated gene *hag* (**Figure 3-9**), as was also seen for deletion of *flgN* (**Figure 3-4**).

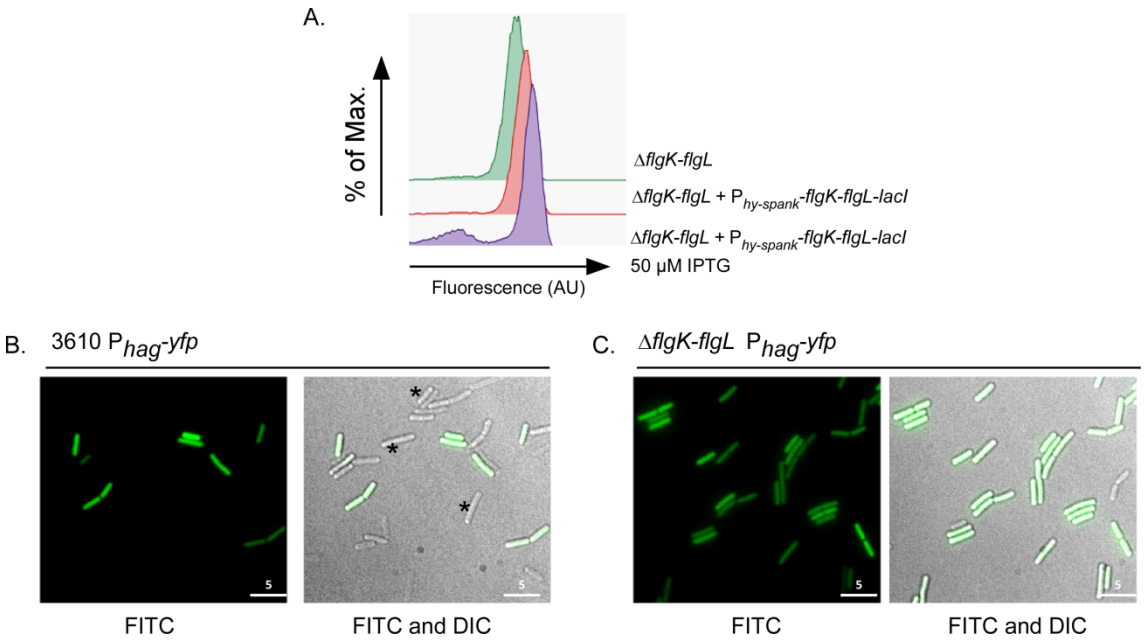

Figure 3-9 Single cell analyses of *hag* transcription in the Δ*flgK-flgL* strain. (A) Flow cytometry analysis of *hag* transcription in strains carrying the P_{hag}-*yfp* transcriptional reporter fusion. Strains shown are: Δ*flgK-flgL* (NRS4071) and Δ*flgK-flgL* + $P_{hy\text{-}spank}$-*flgK-flgL-lacI* (NRS4078) without and with induction with 50 µM IPTG. **(B)** Fluorescence microscopy analysis of the WT (NRS3076) and Δ*flgK-flgL* (NRS4071) strains carrying the P_{hag}-*yfp* transcriptional reporter (false-coloured green). Scale bars represent 5 µm. An asterisk indicates examples cells that do not transcribe *hag*. *Fluorescence microscopy was performed in collaboration with Dr. Victoria Marlow.*

To determine if the translation of *hag* was also altered the P_{hag}'-'*lacZ* was integrated into the Δ*flgK-flgL* strain. β-galactosidase assays showed that the Δ*flgK-flgL* strain displayed a 2-fold decrease in Hag translation when compared with the wild type strain (**Figure 3-5**). Furthermore, upon deletion of *flgK-flgL* Hag could not be detected in the cellular fraction but was instead found in the extracellular milieu (**Figure 3-6**). We confirmed that transcription of the other genes in the operon was not impacted by the *flgK-flgL* deletion using RT-PCR analysis (**Figure 3-3**). In conclusion, deletion of *flgK* and *flgL* generates a strain that phenocopies the single *flgN* mutant as demonstrated by physiological, biochemical and single cell analyses. This is consistent with *Bs*-FlgN functioning as an orthologue of *S*T-FlgN.

3.7 Over-expression of *flgK* and *flgL* does not restore motility to a Δ*flgN* strain

In *Salmonella* deletion of *flgN* can be compensated for by over-expression of *flgK* and *flgL* (Aldridge *et al.*, 2003). This is because FlgN is not exclusively required for the secretion of its substrates, but rather protects FlgK and FlgL from proteolysis and ensures that the substrates are efficiently transported to the export machinery (Aldridge *et al.*, 2003, Thomas *et al.*, 2004). To test if this was the case for the *B. subtilis flgN* deletion, the coding regions of *flgK* and *flgL* were integrated in the Δ*flgN* strain at a heterologous site on the chromosome under the control of an IPTG inducible promoter. Surprisingly, induction of the *flgK-flgL* coding region was unable to restore motility to the Δ*flgN* strain as determined by assaying swarming motility (**Figure 3-10**).

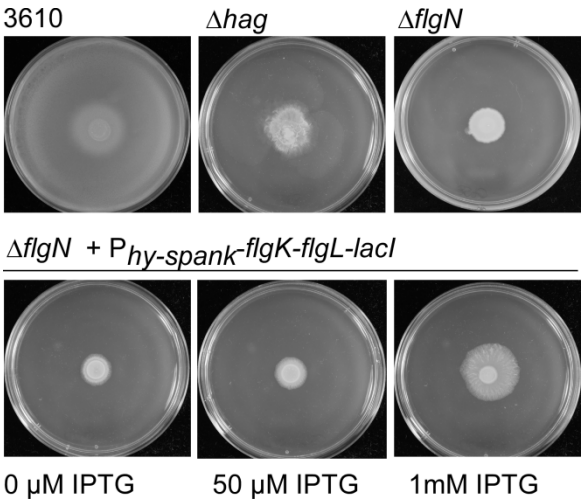

Figure 3-10 Swarm expansion assay of the Δ*flgN* strain when *flgK-flgL* are over-expressed. Photographs of swarm expansion plates taken after 6 hours incubation at 37 °C. Strains shown are wild-type (3610), Δ*hag* (DS1677) Δ*flgN* (NRS3570) and Δ*flgN* + $P_{hy\text{-}spank}$-*flgK-flgL-lacI* (NRS4043) without and with induction with 50 µM IPTG or 1mM IPTG.

To confirm that the flagellar filament is not polymerised upon over-expression of *flgK-flgL,* cellular protein samples (which include assembled flagella) were separated by SDS-PAGE and stained with Coomassie brilliant blue. Hag appears as a dominant protein band at ~36 kDa (**Figure 3-11A**), and can be easily identified by comparison with proteins harvested from the Δ*hag* and wild-type strains (Diethmaier *et al.*, 2011). The identity of the Hag protein identified

in this manner was confirmed by mass spectrometry (**Figure 3-11B**). When compared with the wild-type, analysis of the cellular proteins for the Δ*flgN* strain indicated that Hag was not associated with the cell fraction (**Figure 3-11A**). This is entirely consistent with the data presented above (**Figure 3-6** and **Figure 3-10**). As expected, the presence of the Hag band could be restored by the re-introduction of *flgN* on the chromosome upon induction with 50 µM IPTG (**Figure 3-11A**). However, introduction of *flgK-flgL* in the Δ*flgN* background at a heterologous site could not complement Δ*flgN* with respect to Hag polymerisation, even in the presence of 1 mM IPTG.

A.

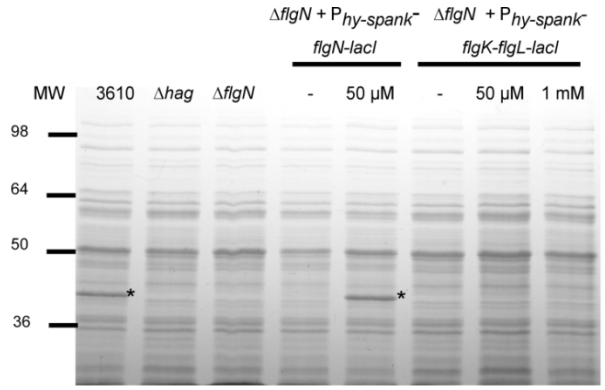

B.

MR**INHNIAALNTLNRL**SSNNSASQKNMEKLSSGLRI
NR**AGDDAAGLAISEK**MRGQIRGLEMASK**NSQDGISL**
IQTAEGALTETHAILQRVRELVVQAGNTGTQDKATD
LQSIQDEISALTDEIDGISNRTEFNGK**KLLDGTYKV**
DTATPANQKNLVFQIGANATQQISVNIEDMGADALG
IKEADGSIAALHSVNDLDVTKFADNAADTADIGFDA
QLKVVDEANQVSSQRAK**LGAVQNRLEHTINNLSASG**
ENLTAAESRIRDVDMAKEMSEFTK**NNILSQASQAML**
AQANQQPQNVLQLLR

Figure 3-11 Detection of Hag in the Δ*flgN* strain when *flgK and flgL* are over-expressed. (A) Coomassie gel analysis of total cell proteins of 3610, Δ*hag* (DS1677), Δ*flgN* (NRS3570), Δ*flgN* + $P_{hy\text{-}spank}$-*flgN-lacI* (NRS3578), Δ*flgN* + $P_{hy\text{-}spank}$-*flgK-flgL-lacI* (NRS4043) without and with induction with 50 µM IPTG or 1mM IPTG. The Hag protein was subsequently identified by mass spectrometry analysis and is marked with an asterix. MW represents molecular weight (kDa). **(B)** The protein sequence of Hag is shown with amino acids from peptide sequences which were identified by mass spectrometry analysis in the identification of Hag in whole cell lysates highlighted in bold.

The inability of *flgK-flgL* over-expression to compensate for deletion of *Bs-flgN* could be due to disruption of flagellar biosynthesis at an earlier stage. However this possibility was ruled out as it was demonstrated that the flagellar hook protein, FlgE could be detected in whole cell

lysates (which include assembled flagella) for both the wild-type and Δ*flgN* strains by Western blot analysis (**Figure 3-12**).

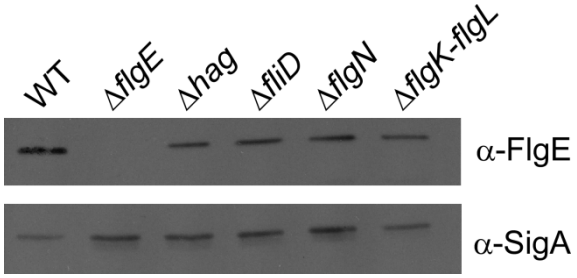

Figure 3-12 Western blot analysis of FlgE in Δ*flgN* and Δ*flgK-flgL* strains. Western blot analysis of whole cell protein fractions (including assembled flagella) of the wild-type (NCIB3610), Δ*flgE* (NRS4042), Δ*hag* (DS1677), Δ*fliD* (NRS4041), Δ*flgN* (NRS3570) and Δ*flgK-flgL* (NRS4060) probed with the α-FlgE antibody.

3.8 Probing the export and interactions of FlgK

3.8.1 Characterisation of strains carrying His-tagged *flgK* alleles

The inability of heterologous *flgK-flgL* expression to complement the *flgN* mutant strain is suggestive of a strict dependence on FlgN for FlgK and FlgL protein stability or secretion. In an attempt to test if FlgK was unstable in the absence of *flgN,* strains were constructed to enable detection of FlgK by fusing FlgK to a poly-Histidine epitope tag. However, the presence of such an epitope tag at either the N- or C-terminus of the protein rendered FlgK non-functional, as determined by a non-motile phenotype (**Figure 3-13**). Experiments with these strains were therefore not pursued.

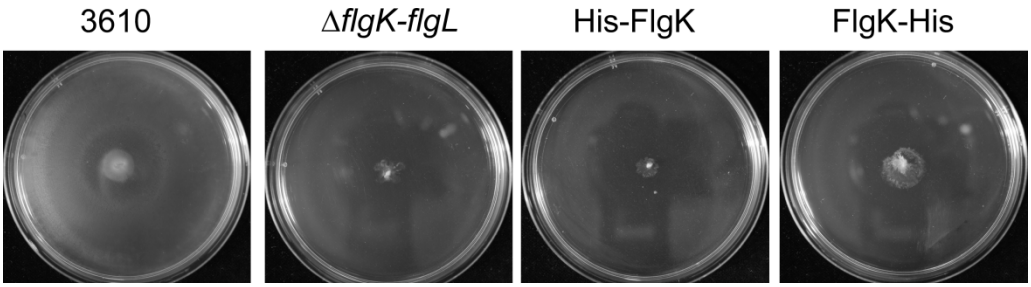

Figure 3-13 Swim expansion assay for strains carrying a poly-Histidine epitope tag fused to FlgK. Swim expansion assay of wild-type (NCIB3610), Δ*flgK-flgL* (NRS4060), His-*flgK* (NRS4812) and *flgK*-His (NRS4801). Photographs were taken after 24 hours incubation at room temperature.

3.8.2 Purification of flagellar hook-basal bodies

As a method of attempting to assess FlgK assembly at the flagellar hook junction we aimed to purify flagellar hook-basal bodies from both the wild-type and Δ*flgN* strains and analyse the protein components of the complex by mass spectrometry (Aizawa *et al.*, 1985, Kubori *et al.*, 1997). While the flagellar fraction of the wild-type strain was enriched successfully (**Figure 3-14** and Table 3-1), the same was not possible for the Δ*flgN* strain. This is most likely because this methodology is dependent on an intact flagellar filament for isolation of the complex and the *flgN* mutant does not form a flagellar filament (**Figure 3-7**).

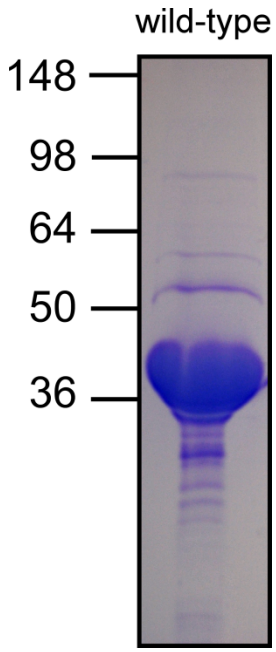

Figure 3-14 SDS-PAGE analysis of proteins isolated after hook-basal body enrichment. Coomassie stained SDS-PAGE gel analysis of flagellar hook-basal body proteins enriched from the wild-type strain (NCIB3610). Protein molecular weights (kDa) are indicated on the left.

Table 3-1 Mass spectrometry analysis of proteins identified from hook-basal body enrichment of NCIB3610. The top 12 proteins from the NCIB3610 sample are presented as identified by their Mascot protein score.

Protein Rank	Protein Description	Mascot Protein Score	Coverage (%)	Unique Peptides	No. Peptides
1	flagellin [Bacillus subtilis subsp. subtilis str. 168]	13717.54	96.71	38	45
2	flagellar basal body rod protein FlgG [Bacillus subtilis subsp. subtilis str. 168]	6251.24	96.97	27	27
3	elongation factor Tu [Bacillus subtilis subsp. subtilis str. 168]	6107.34	92.42	38	38
4	surfactin synthetase [Bacillus subtilis subsp. subtilis str. 168]	3582.23	34.80	84	104
5	surfactin synthetase [Bacillus subtilis subsp. subtilis str. 168]	3267.57	38.44	77	97
6	flagellar MS-ring protein [Bacillus subtilis subsp. subtilis str. 168]	3254.30	70.34	32	32
7	flagellar hook-associated protein FlgK [Bacillus subtilis subsp. subtilis str. 168]	2784.52	73.77	27	27
8	putative flagellin [Bacillus subtilis subsp. subtilis str. 168]	2249.41	48.75	1	11
9	glyceraldehyde-3-phosphate dehydrogenase [Bacillus subtilis subsp. subtilis str. 168]	1957.55	54.63	15	15
10	30S ribosomal protein S2 [Bacillus subtilis subsp. subtilis str. 168]	1776.43	84.55	26	26
11	flagellar capping protein [Bacillus subtilis subsp. subtilis str. 168]	1765.60	63.25	29	29
12	flagellar hook-associated protein FlgL [Bacillus subtilis subsp. subtilis str. 168]	1693.66	67.45	16	16

3.9 Phosphorylation of FlgN and motility

3.9.1 Testing the functionality of FlgN fused to GFP

Global proteomic strategies have identified a plethora of targets for both tyrosine and arginine kinases in *B. subtilis*, with one such target being *Bs*-FlgN, which can be tyrosine phosphorylated on amino acid 49 (Macek *et al.*, 2007) and arginine phosphorylated on amino acid 60 (Elsholz *et al.*, 2012). Having demonstrated that *Bs*-FlgN is required for flagellar biosynthesis, we were presented with the ideal system to assess the role of tyrosine and arginine phosphorylation in controlling protein function *in vivo*.

Previous work has indicated that the sub-cellular localisation of *Bs*-FlgN is altered upon deletion of *ptkA*, which encodes a tyrosine kinase (Jers *et al.*, 2010). Data from fluorescence microscopy experiments suggested that *Bs*-FlgN co-localised with PtkA during stationary phase but was found at the cell poles during exponential phase (Jers *et al.*, 2010). To test if there was a link between the function of FlgN in flagellar assembly and its PtkA-dependent localisation pattern, the *flgN* coding region was fused to the *gfp* gene under the control of a xylose promoter and firstly integrated into the Δ*flgN* strain. The functionality of this fusion protein was tested in a swarming assay. As shown in **Figure 3-15A**, induction of FlgN-GFP with 0.5 % xylose was not sufficient to complement the motility defect of the *flgN* deletion. This was not due to a lack of protein production as the fusion protein could be detected in a Western blot with a GFP-specific antibody. Rather it seems that the introduction of GFP at the C-terminus of FlgN disrupts the function of the protein. This would be in line with *Bs*-FlgN being an orthologue of *S*T-FlgN, as the C-terminus of *S*T-FlgN is essential for interaction with its substrates, FlgK and FlgL.

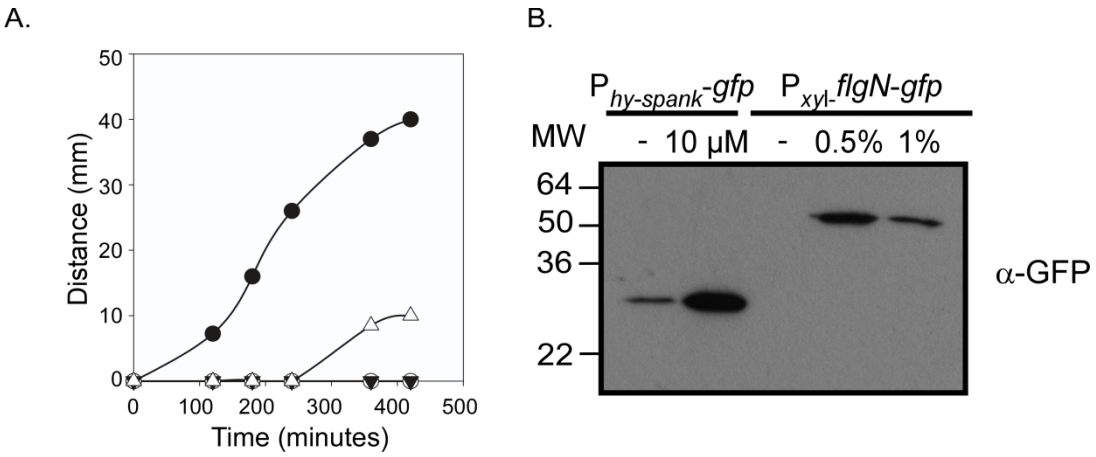

Figure 3-15 Swarm expansion assay for FlgN fused to GFP. (A) Quantitative swarm expansion assays for the wild-type (3610; filled circle), Δ*hag* (DS1677; hollow circle), Δ*flgN* + P_{xyl}-*flgN-gfp* (NRS3603) without induction (filled triangle) and with induction with 0.5% xylose (hollow triangle). **(B)** Western blot analysis of GFP expression in $P_{hy\text{-}spank}$-*gfp-lacI* (NRS 1467) without or with induction with 10 µM IPTG and *ΔflgN* + P_{xyl}-*flgN-gfp-lacI* (NRS3603) without or with induction with 0.5 % xylose.

3.9.2 Mutation of FlgN phosphorylation sites does not impact motility

As an alternative means of assessing the effect of phosphorylation on the physiological function of FlgN, site-directed mutagenesis was used to mutate the reported tyrosine and arginine phosphorylation sites of FlgN to (i) alanine to assess the effects of preventing phosphorylation, or (ii) glutamic acid to assess the effects of mimicking the negative charge associated with phosphorylation. Mutated *flgN* alleles replaced the wild-type *flgN* on the chromosome.

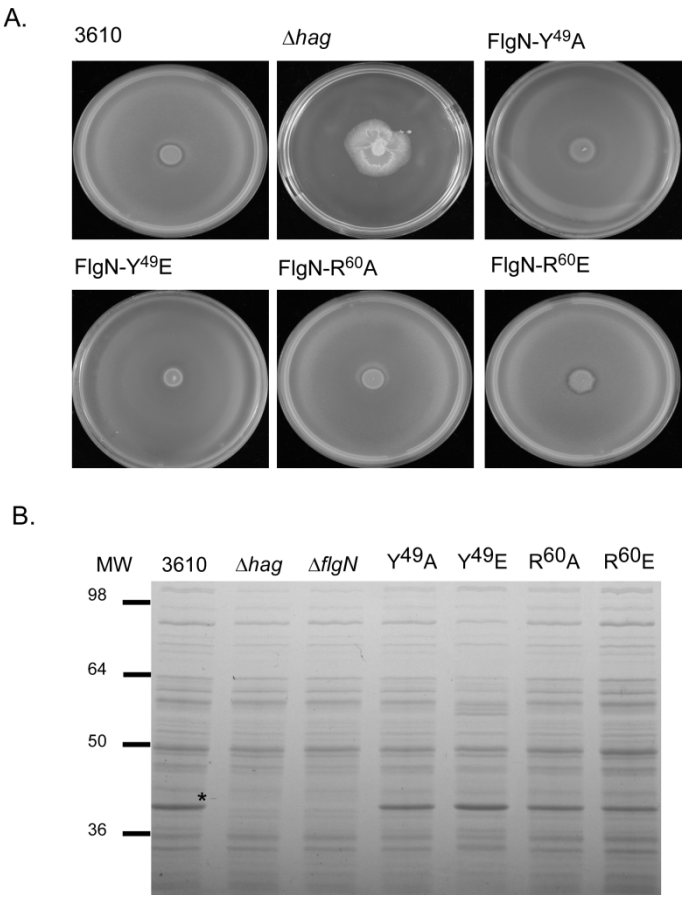

Figure 3-16 Motility analysis of strains carrying mutations of reported FlgN phosphorylation sites. (A) Photographs of swarm expansion plates taken after 6 hours incubation at 37 °C. Strains shown are wild-type (3610), Δ*hag* (DS1677), *flgN* $Y^{49}A$ (NRS3571), *flgN* $Y^{49}E$ (NRS3724), *flgN* $Y^{49}A$ (NRS4063) and *flgN* $Y^{49}E$ (NRS4017). **(B)** Coomassie gel analysis of cellular fractions of 3610, Δ*hag* (DS1677), *flgN* $Y^{49}A$ (NRS3571), *flgN* $Y^{49}E$ (NRS3724), *flgN* $Y^{49}A$ (NRS4063) and *flgN* $Y^{49}E$ (NRS4017). The Hag protein is marked with an asterisk.

Tyrosine at position 49 of FlgN has been reported to be phosphorylated by PtkA by both mass spectrometry approaches and *in vitro* kinase assays. To assess the impact of this residue on motility, tyrosine 49 was mutated to alanine (FlgN-$Y^{49}A$) or glutamic acid (FlgN-$Y^{49}E$) and the effects on motility assessed. As shown in **Figure 3-16A**, both strains exhibited a motility phenotype that was indistinguishable from the wild-type. Subsequently, strains were constructed where the coding region of *flgN* on the chromosome was mutated such that the arginine at position 60 was replaced with either alanine or glutamic acid. The motility phenotypes of these strains were tested and found to swarm at the same rate as the wild-type strain (**Figure 3-16A**). SDS-PAGE analysis of whole cell lysates also showed that Hag was synthesised and cellular localisation was directly comparable to wild-type for each of the point

mutation strains (**Figure 3-16B**). These data demonstrate that neither mutation of the previously defined tyrosine nor arginine phosphorylation sites had an effect on the function of FlgN in the NCIB3610 *B. subtilis* strain.

3.10 Discussion

This work identifies *flgN* of *B. subtilis* as being required for flagellar motility. These experiments demonstrate that the main role for FlgN is to enable flagellar filament polymerisation. The data presented allow us to conclude that *Bs*-FlgN is indeed an orthologue of FlgN from *S.* Typhimurium, but in *B. subtilis* it would appear that there is a strict reliance on FlgN for the secretion and placement of FlgK and FlgL at the hook-filament junction. However, mutation of the identified *Bs*-FlgN phosphorylation sites failed to impact motility. Possible explanations for this are discussed.

3.10.1 The role of FlgN in the regulation of flagellar biosynthesis

This work suggests that FlgN partially mediates flagella biosynthesis through its ability to regulate *hag* transcription and translation. In wild-type *B. subtilis* the sigma factor σ^D (*sigD*) needed for *hag* transcription is only transcribed in a sub-population of cells, resulting in bimodal expression of *hag* (Kearns & Losick, 2005, Cozy & Kearns, 2010). Deletion of *flgN* sees *hag* transcribed in every cell, albeit at a lower level (**Figure 3-4**), indicating that σ^D is active in every cell in this genetic background. Consistent with this, cell chaining was not observed in the absence of *flgN*, inferring that the autolysins, also under the control of a σ^D-driven promoter (Marquez *et al.*, 1990), are transcribed in all cells. It is known that σ^D can be regulated by both transcription of the *sigD* gene and by the anti-sigma factor, FlgM (Cozy & Kearns, 2010) Therefore, the change in *hag* transcription upon deletion of *flgN* might be explained by a change in regulation by the anti-sigma factor, FlgM. In *S.* Typhimurium FlgM regulates the transcription of late class σ^{28}-regulated flagellar genes by both sequestering free σ^{28} and destabilising the σ^{28} RNA polymerase holoenzyme complex (Chadsey *et al.*, 1998). Upon completion of HBB assembly, FlgM is secreted and σ^{28} is able to activate target promoters (Kutsukake, 1994). It has been previously reported that FlgN is able to regulate the translation of FlgM in *S.* Typhimurium (Karlinsey *et al.*, 2000a), therefore raising the possibility that in the

Δ*flgN* strain translation of FlgM is decreased allowing σ^D to trigger transcription of *hag* in all cells. However, the transcriptional profile of *hag* is also altered in the absence of *flgK* and *flgL*. These findings indicate that it is the hook-filament junction itself that acts as a signal to regulate *hag* transcription. Traditionally completion of the hook is viewed as a checkpoint for flagellar assembly (Hughes *et al.*, 1993). Our data infer that, at least in *B. subtilis*, completion of the hook-filament junction could additionally function as an important regulatory checkpoint. These effects could conceivably occur by directly affecting the production, activity or secretion of FlgM, or by modulating FlgN, which could in turn control FlgM. Such regulation has not been studied previously in *S.* Typhimurium. The regulation of FlgM in *B. subtilis* is poorly understood and so whether FlgN, FlgK or FlgL impact FlgM remains to be determined.

Deletion of *flgN* also sees a 2-fold decrease in *hag* translation (**Figure 3-5**). This effect could be due to translational regulation as is seen for the Δ*flgE* strain (**Figure 3-5**) (Mukherjee *et al.*, 2011). Indeed, recent studies in *B. subtilis* have identified the RNA binding protein CsrA, the CsrA regulatory protein FliW and the molecular chaperone FliS as having roles in controlling Hag translation or secretion (Yakhnin *et al.*, 2007, Mukherjee *et al.*, 2011, Mukherjee *et al.*, 2013). When cellular levels of Hag are depleted, FliW binds to CsrA leaving it unable to occlude the *hag* Shine-Dalgarno sequence, allowing translation to proceed. When Hag protein accumulates in the cytoplasm it is able to interact with and sequester FliW, resulting in CsrA-mediated repression of translation (Mukherjee *et al.*, 2011). Therefore, inhibition of translation by CsrA relies on accumulation of Hag within the cell. However, the data presented in **Figure 3-6** show that in the absence of *flgN*, Hag does not accumulate in the cytoplasm but in the extracellular milieu. This not only suggests that CsrA is not responsible for the observed decrease in Hag translation, but is also in keeping with the hypothesis that FlgN is required for the assembly of FlgK and FlgL; in the absence of the hook-filament junction flagellin cannot be properly assembled and so accumulates in the extracellular milieu (Gygi *et al.*, 1997).

Therefore these data support the hypothesis that the change in the transcriptional profile of *hag* is responsible for the decrease in translation observed.

Consistent with the hypothesis that *Bs*-FlgN is an orthologue of *S*T-FlgN, deletion of *flgK-flgL* from the *B. subtilis* chromosome phenocopied deletion of *flgN* with respect to motility, *hag* transcription and translation and Hag polymerisation (**Figure 3-8**, **Figure 3-9**, **Figure 3-4** and **Figure 3-6**, respectively). However, unexpectedly, over-expression of *flgK-flgL* was not sufficient to complement the motility defect of the Δ*flgN* strain (**Figure 3-10**). In *S.* Typhimurium, FlgK and FlgL have been shown to directly interact with the cytoplasmic domain of FlhA (an integral membrane protein required for protein export), which is thought to allow their secretion in the absence of their cognate chaperone (Minamino *et al.*, 2012). The data presented here would suggest that this is not seen in *B. subtilis* and that FlgN is essential for FlgK and FlgL export. In support of this hypothesis, primary sequence and secondary structure analyses revealed that *B. subtilis* FlgK lacks a stretch of 72 amino acids found at the C-terminus of *S.* Typhimurium FlgK (**Figure 3-17A**). We infer that this region might be important for the interaction of *S.* Typhimurium FlgK with FlhA. The absence of such a region in *B. subtilis* FlgK could contribute towards explaining the essentiality of FlgN for motility even in the presence of excess FlgK. Similarly, short amino acid sequences are also missing from *B. subtilis* FlgL (**Figure 3-17B**). Together these data indicate that there is a stricter reliance on FlgN in *B. subtilis* for export of the hook-filament junction proteins than in *S*. Typhimurium. This is perhaps not surprising given that deletion of *Bs-flgN* causes a complete loss of flagellar biosynthesis, as shown by both Western blot and fluorescence microscopy (**Figure 3-6** and **Figure 3-7**), whereas deletion of *S*T-*flgN* usually sees one or two flagella synthesised per cell (Kutsukake *et al.*, 1994).

A.

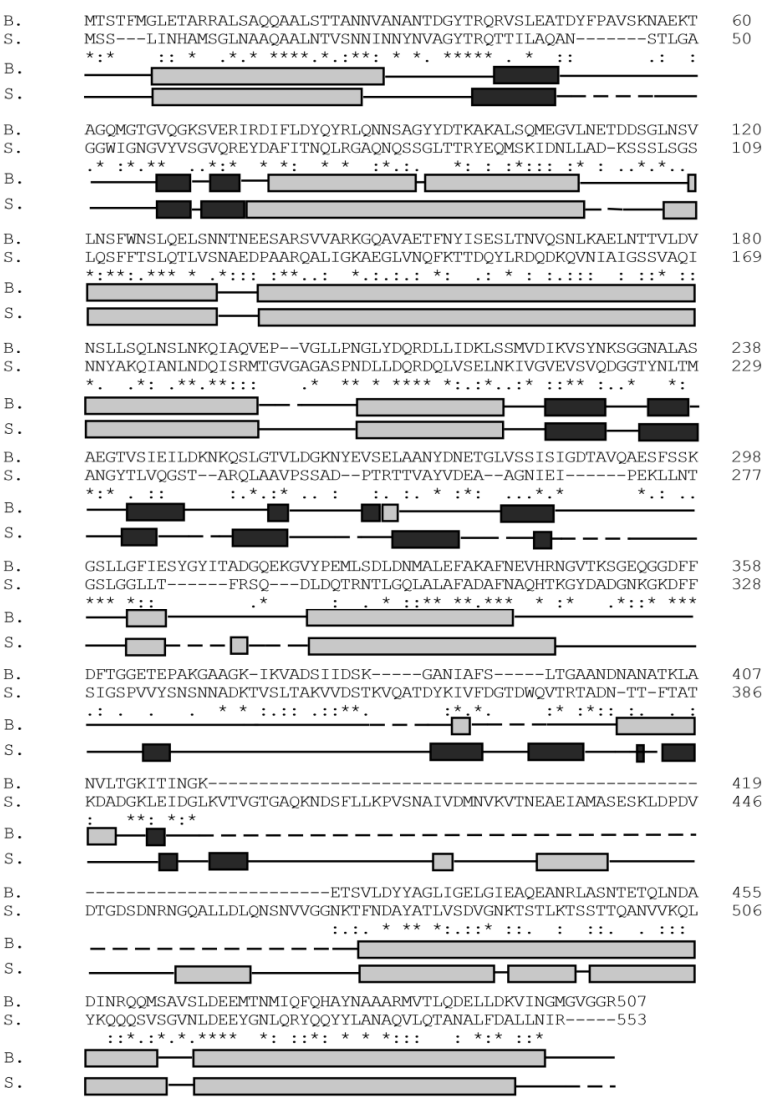
B. MTSTFMGLETARRALSAQQAALSTTANNVANANTDGYTRQRVSLEATDYFPAVSKNAEKT 60
S. MSS---LINHAMSGLNAAQAALNTVSNNINNYNVAGYTRQTTILAQAN-------STLGA 50
B. AGQMGTGVQGKSVERIRDIFLDYQYRLQNNSAGYYDTKAKALSQMEGVLNETDDSGLNSV 120
S. GGWIGNGVYVSGVQREYDAFITNQLRGAQNQSSGLTTRYEQMSKIDNLLAD-KSSSLSGS 109
B. LNSFWNSLQELSNNTNEESARSVVARKGQAVAETFNYISESLTNVQSNLKAELNTTVLDV 180
S. LQSFFTSLQTLVSNAEDPAARQALIGKAEGLVNQFKTTDQYLRDQDKQVNIAIGSSVAQI 169
B. NSLLSQLNSLNKQIAQVEP--VGLLPNGLYDQRDLLIDKLSSMVDIKVSYNKSGGNALAS 238
S. NNYAKQIANLNDQISRMTGVGAGASPNDLLDQRDQLVSELNKIVGVEVSVQDGGTYNLTM 229
B. AEGTVSIEILDKNKQSLGTVLDGKNYEVSELAANYDNETGLVSSISIGDTAVQAESFSSK 298
S. ANGYTLVQGST--ARQLAAVPSSAD--PTRTTVAYVDEA--AGNIEI------PEKLLNT 277
B. GSLLGFIESYGYITADGQEKGVYPEMLSDLDNMALEFAKAFNEVHRNGVTKSGEQGGDFF 358
S. GSLGGLLT------FRSQ---DLDQTRNTLGQLALAFADAFNAQHTKGYDADGNKGKDFF 328
B. DFTGGETEPAKGAAGK-IKVADSIIDSK-----GANIAFS-----LTGAANDNANATKLA 407
S. SIGSPVVYSNSNNADKTVSLTAKVVDSTKVQATDYKIVFDGTDWQVTRTADN-TT-FTAT 386
B. NVLTGKITINGK---------- 419
S. KDADGKLEIDGLKVTVGTGAQKNDSFLLKPVSNAIVDMNVKVTNEAEIAMASESKLDPDV 446
B. ----------ETSVLDYYAGLIGELGIEAQEANRLASNTETQLNDA 455
S. DTGDSDNRNGQALLDLQNSNVVGGNKTFNDAYATLVSDVGNKTSTLKTSSTTQANVVKQL 506
B. DINRQQMSAVSLDEEMTNMIQFQHAYNAAARMVTLQDELLDKVINGMGVGGR507
S. YKQQQSVSGVNLDEEYGNLQRYQQYYLANAQVLQTANALFDALLNIR-----553

B.

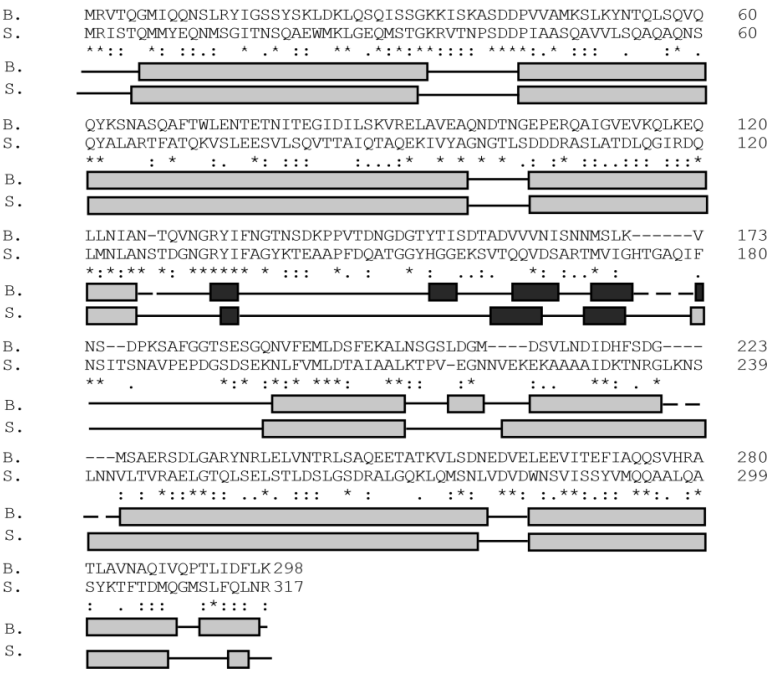
B. MRVTQGMIQQNSLRYIGSSYSKLDKLQSQISSGKKISKASDDPVVAMKSLKYNTQLSQVQ 60
S. MRISTQMMYEQNMSGITNSQAEWMKLGEQMSTGKRVTNPSDDPIAASQAVVLSQAQAQNS 60
B. QYKSNASQAFTWLENTETNITEGIDILSKVRELAVEAQNDTNGEPERQAIGVEVKQLKEQ 120
S. QYALARTFATQKVSLEESVLSQVTTAIQTAQEKIVYAGNGTLSDDDRASLATDLQGIRDQ 120
B. LLNIAN-TQVNGRYIFNGTNSDKPPVTDNGDGTYTISDTADVVVNISNNMSLK------V 173
S. LMNLANSTDGNGRYIFAGYKTEAAPFDQATGGYHGGEKSVTQQVDSARTMVIGHTGAQIF 180
B. NS--DPKSAFGGTSESGQNVFEMLDSFEKALNSGSLDGM----DSVLNDIDHFSDG---- 223
S. NSITSNAVPEPDGSDSEKNLFVMLDTAIAALKTPV-EGNNVEKEKAAAAIDKTNRGLKNS 239
B. ---MSAERSDLGARYNRLELVNTRLSAQEETATKVLSDNEDVELEEVITEFIAQQSVHRA 280
S. LNNVLTVRAELGTQLSELSTLDSLGSDRALGQKLQMSNLVDVDWNSVISSYVMQQAALQA 299
B. TLAVNAQIVQPTLIDFLK298
S. SYKTFTDMQGMSLFQLNR317

Figure 3-17 Primary sequence and secondary structure alignments of FlgK and FlgL. Primary sequence and secondary structure alignments for **(A)** FlgK from *B. subtilis* and *S.* Typhimurium and **(B)** FlgL from *B. subtilis* and *S.* Typhimurium. B. represents *B. subtilis* and S represents *S.* Typhimurium. For primary sequence alignments an asterisk indicates a fully conserved amino acid, a colon indicates a highly conserved amino acid and a full stop indicates a weakly conserved amino acid. Gaps indicate no homology. Dashed lines indicate a break in the sequence. For secondary structure alignments light grey boxes indicate α-helices, dark grey rectangles indicate β-sheets, solid lines indicate coiled coils and dashed lines indicate a break in the sequence.

Despite extensive efforts, we were unable to prove that in the absence of *Bs-flgN*, FlgK and FlgL are not secreted. To assess this an antibody specific to FlgK could be raised and used to probe lysates collected from the extracellular milieu of a Δ*flgN* strain. In *S.* Typhimurium FlgN interacts with FlgK and FlgL (Fraser *et al*, 1999). We did not observe such an interaction in *B. subtilis* using the bacterial two hybrid experiments (in collaboration with Dr. Phillip Aldridge, Newcastle University, data not shown), but this could be due to limitations of the method used. Biochemical methods could be used to test for such interactions *in vitro*.

3.10.2 The role of FlgN phosphorylation

Tyrosine phosphorylation has been implicated in the control of diverse biological processes in *B. subtilis*, including DNA replication (Petranovic *et al.*, 2007), exopolysaccharide synthesis (Mijakovic *et al.*, 2003) and biofilm formation (Kiley & Stanley-Wall, 2010). The *Bs*-FlgN flagellar chaperone protein has been shown to be tyrosine phosphorylated and indeed, the sub-cellular localisation of *Bs*-FlgN was reported to be impacted by deletion of the tyrosine kinase PtkA (Jers *et al.*, 2010). These data, in combination with the knowledge that tyrosine phosphorylation is required for the formation of a wild-type biofilm, led to the hypothesis that tyrosine kinases may represent a means by which bacteria regulate the switch from motility to biofilm formation.

During the course of this work, the Gerth group and colleagues showed that *Bs*-FlgN was also phosphorylated on arginine (Elsholz *et al.*, 2012), representing an additional means by which

FlgN function may be regulated. Moreover, deletion of the arginine phosphatase, *ywlE*, leads to an increase in transcription of σ^D-dependent genes (Elsholz *et al.*, 2012), pointing towards an active role for arginine phosphorylation in the regulation or assembly of the flagellum (Elsholz *et al.*, 2012).

However, despite this prior information, site-directed mutagenesis of the reported FlgN tyrosine and arginine phosphorylation sites *in vivo* failed to impact motility of *B. subtilis.* These findings led us to conclude that a dominant role for phosphorylation of these residues does not exist. When these findings are considered in a wider context of the function of post-translational modifications they may not be surprising. For instance in eukaryotes, it has been suggested that many phosphorylation events are non-functional (Landry *et al.*, 2009). Both FlgN phospho-sites investigated here were originally identified by mass spectrometry (Macek *et al.*, 2007, Elsholz *et al.*, 2012), which despite being sensitive does not always give information on the stoichiometry of a modification (Landry *et al.*, 2009, Beltrao *et al.*, 2012). Additionally, a site may be phosphorylated but only at a very low stoichiometry. If this modification does not harm the cell, there may not be enough selective pressure for the site to be mutated to a non-phosphorylatable amino acid (Landry *et al.*, 2009). In *B. subtilis*, 21 proteins have been identified as being tyrosine phosphorylated (Mijakovic *et al.*, 2003, Levine *et al.*, 2006, Mijakovic *et al.*, 2006, Macek *et al.*, 2007, Petranovic *et al.*, 2009), while 87 proteins are arginine phosphorylated (Elsholz *et al.*, 2012). In contrast, only two tyrosine kinases (Mijakovic *et al.*, 2003, Gerwig *et al.*, 2014) and one arginine kinase have been identified in *B. subtilis* (Fuhrmann *et al.*, 2009), thereby suggesting that each kinase is promiscuous. This may infer that random encounters between kinases and phosphorylatable sites on different proteins might result in non-specific and non-functional phosphorylation events. Alternatively, FlgN might act as a phosphate-sink or store to remove free phosphate from the system (Sourjik & Schmitt, 1998).

The original aim of this study was to establish if tyrosine phosphorylation might be a key factor in regulating both motility and biofilm formation. The data presented in this chapter suggest that phosphorylation of *Bs*-FlgN does not impact motility. Currently, no other proteins predicted to play a role in flagellar regulation or biosynthesis have been identified as being modified on tyrosine by proteomic approaches. Furthermore, deletion of the gene encoding the tyrosine kinase PtkA does not impact motility (unpublished data, NSW group). Collectively, these data suggest that tyrosine phosphorylation does not play a role in *B. subtilis* flagellar motility.

3.10.3 Concluding remarks

The regulation and biosynthesis of the bacterial flagellum is best understood for Gram-negative bacterial species such as *S.* Typhimurium. However, recent work on *B. subtilis* has begun to illuminate how Gram-positive bacterial species are able to coordinate flagellar assembly. These studies have uncovered key differences between Gram-negative and Gram-positive bacterial flagella as well as having highlighted many conserved mechanisms. The data presented here illustrates that FlgN from *B. subtilis* is essential for flagellar filament polymerisation and therefore motility. We propose that *Bs*-FlgN is an orthologue of the *S.* Typhimurium chaperone protein, FlgN and is required for the export and assembly of FlgK and FlgL at the hook-filament junction. By way of contrast, in the absence of *Bs-flgN*, flagellar filaments are not detectable and over-expression of *flgK-flgL* is not sufficient to overcome the motility defect exhibited by the Δ*flgN* strain. Therefore, while *Bs*-FlgN bears functional similarity to S. Typhimurium FlgN, there are crucial differences which suggest that there is a stricter dependence on FlgN for the export of FlgK and FlgL in *B. subtilis*.

The function of phosphorylation of FlgN with regard to motility was also of interest. Only a limited number of studies have investigated the *in vivo* role of the effect of tyrosine or arginine phosphorylation of specific substrate proteins in *B. subtilis* (Fuhrmann *et al.*, 2009), with many

instead focussing experiments on the role of phosphorylation *in vitro* (Mijakovic *et al.*, 2006) or in strains where the kinase has been deleted (Petranovic *et al.*, 2007, Jers *et al.*, 2010). There is evidence to support the claim that bacterial phosphoproteins/phosphorylated residues are more conserved than non-phosphorylated proteins (Macek *et al.*, 2007). However, the work presented here suggests that, as in eukaryotes, *in vivo* characterisation of the effect of mutation of each identified bacterial phospho-site is needed to distinguish between functional and non-functional phosphorylation.

4

A mechanical signal transmitted by the flagellum controls signalling in *B. subtilis*

4.1 Experimental aims and objectives

In the natural environment bacteria predominantly live adhered to a surface as part of a biofilm. While many of the components needed for biofilm assembly are known, the mechanism by which microbes sense and respond to contact with a surface is poorly understood. Two component signal transduction pathways allow bacteria to sense and respond to the extracellular environment. The *Bacillus subtilis* DegS-DegU two component system comprises the sensor kinase, DegS and the response regulator, DegU. Phosphorylated DegU (DegU~P) is able to regulate a multitude of different multicellular behaviours. Of note for this work, low levels of DegU~P are required for swarming motility while intermediate levels are needed to promote transcription of *bslA*, which encodes a hydrophobic surface layer protein that coats the biofilm surface. High levels of DegU~P promote the transcription of protease genes, the major protease being subtilisin, encoded by the *aprE* gene, as well as activating transcription of genes needed to synthesise the exopolymer γ-PGA. Furthermore, a high level of DegU~P positively auto-regulates transcription of *degU* itself. The involvement of DegU~P in several specific processes has allowed the development of several different assays to indirectly measure DegU~P levels within the population.

Despite the ability of DegU~P to control several physiological processes, the signal that activates DegS and thus allows DegU~P to accumulate has remained elusive. Unpublished data from our group suggested a tentative link between flagellar assembly and DegU~P levels. Preliminary data from the Kearns group supported this hypothesis (Hsueh *et al.*, 2011). The aim of the work presented in this chapter was to investigate the link between assembly of the flagellum and the DegS-DegU two component signal transduction system. Given the role of DegS-DegU in both flagellar gene regulation and biofilm formation, it was hypothesised that DegS-DegU might present a means by which motile cells are able to detect and respond to the presence of a surface during the initial stages of biofilm formation. The work presented in this

chapter aimed to establish if inhibition of flagellar rotation might trigger activation of the DegS-DegU two component signal transduction system.

4.2 Deletion of *motB* from the chromosome is associated with a non-motile phenotype

To test if flagellar rotation was linked to the activity of the DegS-DegU two component system, an in-frame non-polar deletion in the flagellar stator gene, *motB* was constructed (NRS3494). It is well established that in different bacterial species disruption of the flagellar stator genes perturbs motility but has no effect on biosynthesis of the flagellum itself (Silverman *et al.*, 1976, Berg, 2003). Consistent with this, the *B. subtilis* Δ*motB* strain synthesised flagella, as determined by the presence of the Hag protein in whole cell lysates, but displayed a non-motile phenotype in swarming assays (**Figure 4-1A and C**). The observed motility defect was complemented upon re-introduction of the *motB* coding sequence on the chromosome under the control of an IPTG-inducible promoter ($P_{hy\text{-}spank}$) at the non-essential *amyE* locus (NRS3775), verifying the specificity in the deletion (**Figure 4-1B**). To test the effect of deletion of both stator components a Δ*motAB* (NRS3744) strain was constructed. It was established that the non-polar *motAB* deletion strain synthesised flagella and exhibited a motility defect that could be specifically complemented by heterologous induction of *motAB* transcription using an IPTG dependent promoter (**Figure 4-1B** and **C**). *B. subtilis* can also assemble the sodium driven stator complex, MotPS, however this complex is not functionally important under the experimental conditions used in this work (Ito *et al.*, 2004, Chan *et al.*, 2014).

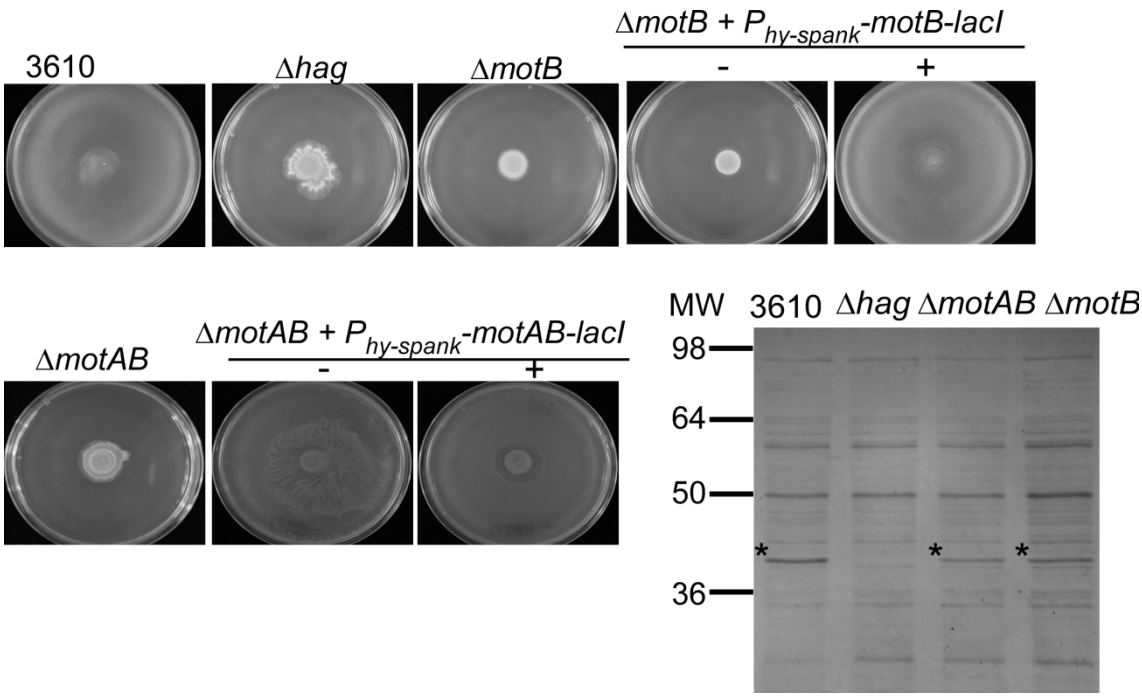

Figure 4-1 Motility and flagellar biosynthesis in strains lacking the flagellar stator genes. (A and B). Photographs of swarm expansion plates taken after incubation for 6 hours at 37 °C. Strains shown are **(A)** NCIB3610 (wild-type), Δ*hag* (DS1677), Δ*motB* (NRS3494), Δ*motB* + $P_{hy\text{-}spank}$-*motB-lacI* (NRS3775) grown in the absence (-) and presence (+) of 50 µM IPTG. **(B)** Δ*motAB* (NRS3744), Δ*motAB* + $P_{hy\text{-}spank}$-*motAB-lacI* (NRS4387) grown in the absence (-) and presence (+) of 50 µM IPTG. **(C)** Coomassie stained SDS-PAGE analysis of total cell protein (including assembled flagella) examining Hag polymerisation for strains, NCIB3610 (wild-type), Δ*hag* (DS1677), Δ*motAB* (NRS3744) and Δ*motB* (NRS3494). The Hag protein is indicated by the presence of an asterisk. MW indicates molecular weights in kDa.

4.3 Deletion of *motB* from the chromosome results in an increase in γ-poly-$_{D\text{-}L}$-glutamic acid production

4.3.1 Δ*motB* and Δ*motAB* strains display a mucoid colony morphology

Strikingly, as shown in **Figure 4-2A**, the Δ*motB* strain displayed a mucoid colony phenotype after growth overnight on LB solidified with 1.5 % agar. The mucoid colony morphology was specific to deletion of *motB* as the colony morphology reverted to the flat, dry phenotype exhibited by the wild-type strain upon heterologous expression of *motB* (**Figure 4-2**). An identical phenotype was also noted for the Δ*motAB* strain (**Figure 4-2B**). Production of the exopolymer poly-γ-$_{DL}$-glutamic acid (γ-PGA) has previously been linked with mucoid colony morphology in *B. subtilis* (Stanley & Lazazzera, 2005). The relationship between the mucoid

colony morphology of the *motB* deletion strain and γ-PGA production was confirmed as the mucoid phenotype was lost upon deletion of the *pgsB* gene, which encodes a γ-PGA synthetase, in the Δ*motB* background (**Figure 4-2B**).

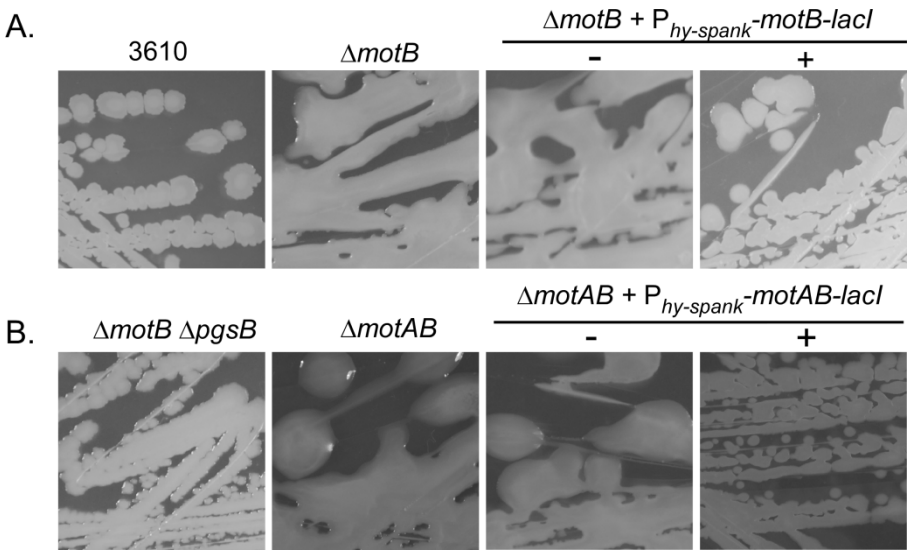

Figure 4-2 Colony morphology of Δ*motB* and Δ*motAB* strains. Colony morphology of **(A)** NCIB3610 (wild-type), Δ*motB* (NRS3494) and Δ*motB* + $P_{hy\text{-}spank}$-*motB-lacI* (NRS3775) grown in the absence (-) and presence (+) of 50 µM IPTG. **(B)** Δ*motB* Δ*pgsB::spc* (NRS3434), Δ*motAB* (NRS3744) and Δ*motAB* + $P_{hy\text{-}spank}$-*motAB-lacI* (NRS4387) grown in the absence (-) and presence (+) of 50 µM IPTG. *The NRS3494 and NRS3775 strains were originally constructed by Dr. Adam Ostrowski and their colony morphologies noted.*

To test if γ-PGA was also produced by the Δ*motB* strain upon growth in liquid culture, γ-PGA was biochemically extracted from culture supernatants collected at the onset of stationary phase. As shown in **Figure 4-3**, γ-PGA can be identified by SDS-PAGE analysis upon deletion of *motB*. This effect is lost by either heterologous expression of *motB* or deletion of *pgsB* in the Δ*motB* strain background.

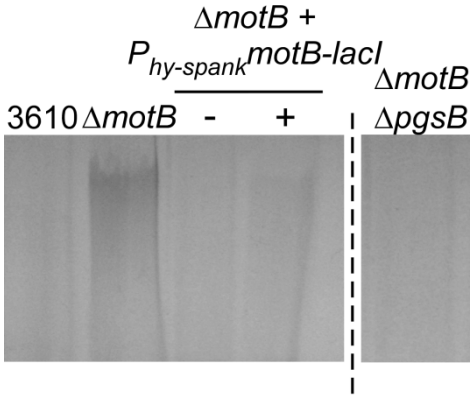

Figure 4-3 SDS-PAGE analysis of γ-PGA extracted from the Δ*motB* strain grown in liquid culture. γ-PGA was biochemically extracted from NCIB3610 (wild-type), Δ*motB* (NRS3494), Δ*motB* + $P_{hy\text{-}spank}$-*motB-lacI* (NRS3775) grown in the absence (-) and presence (+) of 50 μM IPTG and Δ*motB* Δ*pgsB::spc* (NRS3434) strains and resolved by SDS-PAGE. Dashed line separates data from two unique gels.

4.3.2 Poly-γ-glutamic acid production in the absence of *motB* is due to increased transcription of the γ–poly-$_{D\text{-}L}$-glutamic acid biosynthetic operon

Increased γ-PGA production in the absence of *motB* was predicted to be the consequence of: (i) decreased hydrolysis of γ-PGA and/or (ii) increased biosynthesis of γ-PGA. γ-PGA biosynthesis is driven by the protein products of the *pgsB* operon, while turnover is catalysed by the endo-γ-glutamyl peptidase, PgdS (schematic diagram shown in **Figure 4-4A**) (Candela & Fouet, 2006). Firstly, to test the hypothesis that increased γ-PGA production was due to decreased hydrolysis the colony morphologies of Δ*pgdS* and Δ*motB* Δ*pgdS* strains were compared. It was predicted that if decreased hydrolysis alone was sufficient to increase the level of γ-PGA secreted, a Δ*pgdS* strain should display a colony phenotype similar to that of the Δ*motB* strain. As shown in **Figure 4-4B**, deletion of *pgdS* exhibited a dry colony morphology. Moreover, γ-PGA could not be extracted when the Δ*pgdS* strain was grown in liquid culture (**Figure 4-4C**). Deletion of *pgdS* in the Δ*motB* strain phenocopied the Δ*motB* strain (compare **Figure 4-4C** with **Figure 4-2A**), while γ-PGA extracted from the double mutant Δ*pgdS* Δ*motB* strain could be resolved at a higher molecular weight by SDS-PAGE when compared with Δ*motB* alone (**Figure 4-4C**). This is consistent with the PgdS hydrolase retaining activity in the

absence of *motB*. Together, these data indicate that the increased γ-PGA production observed in the Δ*motB* strain is not due to decreased hydrolysis.

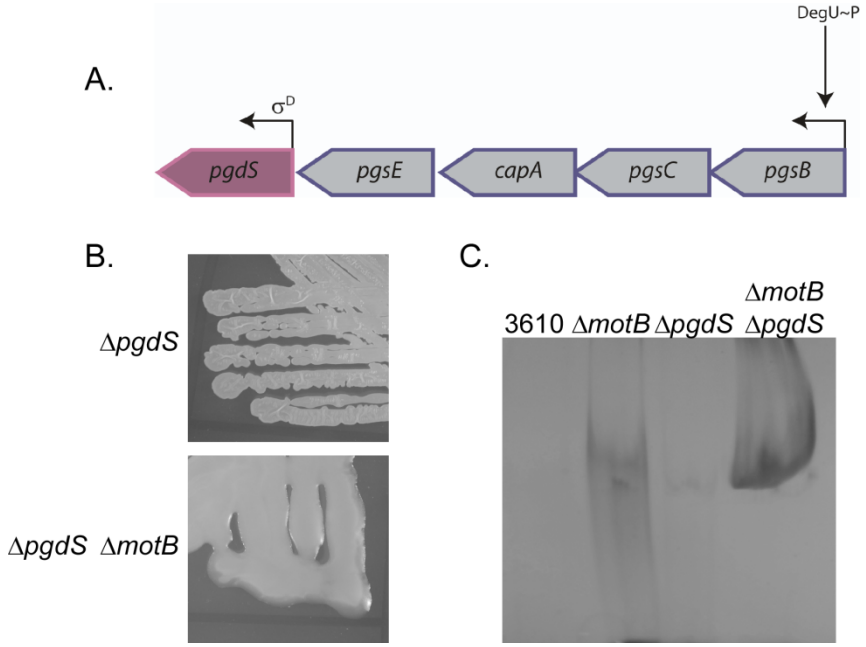

Figure 4-4 Assaying production of γ-PGA upon deletion of the gene that encodes the γ-PGA hydrolase enzyme, PgdS. (A) Schematic diagram of the γ-PGA synthesis operon and γ-PGA hydrolase gene. Arrows represent open reading frames (ORF), with the direction of the arrow indicating the direction of the ORF. The bent arrow represents the promoter located before the *pgdS* gene, which is driven by the alternative sigma factor, σ^D, as indicated. The promoter preceding the *pgsB* gene is activated by high levels of DegU~P. **(B)** Colony morphology of Δ*pgdS::cml* (NRS3347) and Δ*pgdS::cml* Δ*motB* (NRS3348). **(C)** SDS-PAGE analysis of γ-PGA extracted from liquid cultures of: NCIB3610 (wild-type), Δ*motB* (NRS3494), Δ*pgdS::cml* (NRS3347) and Δ*pgdS::cml* Δ*motB* (NRS3348). *Colony morphology images in part B were contributed by Ms. Emma Bissett.*

Consistent with deletion of *motB* triggering increased γ-PGA biosynthesis, RT-PCR analysis showed that transcription of the *pgsB* coding region (which encodes a γ-PGA synthetase) could not be detected in NCIB3610, but was detectable upon deletion of *motB* (**Figure 4-5**). This effect was complemented by heterologous expression of the *motB* coding region under the control of an IPTG-inducible promoter. In contrast, the *pgdS* coding region was transcribed in NCIB3610, Δ*motB* and the complemented strain. These data demonstrate that deletion of *motB* results in increased transcription of *pgsB*, triggering increased biosynthesis of the exopolymer γ-PGA.

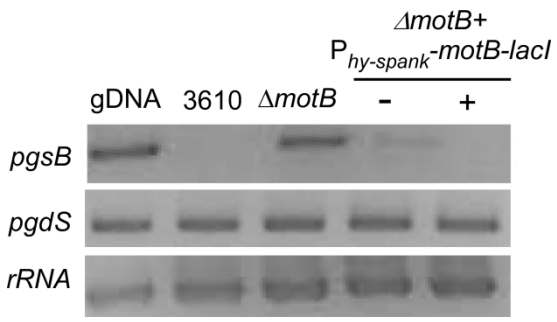

Figure 4-5 RT-PCR analysis of *pgsB* and *pgdS* transcription. Regions of DNA internal to *pgsB* and *pgdS* were amplified from cDNA generated from NCIB3610 (wild-type) Δ*motB* (NRS3494) and Δ*motB* + $P_{hy\text{-}spank}$-*motB-lacI* (NRS3775) strains grown in the absence and presence of 50 μM IPTG. Genomic DNA (gDNA) was used as a template PCR reactions as a positive control and the ribosomal 16S rRNA amplified as an internal control.

4.4 Increasing *degU32hy* expression allows poly-γ-glutamic acid production in *B. subtilis* NCIB3610

Consistent with the hypothesis that flagellar rotation might control the activity of the DegS-DegU two component system, production of γ-PGA is linked with high levels of DegU~P (Stanley & Lazazzera, 2005, Osera *et al.*, 2009). Transcription of the γ-PGA synthetase gene, *pgsB* is directly regulated by DegU~P (Ohsawa *et al.*, 2009), supporting the hypothesis that γ-PGA biosynthesis is increased in the Δ*motB* strain due to an increase in the level of DegU~P. It is worth noting that in certain *B. subtilis* isolates, such as R0-FF-1, γ-PGA is a component of the biofilm matrix (Stanley & Lazazzera, 2005, Morikawa *et al.*, 2006). However, in NCIB3610 this is not the case as γ-PGA is not synthesised, despite the presence of an intact γ-PGA biosynthetic operon on the chromosome (Branda *et al.*, 2006, Srivatsan *et al.*, 2008, Earl *et al.*, 2012). It was therefore hypothesised that in NCIB3610 the DegU~P levels are suppressed and that this suppression was alleviated upon deletion of *motB*. To test if directly increasing the level of DegU~P was sufficient to allow biosynthesis of γ-PGA by NCIB3610, the ability of a synthetic strain of NCIB3610 (NRS1325) to biosynthesise γ-PGA was tested. This strain contains a disruption in the native *degU* gene and carries an allele of *degU* (*degU32hy*) that encodes a DegU protein variant that carries a $H^{12}L$ amino acid mutation. The expression of *degU32hy* is under the control of an IPTG-inducible promoter ($P_{hyspank}$) and the construct is integrated on

the chromosome at the non-essential *amyE* locus (Verhamme *et al.*, 2007) (**Figure 4-6A**). The *degU32hy* gene encodes a DegU variant that is described as exhibiting a slower rate of dephosphorylation by comparison with the wild-type protein, thus increasing the level of DegU~P in the cell (Dahl *et al.*, 1992). As shown in **Figure 4-6B**, induction of *degU32hy* expression with 25 μM IPTG resulted in a highly mucoid colony phenotype. The relationship between the mucoid colony morphology and γ-PGA production was confirmed as γ-PGA could be biochemically extracted from culture supernatant collected at the onset of stationary phase upon induction of *degU32hy* expression (**Figure 4-6C**). Moreover, disruption of the γ-PGA synthetase gene, *pgsB*, in this background abolished γ-PGA production as assessed by the presence of flat, dry colonies (**Figure 4-6D**) and a lack of exopolymer extraction from the culture supernatant (**Figure 4-6C**).

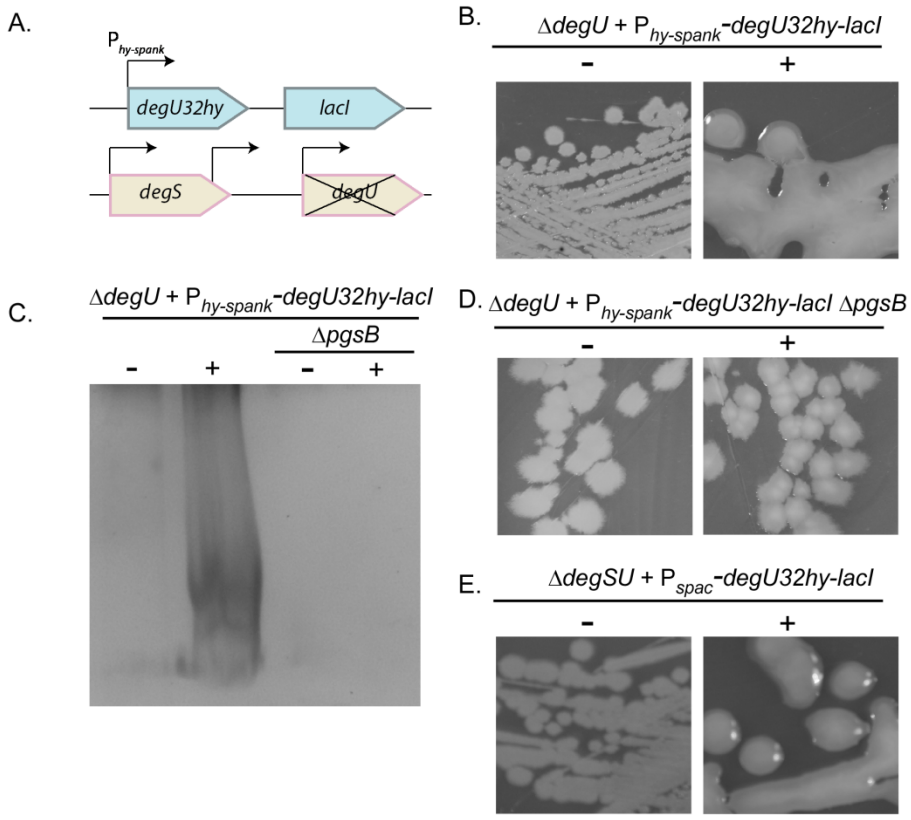

Figure 4-6 Expression of the *degU32hy* gene and its effect on γ-PGA production. (A) Schematic diagram of the construction of the Δ*degU::cml* + $P_{hy\text{-}spank}$-*degU32hy-lacI* strain (NRS1325). Bent arrows represent the promoters located before each gene. **(B)** Colony morphology of the Δ*degU::cml* + $P_{hy\text{-}spank}$-*degU32hy-lacI* (NRS1325) strain without (-) and with (+) induction with 25 µM IPTG. **(C)** SDS-PAGE of γ-PGA collected from cultures of Δ*degU::cml* + $P_{hy\text{-}spank}$-*degU32hy-lacI* (NRS1325) and Δ*degU::cml* + $P_{hy\text{-}spank}$-*degU32hy-lacI* + Δ*pgsB::spc* (NRS3770) grown to the onset of stationary phase in the absence or presence of 25 µM IPTG. **(D)** Colony morphology of the Δ*degU::cml* + $P_{hy\text{-}spank}$-*degU32hy-lacI* + Δ*pgsB::spc* (NRS3770) strain without (-) and with (+) induction with 25 µM IPTG. **(E)** Colony morphology of the Δ*degSU::spc* + P_{spac}-*degU32hy-lacI* (NRS4419) strain without (-) and with (+) induction with 50 µM IPTG.

Intriguingly, a strain carrying the *degU32hy* allele (under the control of the IPTG-inducible promoter, P_{spac}) retained the ability to biosynthesise γ-PGA in the absence of *degS*, as defined by a mucoid colony morphology (**Figure 4-6E**). These findings indicate that DegU $H^{12}L$ can be phosphorylated by another kinase or by a small molecular phosphoryl donor such as acetyl phosphate (Wolfe *et al.*, 2003, Wolfe *et al.*, 2008). Such a mechanism has been suggested previously for the accumulation of low levels of native DegU~P in the absence of *degS* (Kobayashi, 2007, Verhamme *et al.*, 2007). These data highlight that increasing the level of

DegU~P in NCIB3610 results in γ-PGA production. This is replicated upon deletion of *motB*, suggesting that upon inhibition of flagellar rotation DegU~P levels are increased.

4.5 The Δ*motB* strain displays increased DegU~P activity

4.5.1 Deletion of *motB* increases *degU* transcription

Due to the lability of phosphorylated aspartate residues, DegU~P levels have never been directly measured *in vivo*. Instead DegU~P levels are inferred from indirect measurements of (i) transcription of DegU~P target genes or (ii) measurement of the activation or inhibition of DegU~P regulated processes (Kobayashi, 2007, Verhamme *et al.*, 2007, Hsueh *et al.*, 2011). To determine if DegU~P levels were increased in the Δ*motB* strain two approaches were taken. Firstly, transcription of *degU* was quantified upon deletion of *motB* as an indirect measure of DegU~P levels. DegU~P positively auto-regulates transcription of *degU,* therefore measuring the level of activity from the *degU* promoter provides an indirect measurement of DegU~P in the cell (Kobayashi, 2007, Veening *et al.*, 2008) (**Figure 4-7A**). To this end, a P_{degU}-*lacZ* transcriptional reporter fusion was constructed and integrated into the wild-type, Δ*motAB* Δ*motB* and Δ*motB* complemented strains. Cells were harvested from cultures grown to the onset of stationary phase, and β-galactosidase assays performed. As shown in **Figure 4-7B**, in Δ*motB* transcription of *degU* was increased approximately four-fold when compared to the wild-type (P<0.01). This effect was specific to deletion of *motB* as transcription of *degU* could be restored to wild-type levels by expression of *motB* from an IPTG-inducible promoter integrated at a non-essential locus (**Figure 4-7B**).

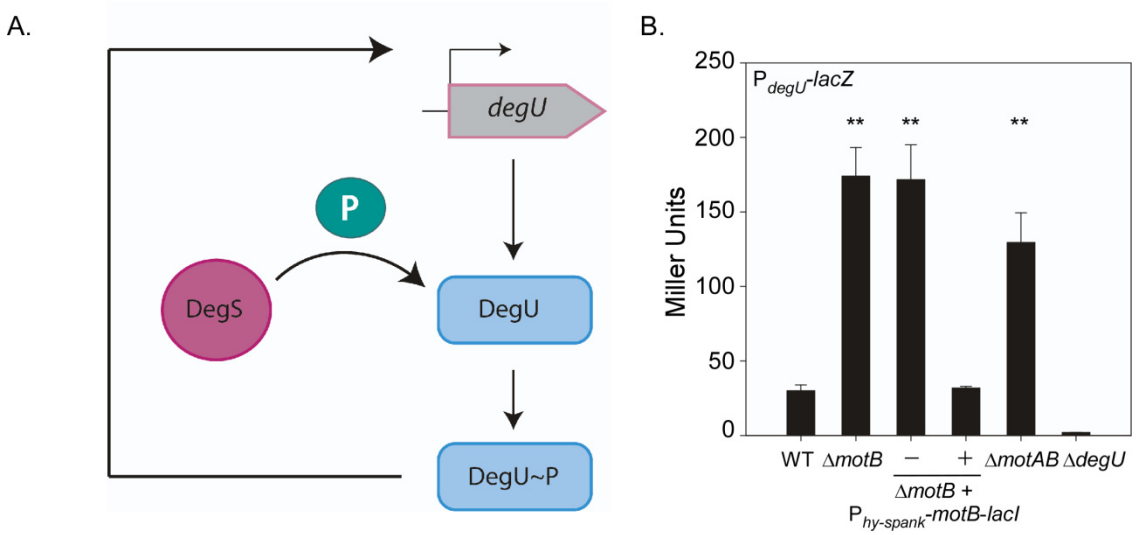

Figure 4-7 Quantification of *degU* transcription in the absence of the flagellar stator genes. (A) Schematic diagram of the effect of DegU~P on transcription of the *degU* gene. The bent blue arrow signifies the *degU* promoter, the bent black arrow represents the positive autoregulatory effect of DegU~P on the *degU* gene and the pink arrow represents transfer of the phosphoryl group to DegU, catalysed by DegS. **(B)** β-galactosidase assays of strains carrying the P_{degU}-*lacZ* transcriptional reporter fusion. Strains shown are WT (NRS4351), Δ*motB* (NRS4345), Δ*motB* + $P_{hy\text{-}spank}$-*motB-lacI* (NRS4396) grown in the absence or presence of 50 µM IPTG, Δ*motAB* (NRS4354) and Δ*degU::cml* (NRS4373). All cells were collected at the onset of stationary phase. Error bars represent standard error of the mean. An asterisk denotes significance as calculated by the Student's t-test where * represents *P*<0.05, ** *P*<0.01 and *** *P*<0.001.

4.5.2 Deletion of *motB* increases *aprE* transcription and total secreted protease activity

Secondly, exoprotease production was quantified. High levels of DegU~P are closely associated with exoprotease biosynthesis (Dahl *et al.*, 1992, Kobayashi, 2007, Verhamme *et al.*, 2007). DegU~P positively regulates transcription of the *aprE* gene, which encodes the alkaline protease subtilisin (Mukai *et al.*, 1990). It was therefore hypothesised that if DegU~P levels were high in the absence of *motB* this would correlate with an increase in *aprE* transcription and, moreover, an increase in the total protease activity in the extracellular environment. To establish if *aprE* transcription was altered in the Δ*motB* and Δ*motAB* strains, a P_{aprE}-*lacZ* transcriptional reporter fusion was integrated at the non-essential *thrC* locus. Cells were harvested for β-galactosidase activity assays and the culture supernatant collected for measurement of extracellular protease activity. Transcription of *aprE* was increased

approximately three-fold in the Δ*motB* strain (*P*<0.001) and two-fold in the Δ*motAB* strain (*P*<0.01) when compared with the wild-type (**Figure 4-8A**). The increase in transcription was specific as induction of *motB* transcription in the *motB* deletion strain reduced *aprE* transcription levels back to wild-type levels (**Figure 4-8A**). In accordance with these data, total protease activity was increased by 2-fold upon deletion of *motB* and 1.6-fold in the Δ*motAB* strain (**Figure 4-8B**) (*P*<0.01).

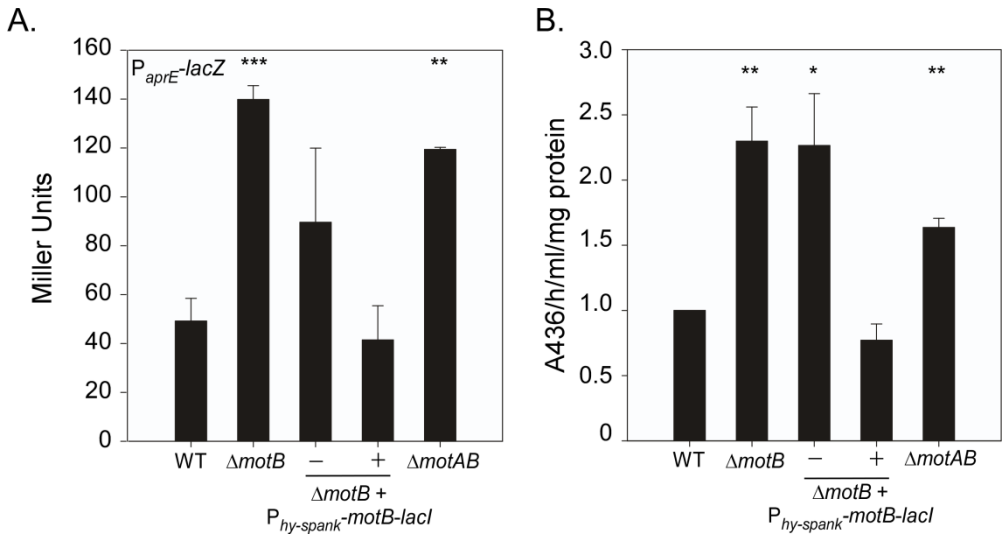

Figure 4-8 Quantification of protease gene transcription and protease activity in the absence of the flagellar stator genes. (A) β-galactosidase assays of strains carrying the P_{aprE}-*lacZ* transcriptional reporter fusion. Strains shown are WT (wild-type NRS1561), Δ*motB* (NRS3440), Δ*motB* + $P_{hy\text{-}spank}$-*motB-lacI* (NRS3858) grown in the absence or presence of 50 µM IPTG and Δ*motAB* (NRS4093). All cells were collected at the onset of stationary phase. **(B)** Total protease activity assays performed with the supernatant collected from cells grown in part (A). Data in parts A and B and are plotted as the average of at least 3 independent replicates; in B data are represented as a fold-change relative to the wild-type strain which was assigned value of 1. Error bars represent standard error of the mean. An asterisk denotes significance as calculated by the Student's t-test where * represents *P*<0.05, ** *P*<0.01 and *** *P*<0.001.

4.5.3 Up-regulation of DegU~P regulated processes in the absence of *motB* requires *degS*

Previous work (along with experiments presented in this chapter) has indicated that DegU can be phosphorylated in the absence of DegS (Kobayashi, 2007, Verhamme *et al.*, 2007) (**Figure 4-6D**). To demonstrate that the up-regulation in DegU~P processes seen in the Δ*motB* strain was transmitted through DegS, the *degS* gene was disrupted in the Δ*motB* background and γ-PGA production assessed by colony morphology. As seen in **Figure 4-9**, the colony morphology of the Δ*motB* Δ*degS* strain reverted to that of the wild-type. Collectively, these findings demonstrate that deletion of the flagellar stator gene, *motB*, causes an increase in the DegU~P level within the population, leading to an up-regulation of at least two distinct DegU~P regulated processes. These effects are reliant on the presence of DegS.

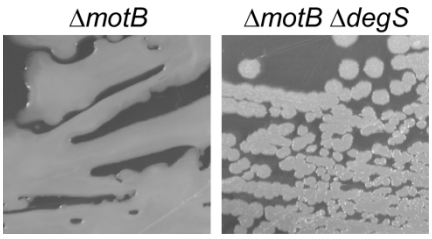

Figure 4-9 Colony morphology of Δ*motB* in the presence and absence of the *degS* gene. Colony morphology of Δ*motB* (NRS3494) and Δ*motB* Δ*degS::cml* (NRS3498).

4.6 Mutation of *motB* to prevent proton binding increases the level of DegU~P within the cell

4.6.1 Expression of *motB D²⁴A* cannot complement the motility defect of a *ΔmotB* strain

Given the importance of MotB in the generation of torque, it was hypothesised that the increase in DegU~P regulated processes in the Δ*motB* background might be linked with the inhibition of flagellar rotation. Torque is generated by specific interactions between the rotor and stator components (Zhou *et al.*, 1998a). The stator complex, which in *Escherichia coli* comprises a complex of four MotA proteins and two MotB proteins, forms two proton

channels (Braun *et al.*, 2004, Kojima & Blair, 2004). It is thought that proton flux through the channels triggers a conformational change that alters the electrostatic interactions between MotA and the rotor protein FliG, resulting in torque generation (Zhou *et al.*, 1998a, Braun *et al.*, 1999) (Schematic diagram in **Figure 4-10A**). Although the precise mechanisms by which torque is generated are not yet fully understood, it has been shown that protonation of a conserved aspartate residue in the MotB transmembrane domain is essential (Sharp *et al.*, 1995, Zhou *et al.*, 1998b). To test if disruption of proton flux through the MotAB complex, and therefore inhibition of flagellar rotation, were key to triggering an increase in DegU~P levels, the conserved aspartate residue of *motB* (aspartate 24 in *B. subtilis*; **Figure 4-10B**) was mutated to alanine (*motB* $D^{24}A$) by site-directed mutagenesis.

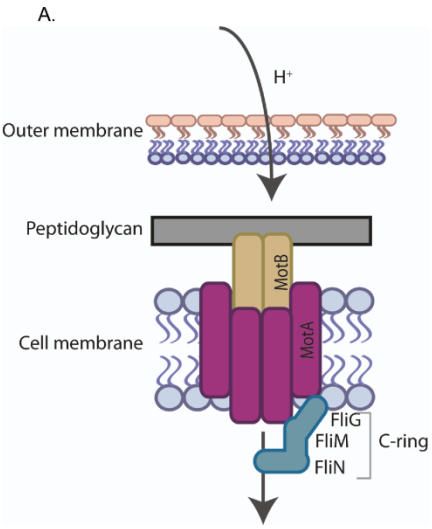

B.

```
E.      MKNQAHPIIVVKRRKAKSHGAAHGSWKIAYADFMTAMMAFFLVMWLISISSPKELIQIAE
B.      --------MARKKKKKHEDEHVDESWLVPYADILTLLLALFIVLYASSSIDAAKFQMLSK
                :. *::* :..  .. ** : ***::* ::*:*:*::  *  .  ::  :::

E.      YFRTPLATAVTGGDRISNSESPIPGGGD--DYTQSQG-EVNKQPNIEELKKRMEQSRLRK
B.      SF----NEVFTGGTGVLDYSSVTPPENESDGIDEVKKEKEEKEKNKKEKEKAADQEELEN
         *      ..***  : : .*  *   :     : :  : :*: * :* :*  :*..*.:

E.      LRGDLDQLIESDPKLRALRPHLKIDLVQEGLRIQIIDSQNRPMFRTGSADVEPYMRDILR
B.      VKSQVEKFIKD----KKLEHQLETKMTSEGLLITIKDS---IFFDSGKATIRKEDVPLAK
        ::.::::::*:.    : *. :*: .:..*** * * **    :* :*.* :.     : :

E.      AIAP-VLNGIPNRISLSGHTDDFPYASGEKGYSNWELSADRANASRRELMVGGLDSGKVL
B.      EISNLLVINPPRNIIISGHTDNMPIKNSE-FQSNWHLSVMRAVNFMGLLIENPKLDAKVF
         *:  ::   *..* :*****::*  ..*   ***.**. **      *:     ..**:

E.      RVVGMAATMRL--SDRGPDDAVNRRISLLVLNKQAEQAILHENAESQNEPVSALEKPEVA
B.      SAKGYGEYKPVASNKTAEGRSKNRRVEVLILPRGAAET---------NEK----------
         . * .    :  .. .   : ***:.:*:* : * ::         **

E.      PQVSVPTMPSAEPR
B.      --------------
```

Figure 4-10 Schematic of the flagellar motor and conservation of a conserved aspartic acid residue in the MotB protein. (A) Schematic diagram of the *E. coli* flagellar motor proteins MotA, MotB and FliG. Protons flow through the MotAB channel and are bound by a conserved aspartic acid residue in MotB. This results in a conformational change such that the interaction between MotA and FliG is altered, resulting in the generation of torque. **(B)** Primary sequence alignment of *B. subtilis* MotB (indicated by B.) and *E. coli* MotB (indicated by E.) generated using Clustal Omega (http://www.ebi.ac.uk/Tools/msa/clustalo/). The conserved aspartic acid (at position 24 in *B. subtilis*, and position 32 in *E. coli*) is highlighted in bold underline. An asterisk indicates a fully conserved amino acid, a colon indicates a highly conserved amino acid and a full stop indicates a weakly conserved amino acid. Gaps indicate no homology. Dashed lines indicate a break in the sequence.

The *motB* $D^{24}A$ allele was first integrated into the wild-type strain at a non-essential site on the chromosome under the control of an IPTG-inducible promoter. Upon induction of expression with 1 mM IPTG, the mutated *motB* allele conferred a dominant-negative phenotype with respect to both swarming motility (**Figure 4-11A**) and γ-PGA production (**Figure 4-11B**). These findings demonstrate that the MotB-$D^{24}A$ protein is synthesised and is functional as it has a dominant phenotype over the native MotB. Next, the construct was integrated into the Δ*motB* strain background. As expected, in contrast to complementation of the *motB* strain with the wild-type allele of *motB*, induction of *motB* $D^{24}A$ transcription did not restore motility to the *motB* deletion strain (**Figure 4-11C**).

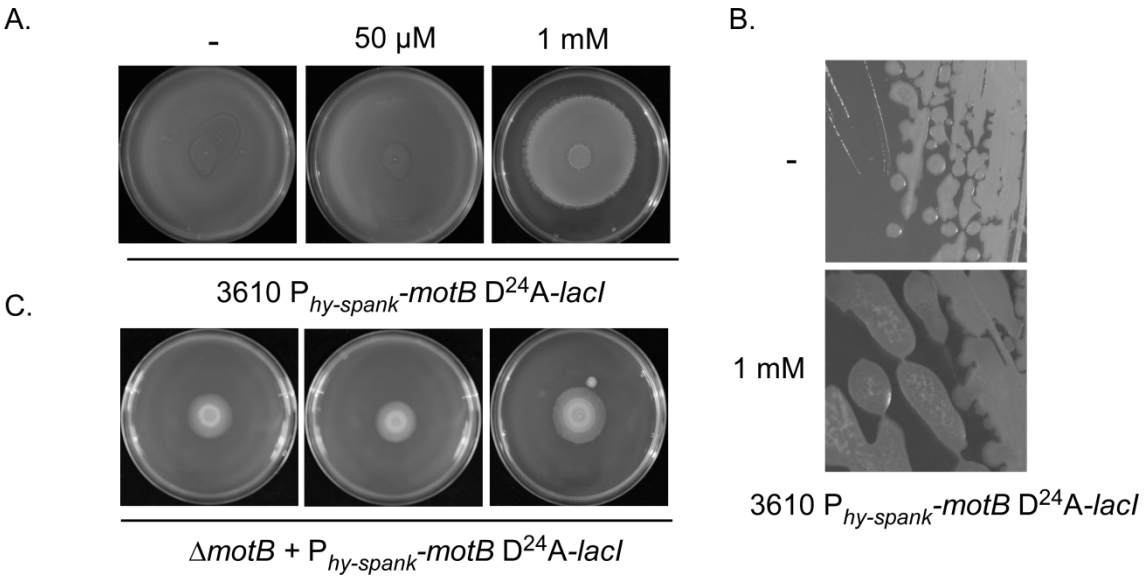

Figure 4-11 Characterisation of the *motB* $D^{24}A$ allele in *B. subtilis*. (A) Photographs of swarm expansion assay plates taken after 6 hours incubation at 37 °C using strain 3610 $P_{hy\text{-}spank}$-*motB* $D^{24}A$-*lacI* (NRS3868) grown in the absence and presence of 50 µM or 1mM IPTG and **(B)** Colony morphology of 3610 $P_{hy\text{-}spank}$-*motB*-$D^{24}A$-*lacI* (NRS3868) grown on LB agar overnight at 37 °C in the absence and presence of 1 mM IPTG. **(C)** Photographs of swarm expansion assay plates taken after 6 hours incubation at 37 °C. Strains shown are: Δ*motB* + $P_{hy\text{-}spank}$-*motB* $D^{24}A$-*lacI* (NRS3867) grown in the absence and presence of 50 µM or 1mM IPTG.

4.6.2 Mutation of *motB* to disturb proton flux phenocopies the *ΔmotB* strain.

Next the effect of the *motB* $D^{24}A$ mutation with regard to *degU* transcription, *aprE* transcription and exoprotease activity was quantified. It was determined that induction of *motB* $D^{24}A$ expression was unable to complement Δ*motB* with respect to both *degU* and *aprE* transcription, which remained 5-fold and 3-fold higher than in the wild-type, respectively (**Figure 4-11A** and **B**). Similarly protease activity was maintained at a higher level in the presence of *motB* $D^{24}A$ (**Figure 4-11C**).

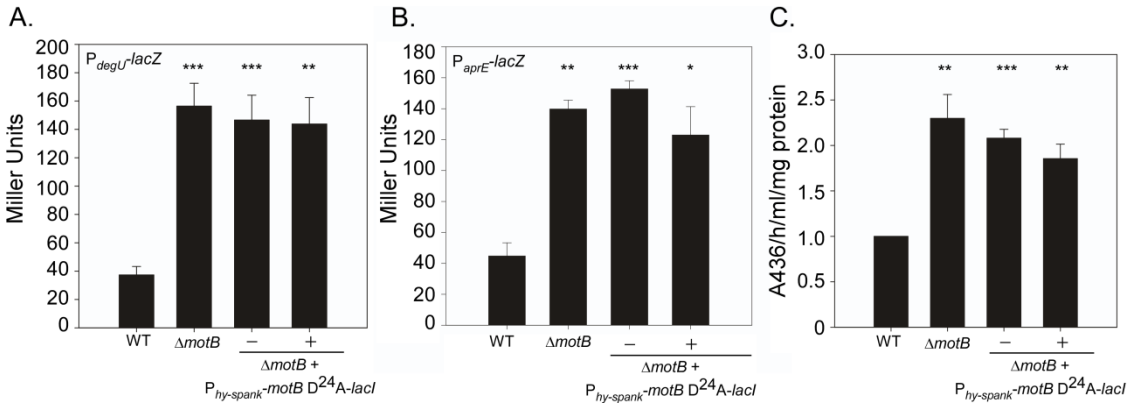

Figure 4-12 Quantification of the effect of MotB $D^{24}A$ on *degU* and *aprE* transcription and exoprotease activity. (A) β-galactosidase assays of strains carrying the P_{degU}-*lacZ* transcriptional reporter fusion. Strains shown are WT (wild-type NRS4351), Δ*motB* (NRS4345), Δ*motB* + $P_{hy\text{-}spank}$-*motB*-$D^{24}A$-*lacI* (NRS4397) grown in the absence or presence of 50 μM IPTG and Δ*degU::cml* (NRS4373). **(B)** β-galactosidase assays of strains carrying the P_{aprE}-*lacZ* transcriptional reporter fusion. Strains shown are WT (NRS1561), Δ*motB* (NRS3440), Δ*motB* + $P_{hy\text{-}spank}$-*motB*-$D^{24}A$-*lacI* (NRS3870) grown in the absence or presence of 50 μM IPTG. All cells in (A) and (B) were collected at the onset of stationary phase. **(C)** Total protease activity assays performed with supernatants collected from cells grown in part (B). Data in parts A, B and C are plotted as the average of at least 3 independent replicates. In part C data are represented as a fold change relative to the wild-type strain which was assigned a value of 1. Error bars represent standard error of the mean. An asterisk denotes significance as calculated by the Student's t-test where * represents $P<0.05$; ** $P<0.01$; and *** $P<0.001$. *Protease activity assays were carried out in collaboration with Dr. Victoria Marlow.*

γ-PGA production was also assessed by observation of a mucoid colony morphology and analysis of exopolymers extracted from culture supernatants (**Figure 4-12**). These data support the hypothesis that perturbation of proton flux through the Mot complex, and therefore flagellar rotation, is necessary to trigger an increase in DegU~P activity.

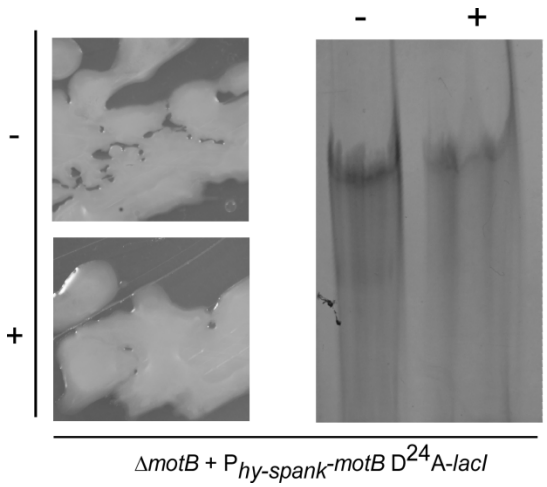

Figure 4-13 γ-PGA production in the presence of the MotB D^{24}A protein variant. Colony morphology (left panel) of Δ*motB* + P$_{hy\text{-}spank}$-*motB*-D^{24}A-*lacI* (NRS3870) grown on LB agar in the absence and presence of 50 μM IPTG overnight at 37 °C, and SDS-PAGE analysis (right panel) of γ-PGA collected from cultures of Δ*motB* + P$_{hy\text{-}spank}$-*motB*-D^{24}A-*lacI* (NRS3870) grown in the absence or presence of 50 μM IPTG.

4.7 Engaging the flagellar clutch causes an increase in DegU~P levels

4.7.1 The clutch function of EpsE stops flagellar motility

To assess if the increase in DegU~P regulated processes was specific to deletion or mutation of the flagellar stator genes, the effect of perturbing flagellar rotation by an alternative genetic means was tested. The *epsE* gene encodes a bi-functional protein, EpsE, that can act as (i) a flagellar clutch to disable flagellar rotation and (ii) a glycosyltransferase enzyme required for the formation of robust biofilms (Blair *et al.*, 2008, Guttenplan *et al.*, 2010). Over-expression of *epsE* under the control of an IPTG-inducible promoter inhibits motility by interaction with FliG, thereby disengaging the rotor from the stator (Blair *et al.*, 2008, Guttenplan *et al.*, 2010) (schematic shown in **Figure 4-14A**). To test if inhibition of flagellar rotation by over-expression of *epsE* would also trigger an increase in DegU~P levels, the coding region of *epsE* was integrated at a non-essential locus on the chromosome under the control of an IPTG-inducible promoter.

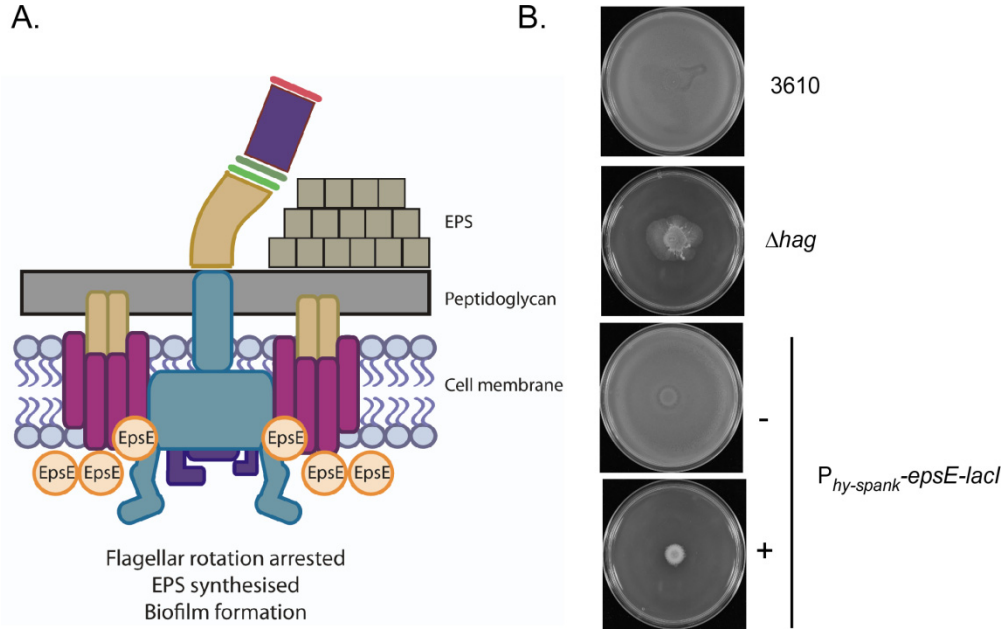

Figure 4-14 Effects of over-expression of *epsE* on swarming motility. **(A)** Schematic diagram of EpsE and its role in stopping flagellar rotation. **(B)** Swarm expansion assay for NCIB3610 (wild-type), Δ*hag* (DS1677) and $P_{hy\text{-}spank}$-*epsE* (NRS4085) in the absence (-) or presence (+) of 1 mM IPTG.

Firstly, the motility phenotype of the $P_{hyspank}$-*epsE-lacI* strain was assessed. As expected, this strain showed a swarming phenotype that was comparable to the wild-type strain in the absence of induction, but motility was lost entirely in the presence of 1 mM IPTG (**Figure 4-14B**).

4.7.2 Expression of *epsE* increases transcription of genes activated by high levels of DegU~P

As the motility phenotype was entirely in line with the previous report (Guttenplan *et al.*, 2010), the effect of over-expression of *epsE* on *degU* transcription was tested next. Both the wild-type and the *epsE* strains were grown to mid-exponential phase, at which point expression of *epsE* was induced by the addition of IPTG. Samples were collected over time to assess β-galactosidase activity. Induction of *epsE* resulted in a 4-fold increase in *degU* transcription by comparison with either the wild-type or the *epsE* strain grown in the absence of IPTG induction (**Figure 4-15**).

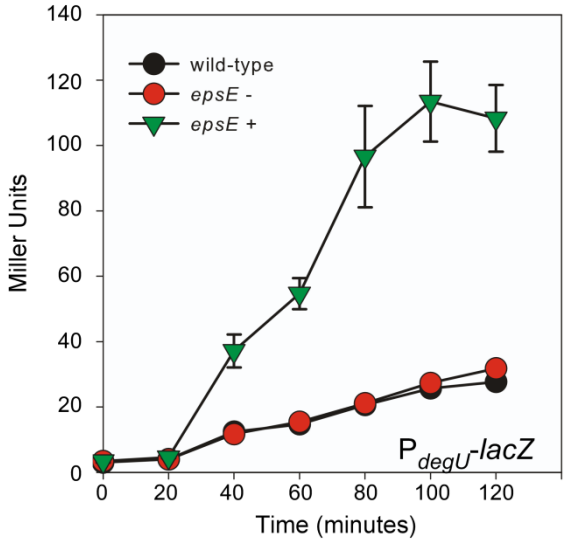

Figure 4-15 The effect of over-expression of *epsE* on *degU* trancription over time. β-galactosidase assays of strains carrying the P_{degU}-*lacZ* transcriptional reporter fusion. Cells were grown to 0.5 OD_{600} and induced with 1mM IPTG (final concentration). Strains shown are: wild-type (NRS4351) and *epsE* ($P_{hy\text{-}spank}$-*epsE-lacI;* NRS4374). The - and + symbols indicate the absence or presence of IPTG. Data are plotted as the average of at least 3 independent replicates. Error bars represent standard error of the mean.

To test if the up-regulation of *degU* transcription observed upon induction of *epsE* translated to an increase in DegU~P-regulated processes, the effect of over-expression of *epsE* on *aprE* transcription and total protease activity was tested. As seen for *degU* transcription, *aprE* transcription was increased 3-fold upon inhibition of flagellar rotation (**Figure 4-16A**). In accordance with the *aprE* transcription analysis data, 120 minutes after induction of *epsE* total protease activity was over 2-fold higher than the wild-type levels ($P<0.001$), while the protease activity in the absence of IPTG induction was not significantly different from the wild-type (**Figure 4-16B**).

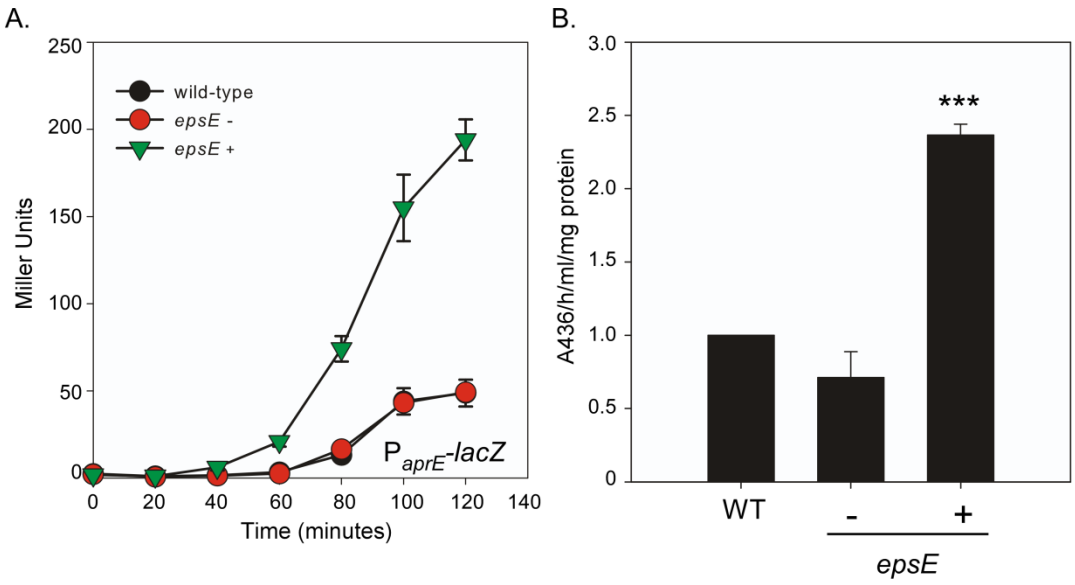

Figure 4-16 The effects of over-expression of *epsE* on *aprE* transcription and exoprotease activity. (A) β-galactosidase assays of strains carrying the P_{aprE}-*lacZ* transcriptional reporter fusion. Cells were grown to 0.5 OD_{600} and induced with 1mM IPTG (final concentration). Strains shown are: wild-type (NRS1561) and *epsE* ($P_{hy\text{-}spank}$-*epsE-lacI;* NRS4345). The - and + symbols indicate the absence or presence of IPTG. **(B)** Total protease activity assays performed with supernatants collected from cells grown in part (A). Data in parts A and B are plotted as the average of at least 3 independent replicates. In part B data are represented as a fold change relative to the wild-type strain which was assigned value of 1. Error bars represent standard error of the mean. An asterisk denotes significance as calculated by the Student's t-test where *** represents $P<0.001$.

Furthermore, the effect of inhibition of flagellar rotation on transcription of the *bslA* gene was also measured. The *bslA* promoter is the main target of DegU~P during biofilm formation by *B. subtilis* (Kobayashi, 2007, Ostrowski *et al.*, 2011) (**Figure 4-17A**). Therefore, it was hypothesised that an increase in DegU~P levels by inhibition of flagellar rotation would result in increased *bslA* transcription. A P_{bslA}-*lacZ* transcriptional reporter fusion was integrated into the *epsE* strain and activity measured over time by β-galactosidase assays. A similar trend to that reported for *degU* and *aprE* transcription was observed. Induction of expression of *epsE* resulted in a 3-fold increase in transcription by comparison with the wild-type (**Figure 4-17B**).

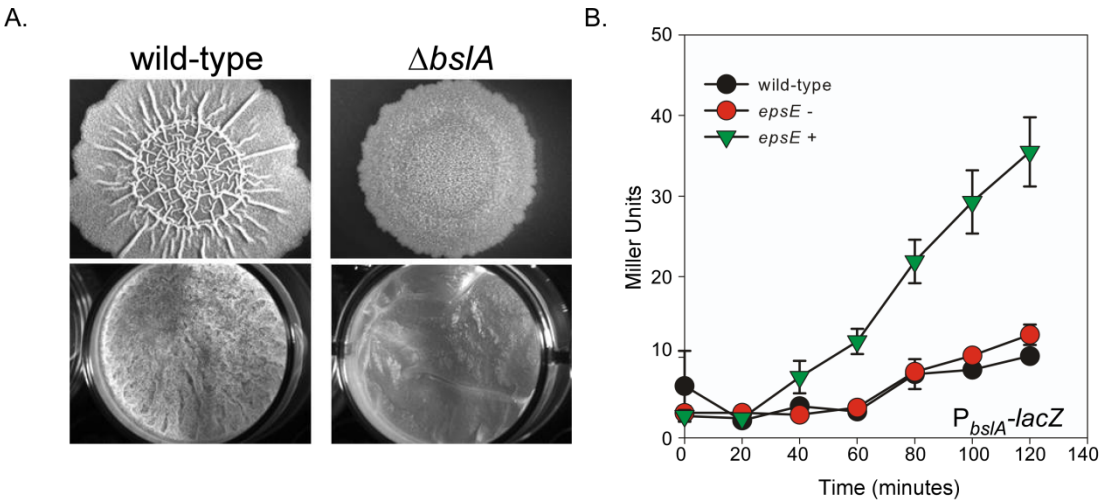

Figure 4-17 Quantification of the effect of over-expression of *epsE* on *bslA* transcription over time. (A) Complex colony (top panel) and pellicle (bottom panel) phenotypes of the wild-type strain (NCIB3610) and the Δ*bslA* strain (NRS2097) (Hobley *et al.*, 2013). **(B)** β-galactosidase assays of strains carrying the P_{bslA}-*lacZ* transcriptional reporter fusion. Cells were grown to 0.5 OD_{600} and induced with 1 mM IPTG (final concentration). Strains shown are: wild-type (NRS2052) and *epsE* ($P_{hy\text{-}spank}$-*epsE-lacI;* NRS4405). The - and + symbols indicate growth in the absence or presence of IPTG. Data are plotted as the average of at least 3 independent replicates. Error bars represent standard error of the mean.

Consistent with DegU~P directing both *bslA* transcription (Kobayashi, 2007, Verhamme *et al.*, 2009) and exoprotease production (Mukai *et al.*, 1990), it was noted that the level of *degU* transcription started to increase 20 minutes after IPTG induction of *epsE* transcription, whereas both *bslA* and *aprE* transcription began to rise 40 minutes post-induction (compare **Figure 4-15** with **Figure 4-16** and **Figure 4-17**). These data demonstrate that that *bslA* and *aprE* are only transcribed after the level of DegU~P increases, as inferred from the level of transcription from the *degU* promoter.

4.7.3 Expression of *epsE* increases γ–poly-$_{D\text{-}L}$-glutamic acid production

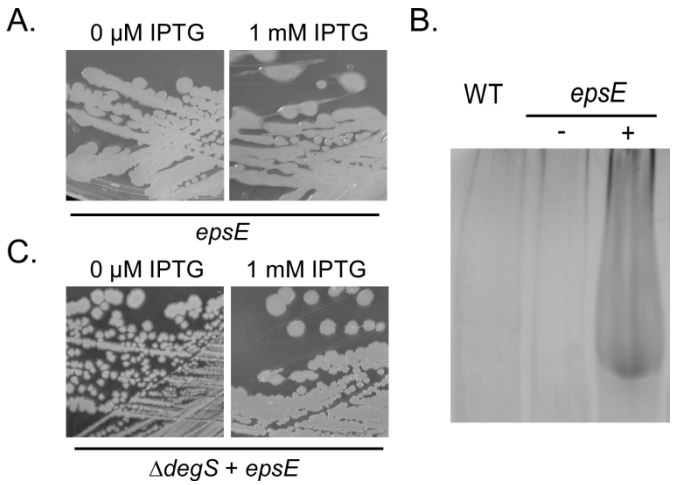

Figure 4-18 γ-PGA biosynthesis upon induction of *epsE* transcription. (A) Colony morphology of the *epsE* strain (*amyE::*P$_{hy\text{-}spank}$*-epsE-lacI*; NRS4085) grown on LB plates overnight at 37 °C in the absence and presence of 1 mM IPTG induction. **(B)** SDS-PAGE analysis of γ-PGA extracted from the culture supernatants of the WT (NCIB3610) and *epsE* (3610 *amyE::*P$_{hy\text{-}spank}$*-epsE-lacI*; NRS4085) strains in the absence (-) or presence (+) of 1 mM IPTG. **(C)** Colony morphology of the *epsE* strain (*amyE::*P$_{hy\text{-}spank}$ *-epsE-lacI* Δ*degS::cml* (NRS4399)) grown on LB plates overnight at 37 °C in the absence and presence of 1 mM IPTG induction.

The ability of a strain over-expressing *epsE* to synthesise γ-PGA was also assessed. Induction of *epsE* expression overnight on LB-agar plates containing 1 mM IPTG yielded a mucoid colony phenotype (**Figure 4-18**). Consistent with the colony phenotypes, γ-PGA could only be extracted upon induction of *epsE* expression. To determine if γ-PGA production, and hence the increased DegU~P levels, was reliant on input from DegS, the *degS* gene was disrupted in the *epsE* strain and γ-PGA production monitored using colony phenotype in the absence and presence of IPTG. A dry, flat colony morphology was observed. These findings indicate that the signal that causes a profound increase in DegU~P activity (as inferred from the assessment of several proxies of DegU~P activity) when flagellar rotation is attenuated is transmitted through the sensor kinase, DegS.

This work clearly shows that over-expression of the *epsE* gene results in an increase in DegU~P levels, which is reflected by an up-regulation of *bslA* transcription, exoprotease activity and γ-

PGA production. As for the *motB* strain (**Figure 4-9**), these effects require DegS. In concert, data describing the ability of deletion or mutation of *motB*, or indeed over-expression of *epsE*, to markedly increase DegU~P regulated processes supports the hypothesis that inhibition of flagellar rotation triggers an increase in DegU~P levels. However, given the bi-functional nature of the EpsE protein further experiments were undertaken to confirm these findings.

4.7.4 The clutch function of EpsE is essential for the increase in DegU~P regulated processes

To ensure that any effect on DegU~P was specific to the clutch activity of *epsE* and not due to the glycosyltransferase function, site-directed mutagenesis was used to mutate aspartate 94 to alanine (*epsE* $D^{94}A$) to yield a protein variant that retained clutch activity but lost glycosyltransferase functionality. In parallel, lysine 106 was mutated to glutamic acid (*epsE* $K^{106}E$) to yield a protein variant that lost clutch activity but possessed glycosyltransferase activity. Both single amino acid mutations have been previously characterised by Guttenplan *et al* (Guttenplan *et al.*, 2010).

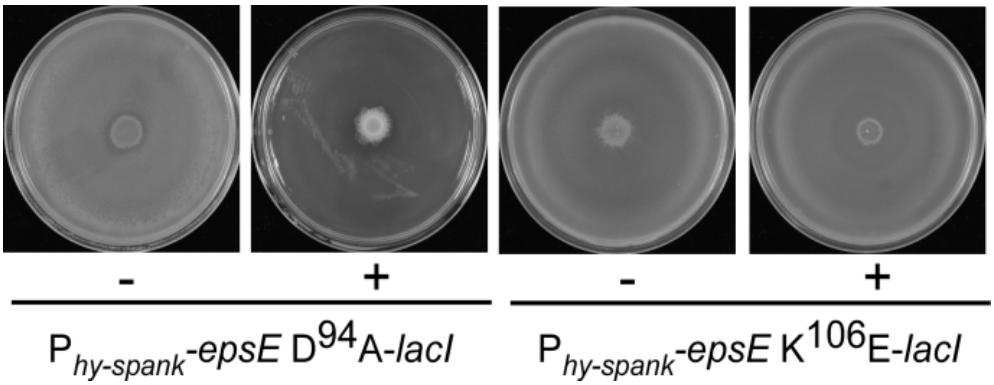

Figure 4-19 Swarming motility phenotypes of *epsE* $D^{94}A$ and *epsE* $K^{106}E$ strains. Photographs of swarming assays of $P_{hy\text{-}spank}$-*epsE* $D^{94}A$-*lacI* (NRS4388) and $P_{hy\text{-}spank}$-*epsE* $K^{106}E$-*lacI* (NRS4389) strains incubated in the absence (-) or presence (+) of 1 mM IPTG taken after incubation at 37°C for 6 hours.

Firstly, the motility phenotypes of these strains were assessed to ensure that the point mutations introduced functioned as expected. As shown in **Figure 4-19**, induction of the *epsE*

D^{94}A coding region inhibited swarming motility, while induction of the *epsE* K^{106}E coding region in the otherwise wild-type strain had no impact on swarming motility.

As these phenotypes are entirely in line with the previous report (Guttenplan *et al.*, 2010), strains were constructed where either the P_{degU}-*lacZ*, P_{aprE}-*lacZ* or P_{bslA}-*lacZ* transcriptional reporter fusions were integrated into each strain at non-essential loci. The effects of expression of the *epsE* mutant alleles on *degU* transcription, *aprE* transcription, exoprotease activity and *bslA* transcription were measured as previously for the wild-type allele of *epsE* (**Figure 4-15**, **Figure 4-16** and **Figure 4-17**, respectively).

Induction of *epsE* D^{94}A expression resulted in a 3-fold increase in *degU* transcription by comparison with the wild-type strain (compare **Figure 4-20A** with **Figure 4-15**). Similar phenotypes were observed for *bslA* transcription (a 3-fold increase upon induction of *epsE* D^{94}A; compare **Figure 4-20B** with **Figure 4-17B**) and *aprE* transcription (4-fold increase upon induction of *epsE* D^{94}A; compare **Figure 4-20C** with **Figure 4-16A**). Total protease activity was also increased approximately 4-fold upon IPTG induction of *epsE* D^{94}A (**Figure 4-20D** compared with **Figure 4-16B**). Induction of *epsE* K^{106}E had no effect on the transcription of the any DegU~P regulated genes tested (**Figure 4-20**).

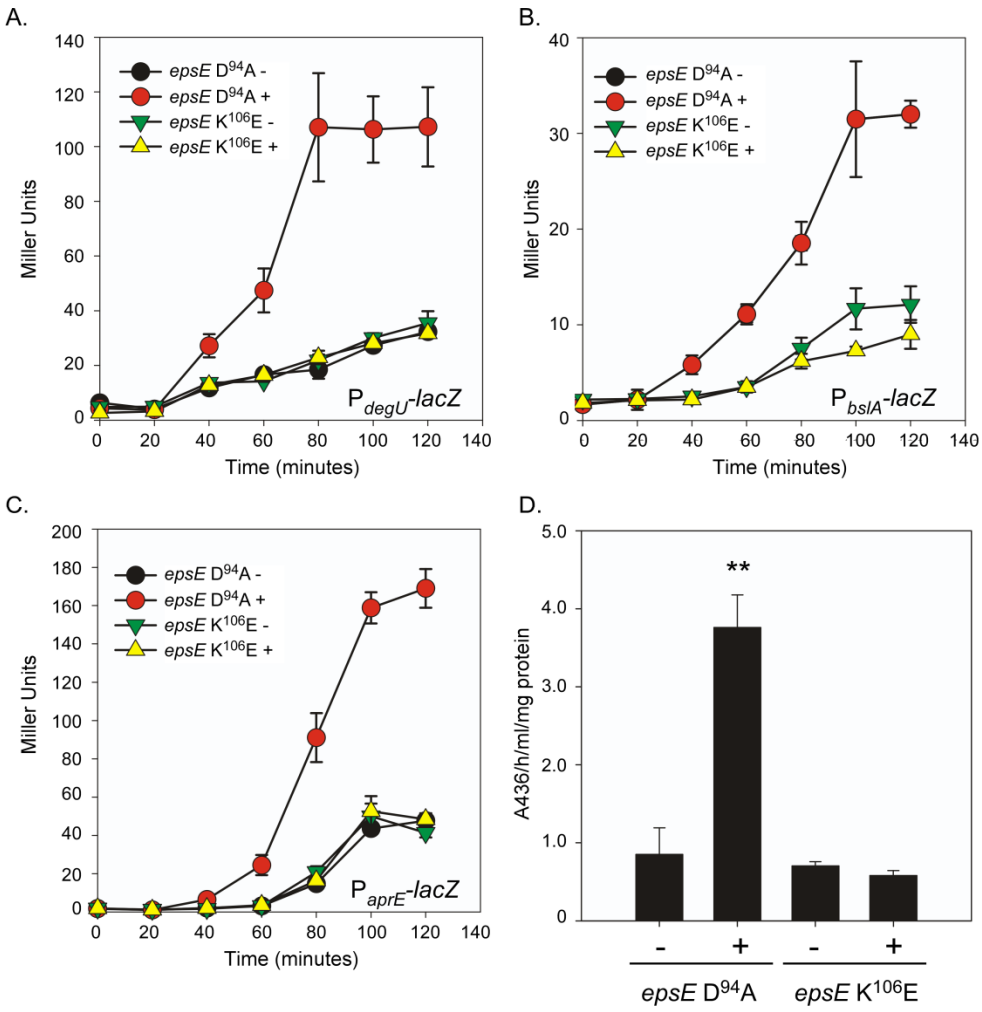

Figure 4-20 Quantification of the effects of EpsE protein variants on DegU~P regulated processes. β-galactosidase assays of strains carrying the **(A)** P_{degU}-*lacZ* **(B)** P_{bslA}-*lacZ* or **(C)** P_{aprE}-*lacZ* transcriptional reporter fusions. Cells were grown to 0.5 OD_{600} and induced with 1 mM IPTG (final concentration). Strains shown are: **(A)** *epsE* $D^{94}A$ ($P_{hy\text{-}spank}$-*epsE*-$D^{94}A$-*lacI*; NRS4392) and *epsE* $K^{106}E$ ($P_{hy\text{-}spank}$-*epsE*-$K^{106}E$-*lacI*; NRS4394) **(B)** $P_{hy\text{-}spank}$-*epsE*-$D^{94}A$-*lacI* (NRS4406) and $P_{hy\text{-}spank}$-*epsE*-$K^{106}E$-*lacI* (NRS4407); **(C)** $P_{hy\text{-}spank}$-*epsE*-$D^{94}A$-*lacI* (NRS4393) and $P_{hy\text{-}spank}$-*epsE*-$K^{106}E$-*lacI* (NRS4395). The – and + symbols denote without or with induction with 1 mM IPTG, respectively. **(D)** Total protease activity assays performed with supernatants collected from cells grown in part C after 120 minutes of growth in the absence (-) or presence (+) of 1 mM IPTG. Data are represented as a fold change relative to the wild-type strain which was assigned value of 1. An asterisk denotes significance as calculated by the Student's t-test, where ** represents $P<0.01$. For all parts of this figure data are represented as the average of at least 3 independent biological replicates and error bars represent standard error of the mean.

Finally, the impact of the EpsE protein variants on γ-PGA production was determined. A mucoid colony morphology could only be detected when *epsE* $D^{94}A$ was grown on LB agar at 37 °C overnight in the presence of 1 mM IPTG (**Figure 4-21A**). Colonies remained flat and dry in the absence of IPTG or indeed when expression of *epsE* $K^{106}E$ was induced. The mucoid

phenotype of *epsE* $D^{94}A$ was reliant on the presence of the *degS* gene, as was also noted for the mucoid colony morphology of the *epsE* wild-type and Δ*motB* strains (**Figure 4-21B**). Moreover, γ-PGA could also be extracted from liquid culture supernatants of *epsE* $D^{94}A$ grown in the presence of 1 mM IPTG (**Figure 4-21C**).

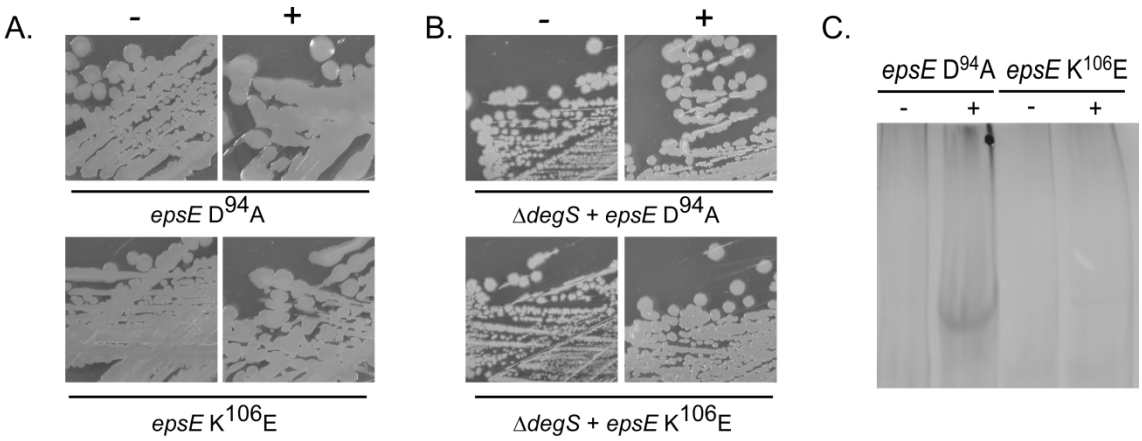

Figure 4-21 γ-PGA production in strains carrying EpsE protein variants in the presence and absence of the *degS* gene. (A) Colony morphologies of *epsE* $D^{94}A$ ($P_{hy\text{-}spank}$-*epsE*-$D^{94}A$-*lacI*; NRS4388) and *epsE* $K^{106}E$ ($P_{hy\text{-}spank}$-*epsE*-$K^{106}E$-*lacI*; NRS4389) in the absence (-) or presence (+) of 1 mM IPTG. **(B)** Colony morphology of Δ*degS epsE* $D^{94}A$ ($P_{hy\text{-}spank}$-*epsE*-$D^{94}A$-*lacI* Δ*degS::cml;* NRS4400) and Δ*degS epsE* $K^{106}E$ ($P_{hy\text{-}spank}$-*epsE*-$K^{106}E$-*lacI* Δ*degS::cml;* NRS4401) in the absence (-) and presence (+) of 1 mM IPTG after growth overnight at 37°C. **(C)** SDS-PAGE of γ-PGA collected from cultures of *epsE* $D^{94}A$ ($P_{hy\text{-}spank}$-*epsE*-$D^{94}A$-*lacI thrC::*P_{aprE}-*lacZ;* NRS4393) and *epsE* $K^{106}E$ ($P_{hy\text{-}spank}$-*epsE*-$K^{106}E$-*lacI thrC::*P_{aprE}-*lacZ;* NRS4395), grown in the absence or presence of 1 mM IPTG, at the onset of stationary phase.

Taken together, these data indicate that inhibition of flagellar rotation by EpsE results in an increase in DegU~P levels, which is reflected by an up-regulation of *bslA* transcription, exoprotease activity and γ-PGA production. As proven for the *motB* strain (**Figure 4-9**), DegS is responsible for increasing the levels of DegU~P upon induction of EpsE. Thus the signal generated by inhibition of flagellar rotation when EpsE is present is likely to be the same as when flagellar rotation is inhibited due to mutation or disruption of MotB.

4.8 Tangling of flagella increases DegU~P activity

Data presented thus far indicate that inhibition of flagellar rotation by genetic manipulation activates the DegS-DegU two component signal transduction system, suggesting that the flagellum is able to act as a mechanosensor to control signal transduction. To corroborate these findings, a non-genetic method to block flagellar rotation was used (Meister *et al.*, 1987). It was postulated that if the flagellum were able to act as a mechanosensor, physical perturbation of flagellar rotation should result in an increase in DegU~P levels. To test this hypothesis an antibody raised against the flagellar filament protein, Hag, was used to tangle flagella and the impact on *degU* transcription measured.

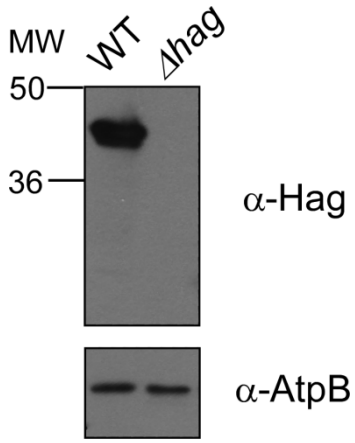

Figure 4-22 Western blot analysis of the specificity of the Hag anti-serum. Western blot analysis of whole cell proteins (including assembled flagella) extracted from WT (NCIB3610) or Δ*hag* (DS1677) strains probed with Hag-specific anti-serum. An antibody specific to the membrane protein AtpB was used as a loading control. MW indicates molecular weight in kDa.

Firstly, the specificity of the Hag antibody was ascertained by Western blotting. As shown in **Figure 4-22**, the Hag protein was detectable in the wild-type strain but not in a Δ*hag* strain. To ensure that any effects on *degU* transcription were specific to the Hag antibody, and not due to off-target effects of the serum, three independent pre-immune sera were used as controls. The wild-type strain carrying the P_{degU}-*lacZ* transcriptional reporter fusion was grown in liquid culture to mid-exponential phase at which point either pre-immune sera or the Hag anti-serum

(1:20 dilution) was added. Swimming motility was immediately checked by real-time live single cell microscopy (**Figure 4-23A**) and samples were collected over time for β-galactosidase assays. Analysis demonstrated that transcription from the *degU* promoter was up-regulated only 15 minutes after addition of the antibody, and increased 4-fold by comparison with the pre-immune sera controls after 30 minutes (**Figure 4-23B**) (P<0.001). This trend of increased transcription was maintained over the course of the experiment (**Figure 4-23B**). To further validate these data, exoprotease activity assays were undertaken with samples collected at the end of each time-course. The mean level of exoprotease activity for the three pre-immune sera controls was calculated and compared with that of the experimental sample incubated with Hag anti-sera. Analysis demonstrated a statistically significant (P=0.001) 13-fold increase in exoprotease activity upon inhibition of flagellar rotation by tangling of the flagella (**Figure 4-23C**). Collectively, these data unequivocally demonstrate that inhibition of rotation of the *B. subtilis* flagellum either genetically or mechanically results in an increase in *degU* transcription and DegU~P regulated processes, findings that are consistent with the activation of the sensor kinase, DegS.

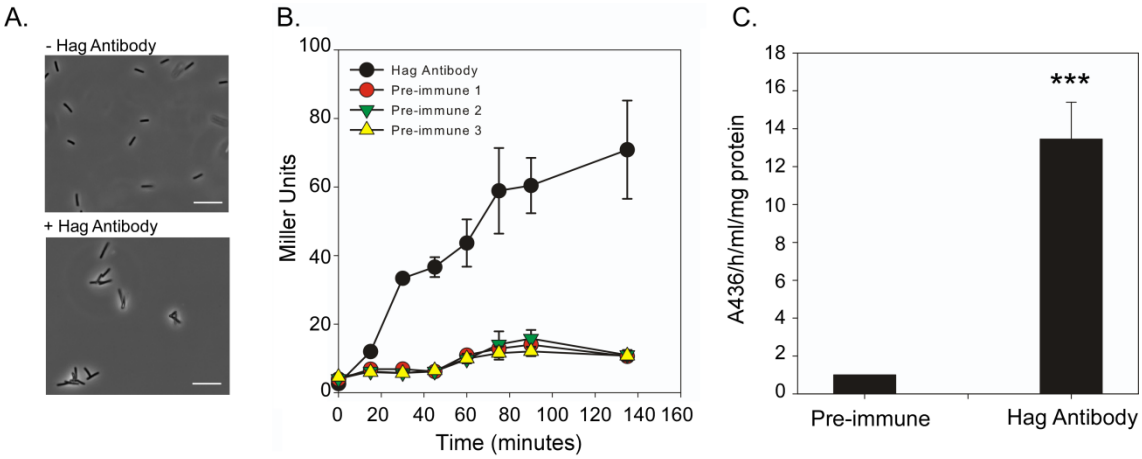

Figure 4-23 Assessment of the effects of tangling flagella on DegU~P activity. (A) Micrographs of cells containing the P_{degU}-*lacZ* transcriptional reporter fusion (NRS4351) grown in the presence or absence of Hag antibody in sera. Micrographs are static images taken from movies filmed 5 minutes after the addition of antibody to the culture. Scale bars represent 100 pixels. Still micrographs are taken from movies that are available online (http://onlinelibrary.wiley.com/doi/10.1111/mmi.12342/suppinfo) **(B)** β-galactosidase assays of the wild-type strain carrying the P_{degU}-*lacZ* transcriptional reporter fusion (NRS4351) grown in the presence of a 1:20 dilution of either pre-immune sera or the Hag specific antibody. Three independent pre-immune sera were used as controls. Data are plotted as the average of at least three independent replicates. Error bars represent standard error of the mean. **(C)** Exoprotease activity of samples harvested at the end of the time-course presented in part B. Data are represented as a fold change relative to the data acquired from samples treated with pre-immune sera, which was assigned value of 1. Data are represented as the average of at least 3 independent biological replicates and error bars represent standard error of the mean. An asterisk denotes significance as calculated by the Student's t-test, where *** represents P <0.001.

4.9 Discussion

In the natural environment bacteria predominantly live adhered to a surface as part of a biofilm (Costerton *et al.*, 1995, Vlamakis *et al.*, 2013). However, how a motile cell is able to sense and respond to the presence of a surface is, for most bacterial species, poorly understood. Experiments presented in this chapter show that inhibition of flagellar rotation acts as a signal to trigger an increase in the level of DegU~P via the sensor kinase DegS. This is a regulatory pathway that is needed for biofilm formation by the Gram-positive bacterium *B. subtilis* (Stanley & Lazazzera, 2005, Kobayashi, 2007, Verhamme *et al.*, 2007). These findings clearly demonstrate that *B. subtilis* can effectively use the flagellum for both signal transduction purposes and as a mechanical device for propulsion. These experiments lend support to the hypothesis that inhibition of flagellar rotation would occur due to physical contact with a surface, and that the consequential activation of a signal transduction pathway may present a mechanism by which flagellated organisms detect and respond to a surface.

Following publication of this work, a study by Kearns and colleagues confirmed our findings by showing that γ-PGA is produced in the absence of *motA* and that this was reliant upon DegS-DegU. (Chan *et al.*, 2014). Furthermore, this study showed that mutation of residues corresponding to arginine 90, proline 173 and proline 222 in *E. coli* MotA, abolished motility in *B. subtilis* (Chan *et al.*, 2014). These results therefore confirmed that the residues required for torque generation are conserved between *E. coli* and *B. subtilis*. Interestingly, a transposon mutagenesis screen revealed that deletion of *flgL*, *fliD* or *fliT* also disrupted γ-PGA production in the Δ*motA* strain background, although this effect was not due to transcriptional regulation of the genes required for the synthesis or the hydrolysis of γ-PGA (Chan *et al.*, 2014). FlgL, FliD and FliT could instead alter the activity of the synthetase and hydrolase proteins. Alternatively this may indicate involvement of the flagellar filament in signal transduction. Further analysis of these strains to check their phenotypes with regard to other DegU~P regulated behaviours

could enhance our knowledge in this regard. Preliminary data from the NSW group tentatively suggests that the γ-PGA phenotype of Δ*flgK-flgL* and Δ*fliD* strains might differ between surface and liquid growth.

4.9.1 Activation of the DegS-DegU two component system

Previous work has highlighted a role of DegU~P in controlling flagellar assembly (Amati *et al.*, 2004, Hsueh *et al.*, 2011). Indeed it has been shown that DegU is preferentially activated in genetic backgrounds that promote the formation of chains of cells, with further experiments tentatively suggesting that DegU might play a role in sensing the status of flagellar assembly (Hsueh *et al.*, 2011). The data presented herein demonstrate that the DegS-DegU two component regulatory system is activated when the flagellum stops rotating. Therefore DegU~P has a role in both flagellar biosynthesis and in responding to signals inputted by the flagellum. Data demonstrating that inhibition of flagellar rotation acts as a trigger to activate the DegS-DegU two component system allows the *B. subtilis* flagellum to be classified as a mechanosensor that controls bacterial cell behaviour. To the best of our knowledge this is the first example of a classical two component system that can be activated in response to a mechanical signal, namely the inhibition of flagellar rotation. It is suggested that repression of flagellar rotation occurs when the flagellum encounters a surface; a process that is mimicked in this study by flagella tangling experiments (**Figure 4-23**).

4.9.2 Surface sensing by the flagellum

These findings add *B. subtilis* to the small list of microorganisms for which surface sensing has been linked with downstream alterations in gene transcription and protein synthesis (McCarter *et al.*, 1988, Kawagishi *et al.*, 1996). For example, transcriptomic and proteomic screens have shown that genes and proteins are differentially regulated between liquid and surface grown bacteria (Kim & Surette, 2004, Wang *et al.*, 2004). Moreover, in *Vibrio parahaemolyticus*, which possesses a dual flagellar system, it has been shown that slowing the

rotational speed of the polar flagellum triggers gene expression changes that result in the transcription of genes essential for the synthesis of lateral flagella (McCarter *et al.*, 1988, Kawagishi *et al.*, 1996). Furthermore, inhibition of rotation of the polar flagellum also impacts genes associated with cyclic-di-GMP signalling and virulence, thereby suggestive of a global role for flagellar mediated surface sensing in controlling bacterial cell physiology (Gode-Potratz *et al.*, 2011).

4.9.3 The transition from motility to attachment

The attachment of bacteria to a surface is the first step in the formation of a biofilm, where the initial stage of adhesion is often mediated by flagella or pili based motility (O'Toole *et al.*, 2000). Indeed, several studies have identified flagella, or flagellar motility, as a key aspect of biofilm development and biofilm "microanatomy" (O'Toole & Kolter, 1998, Pratt & Kolter, 1998, Watnick & Kolter, 1999, Lemon *et al.*, 2007, Friedlander *et al.*, 2013, Serra *et al.*, 2013). The subsequent transition to persistent adhesion is often mediated by polysaccharides (Watnick & Kolter, 1999). In *Caulobacter crescentus* a direct link between surface-sensing by the flagellum and irreversible adhesion has been shown, where upon reaching the surface, pili-dependent inhibition of flagellum rotation stimulates concomitant synthesis of the holdfast, promoting permanent attachment (Li *et al.*, 2012). Moreover, exopolysaccharides have been shown to "wheel-lock" flagellar rotation resulting in coordination of motility inhibition and stimulation of biofilm formation (Zorraquino *et al.*, 2013). Such a "locking" of the flagellum does not occur when *epsE* is expressed in *B. subtilis*; the flagella are not immobilised but are unpowered and able to rotate by Brownian motion (Blair *et al.*, 2008). Alternatively, or indeed additionally, flagellar brake or clutch activity can play a role in the transition between motility and biofilm formation to ensure separation of these mutually exclusive cell behaviours (Blair *et al.*, 2008, Pilizota *et al.*, 2009, Boehm *et al.*, 2010, Paul *et al.*, 2010). This can be exemplified by the *B. subtilis* flagellar clutch, EpsE, which was utilised in this study. It is of interest to note that EpsE is encoded within the *epsA-O* operon that is required for the synthesis of one of the

major structural components of the biofilm, the exopolysaccharide. EpsE therefore links inhibition of motility to exopolysaccharide production and biofilm formation (Blair *et al.*, 2008, Guttenplan *et al.*, 2010, Guttenplan & Kearns, 2013). Experiments detailed in this chapter indicate that induction of EpsE will reinforce biofilm formation through increased biosynthesis of BslA (Fig. 4-20); a bacterial hydrophobin that coats the *B. subtilis* biofilm (Kobayashi & Iwano, 2012, Hobley *et al.*, 2013) and functions synergistically with the exopolysaccharide and TasA amyloid fibres to facilitate assembly of the biofilm matrix (Ostrowski *et al.*, 2011). Therefore EpsE can serve three functions: (i) to stop rotation of the flagellum (ii) to promote the synthesis of BslA through increasing DegU~P levels and (iii) to catalyse synthesis of the EPS. Proteins functionally similar to EpsE with regard to stopping flagellar rotation have been classed as flagellar "brakes" in *E. coli* (Boehm *et al.*, 2010, Paul *et al.*, 2010) and *Rhodobacter sphaeroides* (Pilizota *et al.*, 2009). Therefore, the ability of a single protein to inhibit flagellar rotation appears to be a general mechanism used by bacteria to facilitate the transition to a sessile state.

4.9.4 Concluding remarks

The experiments presented in this chapter uncover a major and novel role for the *B. subtilis* flagellum as a mechanosensor. This study adds to the small but growing body of evidence indicating that the flagellum is utilised by the cell to explore and respond to external stimuli in diverse bacterial species (Belas & Suvanasuthi, 2005, Wang *et al.*, 2005, Gode-Potratz *et al.*, 2011, Friedlander *et al.*, 2013). The activation of the DegS-DegU two component signal transduction pathway upon inhibition of flagellar rotation allows a connection to be made between initial surface contact and the subsequent development of a biofilm. These experiments lend support to the hypothesis that inhibition of flagellar rotation would occur due to physical contact with a surface, and that the consequential activation of a signal transduction pathway may present a mechanism by which many flagellated organisms detect and respond to a surface.

5
Conclusions and outlook

Bacteria live in diverse and challenging environments. To enable their survival in the presence of a variety of external stresses, cells must be able to sense and respond to a plethora of external stimuli. Signal transduction pathways present a means by which bacteria can detect and integrate signals such as pH, temperature and nutrient status to elicit an appropriate response that will allow their continued survival and propagation. This study aimed to investigate the role of signal transduction pathways in mediating the switch between flagellar motility and biofilm formation in *B. subtilis*.

5.1 Investigating a potential role for tyrosine phosphorylation in motility

When this study began a role for tyrosine phosphorylation in biofilm formation had only just been recognised (Kiley & Stanley-Wall, 2010). In parallel, a second study showed that the putative motility protein YvyG could be phosphorylated on tyrosine, and that this phosphorylation event may impact the localisation of the protein (Jers *et al.*, 2010). As such, a link between flagellar motility, biofilm formation and tyrosine phosphorylation was hypothesised.

The experiments presented in Chapter 3 established the role of YvyG (re-named to FlgN) as an orthologue of the *S.* Typhimurium T3SS flagellar chaperone protein, FlgN. Crucially, this work has identified key differences between *Bs*-FlgN and *S*T-FlgN; *Bs*-FlgN appears to be essential for flagellar biosynthesis, whereas in *Salmonella* a few flagella can be assembled per cell in the absence of *flgN* (Kutsukake, 1994). Furthermore, in *B. subtilis* deletion of either *flgK* and *flgL* or *flgN* altered transcription of the *hag* gene. These findings infer that the hook-filament junction itself may act as a regulatory checkpoint to control flagellar assembly. When considered in the context of other recent *B. subtilis* flagella studies (Courtney *et al.*, 2012, Mukherjee *et al.*, 2013) these differences are not surprising and further suggest that flagellar assembly in *B. subtilis* is controlled by both conserved and species-specific mechanisms. In future it would be of interest to delineate if other Gram-positive species also share these alternative regulatory

processes. Recent work has identified novel components of the Epsilonproteobacterium *Campylobacter jejuni* flagellum, indicating that even within Gram-negative bacteria there are key functional differences with regard to flagellum structure and regulation (Gao *et al.*, 2014). Such differences likely allow different bacteria to adapt to their local environments

The effects of phosphorylation of *Bs*-FlgN were also assessed. Using a site-directed mutagenesis approach, it was shown that mutation of the identified *Bs*-FlgN phosphorylation site does not impact motility. Indeed, mutation of a subsequently identified arginine phosphorylation site (Elsholz *et al.*, 2012) also failed to yield any phenotype with regard to motility. It is possible that *Bs*-FlgN is able to play a role in an additional process that is regulated by phosphorylation, but this seems unlikely given the position of the *flgN* gene in an operon associated with flagellar biosynthesis. Instead phosphorylation of FlgN may be non-specific, as often occurs for eukaryotes, or FlgN may act as a phosphate sink (Sourjik & Schmitt, 1998, Landry *et al.*, 2009). Alternatively, mutation of Y49 may only impact motility alongside mutation of other sites of post-translational modification. Previous work by the Mijakovic group suggested that the sub-cellular localisation of *Bs*-FlgN was altered upon deletion of the tyrosine kinase, *ptkA* from the chromosome (Jers *et al.*, 2010). However, a *Bs*-FlgN-GFP translational fusion protein constructed as part of this study was non-functional, and indeed deletion of *ptkA* does not confer a phenotype with regard to swimming or swarming motility (NSW lab, unpublished). Therefore, the effect that the alteration of the cellular location of *Bs*-FlgN has remains to be determined. Nonetheless, this work illustrates that phosphorylation sites identified by mass spectrometry approaches must be investigated at a functional level before any significance can be inferred from their modification.

Taken together, this section of work ascribed a function to *Bs*-FlgN as a flagellar chaperone protein and established that tyrosine phosphorylation of *Bs*-FlgN is not important for its function. In conclusion, it is likely that tyrosine phosphorylation does not regulate motility and

that this means of signal transduction does not represent a pathway that controls the transition from motility to a sessile lifestyle in *B. subtilis*.

5.2 The *B. subtilis* flagellum as a mechanosensor that controls signalling

Two component signal transduction systems represent the prototypical signalling pathway that bacteria use to sense and respond to external stimuli. In *B. subtilis* the DegS-DegU two component signal transduction pathway is unusual in that the response regulator, DegU, can elicit different responses depending on the level of phosphorylated DegU within the cell (Kobayashi, 2007, Verhamme *et al.*, 2007). Of particular note to this work, low levels of DegU~P support swarming motility and mid-levels promote biofilm formation (Verhamme *et al.*, 2007). Due to the labile nature of aspartic acid phosphorylation, DegU~P levels have never been directly measured. It is possible to mimic aspartic acid phosphorylation of response regulators using beryllofluoride (Yan *et al.*, 1999). However, this technique is technically challenging and has only been used in *in vitro* structural and biochemical experiments (Yan *et al.*, 1999). Other methods for detecting response regulator phosphorylation are now becoming available and have been used successfully for signalling systems in other bacterial species (Barbieri & Stock, 2008), but none have been tested or optimised for DegU, or indeed for any other *B. subtilis* response regulator. Therefore in this work DegU~P levels are inferred from established and recognised assays which, although indirect, provide robust and reproducible indications of DegU~P activity.

In combination with work from the Kearns group (Hsueh *et al.*, 2011), our preliminary experiments suggested that DegS-DegU may link the transition from motility to biofilm formation. Indeed, data presented in Chapter 4 identify the *B. subtilis* flagellum as a mechanosensor. When flagellar rotation was perturbed by either genetic or physical means, an increase in the level and activity of DegU~P was observed. This was measured as an increase in

(i) the transcription of target genes, including *degU*, *bslA* and *aprE*, (ii) the production of the exopolymer γ-PGA and (iii) total secreted protease activity.

5.2.1 The role of the flagellum in bacterial gene expression

The bacterial flagellum has been shown by other studies to not only be crucial for motility, but also to play a role in other bacterial processes due to its ability to monitor changes in the external environment. During swarming the *S.* Typhimurium flagellum senses external moisture (Wang *et al.*, 2005). Under conditions of poor hydration, the flagellum restricts its own biosynthesis via a regulatory mechanism that prevents secretion of the anti-sigma factor FlgM to inhibit the transcription of class III flagellar genes (Wang *et al.*, 2005). Rotation of the flagellum has also been suggested to increase hydration to overcome surface friction and promote swarming motility (Partridge & Harshey, 2013). The marine bacterium *Vibrio parahaemolyticus* uses a polar flagellum driven by sodium-motive force for swimming motility and lateral flagella driven by proton-motive force for swarming motility. Impedance of rotation of the polar flagellum evokes changes in downstream gene expression such that lateral flagella are expressed, promoting swarming motility (Kawagishi *et al.*, 1996). Inhibition of polar flagellar rotation in this bacterium also impacts transcription of genes involved in c-di-GMP synthesis and virulence (Gode-Potratz *et al.*, 2011). In combination these studies are suggestive of a global role for flagellar mediated surface-sensing in bacterial physiology.

5.2.2 Mechanisms of bacterial surface-sensing

There are, of course, outstanding questions that follow the discovery that the *B. subtilis* flagellum acts as a mechanosensor to control the DegS-DegU two component system; including how a slowing or lack of flagellar rotation is sensed and how the response is potentiated. There are several mechanisms by which this might occur. One possibility is that DegS, as a cytoplasmic sensor kinase, interacts with components of the flagellar motor when rotation is stopped. In *E. coli* the c-di-GMP binding protein, YcgR, has been shown to interact

with the flagellar motor proteins FliG, FliM (Paul *et al.*, 2010) and MotA (Boehm *et al.*, 2010) when c-di-GMP levels are high, resulting in the inhibition of motility. Alternatively, DegS may interact with components of the chemotaxis signalling system. In *Pseudomonas aeruginosa* the c-di-GMP phosphodiesterase, Pch, interacts with the CheA kinase (Kulasekara *et al.*, 2013). CheA phosphorylates CheY and causes the flagellum to rotate in a clockwise direction and change trajectory (Kulasekara *et al.*, 2013). Interaction of Pch with CheA is essential for the localisation of Pch to the flagellum and the subsequent decrease in c-di-GMP levels that permit the cell to remain motile. Therefore, there is precedent for the interaction of signalling components with flagellar or chemotaxis proteins. In *B. subtilis* such interactions could be tested for by co-immunoprecipitation experiments in combination with mass spectrometry.

An alternative mechanism may involve the stator-associated transmembrane protein, FliL. Previous studies have identified FliL as a possible intermediary between the inhibition of flagellar rotation and signal transduction (Belas & Suvanasuthi, 2005, Cusick *et al.*, 2012). Moreover, recent studies in different bacterial species have identified several roles for FliL in bacterial motility and surface-sensing (Lee *et al.*, 2013). For example, FliL has been shown to be associated with, and enhance the function of, the flagellar stator (Suaste-Olmos *et al.*, 2010, Motaleb *et al.*, 2011), with evidence now suggesting that over-expression of FliL alongside MotA and MotB is sufficient to overcome surface friction associated with swarming on hard agar (Partridge & Harshey, 2013). Given that the function of FliL does not appear to be strictly conserved between bacterial species it will be of interest to determine if FliL is also a key player in surface-sensing and flagellar rotation in *B. subtilis*. Conversely, the possibility that DegS might directly sense changes in the intracellular environment that are triggered by a lack of flagellar rotation, such as ion flux (Kawagishi *et al.*, 1996), cannot be excluded. The cell membrane could conceivably be altered by disruption of flagellar rotation due to an increase in membrane potential, as appears to occur for *Vibrio cholerae* during attachment to a surface (Van Dellen *et al.*, 2008). Intriguingly, recent work in *E. coli* has identified the flagellar stator,

not the flagellar filament, as a mechanosensor that is able to remodel itself in a load dependent manner (Lele *et al.*, 2013, Tipping *et al.*, 2013a). It is therefore possible that the increase in the number of stators required to drive flagellar torque under high loads might itself act as a signal to impact downstream signalling pathways.

Furthermore, inhibition of flagellar rotation could alter the localisation of DegS or DegU. In *Pseudomonas aeruginosa* the chemotaxis-like Wsp signal transduction system, which is essential for biofilm formation, has been shown to produce c-di-GMP in response to surface growth (Guvener & Harwood, 2007, O'Connor *et al.*, 2012). Upon growth on a surface the Wsp pathway is activated and the phosphorylated response regulator, WspR forms clusters that can be visualised by fluorescence microscopy (Guvener & Harwood, 2007). These clusters are essential for c-di-GMP activity (Huangyutitham *et al.*, 2013). It would be intriguing to assess if upon stopping of the flagellar motor DegU~P also forms clusters to potentiate its response.

The data presented in this thesis show that a complete lack of flagellar rotation triggers an increase in DegU~P levels. However, *B. subtilis* is reported to assemble approximately 26 flagella per cell (Guttenplan *et al.*, 2013). Future studies could aim to address if all flagella must be stopped to achieve activation of DegS-DegU. Alternatively, perhaps a slowing of flagellar rotation would be sufficient to impact downstream gene expression. This work also does not assess if cell-cell contact could promote an increase in DegU~P activity by interfering with flagellar rotation. This scenario would be plausible within the confines of a bacterial community such as the biofilm.

The data presented measure DegU~P as a function of several accepted proxies. The up-regulation in DegU~P required the presence of the sensor kinase, DegS. One way in which the necessity of DegU phosphorylation could be further confirmed would be by introducing the *degU146* mutation (section 1.3.1), to change the phosphorylatable aspartic acid residue to

asparagine, into the Δ*motB* strain. Such a mutation should not support any up-regulation of any measurement of DegU~P.

It will be of interest in the future to determine the underlying molecular details of DegS activation. Given that the N-terminal input domain of DegS lacks homology to other proteins, a structural approach could help to illuminate if DegS responds to a specific molecule or ligand. Alternatively, DegS may be stimulated by interaction with another protein. How the multiple mechanisms that regulate DegS-DegU are integrated will be a complex problem to solve. One conjecture is that the specific environmental conditions will confer which specific regulatory means are employed. Looking beyond DegS-DegU, transcriptomics studies could reveal if inhibition of flagellar rotation specifically up-regulates the DegS-DegU two component system, or if rather there are additional signalling pathways that the flagellum can control. A similar approach could also be taken in other bacterial species. For example, the *Listeria monocytogenes* genome encodes a homologue of the *B. subtilis* DegU protein, although a cognate sensor kinase has not been identified. In *L. monocytogenes* DegU also plays a role in motility and in biofilm formation (Gueriri *et al.*, 2008). It would therefore be interesting to test if stopping the flagellar motor in this bacterium also impacts DegU regulated behaviours. These studies could clarify if our hypothesis that the flagellum acts as a mechanosensor to control signalling in other flagellated bacterial species holds true.

5.2.3 A model for *B. subtilis* biofilm development

Given the role of DegU in biofilm development, the discovery that the flagellum can act as a mechanosensor to control DegU~P levels not only furthers our knowledge on the role of the flagellum in signal transduction, but also allows our model for the role of DegU in the development of the *B. subtilis* biofilm to be progressed. This model is summarised in **Figure 5-1**. The first step in the formation of a biofilm involves surface contact. We propose that when the cell reaches a surface flagellar rotation is impeded, mimicked in this study by flagella

tangling experiments. This would subsequently cause an accumulation in DegU~P, likely via activation of the DegS sensor kinase. The experiments used in this study to perturb flagellar rotation all cause a complete loss of motility. However, given the peritrichous patterning of the *B. subtilis* cell it is possible that upon reaching a surface flagellar rotation is initially only slowed or that only a sub-population of flagella stop rotation. This may allow DegU~P levels to increase to a point where transcription of *bslA* is triggered. Alternatively, mid-levels of DegU~P may be maintained by some of the regulatory mechanisms summarised in section 1.3.1. However, production of BslA alone is not sufficient to allow biofilm formation to proceed. Transcription of the *tapA* and *epsA* operons is essential for construction of the biofilm and their expression would require low levels of Spo0A~P. Data recently published from the NSW group allows us to tentatively suggest that DegU~P can control Spo0A~P levels (Marlow *et al.*, 2014b). Perhaps a mid-level of DegU~P could allow sufficient accumulation of Spo0A~P to indirectly promote *eps* and *tapA* transcription. Alternatively, or indeed additionally, other signals may be recognised by the sensor kinases of the Spo0A pathway to initiate matrix gene transcription. For example, upon an increase in cell density the gene encoding surfactin is transcribed. Surfactin has been shown to induce potassium leakage and promote activation of the Spo0A phosphorelay (Lopez *et al.*, 2009). As well as being activated upon reaching a surface, cell density might also perturb flagellar rotation, further resulting in increased DegU~P levels.

Upon expression of the *epsA* operon, the bi-functional EpsE protein is produced, which promotes exopolysaccharide synthesis and also contributes to inhibition of flagellar rotation (Blair *et al.*, 2008). In combination with prolonged surface contact, the clutch activity of EpsE could cause DegU~P levels to rise further. This scenario would see DegU~P reach a level that is compatible with inhibition of expression from the *tapA* and *epsA* operons. Furthermore, protease gene expression would be activated and the sporulation pathway initiated.

Therefore, this model suggests that DegU~P plays a role through the entire process of biofilm formation.

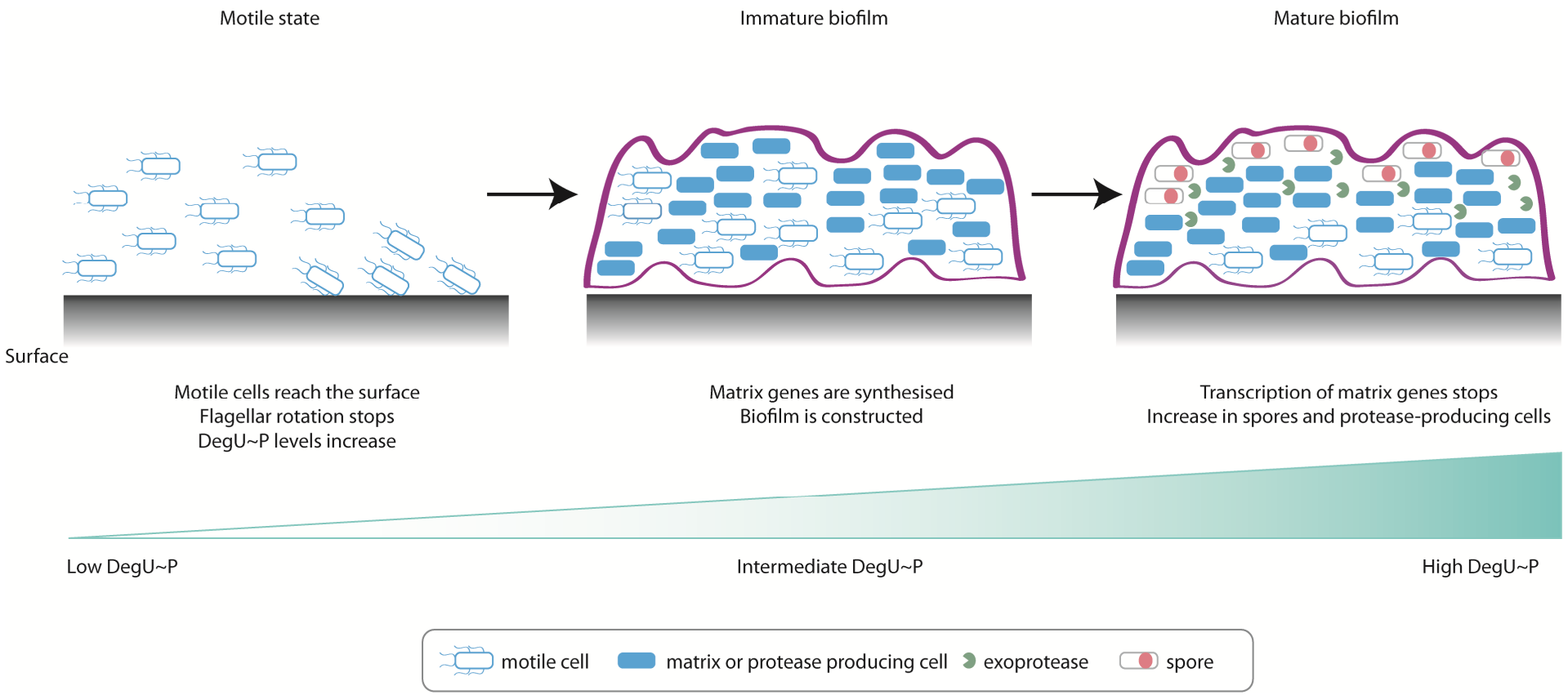

Figure 5-1 A model for the development of the *B. subtilis* biofilm. Upon reaching a surface flagellar rotation will stop. This leads to an increase in DegU~P levels, inferred from several proxies, which triggers transcription of *bslA*. The other matrix operons are also transcribed via activation of the Spo0A pathway by various means. Some motile cells remain within the biofilm. As the biofilm matures the increase in DegU~P and Spo0A~P will drive cell differentiation so that exoproteases are synthesised and secreted and a sub-population of cells develop into spores. Biofilm maturation occurs as the level of DegU~P increases.

In summary, this study has successfully contributed to our knowledge of motility and the link to biofilm formation in *B. subtilis*. The identification of *Bs*-FlgN as an orthologue of *S*T-FlgN and analysis of its function has demonstrated that *B. subtilis* can use both conserved and species-specific mechanisms to control flagellar biosynthesis. Furthermore, the findings that mutation of the identified tyrosine and arginine phosphorylation sites establish that, as for eukaryotic substrates, it is likely that prokaryotic proteins are also subject to non-functional post-translational modifications. Additionally, the identification of the *B. subtilis* flagellum as a mechanosensor has demonstrated for the first time that a canonical two component system can be activated by the flagellum. This work also further illustrates the multi-functional nature of the flagellum, proving that what was once assumed to solely act as a device for propulsion can actually function to detect external stimuli and relay this information to a signal transduction pathway. Overall, these findings enhance our understanding of how the *B. subtilis* cell regulates motility, senses changes in its external environment and responds to mediate its transition to a sessile lifestyle.

6
References

Aguilar, C., Vlamakis, H., Guzman, A., Losick, R. & Kolter, R., (2010) KinD is a checkpoint protein linking spore formation to extracellular-matrix production in *Bacillus subtilis* biofilms. *mBio* **1**.

Aizawa, S. I., Dean, G. E., Jones, C. J., Macnab, R. M. & Yamaguchi, S., (1985) Purification and characterization of the flagellar hook-basal body complex of *Salmonella* Typhimurium. *J Bacteriol* **161**: 836-849.

Aldridge, P., Karlinsey, J. & Hughes, K. T., (2003) The type III secretion chaperone FlgN regulates flagellar assembly via a negative feedback loop containing its chaperone substrates FlgK and FlgL. *Mol Microbiol* **49**: 1333-1345.

Aldridge, P. D., Karlinsey, J. E., Aldridge, C., Birchall, C., Thompson, D., Yagasaki, J. & Hughes, K. T., (2006) The flagellar-specific transcription factor, sigma28, is the Type III secretion chaperone for the flagellar-specific anti-sigma28 factor FlgM. *Genes Dev* **20**: 2315-2326.

Allan, C., Burel, J. M., Moore, J., Blackburn, C., Linkert, M., Loynton, S., Macdonald, D., Moore, W. J., Neves, C., Patterson, A., Porter, M., Tarkowska, A., Loranger, B., Avondo, J., Lagerstedt, I., Lianas, L., Leo, S., Hands, K., Hay, R. T., Patwardhan, A., Best, C., Kleywegt, G. J., Zanetti, G. & Swedlow, J. R., (2012) OMERO: flexible, model-driven data management for experimental biology. *Nature methods* **9**: 245-253.

Amati, G., Bisicchia, P. & Galizzi, A., (2004) DegU-P represses expression of the motility *fla-che* operon in *Bacillus subtilis*. *J Bacteriol* **186**: 6003-6014.

Arnaud, M., Chastanet, A. & Debarbouille, M., (2004) New vector for efficient allelic replacement in naturally nontransformable, low-GC-content, gram-positive bacteria. *Applied and environmental microbiology* **70**: 6887-6891.

Auvray, F., Ozin, A. J., Claret, L. & Hughes, C., (2002) Intrinsic membrane targeting of the flagellar export ATPase FliI: interaction with acidic phospholipids and FliH. *J Mol Biol* **318**: 941-950.

Bai, U., Mandic-Mulec, I. & Smith, I., (1993) SinI modulates the activity of SinR, a developmental switch protein of *Bacillus subtilis*, by protein-protein interaction. *Genes Dev* **7**: 139-148.

Bange, G., Kummerer, N., Engel, C., Bozkurt, G., Wild, K. & Sinning, I., (2010) FlhA provides the adaptor for coordinated delivery of late flagella building blocks to the type III secretion system. *Proc Natl Acad Sci U S A* **107**: 11295-11300.

Banse, A. V., Chastanet, A., Rahn-Lee, L., Hobbs, E. C. & Losick, R., (2008) Parallel pathways of repression and antirepression governing the transition to stationary phase in *Bacillus subtilis*. *Proc Natl Acad Sci U S A* **105**: 15547-15552.

Barbieri, C. M. & Stock, A. M., (2008) Universally applicable methods for monitoring response regulator aspartate phosphorylation both in vitro and in vivo using Phos-tag-based reagents. *Analytical biochemistry* **376**: 73-82.

Belas, R. & Suvanasuthi, R., (2005) The ability of *Proteus mirabilis* to sense surfaces and regulate virulence gene expression involves FliL, a flagellar basal body protein. *J Bacteriol* **187**: 6789-6803.

Beltrao, P., Albanese, V., Kenner, L. R., Swaney, D. L., Burlingame, A., Villen, J., Lim, W. A., Fraser, J. S., Frydman, J. & Krogan, N. J., (2012) Systematic functional prioritization of protein posttranslational modifications. *Cell* **150**: 413-425.

Bennett, J. C. & Hughes, C., (2000) From flagellum assembly to virulence: the extended family of type III export chaperones. *Trends Microbiol* **8**: 202-204.

Bennett, J. C., Thomas, J., Fraser, G. M. & Hughes, C., (2001) Substrate complexes and domain organization of the *Salmonella* flagellar export chaperones FlgN and FliT. *Mol Microbiol* **39**: 781-791.

Berg, H. C., (2003) The rotary motor of bacterial flagella. *Annual review of biochemistry* **72**: 19-54.

Birnboim, H. C. & Doly, J., (1979) A rapid alkaline extraction procedure for screening recombinant plasmid DNA. *Nucleic Acids Res* **7**: 1513-1523.

Bischoff, D. S. & Ordal, G. W., (1991) Sequence and characterization of *Bacillus subtilis* CheB, a homolog of Escherichia coli CheY, and its role in a different mechanism of chemotaxis. *The Journal of biological chemistry* **266**: 12301-12305.

Blair, D. F. & Berg, H. C., (1988) Restoration of torque in defective flagellar motors. *Science* **242**: 1678-1681.

Blair, K. M., Turner, L., Winkelman, J. T., Berg, H. C. & Kearns, D. B., (2008) A molecular clutch disables flagella in the *Bacillus subtilis* biofilm. *Science* **320**: 1636-1638.

Boehm, A., Kaiser, M., Li, H., Spangler, C., Kasper, C. A., Ackermann, M., Kaever, V., Sourjik, V., Roth, V. & Jenal, U., (2010) Second messenger-mediated adjustment of bacterial swimming velocity. *Cell* **141**: 107-116.

Bourret, R. B., (2010) Receiver domain structure and function in response regulator proteins. *Curr Opin Microbiol* **13**: 142-149.

Branda, S. S., Chu, F., Kearns, D. B., Losick, R. & Kolter, R., (2006) A major protein component of the *Bacillus subtilis* biofilm matrix. *Mol Microbiol* **59**: 1229-1238.

Branda, S. S., Gonzalez-Pastor, J. E., Ben-Yehuda, S., Losick, R. & Kolter, R., (2001) Fruiting body formation by *Bacillus subtilis*. *Proc Natl Acad Sci U S A* **98**: 11621-11626.

Branda, S. S., Gonzalez-Pastor, J. E., Dervyn, E., Ehrlich, S. D., Losick, R. & Kolter, R., (2004) Genes involved in formation of structured multicellular communities by *Bacillus subtilis*. *J Bacteriol* **186**: 3970-3979.

Braun, T. F., Al-Mawsawi, L. Q., Kojima, S. & Blair, D. F., (2004) Arrangement of core membrane segments in the MotA/MotB proton-channel complex of *Escherichia coli*. *Biochemistry* **43**: 35-45.

Braun, T. F., Poulson, S., Gully, J. B., Empey, J. C., Van Way, S., Putnam, A. & Blair, D. F., (1999) Function of proline residues of MotA in torque generation by the flagellar motor of *Escherichia coli*. *J Bacteriol* **181**: 3542-3551.

Braun, V. & Schmitz, G., (1980) Excretion of a protease by *Serratia marcescens*. *Archives of microbiology* **124**: 55-61.

Britton, R. A., Eichenberger, P., Gonzalez-Pastor, J. E., Fawcett, P., Monson, R., Losick, R. & Grossman, A. D., (2002) Genome-wide analysis of the stationary-phase sigma factor (sigma-H) regulon of *Bacillus subtilis*. *J Bacteriol* **184**: 4881-4890.

Buchan, D. W., Minneci, F., Nugent, T. C., Bryson, K. & Jones, D. T., (2013) Scalable web services for the PSIPRED Protein Analysis Workbench. *Nucleic Acids Res* **41**: W349-357.

Buelow, D. R. & Raivio, T. L., (2010) Three (and more) component regulatory systems - auxiliary regulators of bacterial histidine kinases. *Mol Microbiol* **75**: 547-566.

Burbulys, D., Trach, K. A. & Hoch, J. A., (1991) Initiation of sporulation in *B. subtilis* is controlled by a multicomponent phosphorelay. *Cell* **64**: 545-552.

Calvio, C., Celandroni, F., Ghelardi, E., Amati, G., Salvetti, S., Ceciliani, F., Galizzi, A. & Senesi, S., (2005) Swarming differentiation and swimming motility in *Bacillus subtilis* are controlled by *swrA*, a newly identified dicistronic operon. *J Bacteriol* **187**: 5356-5366.

Candela, T. & Fouet, A., (2006) Poly-gamma-glutamate in bacteria. *Mol Microbiol* **60**: 1091-1098.

Carabetta, V. J., Tanner, A. W., Greco, T. M., Defrancesco, M., Cristea, I. M. & Dubnau, D., (2013) A complex of YlbF, YmcA and YaaT regulates sporulation, competence and biofilm formation by accelerating the phosphorylation of Spo0A. *Mol Microbiol* **88**: 283-300.

Chadsey, M. S., Karlinsey, J. E. & Hughes, K. T., (1998) The flagellar anti-sigma factor FlgM actively dissociates *Salmonella* Typhimurium sigma28 RNA polymerase holoenzyme. *Genes Dev* **12**: 3123-3136.

Chai, Y., Beauregard, P. B., Vlamakis, H., Losick, R. & Kolter, R., (2012) Galactose metabolism plays a crucial role in biofilm formation by *Bacillus subtilis*. *mBio* **3**: e00184-00112.

Chai, Y., Chu, F., Kolter, R. & Losick, R., (2008) Bistability and biofilm formation in *Bacillus subtilis*. *Mol Microbiol* **67**: 254-263.

Chai, Y., Kolter, R. & Losick, R., (2009) Paralogous antirepressors acting on the master regulator for biofilm formation in *Bacillus subtilis*. *Mol Microbiol* **74**: 876-887.

Chai, Y., Norman, T., Kolter, R. & Losick, R., (2010) An epigenetic switch governing daughter cell separation in *Bacillus subtilis*. *Genes Dev* **24**: 754-765.

Chan, J. M., Guttenplan, S. B. & Kearns, D. B., (2014) Defects in the flagellar motor increase synthesis of poly-gamma-glutamate in *Bacillus subtilis*. *J Bacteriol* **196**: 740-753.

Chen, Y., Cao, S., Chai, Y., Clardy, J., Kolter, R., Guo, J. H. & Losick, R., (2012) A *Bacillus subtilis* sensor kinase involved in triggering biofilm formation on the roots of tomato plants. *Mol Microbiol* **85**: 418-430.

Chen, Y., Yan, F., Chai, Y., Liu, H., Kolter, R., Losick, R. & Guo, J. H., (2013) Biocontrol of tomato wilt disease by *Bacillus subtilis* isolates from natural environments depends on conserved genes mediating biofilm formation. *Environmental microbiology* **15**: 848-864.

Chen, Y. F. & Helmann, J. D., (1992) Restoration of motility to an *Escherichia coli fliA* flagellar mutant by a *Bacillus subtilis* sigma factor. *Proc Natl Acad Sci U S A* **89**: 5123-5127.

Cheung, J. & Hendrickson, W. A., (2010) Sensor domains of two-component regulatory systems. *Curr Opin Microbiol* **13**: 116-123.

Chevance, F. F. & Hughes, K. T., (2008) Coordinating assembly of a bacterial macromolecular machine. *Nature reviews. Microbiology* **6**: 455-465.

Chu, F., Kearns, D. B., Branda, S. S., Kolter, R. & Losick, R., (2006) Targets of the master regulator of biofilm formation in Bacillus subtilis. *Mol Microbiol* **59**: 1216-1228.

Chu, F., Kearns, D. B., McLoon, A., Chai, Y., Kolter, R. & Losick, R., (2008) A novel regulatory protein governing biofilm formation in *Bacillus subtilis*. *Mol Microbiol* **68**: 1117-1127.

Chumsakul, O., Takahashi, H., Oshima, T., Hishimoto, T., Kanaya, S., Ogasawara, N. & Ishikawa, S., (2011) Genome-wide binding profiles of the *Bacillus subtilis* transition state regulator AbrB and its homolog Abh reveals their interactive role in transcriptional regulation. *Nucleic Acids Res* **39**: 414-428.

Costerton, J. W., Lewandowski, Z., Caldwell, D. E., Korber, D. R. & Lappin-Scott, H. M., (1995) Microbial biofilms. *Annual review of microbiology* **49**: 711-745.

Courtney, C. R., Cozy, L. M. & Kearns, D. B., (2012) Molecular characterization of the flagellar hook in *Bacillus subtilis*. *J Bacteriol* **194**: 4619-4629.

Cousin, C., Derouiche, A., Shi, L., Pagot, Y., Poncet, S. & Mijakovic, I., (2013) Protein-serine/threonine/tyrosine kinases in bacterial signaling and regulation. *FEMS microbiology letters* **346**: 11-19.

Cozy, L. M. & Kearns, D. B., (2010) Gene position in a long operon governs motility development in *Bacillus subtilis*. *Mol Microbiol* **76**: 273-285.

Cozy, L. M., Phillips, A. M., Calvo, R. A., Bate, A. R., Hsueh, Y. H., Bonneau, R., Eichenberger, P. & Kearns, D. B., (2012) SlrA/SinR/SlrR inhibits motility gene expression upstream of a hypersensitive and hysteretic switch at the level of sigma(D) in *Bacillus subtilis*. *Mol Microbiol* **83**: 1210-1228.

Cusick, K., Lee, Y. Y., Youchak, B. & Belas, R., (2012) Perturbation of FliL interferes with *Proteus mirabilis* swarmer cell gene expression and differentiation. *J Bacteriol* **194**: 437-447.

Dahl, M. K., Msadek, T., Kunst, F. & Rapoport, G., (1991) Mutational analysis of the *Bacillus subtilis* DegU regulator and its phosphorylation by the DegS protein kinase. *J Bacteriol* **173**: 2539-2547.

Dahl, M. K., Msadek, T., Kunst, F. & Rapoport, G., (1992) The phosphorylation state of the DegU response regulator acts as a molecular switch allowing either degradative enzyme synthesis or expression of genetic competence in *Bacillus subtilis*. *The Journal of biological chemistry* **267**: 14509-14514.

De Mot, R. & Vanderleyden, J., (1994) The C-terminal sequence conservation between OmpA-related outer membrane proteins and MotB suggests a common function in both gram-positive and gram-negative bacteria, possibly in the interaction of these domains with peptidoglycan. *Mol Microbiol* **12**: 333-334.

Dervyn, E., Noirot-Gros, M. F., Mervelet, P., McGovern, S., Ehrlich, S. D., Polard, P. & Noirot, P., (2004) The bacterial condensin/cohesin-like protein complex acts in DNA repair and regulation of gene expression. *Mol Microbiol* **51**: 1629-1640.

Diethmaier, C., Pietack, N., Gunka, K., Wrede, C., Lehnik-Habrink, M., Herzberg, C., Hubner, S. & Stulke, J., (2011) A novel factor controlling bistability in *Bacillus subtilis*: the YmdB protein affects flagellin expression and biofilm formation. *J Bacteriol* **193**: 5997-6007.

Do, T. H., Suzuki, Y., Abe, N., Kaneko, J., Itoh, Y. & Kimura, K., (2011) Mutations suppressing the loss of DegQ function in *Bacillus subtilis* (natto) poly-gamma-glutamate synthesis. *Applied and environmental microbiology* **77**: 8249-8258.

Dogsa, I., Brloznik, M., Stopar, D. & Mandic-Mulec, I., (2013) Exopolymer diversity and the role of levan in *Bacillus subtilis* biofilms. *PloS one* **8**: e62044.

Domka, J., Lee, J., Bansal, T. & Wood, T. K., (2007) Temporal gene-expression in *Escherichia coli* K-12 biofilms. *Environmental microbiology* **9**: 332-346.

Dyer, C. M., Vartanian, A. S., Zhou, H. & Dahlquist, F. W., (2009) A molecular mechanism of bacterial flagellar motor switching. *J Mol Biol* **388**: 71-84.

Earl, A. M., Eppinger, M., Fricke, W. F., Rosovitz, M. J., Rasko, D. A., Daugherty, S., Losick, R., Kolter, R. & Ravel, J., (2012) Whole-genome sequences of *Bacillus subtilis* and close relatives. *J Bacteriol* **194**: 2378-2379.

Elsholz, A. K., Turgay, K., Michalik, S., Hessling, B., Gronau, K., Oertel, D., Mader, U., Bernhardt, J., Becher, D., Hecker, M. & Gerth, U., (2012) Global impact of

protein arginine phosphorylation on the physiology of *Bacillus subtilis*. *Proc Natl Acad Sci U S A* **109**: 7451-7456.

Epstein, A. K., Pokroy, B., Seminara, A. & Aizenberg, J., (2011) Bacterial biofilm shows persistent resistance to liquid wetting and gas penetration. *Proc Natl Acad Sci U S A* **108**: 995-1000.

Estacio, W., Anna-Arriola, S. S., Adedipe, M. & Marquez-Magana, L. M., (1998) Dual promoters are responsible for transcription initiation of the *fla/che* operon in *Bacillus subtilis*. *J Bacteriol* **180**: 3548-3555.

Evans, L. D., Poulter, S., Terentjev, E. M., Hughes, C. & Fraser, G. M., (2013) A chain mechanism for flagellum growth. *Nature* **504**: 287-290.

Evans, L. D., Stafford, G. P., Ahmed, S., Fraser, G. M. & Hughes, C., (2006) An escort mechanism for cycling of export chaperones during flagellum assembly. *Proc Natl Acad Sci U S A* **103**: 17474-17479.

Feng, F. & Zhou, J. M., (2012) Plant-bacterial pathogen interactions mediated by type III effectors. *Curr Opin Plant Biol* **15**: 469-476.

Flemming, H. C. & Wingender, J., (2010) The biofilm matrix. *Nature reviews. Microbiology* **8**: 623-633.

Francez-Charlot, A., Frunzke, J., Reichen, C., Ebneter, J. Z., Gourion, B. & Vorholt, J. A., (2009) Sigma factor mimicry involved in regulation of general stress response. *Proc Natl Acad Sci U S A* **106**: 3467-3472.

Fraser, G. M., Bennett, J. C. & Hughes, C., (1999) Substrate-specific binding of hook-associated proteins by FlgN and FliT, putative chaperones for flagellum assembly. *Mol Microbiol* **32**: 569-580.

Fraser, G. M. & Hughes, C., (1999) Swarming motility. *Curr Opin Microbiol* **2**: 630-635.

Friedlander, R. S., Vlamakis, H., Kim, P., Khan, M., Kolter, R. & Aizenberg, J., (2013) Bacterial flagella explore microscale hummocks and hollows to increase adhesion. *Proc Natl Acad Sci U S A* **110**: 5624-5629.

Fuhrmann, J., Schmidt, A., Spiess, S., Lehner, A., Turgay, K., Mechtler, K., Charpentier, E. & Clausen, T., (2009) McsB is a protein arginine kinase that phosphorylates and inhibits the heat-shock regulator CtsR. *Science* **324**: 1323-1327.

Fujita, M., Gonzalez-Pastor, J. E. & Losick, R., (2005) High- and low-threshold genes in the Spo0A regulon of *Bacillus subtilis*. *J Bacteriol* **187**: 1357-1368.

Fukuoka, H., Wada, T., Kojima, S., Ishijima, A. & Homma, M., (2009) Sodium-dependent dynamic assembly of membrane complexes in sodium-driven flagellar motors. *Mol Microbiol* **71**: 825-835.

Gao, B., Lara-Tejero, M., Lefebre, M., Goodman, A. L. & Galan, J. E., (2014) Novel components of the flagellar system in epsilonproteobacteria. *mBio* **5**.

Gao, R., Mack, T. R. & Stock, A. M., (2007) Bacterial response regulators: versatile regulatory strategies from common domains. *Trends Biochem Sci* **32**: 225-234.

Gerwig, J., Kiley, T. B., Gunka, K., Stanley-Wall, N. & Stulke, J., (2014) The protein tyrosine kinases EpsB and PtkA differentially affect biofilm formation in *Bacillus subtilis*. *Microbiology*.

Gode-Potratz, C. J., Kustusch, R. J., Breheny, P. J., Weiss, D. S. & McCarter, L. L., (2011) Surface sensing in *Vibrio parahaemolyticus* triggers a programme of gene expression that promotes colonization and virulence. *Mol Microbiol* **79**: 240-263.

Gonzalez-Pedrajo, B., Fraser, G. M., Minamino, T. & Macnab, R. M., (2002) Molecular dissection of *Salmonella* FliH, a regulator of the ATPase FliI and the type III flagellar protein export pathway. *Mol Microbiol* **45**: 967-982.

Gonzalez-Pedrajo, B., Minamino, T., Kihara, M. & Namba, K., (2006) Interactions between C ring proteins and export apparatus components: a possible mechanism for facilitating type III protein export. *Mol Microbiol* **60**: 984-998.

Grangeasse, C., Nessler, S. & Mijakovic, I., (2012) Bacterial tyrosine kinases: evolution, biological function and structural insights. *Philosophical transactions of the Royal Society of London. Series B, Biological sciences* **367**: 2640-2655.

Gueriri, I., Cyncynatus, C., Dubrac, S., Arana, A. T., Dussurget, O. & Msadek, T., (2008) The DegU orphan response regulator of *Listeria monocytogenes* autorepresses its own synthesis and is required for bacterial motility, virulence and biofilm formation. *Microbiology* **154**: 2251-2264.

Guerout-Fleury, A. M., Frandsen, N. & Stragier, P., (1996) Plasmids for ectopic integration in *Bacillus subtilis*. *Gene* **180**: 57-61.

Guttenplan, S. B., Blair, K. M. & Kearns, D. B., (2010) The EpsE flagellar clutch is bifunctional and synergizes with EPS biosynthesis to promote *Bacillus subtilis* biofilm formation. *PLoS genetics* **6**: e1001243.

Guttenplan, S. B. & Kearns, D. B., (2013) Regulation of flagellar motility during biofilm formation. *FEMS microbiology reviews* **37**: 849-871.

Guttenplan, S. B., Shaw, S. & Kearns, D. B., (2013) The cell biology of peritrichous flagella in Bacillus subtilis. *Mol Microbiol* **87**: 211-229.

Guvener, Z. T. & Harwood, C. S., (2007) Subcellular location characteristics of the *Pseudomonas aeruginosa* GGDEF protein, WspR, indicate that it produces cyclic-di-GMP in response to growth on surfaces. *Mol Microbiol* **66**: 1459-1473.

Gygi, D., Fraser, G., Dufour, A. & Hughes, C., (1997) A motile but non-swarming mutant of *Proteus mirabilis* lacks FlgN, a facilitator of flagella filament assembly. *Mol Microbiol* **25**: 597-604.

Hamoen, L. W., Van Werkhoven, A. F., Venema, G. & Dubnau, D., (2000) The pleiotropic response regulator DegU functions as a priming protein in competence development in *Bacillus subtilis*. *Proc Natl Acad Sci U S A* **97**: 9246-9251.

Hamon, M. A. & Lazazzera, B. A., (2001) The sporulation transcription factor Spo0A is required for biofilm development in *Bacillus subtilis*. *Mol Microbiol* **42**: 1199-1209.

Hamon, M. A., Stanley, N. R., Britton, R. A., Grossman, A. D. & Lazazzera, B. A., (2004) Identification of AbrB-regulated genes involved in biofilm formation by *Bacillus subtilis*. *Mol Microbiol* **52**: 847-860.

Harwood, C. R. & Cutting, S. M., (1990) Molecular biological methods for *Bacillus*. John Wiley &Sons Ltd. Chichester, England.

Helmann, J. D., Marquez, L. M. & Chamberlin, M. J., (1988) Cloning, sequencing, and disruption of the *Bacillus subtilis* sigma 28 gene. *J Bacteriol* **170**: 1568-1574.

Henner, D. J., Yang, M. & Ferrari, E., (1988) Localization of *Bacillus subtilis* sacU(Hy) mutations to two linked genes with similarities to the conserved procaryotic family of two-component signalling systems. *J Bacteriol* **170**: 5102-5109.

Higgins, D. & Dworkin, J., (2012) Recent progress in Bacillus subtilis sporulation. *FEMS microbiology reviews* **36**: 131-148.

Hobley, L., Ostrowski, A., Rao, F. V., Bromley, K. M., Porter, M., Prescott, A. R., MacPhee, C. E., van Aalten, D. M. & Stanley-Wall, N. R., (2013) BslA is a self-assembling bacterial hydrophobin that coats the *Bacillus subtilis* biofilm. *Proc Natl Acad Sci U S A* **110**: 13600-13605.

Hosking, E. R., Vogt, C., Bakker, E. P. & Manson, M. D., (2006) The *Escherichia coli* MotAB proton channel unplugged. *J Mol Biol* **364**: 921-937.

Houry, A., Gohar, M., Deschamps, J., Tischenko, E., Aymerich, S., Gruss, A. & Briandet, R., (2012) Bacterial swimmers that infiltrate and take over the biofilm matrix. *Proc Natl Acad Sci U S A* **109**: 13088-13093.

Hsueh, Y. H., Cozy, L. M., Sham, L. T., Calvo, R. A., Gutu, A. D., Winkler, M. E. & Kearns, D. B., (2011) DegU-phosphate activates expression of the anti-sigma factor FlgM in *Bacillus subtilis*. *Mol Microbiol* **81**: 1092-1108.

Huangyutitham, V., Guvener, Z. T. & Harwood, C. S., (2013) Subcellular clustering of the phosphorylated WspR response regulator protein stimulates its diguanylate cyclase activity. *mBio* **4**: e00242-00213.

Hughes, K. T., Gillen, K. L., Semon, M. J. & Karlinsey, J. E., (1993) Sensing structural intermediates in bacterial flagellar assembly by export of a negative regulator. *Science* **262**: 1277-1280.

Irnov, I. & Winkler, W. C., (2010) A regulatory RNA required for antitermination of biofilm and capsular polysaccharide operons in Bacillales. *Mol Microbiol* **76**: 559-575.

Ishii, H., Tanaka, T. & Ogura, M., (2013) The *Bacillus subtilis* response regulator gene *degU* is positively regulated by CcpA and by catabolite-repressed synthesis of ClpC. *J Bacteriol* **195**: 193-201.

Ito, M., Hicks, D. B., Henkin, T. M., Guffanti, A. A., Powers, B. D., Zvi, L., Uematsu, K. & Krulwich, T. A., (2004) MotPS is the stator-force generator for motility of alkaliphilic *Bacillus*, and its homologue is a second functional Mot in *Bacillus subtilis*. *Mol Microbiol* **53**: 1035-1049.

Ito, M., Terahara, N., Fujinami, S. & Krulwich, T. A., (2005) Properties of motility in *Bacillus subtilis* powered by the H+-coupled MotAB flagellar stator, Na+-coupled MotPS or hybrid stators MotAS or MotPB. *J Mol Biol* **352**: 396-408.

Jarrell, K. F. & McBride, M. J., (2008) The surprisingly diverse ways that prokaryotes move. *Nature reviews. Microbiology* **6**: 466-476.

Jers, C., Kobir, A., Sondergaard, E. O., Jensen, P. R. & Mijakovic, I., (2011) *Bacillus subtilis* two-component system sensory kinase DegS is regulated by serine phosphorylation in its input domain. *PloS one* **6**: e14653.

Jers, C., Pedersen, M. M., Paspaliari, D. K., Schutz, W., Johnsson, C., Soufi, B., Macek, B., Jensen, P. R. & Mijakovic, I., (2010) *Bacillus subtilis* BY-kinase PtkA controls enzyme activity and localization of its protein substrates. *Mol Microbiol* **77**: 287-299.

Johansson, J., Mandin, P., Renzoni, A., Chiaruttini, C., Springer, M. & Cossart, P., (2002) An RNA thermosensor controls expression of virulence genes in *Listeria monocytogenes*. *Cell* **110**: 551-561.

Jones, S. E. & Knight, K. L., (2012) *Bacillus subtilis*-mediated protection from *Citrobacter rodentium*-associated enteric disease requires espH and functional flagella. *Infection and immunity* **80**: 710-719.

Jones, S. E., Paynich, M. L., Kearns, D. B. & Knight, K. L., (2014) Protection from intestinal inflammation by bacterial exopolysaccharides. *Journal of immunology* **192**: 4813-4820.

Karlinsey, J. E., Lonner, J., Brown, K. L. & Hughes, K. T., (2000a) Translation/secretion coupling by type III secretion systems. *Cell* **102**: 487-497.

Karlinsey, J. E., Tanaka, S., Bettenworth, V., Yamaguchi, S., Boos, W., Aizawa, S. I. & Hughes, K. T., (2000b) Completion of the hook-basal body complex of the *Salmonella* typhimurium flagellum is coupled to FlgM secretion and fliC transcription. *Mol Microbiol* **37**: 1220-1231.

Kawagishi, I., Imagawa, M., Imae, Y., McCarter, L. & Homma, M., (1996) The sodium-driven polar flagellar motor of marine *Vibrio* as the mechanosensor that regulates lateral flagellar expression. *Mol Microbiol* **20**: 693-699.

Kazetani, K., Minamino, T., Miyata, T., Kato, T. & Namba, K., (2009) ATP-induced FliI hexamerization facilitates bacterial flagellar protein export. *Biochemical and biophysical research communications* **388**: 323-327.

Kearns, D. B., (2010) A field guide to bacterial swarming motility. *Nature reviews. Microbiology* **8**: 634-644.

Kearns, D. B., Chu, F., Branda, S. S., Kolter, R. & Losick, R., (2005) A master regulator for biofilm formation by Bacillus subtilis. *Mol Microbiol* **55**: 739-749.

Kearns, D. B., Chu, F., Rudner, R. & Losick, R., (2004) Genes governing swarming in *Bacillus subtilis* and evidence for a phase variation mechanism controlling surface motility. *Mol Microbiol* **52**: 357-369.

Kearns, D. B. & Losick, R., (2003) Swarming motility in undomesticated *Bacillus subtilis*. *Mol Microbiol* **49**: 581-590.

Kearns, D. B. & Losick, R., (2005) Cell population heterogeneity during growth of *Bacillus subtilis*. *Genes Dev* **19**: 3083-3094.

Khan, I. H., Reese, T. S. & Khan, S., (1992) The cytoplasmic component of the bacterial flagellar motor. *Proc Natl Acad Sci U S A* **89**: 5956-5960.

Kiley, T. B. & Stanley-Wall, N. R., (2010) Post-translational control of *Bacillus subtilis* biofilm formation mediated by tyrosine phosphorylation. *Mol Microbiol* **78**: 947-963.

Kim, W. & Surette, M. G., (2004) Metabolic differentiation in actively swarming *Salmonella*. *Mol Microbiol* **54**: 702-714.

Kinoshita, M., Hara, N., Imada, K., Namba, K. & Minamino, T., (2013) Interactions of bacterial flagellar chaperone-substrate complexes with FlhA contribute to co-ordinating assembly of the flagellar filament. *Mol Microbiol* **90**: 1249-1261.

Kobayashi, K., (2007) Gradual activation of the response regulator DegU controls serial expression of genes for flagellum formation and biofilm formation in *Bacillus subtilis*. *Mol Microbiol* **66**: 395-409.

Kobayashi, K., (2008) SlrR/SlrA controls the initiation of biofilm formation in *Bacillus subtilis*. *Mol Microbiol* **69**: 1399-1410.

Kobayashi, K. & Iwano, M., (2012) BslA(YuaB) forms a hydrophobic layer on the surface of *Bacillus subtilis* biofilms. *Mol Microbiol* **85**: 51-66.

Kojima, S. & Blair, D. F., (2001) Conformational change in the stator of the bacterial flagellar motor. *Biochemistry* **40**: 13041-13050.

Kojima, S. & Blair, D. F., (2004) Solubilization and purification of the MotA/MotB complex of *Escherichia coli*. *Biochemistry* **43**: 26-34.

Konkol, M. A., Blair, K. M. & Kearns, D. B., (2013) Plasmid-encoded ComI inhibits competence in the ancestral 3610 strain of *Bacillus subtilis*. *J Bacteriol* **195**: 4085-4093.

Kovacs, A. T. & Kuipers, O. P., (2011) Rok regulates *yuaB* expression during architecturally complex colony development of *Bacillus subtilis* 168. *J Bacteriol* **193**: 998-1002.

Kubori, T., Okumura, M., Kobayashi, N., Nakamura, D., Iwakura, M. & Aizawa, S. I., (1997) Purification and characterization of the flagellar hook-basal body complex of *Bacillus subtilis*. *Mol Microbiol* **24**: 399-410.

Kulasekara, B. R., Kamischke, C., Kulasekara, H. D., Christen, M., Wiggins, P. A. & Miller, S. I., (2013) c-di-GMP heterogeneity is generated by the chemotaxis machinery to regulate flagellar motility. *eLife* **2**: e01402.

Kutsukake, K., (1994) Excretion of the anti-sigma factor through a flagellar substructure couples flagellar gene expression with flagellar assembly in *Salmonella* Typhimurium. *Mol Gen Genet* **243**: 605-612.

Kutsukake, K., Okada, T., Yokoseki, T. & Iino, T., (1994) Sequence analysis of the *flgA* gene and its adjacent region in *Salmonella* Typhimurium, and identification of another flagellar gene, *flgN*. *Gene* **143**: 49-54.

Laemmli, U. K., (1970) Cleavage of structural proteins during the assembly of the head of bacteriophage T4. *Nature* **227**: 680-685.

Landry, C. R., Levy, E. D. & Michnick, S. W., (2009) Weak functional constraints on phosphoproteomes. *Trends Genet* **25**: 193-197.

Laub, M. T. & Goulian, M., (2007) Specificity in two-component signal transduction pathways. *Annual review of genetics* **41**: 121-145.

Leake, M. C., Chandler, J. H., Wadhams, G. H., Bai, F., Berry, R. M. & Armitage, J. P., (2006) Stoichiometry and turnover in single, functioning membrane protein complexes. *Nature* **443**: 355-358.

Lee, Y. Y., Patellis, J. & Belas, R., (2013) Activity of *Proteus mirabilis* FliL is viscosity dependent and requires extragenic DNA. *J Bacteriol* **195**: 823-832.

Lele, P. P., Hosu, B. G. & Berg, H. C., (2013) Dynamics of mechanosensing in the bacterial flagellar motor. *Proc Natl Acad Sci U S A* **110**: 11839-11844.

Lemon, K. P., Higgins, D. E. & Kolter, R., (2007) Flagellar motility is critical for *Listeria monocytogenes* biofilm formation. *J Bacteriol* **189**: 4418-4424.

Levine, A., Vannier, F., Absalon, C., Kuhn, L., Jackson, P., Scrivener, E., Labas, V., Vinh, J., Courtney, P., Garin, J. & Seror, S. J., (2006) Analysis of the dynamic *Bacillus subtilis* Ser/Thr/Tyr phosphoproteome implicated in a wide variety of cellular processes. *Proteomics* **6**: 2157-2173.

Lewis, R. J., Brannigan, J. A., Offen, W. A., Smith, I. & Wilkinson, A. J., (1998) An evolutionary link between sporulation and prophage induction in the structure of a repressor:anti-repressor complex. *J Mol Biol* **283**: 907-912.

Li, G., Brown, P. J., Tang, J. X., Xu, J., Quardokus, E. M., Fuqua, C. & Brun, Y. V., (2012) Surface contact stimulates the just-in-time deployment of bacterial adhesins. *Mol Microbiol* **83**: 41-51.

Liu, H. T. & Naismith, J. H., (2009) A simple and efficient expression and purification system using two newly constructed vectors. *Protein Expres Purif* **63**: 102-111.

Liu, Y., Zhang, W., Sileika, T., Warta, R., Cianciotto, N. P. & Packman, A., (2009) Role of bacterial adhesion in the microbial ecology of biofilms in cooling tower systems. *Biofouling* **25**: 241-253.

Lopez, D., Fischbach, M. A., Chu, F., Losick, R. & Kolter, R., (2009) Structurally diverse natural products that cause potassium leakage trigger multicellularity in *Bacillus subtilis*. *Proc Natl Acad Sci U S A* **106**: 280-285.

Lundberg, M. E., Becker, E. C. & Choe, S., (2013) MstX and a putative potassium channel facilitate biofilm formation in *Bacillus subtilis*. *PloS one* **8**: e60993.

Macek, B., Gnad, F., Soufi, B., Kumar, C., Olsen, J. V., Mijakovic, I. & Mann, M., (2008) Phosphoproteome analysis of *E. coli* reveals evolutionary conservation of bacterial Ser/Thr/Tyr phosphorylation. *Mol Cell Proteomics* **7**: 299-307.

Macek, B., Mijakovic, I., Olsen, J. V., Gnad, F., Kumar, C., Jensen, P. R. & Mann, M., (2007) The serine/threonine/tyrosine phosphoproteome of the model bacterium *Bacillus subtilis*. *Mol Cell Proteomics* **6**: 697-707.

Macho, A. P., Schwessinger, B., Ntoukakis, V., Brutus, A., Segonzac, C., Roy, S., Kadota, Y., Oh, M. H., Sklenar, J., Derbyshire, P., Lozano-Duran, R., Malinovsky, F. G., Monaghan, J., Menke, F. L., Huber, S. C., He, S. Y. & Zipfel, C., (2014) A bacterial tyrosine phosphatase inhibits plant pattern recognition receptor activation. *Science* **343**: 1509-1512.

Mader, U., Antelmann, H., Buder, T., Dahl, M. K., Hecker, M. & Homuth, G., (2002) *Bacillus subtilis* functional genomics: genome-wide analysis of the DegS-DegU regulon by transcriptomics and proteomics. *Molecular genetics and genomics : MGG* **268**: 455-467.

Marlow, V. L., Cianfanelli, F. R., Porter, M., Cairns, L. S., Dale, J. K. & Stanley-Wall, N. R., (2014a) The prevalence and origin of exoprotease-producing cells in the *Bacillus subtilis* biofilm. *Microbiology* **160**: 56-66.

Marlow, V. L., Porter, M., Hobley, L., Kiley, T. B., Swedlow, J. R., Davidson, F. A. & Stanley-Wall, N. R., (2014b) Phosphorylated DegU manipulates cell fate differentiation in the *Bacillus subtilis* biofilm. *J Bacteriol* **196**: 16-27.

Marquez-Magana, L. M. & Chamberlin, M. J., (1994) Characterization of the sigD transcription unit of *Bacillus subtilis*. *J Bacteriol* **176**: 2427-2434.

Marquez, L. M., Helmann, J. D., Ferrari, E., Parker, H. M., Ordal, G. W. & Chamberlin, M. J., (1990) Studies of sigma D-dependent functions in *Bacillus subtilis*. *J Bacteriol* **172**: 3435-3443.

Mascher, T., (2013) Signaling diversity and evolution of extracytoplasmic function (ECF) sigma factors. *Curr Opin Microbiol* **16**: 148-155.

Mattick, J. S., (2002) Type IV pili and twitching motility. *Annual review of microbiology* **56**: 289-314.

McBride, M. J., (2001) Bacterial gliding motility: multiple mechanisms for cell movement over surfaces. *Annual review of microbiology* **55**: 49-75.

McCarter, L., Hilmen, M. & Silverman, M., (1988) Flagellar dynamometer controls swarmer cell differentiation of *V. parahaemolyticus*. *Cell* **54**: 345-351.

McGuffin, L. J., Bryson, K. & Jones, D. T., (2000) The PSIPRED protein structure prediction server. *Bioinformatics* **16**: 404-405.

McLoon, A. L., Guttenplan, S. B., Kearns, D. B., Kolter, R. & Losick, R., (2011) Tracing the domestication of a biofilm-forming bacterium. *J Bacteriol* **193**: 2027-2034.

Meister, M., Lowe, G. & Berg, H. C., (1987) The proton flux through the bacterial flagellar motor. *Cell* **49**: 643-650.

Middleton, R. & Hofmeister, A., (2004) New shuttle vectors for ectopic insertion of genes into *Bacillus subtilis*. *Plasmid* **51**: 238-245.

Mijakovic, I., Petranovic, D., Macek, B., Cepo, T., Mann, M., Davies, J., Jensen, P. R. & Vujaklija, D., (2006) Bacterial single-stranded DNA-binding proteins are phosphorylated on tyrosine. *Nucleic Acids Res* **34**: 1588-1596.

Mijakovic, I., Poncet, S., Boel, G., Maze, A., Gillet, S., Jamet, E., Decottignies, P., Grangeasse, C., Doublet, P., Le Marechal, P. & Deutscher, J., (2003) Transmembrane modulator-dependent bacterial tyrosine kinase activates UDP-glucose dehydrogenases. *EMBO J* **22**: 4709-4718.

Miller, J., (1972) Experiments in molecular genetics. Cold Spring Harbor Laboratory, Cold Spring Harbor, N.Y.

Minamino, T., (2013) Protein export through the bacterial flagellar type III export pathway. *Biochimica et biophysica acta*.

Minamino, T., Kinoshita, M., Hara, N., Takeuchi, S., Hida, A., Koya, S., Glenwright, H., Imada, K., Aldridge, P. D. & Namba, K., (2012) Interaction of a bacterial flagellar chaperone FlgN with FlhA is required for efficient export of its cognate substrates. *Mol Microbiol* **83**: 775-788.

Minamino, T. & Macnab, R. M., (1999) Components of the *Salmonella* flagellar export apparatus and classification of export substrates. *J Bacteriol* **181**: 1388-1394.

Minamino, T. & MacNab, R. M., (2000a) FliH, a soluble component of the type III flagellar export apparatus of *Salmonella,* forms a complex with FliI and inhibits its ATPase activity. *Mol Microbiol* **37**: 1494-1503.

Minamino, T. & MacNab, R. M., (2000b) Interactions among components of the *Salmonella* flagellar export apparatus and its substrates. *Mol Microbiol* **35**: 1052-1064.

Minamino, T. & Namba, K., (2008) Distinct roles of the FliI ATPase and proton motive force in bacterial flagellar protein export. *Nature* **451**: 485-488.

Mirel, D. B., Lauer, P. & Chamberlin, M. J., (1994) Identification of flagellar synthesis regulatory and structural genes in a sigma D-dependent operon of *Bacillus subtilis*. *J Bacteriol* **176**: 4492-4500.

Morikawa, M., Kagihiro, S., Haruki, M., Takano, K., Branda, S., Kolter, R. & Kanaya, S., (2006) Biofilm formation by a *Bacillus subtilis* strain that produces gamma-polyglutamate. *Microbiology* **152**: 2801-2807.

Morimoto, Y. V., Nakamura, S., Kami-ike, N., Namba, K. & Minamino, T., (2010) Charged residues in the cytoplasmic loop of MotA are required for stator assembly into the bacterial flagellar motor. *Mol Microbiol* **78**: 1117-1129.

Motaleb, M. A., Pitzer, J. E., Sultan, S. Z. & Liu, J., (2011) A novel gene inactivation system reveals altered periplasmic flagellar orientation in a *Borrelia burgdorferi fliL* mutant. *J Bacteriol* **193**: 3324-3331.

Msadek, T., Kunst, F., Henner, D., Klier, A., Rapoport, G. & Dedonder, R., (1990) Signal transduction pathway controlling synthesis of a class of degradative enzymes in *Bacillus subtilis*: expression of the regulatory genes and analysis of mutations in *degS* and *degU*. *J Bacteriol* **172**: 824-834.

Msadek, T., Kunst, F., Klier, A. & Rapoport, G., (1991) DegS-DegU and ComP-ComA modulator-effector pairs control expression of the *Bacillus subtilis* pleiotropic regulatory gene *degQ*. *J Bacteriol* **173**: 2366-2377.

Mukai, K., Kawata, M. & Tanaka, T., (1990) Isolation and phosphorylation of the *Bacillus subtilis degS* and *degU* gene products. *The Journal of biological chemistry* **265**: 20000-20006.

Mukherjee, S., Babitzke, P. & Kearns, D. B., (2013) FliW and FliS Function Independently To Control Cytoplasmic Flagellin Levels in *Bacillus subtilis*. *J Bacteriol* **195**: 297-306.

Mukherjee, S., Yakhnin, H., Kysela, D., Sokoloski, J., Babitzke, P. & Kearns, D. B., (2011) CsrA-FliW interaction governs flagellin homeostasis and a checkpoint on flagellar morphogenesis in *Bacillus subtilis*. *Molecular Microbiol* **82**: 447-461.

Murray, E. J., Strauch, M. A. & Stanley-Wall, N. R., (2009) SigmaX is involved in controlling *Bacillus subtilis* biofilm architecture through the AbrB homologue Abh. *J Bacteriol* **191**: 6822-6832.

Nagorska, K., Bikowski, M. & Obuchowski, M., (2007) Multicellular behaviour and production of a wide variety of toxic substances support usage of *Bacillus subtilis* as a powerful biocontrol agent. *Acta biochimica Polonica* **54**: 495-508.

Newman, J. A. & Lewis, R. J., (2013) Exploring the role of SlrR and SlrA in the SinR epigenetic switch. *Communicative & integrative biology* **6**: e25658.

Newman, J. A., Rodrigues, C. & Lewis, R. J., (2013) Molecular basis of the activity of SinR protein, the master regulator of biofilm formation in *Bacillus subtilis*. *The Journal of biological chemistry* **288**: 10766-10778.

Ng, W. L. & Bassler, B. L., (2009) Bacterial quorum-sensing network architectures. *Annual review of genetics* **43**: 197-222.

Nixon, B. T., Ronson, C. W. & Ausubel, F. M., (1986) Two-component regulatory systems responsive to environmental stimuli share strongly conserved domains with the nitrogen assimilation regulatory genes ntrB and ntrC. *Proc Natl Acad Sci U S A* **83**: 7850-7854.

O'Connor, J. R., Kuwada, N. J., Huangyutitham, V., Wiggins, P. A. & Harwood, C. S., (2012) Surface sensing and lateral subcellular localization of WspA, the receptor in a chemosensory-like system leading to c-di-GMP production. *Mol Microbiol* **86**: 720-729.

O'Toole, G., Kaplan, H. B. & Kolter, R., (2000) Biofilm formation as microbial development. *Annual review of microbiology* **54**: 49-79.

O'Toole, G. A. & Kolter, R., (1998) Flagellar and twitching motility are necessary for *Pseudomonas aeruginosa* biofilm development. *Mol Microbiol* **30**: 295-304.

Ogura, M., Shimane, K., Asai, K., Ogasawara, N. & Tanaka, T., (2003) Binding of response regulator DegU to the *aprE* promoter is inhibited by RapG, which is counteracted by extracellular PhrG in *Bacillus subtilis*. *Mol Microbiol* **49**: 1685-1697.

Ogura, M., Yamaguchi, H., Yoshida, K., Fujita, Y. & Tanaka, T., (2001) DNA microarray analysis of *Bacillus subtilis* DegU, ComA and PhoP regulons: an approach to comprehensive analysis of *B.subtilis* two-component regulatory systems. *Nucleic Acids Res* **29**: 3804-3813.

Ohsawa, T., Tsukahara, K. & Ogura, M., (2009) *Bacillus subtilis* response regulator DegU is a direct activator of *pgsB* transcription involved in gamma-poly-glutamic acid synthesis. *Bioscience, biotechnology, and biochemistry* **73**: 2096-2102.

Osera, C., Amati, G., Calvio, C. & Galizzi, A., (2009) SwrAA activates poly-gamma-glutamate synthesis in addition to swarming in *Bacillus subtilis*. *Microbiology* **155**: 2282-2287.

Ostrowski, A., Mehert, A., Prescott, A., Kiley, T. B. & Stanley-Wall, N. R., (2011) YuaB functions synergistically with the exopolysaccharide and TasA amyloid fibers to allow biofilm formation by *Bacillus subtilis*. *J Bacteriol* **193**: 4821-4831.

Ozin, A. J., Claret, L., Auvray, F. & Hughes, C., (2003) The FliS chaperone selectively binds the disordered flagellin C-terminal D0 domain central to polymerisation. *FEMS microbiology letters* **219**: 219-224.

Pallen, M. J., Penn, C. W. & Chaudhuri, R. R., (2005) Bacterial flagellar diversity in the post-genomic era. *Trends Microbiol* **13**: 143-149.

Parashar, V., Konkol, M. A., Kearns, D. B. & Neiditch, M. B., (2013) A plasmid-encoded phosphatase regulates *Bacillus subtilis* biofilm architecture, sporulation, and genetic competence. *J Bacteriol* **195**: 2437-2448.

Partridge, J. D. & Harshey, R. M., (2013) More than motility: *Salmonella* flagella contribute to overriding friction and facilitating colony hydration during swarming. *J Bacteriol* **195**: 919-929.

Paul, K., Erhardt, M., Hirano, T., Blair, D. F. & Hughes, K. T., (2008) Energy source of flagellar type III secretion. *Nature* **451**: 489-492.

Paul, K., Nieto, V., Carlquist, W. C., Blair, D. F. & Harshey, R. M., (2010) The c-di-GMP binding protein YcgR controls flagellar motor direction and speed to affect chemotaxis by a "backstop brake" mechanism. *Molecular cell* **38**: 128-139.

Pawson, T. & Scott, J. D., (2005) Protein phosphorylation in signaling--50 years and counting. *Trends Biochem Sci* **30**: 286-290.

Peel, M., Donachie, W. & Shaw, A., (1988) Temperature-dependent expression of flagella of *Listeria monocytogenes* studied by electron microscopy, SDS-PAGE and western blotting. *Journal of general microbiology* **134**: 2171-2178.

Perego, M. & Hoch, J. A., (1988) Sequence analysis and regulation of the *hpr* locus, a regulatory gene for protease production and sporulation in *Bacillus subtilis*. *J Bacteriol* **170**: 2560-2567.

Petranovic, D., Grangeasse, C., Macek, B., Abdillatef, M., Gueguen-Chaignon, V., Nessler, S., Deutscher, J. & Mijakovic, I., (2009) Activation of *Bacillus subtilis* Ugd by the BY-kinase PtkA proceeds via phosphorylation of its residue tyrosine 70. *J Mol Microbiol Biotechnol* **17**: 83-89.

Petranovic, D., Michelsen, O., Zahradka, K., Silva, C., Petranovic, M., Jensen, P. R. & Mijakovic, I., (2007) *Bacillus subtilis* strain deficient for the protein-tyrosine kinase PtkA exhibits impaired DNA replication. *Mol Microbiol* **63**: 1797-1805.

Pilizota, T., Brown, M. T., Leake, M. C., Branch, R. W., Berry, R. M. & Armitage, J. P., (2009) A molecular brake, not a clutch, stops the *Rhodobacter sphaeroides* flagellar motor. *Proc Natl Acad Sci U S A* **106**: 11582-11587.

Podgornaia, A. I. & Laub, M. T., (2013) Determinants of specificity in two-component signal transduction. *Curr Opin Microbiol* **16**: 156-162.

Porter, S. L., Wadhams, G. H. & Armitage, J. P., (2011) Signal processing in complex chemotaxis pathways. *Nature reviews. Microbiology* **9**: 153-165.

Pratt, L. A. & Kolter, R., (1998) Genetic analysis of *Escherichia coli* biofilm formation: roles of flagella, motility, chemotaxis and type I pili. *Mol Microbiol* **30**: 285-293.

Rao, C. V., Glekas, G. D. & Ordal, G. W., (2008) The three adaptation systems of *Bacillus subtilis* chemotaxis. *Trends Microbiol* **16**: 480-487.

Romero, D., Aguilar, C., Losick, R. & Kolter, R., (2010) Amyloid fibers provide structural integrity to *Bacillus subtilis* biofilms. *Proc Natl Acad Sci U S A* **107**: 2230-2234.

Romero, D., Vlamakis, H., Losick, R. & Kolter, R., (2011) An accessory protein required for anchoring and assembly of amyloid fibres in *B. subtilis* biofilms. *Mol Microbiol* **80**: 1155-1168.

Russell, A. B., Peterson, S. B. & Mougous, J. D., (2014) Type VI secretion system effectors: poisons with a purpose. *Nature reviews. Microbiology* **12**: 137-148.

Ruzal, S. M. & Sanchez-Rivas, C., (1998) In *Bacillus subtilis* DegU-P is a positive regulator of the osmotic response. *Current microbiology* **37**: 368-372.

Sambrook, J. & Russell, D., (2001) *Molecular Cloning. A laboratory manual*. Cold Springs Harbour Laboratory Press.

Sanchez, A. & Olmos, J., (2004) *Bacillus subtilis* transcriptional regulators interaction. *Biotechnology letters* **26**: 403-407.

Scott, D. J., Leejeerajumnean, S., Brannigan, J. A., Lewis, R. J., Wilkinson, A. J. & Hoggett, J. G., (1999) Quaternary re-arrangement analysed by spectral enhancement: the interaction of a sporulation repressor with its antagonist. *J Mol Biol* **293**: 997-1004.

Serra, D. O., Richter, A. M., Klauck, G., Mika, F. & Hengge, R., (2013) Microanatomy at cellular resolution and spatial order of physiological differentiation in a bacterial biofilm. *mBio* **4**: e00103-00113.

Shapiro, J. A., (1988) Bacteria as Multicellular Organisms. *Scientific American* **258**: 82-89.

Shapiro, J. A., (1998) Thinking about bacterial populations as multicellular organisms. *Annual review of microbiology* **52**: 81-104.

Sharp, L. L., Zhou, J. & Blair, D. F., (1995) Tryptophan-scanning mutagenesis of MotB, an integral membrane protein essential for flagellar rotation in *Escherichia coli*. *Biochemistry* **34**: 9166-9171.

Shimane, K. & Ogura, M., (2004) Mutational analysis of the helix-turn-helix region of *Bacillus subtilis* response regulator DegU, and identification of cis-acting sequences for DegU in the *aprE* and *comK* promoters. *Journal of biochemistry* **136**: 387-397.

Shimoyama, T., Kato, S., Ishii, S. & Watanabe, K., (2009) Flagellum mediates symbiosis. *Science* **323**: 1574.

Sievers, F., Wilm, A., Dineen, D., Gibson, T. J., Karplus, K., Li, W., Lopez, R., McWilliam, H., Remmert, M., Soding, J., Thompson, J. D. & Higgins, D. G., (2011) Fast, scalable generation of high-quality protein multiple sequence alignments using Clustal Omega. *Molecular systems biology* **7**: 539.

Silverman, M., Matsumura, P. & Simon, M., (1976) The identification of the mot gene product with *Escherichia coli*-lambda hybrids. *Proc Natl Acad Sci U S A* **73**: 3126-3130.

Soppa, J., Kobayashi, K., Noirot-Gros, M. F., Oesterhelt, D., Ehrlich, S. D., Dervyn, E., Ogasawara, N. & Moriya, S., (2002) Discovery of two novel families of proteins that are proposed to interact with prokaryotic SMC proteins, and characterization of the *Bacillus subtilis* family members ScpA and ScpB. *Mol Microbiol* **45**: 59-71.

Sourjik, V. & Schmitt, R., (1998) Phosphotransfer between CheA, CheY1, and CheY2 in the chemotaxis signal transduction chain of *Rhizobium meliloti*. *Biochemistry* **37**: 2327-2335.

Sowa, Y., Homma, M., Ishijima, A. & Berry, R. M., (2014) Hybrid-fuel bacterial flagellar motors in *Escherichia coli*. *Proc Natl Acad Sci U S A* **111**: 3436-3441.

Srivatsan, A., Han, Y., Peng, J., Tehranchi, A. K., Gibbs, R., Wang, J. D. & Chen, R., (2008) High-precision, whole-genome sequencing of laboratory strains facilitates genetic studies. *PLoS genetics* **4**: e1000139.

Stanley, N. R., Britton, R. A., Grossman, A. D. & Lazazzera, B. A., (2003) Identification of catabolite repression as a physiological regulator of biofilm formation by *Bacillus subtilis* by use of DNA microarrays. *J Bacteriol* **185**: 1951-1957.

Stanley, N. R. & Lazazzera, B. A., (2005) Defining the genetic differences between wild and domestic strains of *Bacillus subtilis* that affect poly-gamma-dl-glutamic acid production and biofilm formation. *Mol Microbiol* **57**: 1143-1158.

Strauch, M., Webb, V., Spiegelman, G. & Hoch, J. A., (1990) The SpoOA protein of *Bacillus subtilis* is a repressor of the *abrB* gene. *Proc Natl Acad Sci U S A* **87**: 1801-1805.

Suaste-Olmos, F., Domenzain, C., Mireles-Rodriguez, J. C., Poggio, S., Osorio, A., Dreyfus, G. & Camarena, L., (2010) The flagellar protein FliL is essential for swimming in Rhodobacter sphaeroides. *J Bacteriol* **192**: 6230-6239.

Tanaka, T., Kawata, M. & Mukai, K., (1991) Altered phosphorylation of *Bacillus subtilis* DegU caused by single amino acid changes in DegS. *J Bacteriol* **173**: 5507-5515.

Thomas, J., Stafford, G. P. & Hughes, C., (2004) Docking of cytosolic chaperone-substrate complexes at the membrane ATPase during flagellar type III protein export. *Proc Natl Acad Sci U S A* **101**: 3945-3950.

Tipping, M. J., Delalez, N. J., Lim, R., Berry, R. M. & Armitage, J. P., (2013a) Load-dependent assembly of the bacterial flagellar motor. *mBio* **4**.

Tipping, M. J., Steel, B. C., Delalez, N. J., Berry, R. M. & Armitage, J. P., (2013b) Quantification of flagellar motor stator dynamics through in vivo proton-motive force control. *Mol Microbiol* **87**: 338-347.

Titz, B., Rajagopala, S. V., Ester, C., Hauser, R. & Uetz, P., (2006) Novel conserved assembly factor of the bacterial flagellum. *J Bacteriol* **188**: 7700-7706.

Tsukahara, K. & Ogura, M., (2008a) Characterization of DegU-dependent expression of *bpr* in *Bacillus subtilis*. *FEMS microbiology letters* **280**: 8-13.

Tsukahara, K. & Ogura, M., (2008b) Promoter selectivity of the *Bacillus subtilis* response regulator DegU, a positive regulator of the *fla/che* operon and *sacB*. *BMC microbiology* **8**: 8.

Tucker, A. T., Bobay, B. G., Banse, A. V., Olson, A. L., Soderblom, E. J., Moseley, M. A., Thompson, R. J., Varney, K. M., Losick, R. & Cavanagh, J., (2014) A DNA Mimic: The Structure and Mechanism of Action for the Anti-Repressor Protein AbbA. *J Mol Biol* **426**: 1911-1924.

Ulrich, L. E., Koonin, E. V. & Zhulin, I. B., (2005) One-component systems dominate signal transduction in prokaryotes. *Trends Microbiol* **13**: 52-56.

Van Dellen, K. L., Houot, L. & Watnick, P. I., (2008) Genetic analysis of Vibrio cholerae monolayer formation reveals a key role for DeltaPsi in the transition to permanent attachment. *J Bacteriol* **190**: 8185-8196.

Veening, J. W., Hamoen, L. W. & Kuipers, O. P., (2005) Phosphatases modulate the bistable sporulation gene expression pattern in *Bacillus subtilis*. *Mol Microbiol* **56**: 1481-1494.

Veening, J. W., Igoshin, O. A., Eijlander, R. T., Nijland, R., Hamoen, L. W. & Kuipers, O. P., (2008) Transient heterogeneity in extracellular protease production by *Bacillus subtilis*. *Molecular systems biology* **4**: 184.

Verhamme, D. T., Kiley, T. B. & Stanley-Wall, N. R., (2007) DegU co-ordinates multicellular behaviour exhibited by *Bacillus subtilis*. *Mol Microbiol* **65**: 554-568.

Verhamme, D. T., Murray, E. J. & Stanley-Wall, N. R., (2009) DegU and Spo0A jointly control transcription of two loci required for complex colony development by *Bacillus subtilis*. *J Bacteriol* **191**: 100-108.

Vieira, J. & Messing, J., (1982) The pUC plasmids, an M13mp7-derived system for insertion mutagenesis and sequencing with synthetic universal primers. *Gene* **19**: 259-268.

Vlamakis, H., Aguilar, C., Losick, R. & Kolter, R., (2008) Control of cell fate by the formation of an architecturally complex bacterial community. *Genes Dev* **22**: 945-953.

Vlamakis, H., Chai, Y., Beauregard, P., Losick, R. & Kolter, R., (2013) Sticking together: building a biofilm the *Bacillus subtilis* way. *Nature reviews. Microbiology* **11**: 157-168.

Wang, Q., Frye, J. G., McClelland, M. & Harshey, R. M., (2004) Gene expression patterns during swarming in *Salmonella* typhimurium: genes specific to surface growth and putative new motility and pathogenicity genes. *Mol Microbiol* **52**: 169-187.

Wang, Q., Suzuki, A., Mariconda, S., Porwollik, S. & Harshey, R. M., (2005) Sensing wetness: a new role for the bacterial flagellum. *EMBO J* **24**: 2034-2042.

Watnick, P. I. & Kolter, R., (1999) Steps in the development of a *Vibrio cholerae* El Tor biofilm. *Mol Microbiol* **34**: 586-595.

Welch, M., Oosawa, K., Aizawa, S. I. & Eisenbach, M., (1993) Phosphorylation-Dependent Binding of a Signal Molecule to the Flagellar Switch of Bacteria. *Proc Natl Acad Sci USA* **90**: 8787-8791.

West, J. T., Estacio, W. & Marquez-Magana, L., (2000) Relative roles of the *fla/che* P(A), P(D-3), and P(sigD) promoters in regulating motility and *sigD* expression in *Bacillus subtilis*. *J Bacteriol* **182**: 4841-4848.

Wolfe, A. J., Chang, D. E., Walker, J. D., Seitz-Partridge, J. E., Vidaurri, M. D., Lange, C. F., Pruss, B. M., Henk, M. C., Larkin, J. C. & Conway, T., (2003) Evidence that acetyl phosphate functions as a global signal during biofilm development. *Mol Microbiol* **48**: 977-988.

Wolfe, A. J., Parikh, N., Lima, B. P. & Zemaitaitis, B., (2008) Signal integration by the two-component signal transduction response regulator CpxR. *J Bacteriol* **190**: 2314-2322.

Wu, R., Gu, M., Wilton, R., Babnigg, G., Kim, Y., Pokkuluri, P. R., Szurmant, H., Joachimiak, A. & Schiffer, M., (2013) Insight into the sporulation phosphorelay: crystal structure of the sensor domain of *Bacillus subtilis* histidine kinase, KinD. *Protein science : a publication of the Protein Society* **22**: 564-576.

Yakhnin, H., Pandit, P., Petty, T. J., Baker, C. S., Romeo, T. & Babitzke, P., (2007) CsrA of *Bacillus subtilis* regulates translation initiation of the gene encoding the flagellin protein (*hag*) by blocking ribosome binding. *Mol Microbiol* **64**: 1605-1620.

Yan, D., Cho, H. S., Hastings, C. A., Igo, M. M., Lee, S. Y., Pelton, J. G., Stewart, V., Wemmer, D. E. & Kustu, S., (1999) Beryllofluoride mimics phosphorylation of NtrC and other bacterial response regulators. *Proc Natl Acad Sci U S A* **96**: 14789-14794.

Yasbin, R. E. & Young, F. E., (1974) Transduction in *Bacillus subtilis* by bacteriophage SPP1. *Journal of virology* **14**: 1343-1348.

Yasumura, A., Abe, S. & Tanaka, T., (2008) Involvement of nitrogen regulation in *Bacillus subtilis degU* expression. *J Bacteriol* **190**: 5162-5171.

Zhou, J., Fazzio, R. T. & Blair, D. F., (1995) Membrane topology of the MotA protein of *Escherichia coli*. *J Mol Biol* **251**: 237-242.

Zhou, J., Lloyd, S. A. & Blair, D. F., (1998a) Electrostatic interactions between rotor and stator in the bacterial flagellar motor. *Proc Natl Acad Sci U S A* **95**: 6436-6441.

Zhou, J., Sharp, L. L., Tang, H. L., Lloyd, S. A., Billings, S., Braun, T. F. & Blair, D. F., (1998b) Function of protonatable residues in the flagellar motor of *Escherichia coli*: a critical role for Asp 32 of MotB. *J Bacteriol* **180**: 2729-2735.

Zorraquino, V., Garcia, B., Latasa, C., Echeverz, M., Toledo-Arana, A., Valle, J., Lasa, I. & Solano, C., (2013) Coordinated cyclic-di-GMP repression of *Salmonella* motility through YcgR and cellulose. *J Bacteriol* **195**: 417-428.

Appendix A
Synthesised DNA sequences

Regions of DNA synthesised for downstream cloning

Restriction sites are underlined, the first two codons and final two codons of each gene deleted are highlighted in bold and His-tag sequences indicates by bold underline.

Regions of DNA synthesised for cloning into pMAD.

Δ*fliD* used to construct pNW1034

GAATTCACAAGAAATCTAAAACAGAAGATTTTTTTCCAAAAATATGTGTAATCTTATCTCGACT
TAGTCGATATAAACGATAGATTGGGGCATAGGGGATGATCAATTGAACATTGAAAGGCTCACTA
CGTTACAACCTGTTTGGGATCGTTATGATACTCAAATACATAATCAGAAAGATAATGATAACGA
GGTTCCTGTTCATCAAGTTTCATATACCAATCTTGCTGAAATGGTGGGGGAAATGAACAAGCTT
TTGGAACCTTCGCAAGTTCATCTGAAGTTCGAGCTTCATGACAAGTTAAATGAATACTATGTAA
AGGTAATAGAGGACTCTACAAATGAAGTGATCCGCGAAATTCCACCAAAACGGTGGCTTGATTT
TTATGCGGCTATGACTGAATTTCTTGGGTTATTTGTAGATGAAAAAAAGTAGAATAGGAGTGGT
TTGAG**ATGGTCCAATAA**ATGTAATTTGGAGGATGACACATGGCGATCCAAAATCCATATACAGC
CTATCAGCAAAATTCAGTGAATACGGCTACACCCGGGGAGCTGACGCTTATGCTGTATAATGGC
TGTTTGAAATTTATAAGACTTGCCGCTCAGGCCATTGAGAATGATGATATGGAACGTAAAAATG
AAAATCTGATTAAAGCGCAAAATATTATTCAGGAATTAAATTTTACACTTAACCGTAACATAGA
GCTTTCCGCTTCTATGGGTGCGATGTACGATTATATGTATCGCAGATTGGTACAGGCAAATATC
AAAAATGATACGGGCATGCTGGCTGAGGTTGAAGGTTATGTAACAGATTTTCGCGATGCTTGGA
AACAAGCCATTCAAAGTGAGCGGAAGGACCGGCACGGATCAGGCGGGATCGCATGAATAATATA
GATCAACTATACACTGAGACGAAGAGTATGCTGTCACACATACAAAATACGCCGGAAAGCGATG
AACTTTTAAAGCAAATTGAAGACTTTGTGGCTACACGGTCTGAACTGATTCAGGAGATATCTCT
GCCGCTTTCAGGATCC

Δ*flgE* used to construct pNW1036

GAATTCATGACTTCTATAAGTTCAGAATATAAACTGCCTGAAAAAACGAACACTGTGTCGACGA
ACAACAGCAGCTTGGGGAAAGACGAGTTTTTAAAAATATTAATGACTCAAGTTCAAAACCAAGA
TCCGCTTAACCCGATTGACGATAAAGAATTTATCAGCCAGATGGCGACTTTTTCAAGCTTGGAG
CAAATGATGAATCTGAATACGACAATGACTCAATTCGTTGAAAACCAAGATCCGTTTACAACGT
ATGTTGATTGGATGGGAAAAGAAGTATCTTGGACTGATGGTAAAAGTGCAACAGATAAAACAGG
CACAGTAAGCTCTGTTAAACATTTTAAAGGAAATTATTATCTCGTTCTTGATGATGGGACCGAG
ATCAGTCCTGCGAATGTCATGTCTGTGGGACAATCATCTAAATAAAAACATCTGGGGGAATATA
TT**ATGTTACGTTAA**GGAGGGAGGGGAGGCGAGTAATCGCTTCTCCGCTGTTTTATGATTAAAGT
AACCCGTTTGAACGGGCAGCCCTTTACACTGAATGCGCTATTTATTGAACAGATTGAATGTTTT
CCGGATACTACAATTACTCTGTCAAATGGTAAGAAGTTTGTAGTAAAAGAAGATGAAGAAGCTG
TTCTGGAAAAGATCGCAGCTTTCTACCGAAAAATACAAATATTTGCAATGGATCAAGGAATAGA
GGAACCGGAATGAAGAAAAAGTTAATGATCATATTACTAATTATTCTTATCGTAATTGGTGCTC
TCGGGGCGGCGGCTTATTTTGTTTTAGGCGGAAAGTCCGAAAAAAGTGAAGCGAAAAAAAGTAT
TGATGAAATCGTTGCGTCTTCTGTTGATGTAGAAGAGATCACAACAAATTTAAAGTCTGATAAC
ATTATCCGTCTTGCTATTAAACTTGAAACTGATTCTGATAAATCAAAAGAAGAACTTGAGAAAC
GTGATTTCCAAGTGAAAGACGCTGTTATATCACTGCTGGCTGATACGAATGCTGGGATCC

Δ*flgK-flgL* used to construct pNW1042

GGATCCTGTCAGCGAAGGCAATTATTGAACAATTGAAGCGACTTTGCGTTCTGCATGAGCACCT
GCTCACGCTGTCTGAAGAAAAGACGGAAGCGCTCAAAGCCGGCAAAACAAAAGAGCTTTCTAAC

ATTTTGACAAAAGAGCAAAAATATATTCAAGCAATCACGCAGACAGAAGATGACCGGATCAAAA
CAACTTCGGCCTTTCTCGGATATAGCGAAAATAATACTATTTCCGCATGTATCGCCAAAACCTC
AGGCAGTGAAAAGGAAGAGCTGGAACAACTATACGAATCTCTTTCTCAAGTTCTCGGACGTCTG
AAAAAAGTAAATGAGATGAATAGGCAGCTGACAAGAGACGCGCTGCAATTCATCTCTATTTCGT
ACGATATGCTGGTTCCTAAGGAAAATAACTTCAATTACAGCAAATCAATTAAAGCTGAGCTGCC
GAAAAGTAGCAAAATGAAACTGTTTGATTCAAAAGCTTAGCAGAAAGGAATTCAGAAA**ATGACA**
AAGTAAGCGGCTCTTAGGAGTTCGCTTTTTTTATAGTTCAGGAGGTAGAGTGATGCAGATTCCC
AGATTGATTATGCATAGTGTTCAAGGAAAAATTGGTTTAACAACGACGCCTGCCAGCTTAAAAA
TGGAGCAGCCTCAAGCTGATCTAGAGATCGAACAGCCGAGTGCGGAAATGGAAATATCGGTGAC
ACCTGGAAAACTCACGATTGACCAGACACAAGCATGGGAAGAATTAGACAGAAAGCATGTTTTC
AAGAGAATTGAAGAAGCCGCCCAACAAGGGCATGAGGATGTAATGGAGGGAATAGCACGCACTG
CAGAAGAAGGCGACGAGCTTATGAAGATTGAAAATAAGGGGAACCCAATCGCTTCACAAGCAAG
GAGGAACTCTGAAATGCACCAAATTCAATTAGGCGAAAATTATGCTCCTTCTCTTTCGAGGGTG
AAAATACAATATACTCCGTCACAGCTTGATGTGCAGATTACGCCGCGAAAGCCTGGGATCC

His-flgK used to construct pNW1063

GGATCCCCATGTCAGCGAAGGCAATTATTGAACAATTGAAGCGACTTTGCGTTCTGCATGAGCA
CCTGCTCACGCTGTCTGAAGAAAAGACGGAAGCGCTCAAAGCCGGCAAAACAAAAGAGCTTTCT
AACATTTTGACAAAAGAGCAAAAATATATTCAAGCAATCACGCAGACAGAAGATGACCGGATCA
AAACAACTTCGGCCTTTCTCGGATATAGCGAAAATAATACTATTTCCGCATGTATCGCCAAAAC
CTCAGGCAGTGAAAAGGAAGAGCTGGAACAACTATACGAATCTCTTTCTCAAGTTCTCGGACGT
CTGAAAAAAGTAAATGAGATGAATAGGCAGCTGACAAGAGACGCGCTGCAATTCATCTCTATTT
CGTACGATATGCTGGTTCCTAAGGAAAATAACTTCAATTACAGCAAATCAATTAAAGCTGAGCT
GCCGAAAAGTAGCAAAATGAAACTGTTTGATTCAAAAGCTTAGCAGAAAGGAATTCAGAAAATG
CATCACCATCACCATCACCATCACCATCACACATCTACCTTTATGGGGCTTGAAACTGCAAGGC
GGGCGTTAAGCGCTCAGCAGGCAGCGTTAAGCACTACTGCAAATAACGTGGCAAATGCCAATAC
TGATGGTTATACAAGACAGCGGGTCTCATTGGAGGCAACTGACTATTTCCCTGCTGTATCTAAA
AATGCAGAAAAAACAGCGGGACAAATGGGTACGGGCGTTCAAGGAAAATCAGTTGAGAGAATAA
GAGATATCTTTCTTGACTACCAATACCGTCTTCAAAACAACAGTGCCGGATACTATGACACGAA
GGCAAAAGCGCTGTCCCAAATGGAAGGCGTTTTAAATGAAACGGATGACAGCGGCTTGAACAGT
GTGCTCAATTCGTTTTGGAATTCCCTGCAGGAATTATCGAATAATACAAATGAAGAAAGTGCAC
GTTCTGTTGTTGCTCGAAAAGGACAAGCTGTAGCTGAAACGTTTAATTATATTTCTGAATCACT
TACAAATGTCCGGATCC

flgK-His used to construct pNW1065

GAATTCGAAGTGCACAGAAATGGTGTGACCAAGAGCGGTGAACAAGGCGGAGACTTTTTTGATT
TTACTGGCGGTGAAACTGAACCTGCCAAGGGCGCGGCGGGCAAGATCAAAGTGGCTGACAGCAT
AATAGATTCAAAAGGCGCAAACATTGCTTTCTCACTGACTGGCGCAGCCAACGATAACGCAAAT
GCTACAAAATTAGCAAATGTTTTAACCGGTAAAATAACCATTAACGGTAAAGAAACTAGTGTTT
TAGATTATTATGCGGGTCTGATTGGCGAGCTAGGGATCGAAGCTCAAGAGGCTAATCGACTGGC
GTCTAATACAGAAACACAGCTGAATGATGCTGACATAAACCGTCAGCAAATGAGCGCAGTTTCT
TTAGACGAAGAAATGACGAATATGATTCAATTCCAACACGCATACAATGCAGCTGCAAGAATGG
TGACTTTACAAGACGAATTGCTTGATAAAGTGATCAACGGCATGGGTGTTGGAGGAAGGGGAGC
AGGA**CATCACCATCACCATCACCATCACCATCAC**TAGTGGGTGTTGGAGGAAGGGTAGAGTCAC
ATGAGAGTAACACAAGGCATGATACAGCAAAACTCACTGAGATATATCGGTTCAAGCTACTCGA
AGCTGGATAAACTCCAGTCGCAGATTTCTTCAGGAAAAAAAATCTCAAAAGCTTCCGACGATCC
TGTAGTAGCAATGAAAAGCTTAAAGTATAATACGCAACTGTCTCAAGTGCAGCAGTACAAAAGC
AATGCTTCTCAAGCCTTTACCTGGCTCGAAAACACAGAAACAAACATTACAGAAGGAATTGACA

TCTTGTCAAAGGTCAGAGAATTAGCGGTTGAAGCTCAAAATGATACAAACGGCGAGCCGGAGCG
GCAAGCGATTGGCGTAGAGGTAAAGCAGTTAAAGGAACAGCTTTTAAATATTGCGAATACACAA
GTGAACGGCAGATATATCTTTAATGGCACAAATTCAGATAAGCCTCCGGTTACAGATAACGGAG
ACGGAACTTATACGGATCC

Appendix B
Publications

JB Journals.ASM.org

FlgN Is Required for Flagellum-Based Motility by *Bacillus subtilis*

Lynne S. Cairns,[a] Victoria L. Marlow,[a] Taryn B. Kiley,[a] Christopher Birchall,[b] Adam Ostrowski,[a] Phillip D. Aldridge,[b] Nicola R. Stanley-Wall[a]

Division of Molecular Microbiology, College of Life Sciences, University of Dundee, Dundee, United Kingdom[a]; Centre for Bacterial Cell Biology, Newcastle University, Newcastle upon Tyne, United Kingdom[b]

The assembly of the bacterial flagellum is exquisitely controlled. Flagellar biosynthesis is underpinned by a specialized type III secretion system that allows export of proteins from the cytoplasm to the nascent structure. *Bacillus subtilis* regulates flagellar assembly using both conserved and species-specific mechanisms. Here, we show that YvyG is essential for flagellar filament assembly. We define YvyG as an orthologue of the *Salmonella enterica* serovar Typhimurium type III secretion system chaperone, FlgN, which is required for the export of the hook-filament junction proteins, FlgK and FlgL. Deletion of *flgN* (*yvyG*) results in a nonmotile phenotype that is attributable to a decrease in *hag* translation and a complete lack of filament polymerization. Analyses indicate that a *flgK-flgL* double mutant strain phenocopies deletion of *flgN* and that overexpression of *flgK-flgL* cannot complement the motility defect of a Δ*flgN* strain. Furthermore, in contrast to previous work suggesting that phosphorylation of FlgN alters its subcellular localization, we show that mutation of the identified tyrosine and arginine FlgN phosphorylation sites has no effect on motility. These data emphasize that flagellar biosynthesis is differentially regulated in *B. subtilis* from classically studied Gram-negative flagellar systems and questions the biological relevance of some posttranslational modifications identified by global proteomic approaches.

The bacterial flagellum is a complex molecular motor that has been shown to play roles in motility, surface adherence, biofilm structure, and signal transduction (1–4). The flagellum is organized into three main structural components: the basal body, hook, and filament (1). The basal body consists of the flagellar motor, which is required to power rotation of the flagellum, and a type III secretion (T3S) system that permits the export of proteins required for the biosynthesis of the hook and filament. The hook is a flexible joint that permits a change in the angle of rotation of the flagellum, while the filament acts as a propeller to drive movement. Biosynthesis of the flagellum is tightly regulated at the level of transcription. In the Gram-positive bacterium *Bacillus subtilis*, the proteins needed for the hook-basal body (HBB) are transcribed in the 31-gene *fla-che* operon (5, 6). The penultimate gene of this operon, *sigD*, encodes the sigma factor σ^D (7, 8) that activates transcription of the late flagellar genes: the flagellar filament gene *hag*; the flagellar stator genes *motA* and *motB*; the anti-sigma factor *flgM*; the hook-filament junction genes *flgK* and *flgL* (9); and the autolysins (10). In wild-type *B. subtilis*, while all cells transcribe the *fla-che* operon, only a subpopulation of the cells synthesize flagella (11, 12). This is due to heterogeneity in *sigD* transcription such that a threshold level of *sigD* transcription must be reached to allow sufficient σ^D protein to accumulate and activate σ^D-regulated promoters (11). The net result is that transcription is temporally ordered such that the HBB genes are expressed before the filament genes (1).

As well as being controlled at the level of transcription, flagellar biosynthesis is regulated posttranscriptionally by flagellar type III secretion system (T3S) chaperones. Regulation at this level has been described most extensively in *Salmonella enterica* serovar Typhimurium, with little known about the function of chaperones in Gram-positive bacterial species (13, 14). T3S chaperones are small proteins that bind their cognate substrate(s) in the cytoplasm, protecting the substrate from degradation and/or preventing aggregation (15, 16). Chaperones therefore allow the efficient transport of the substrate to the export machinery. Chaperone-substrate complexes reach the secretion apparatus with the aid of the soluble export apparatus proteins FliI and FliH (17), while empty chaperones are recycled with the aid of FliJ (18). Following interaction of the chaperone-substrate complex with the C-terminal cytoplasmic domain of the integral membrane protein FlhA, a series of protein-protein interactions facilitates the entry of the substrate protein to the export gate (19–21), and its subsequent secretion is driven by proton motive force (22, 23). In *S.* Typhimurium, FliS is a specific chaperone for flagellin (24), FliT is specific for the FliD filament cap protein, and FlgN (*ST*-FlgN) is specific for the hook-filament junction proteins, FlgK and FlgL (25, 26). Recently, it has been shown that FliS is required for Hag (flagellin) secretion in *B. subtilis* (13, 14). In addition, *in silico* analysis has suggested that YvyG of *B. subtilis* is an orthologue of the *S.* Typhimurium protein FlgN (27). However, a defined function for YvyG has not yet been determined experimentally.

Several global proteomic screens have been conducted using *B. subtilis* with the goal of examining the extent and diversity of posttranslational modification (28–30). Intriguingly, these experiments identified YvyG as being phosphorylated on tyrosine 49 (29) and arginine 60 (30). Posttranslational modification of proteins can control cell fate in several ways: (i) by altering protein localization and half-life (31), (ii) by controlling protein activity and affinity to ligands (32), and (iii) by the disruption or promotion of protein-protein interactions (33). The *B. subtilis* flagellum

Received 20 February 2014 Accepted 1 April 2014
Published ahead of print 4 April 2014
Address correspondence to Nicola R. Stanley-Wall, n.r.stanleywall@dundee.ac.uk.
Supplemental material for this article may be found at http://dx.doi.org/10.1128/JB.01599-14.

doi:10.1128/JB.01599-14

has recently been shown to be regulated by mechanisms not identified in other bacterial species (34, 35). Therefore, given the potential for YvyG to play a crucial role in the tightly controlled process of flagellar biosynthesis (31, 36), we hypothesized that protein phosphorylation might present an additional route for *B. subtilis* to regulate flagellar assembly and, therefore, motility. Thus, we aimed to define the function of YvyG during motility by *B. subtilis* and to ascertain the *in vivo* role of YvyG tyrosine and arginine phosphorylation.

Work presented here identifies *B. subtilis* YvyG (here referred to as *B. subtilis* FlgN [*Bs*-FlgN]) as an orthologue of the *S.* Typhimurium T3S chaperone FlgN, as previously suggested by *in silico* analysis (27). Consistent with this, we prove for the first time that FlgN is required for both swimming and swarming motility in *B. subtilis*. The lack of motility in the *B. subtilis flgN* deletion strain is linked to a block in flagellar biosynthesis. This is a consequence of a complete lack of filament assembly. Analysis of a Δ*flgK-flgL* double mutant strain demonstrates that the strain phenocopies the *flgN* mutation. Collectively, these data prove that in *B. subtilis* FlgN is required for flagellar assembly, perhaps by acting as a chaperone for FlgK and FlgL. In *S.* Typhimurium, overexpression of *flgK* can compensate for the motility defect of a Δ*flgN* strain (16). However, data presented here demonstrates that in *B. subtilis* deletion of *flgN* cannot be compensated for by the overexpression of *flgK* and *flgL*. This leads to the conclusion that there is a stricter dependence on the presence of FlgN in *B. subtilis* for motility than there is for FlgN in *S.* Typhimurium (16, 36). Finally, through the use of site-directed mutagenesis, we demonstrate that mutation of the tyrosine and arginine phosphorylation sites of FlgN has no effect on the ability of *B. subtilis* to become motile. In summary, these data emphasize that flagellar biosynthesis is differentially regulated in *B. subtilis* in comparison to the classically studied Gram-negative bacteria and additionally raises questions regarding the biological relevance of some posttranslational modifications identified by global proteomic approaches.

MATERIALS AND METHODS

Growth conditions and strain construction. *Escherichia coli* and *Bacillus subtilis* strains were routinely grown in Luria-Bertani (LB) medium (10 g liter^{-1} NaCl, 5 g liter^{-1} yeast extract, 10 g liter^{-1} tryptone) or on LB plates supplemented with 1.5% agar at 37°C unless otherwise stated. *E. coli* strain MC1061 [F′ *lacI*^{q} *lacZ*ΔM15 Tn*10*(*tet*)] was used for the routine construction and maintenance of plasmids. When required, antibiotics were used at the following concentrations: 100 μg ml^{-1} ampicillin, 100 μg ml^{-1} spectinomycin, 25 μg ml^{-1} chloramphenicol, 10 μg ml^{-1} kanamycin (*B. subtilis*), 50 μg ml^{-1} kanamycin (*E. coli*), 1 μg ml^{-1} erythromycin, and 25 μg ml^{-1} lincomycin. Strains were constructed using standard protocols. Phage transductions were carried out as previously described (37). When appropriate, isopropyl β-D-1-thiogalactopyranoside (IPTG) was added at the concentrations indicated in the figures or figure legends. A full list of strains used in this study is provided in Table S1 in the supplemental material.

Construction of in-frame deletion strains. To construct the in-frame deletion of *flgN*, an approach similar to that previously described was used (38). The upstream region of *flgN* was amplified from genomic DNA using primers NSW938 and NSW939, purified, and digested with XbaI and SalI using the restriction sites engineered into the primers. The downstream region of *flgN* was amplified using primers NSW936 and NSW937, purified, and digested with BamHI and XbaI using the restriction sites engineered into the primers. The fragments were simultaneously ligated into pUC19 and sequenced, prior to introduction into pMAD (39), to produce plasmid pNW399. Strain NRS3570 (NCIB3610 Δ*flgN*) was generated by integration and curing of the region contained in pNW399 in strain NCIB3610. Strains NRS4041 (NCIB3610 Δ*fliD*), NRS4042 (NCIB3610 Δ*flgE*), and NRS4060 (NCIB3610 Δ*flgK-flgL*) were constructed in a similar manner using the primers and plasmids detailed in Tables S2 and S3 in the supplemental material, respectively, and in the supplemental methods.

Introduction of site-specific mutations to the chromosome. To introduce site-specific mutations to the chromosome of NCIB3610, a similar approach to that previously described was used (39). Plasmids pNW801 and pNW1012 were used to introduce site-specific mutations in codon 49 of *flgN*. Primers NSW936 and NSW939 were used to amplify a 1,725-bp region of DNA containing the complete *flgN* coding region. The PCR fragment was cloned into pUC19 using SalI and SphI restriction sites engineered into the primers, resulting in plasmid pNW398. Primer sets NSW942 and NSW943 (Y^{49}A) and NSW1436 and NSW1437 (Y^{49}E) were used to introduce point mutations to pNW398 using site-directed mutagenesis by the QuikChange method, according to the manufacturer's instructions (Stratagene). The resulting plasmids were sequenced to ensure that the correct mutations were introduced. The mutated *flgN* coding region was excised and cloned into pMAD for integration into NCIB3610, as described for the construction of in-frame deletion strains. Further plasmids were constructed in an identical manner for *hag* (Hag T^{209}C) and *flgN* (with the R-to-A or R-to-E mutation at position 60 encoded by *flgN* [*flgN*-R^{60}A or *flgN*-R^{60}E, respectively]). Full details of the plasmids and primers used are provided in Tables S2 and S3, respectively, in the supplemental material.

Sigma A antibodies. To overexpress and purify the σ^{A} protein from *B. subtilis* for antibody preparation, the *sigA* gene was amplified from the chromosome of the strain NCIB3610 using primers NSW860 and NSW861. The NcoI and XhoI sites engineered into the primer sequence are underlined in Table S3 in the supplemental material. The resulting PCR product was digested with NcoI and XhoI and cloned into the expression vector pEHISGFPTEV (40) to yield a His$_6$-green fluorescent protein (GFP)-σ^{A} fusion construct named pNW642. A tobacco etch virus (TEV) protease recognition site was placed between the *gfp* and *sigA* coding regions.

E. coli BL21(DE3) cells carrying the pNW642 vector were grown in LB broth containing ampicillin to an optical density at 600 nm (OD$_{600}$) of 0.3 at 37°C. The cells were chilled to 20°C, and protein expression was induced with 50 μM IPTG overnight. Cells were collected by centrifugation and resuspended in lysis buffer (25 mM Tris [pH 7.5], 250 mM NaCl, 5 mM dithiothreitol [DTT], 30 mM imidazole, lysozyme, DNase I, and complete EDTA-free protease inhibitor cocktail [Roche]). Cells were lysed on a French press using pressure at 15,000 lb/in^2, and the cellular debris was removed by centrifugation. The supernatant was filtered through a 0.45-μm-pore-size syringe filter before being loaded onto a 1-ml HiTrap HF immobilized metal affinity chromatography (IMAC) column (GE Healthcare) using loading buffer, and the column was then washed with 10 ml of loading buffer (25 mM Tris [pH 7.5], 250 mM NaCl, 5 mM DTT, 30 mM imidazole). The recombinant His$_6$-GFP-σ^{A} fusion protein was eluted from the column using a gradient of elution buffer (25 mM Tris [pH 7.5], 250 mM NaCl, 5 mM DTT, 500 mM imidazole). The fractions containing the fusion protein were pooled and dialyzed into TEV buffer (50 mM Tris [pH 7.5], 20 mM NaCl, 0.5 mM EDTA, 10% glycerol) using spin concentrators. The dialyzed protein was diluted to 1 mg ml^{-1} in the TEV buffer, and 1.5 mg of TEV protease was added. The reaction solution was incubated overnight at 4°C with agitation. The resulting σ^{A} and GFP proteins were separated using negative IMAC with the loading and elution buffers described above. The unbound fraction, containing σ^{A}, was additionally purified using size exclusion chromatography with a Superdex75 resin (GE Healthcare) and buffer containing 25 mM Tris (pH 7.5) and 250 mM NaCl. The purified protein was concentrated to 1 mg ml^{-1} and sent for rabbit immunization to Dundee Cell Products (Dundee, United Kingdom). The obtained σ^{A} antiserum was affinity pu-

rified against purified recombinant σ^A according to a previously described protocol (41).

Secondary-structure prediction. Primary protein sequences of *S.* Typhimurium FlgN and *B. subtilis* FlgN were aligned using Clustal Omega (http://www.ebi.ac.uk/Tools/msa/clustalo/) (42). The secondary structures were predicted using PsiPred (http://bioinf.cs.ucl.ac.uk/psipred/) (43, 44) and aligned against the primary sequence of the proteins.

RNA extraction and RT-PCR. RNA isolation was carried out as described previously (38) using a RiboPure Bacteria RNA Isolation Kit (Ambion), according to the manufacturer's instructions, and treated with DNase I. To confirm cotranscription of *flgN* with *flgK* and *flgL*, cDNA was synthesized using the *yviE* gene-specific primer NSW1459 in a reaction with SuperScript III (Life Technologies) and subsequently treated with RNase H (NEB) for 20 min at 37°C. To establish if deletion of *flgN* perturbed transcription of *flgK* or *flgL* (and vice versa), cDNA was synthesized using random hexamers in a reaction with SuperScript III (Life Technologies). To amplify internal gene products, the following primer pairs were used: DEN5 and DEN7 (rRNA), NSW1446 and NSW1447 (*flgL*), NSW1444 and NSW1445 (*flgK*), NSW1442 and NSW1443 (*flgN*), and NSW1440 and NSW1441 (*flgM*).

Motility assays. Swimming and swarming analyses were performed as described previously (37) using low-salt LB medium (5 g liter^{-1} NaCl, 5 g liter^{-1} yeast extract, 10 g liter^{-1} tryptone) supplemented with 0.4% and 0.7% Bacto agar, respectively. Plates were incubated at 37°C, and the extent of swimming or swarming was noted at defined time intervals.

Staining of flagella and fluorescence microscopy. Cells carrying the Hag T^{209}C point mutation (45) were grown to mid-exponential phase, and 0.5 ml of cells was harvested by centrifugation at 4,000 × *g*. Cells were washed once with 1× T-Base [1 mM EDTA, 15 mM $(NH_4)_2SO_4$, 80 mM K_2HPO_4, 44 mM KH_2PO_4, 3.4 mM sodium citrate], pelleted, resuspended in 50 μl of T-Base containing 5 μg/ml Alexa Fluor 488 C_5 maleimide dye (Molecular Probes), and incubated for 5 min at room temperature. Cells were washed three times with 500 μl of 1× T-Base and suspended in 50 μl of 1× phosphate-buffered saline (PBS). Two microliters of the cell suspension was spotted onto a thin matrix of 1.5% agarose in water (Ultrapure Agarose; Invitrogen) contained in a 1.7- by 2.8-cm Gene Frame (AB-0578; ABgene House, Epsom, Surrey, United Kingdom) mounted on a standard microscope slide (Super Premium slides; VWR). Each slide was prepared as follows: the gene frame was filled with molten 1.5% agarose and covered firmly with a standard microscope slide to flatten the agarose surface. Following solidification of the agarose, the slide was carefully removed, and the cell suspension was added. Once the cell suspension was dry, the gene frame was sealed with a coverslip (thickness number 1.5; VWR), and images were immediately acquired. Imaging was performed using a DeltaVision Core widefield microscope (Applied Precision) mounted on an Olympus lX71 inverted stand with an Olympus 100× (1.4 numerical aperture [NA]) lens and a CoolSNAPHQ camera (Photometrics) with differential interference contrast (DIC) and fluorescence optics. GFP was imaged using a 100 W Mercury lamp and a fluorescein isothiocyanate (FITC) filter set (excitation, 490/20 nm; emission, 528/38 nm) with an exposure time of 200 ms. DIC images were illuminated with an LED-transmitted light source.

To monitor P_{hag}-*yfp* expression, cells were grown at 37°C in LB medium to an OD_{600} of 1.0, 0.5 ml of the culture was harvested, and cells were washed and resuspended in 1× PBS. The cell suspension was prepared for microscopy and imaged as described above. Yellow fluorescent protein (YFP) fluorescence was imaged using a 100 W Mercury lamp and an FITC filter set (excitation, 490/20 nm; emission, 528/38 nm) with an exposure time of 50 ms. The threshold used to define activation of the transcriptional reporter P_{hag} was set as a YFP fluorescence intensity value greater than 2 standard deviations above the mean background fluorescence. All images were rendered and analyzed postacquisition using OMERO software (www.openmicroscopy.org) (46).

Flow cytometry analysis. The fluorescence of strains harboring *yfp* or *gfp* transcriptional promoter fusions was measured in single cells extracted from planktonic cultures grown to mid-exponential phase and analyzed as described previously (47).

Whole-cell analysis of Hag. Proteins were extracted from planktonic cultures grown to mid-exponential phase. Briefly, cells were harvested by centrifugation at 4,700 × *g*. Cells were suspended in 1× Bugbuster (Novagen) and lysed according to the manufacturer's instructions. Seven micrograms of protein was resolved by SDS-PAGE and stained with Coomassie brilliant blue. Hag was identified by comparison with the Δ*hag* strain (DS1677) and confirmed by mass spectrometry (FingerPrints Proteomics and Mass Spectrometry Facility, University of Dundee).

Western blot analysis. Cellular proteins were extracted as for whole-cell analysis of Hag. Extracellular proteins were extracted from the culture supernatant and processed as detailed previously (48) and suspended in 50 μl of 4× SDS loading dye. Seven micrograms of cellular proteins or 7 μl of extracellular proteins was separated by SDS-PAGE prior to transfer onto polyvinylidene difluoride (PVDF) membrane (Millipore) by electroblotting. Antibodies raised against Hag (a kind gift from Kürsad Turgay) were used at 1:40,000, anti-FlgE (a kind gift from Daniel Kearns) was used at 1:20,000, anti-σ^A was used at 1:500, and goat anti-rabbit or goat anti-mouse horseradish peroxidase (HRP)-conjugated secondary antibodies (both from Pierce) were used at 1:5,000.

β-Galactosidase assays. The β-galactosidase activity of strains harboring *lacZ* promoter reporter fusions was measured as previously described (37, 49). The values presented are the average β-galactosidase activities in Miller units (50) determined from at least three independent samples. Error bars represent the standard errors of the means.

Enrichment of flagellar hook-basal bodies. The flagellar HBB fraction of NCIB3610 was enriched for as described previously (51, 52). Briefly, 1 liter of cells was grown to early exponential phase and harvested by centrifugation at 6,000 × *g* for 45 min at 4°C. The cell pellet was resuspended in 100 ml of sucrose solution (0.5 M sucrose, 0.15 M Tris) with a protease inhibitor tablet (Roche), and cells were homogenized with a loose pestle on ice. To lyse cells and allow spheroplast formation, lysozyme was added to the cell suspension at a final concentration of 0.1 mg ml^{-1}, and samples were incubated at 4°C with stirring for 40 min. Spheroplasts were lysed by addition of Triton X-100 to a final concentration of 1%, and viscosity was decreased by stirring at room temperature for 30 min, allowing endogenous DNases to degrade cellular DNA. Unlysed cells were removed by centrifugation at 4,000 × *g* for 10 min, and EDTA was added to the suspension at a final concentration of 10 mM. To aid removal of contaminating membrane proteins, the pH of the lysate was raised to 10 by addition of NaOH. The lysate then underwent high-speed centrifugation (60,000 × *g* for 60 min), and the pellets were resuspended in alkaline solution (0.1 M KCl-KOH, 0.5 M sucrose, 0.1% Triton X-100, pH 11.0) and centrifuged again. The pellet was then resuspended in 90 ml of TET buffer (10 mM Tris-HCl, 5 mM EDTA, 0.1% Triton X-100, pH 8.0), and a 36% CsCl gradient was established. The solution was centrifuged using a Beckman SW41Ti swinging-bucket rotor at 55,000 × *g* for 16 h at 15°C. The flagellar fraction was visible as a band approximately 2 cm from the bottom of the tube and was collected with a Pasteur pipette and dialyzed against TET buffer. In an attempt to dissociate the flagellar filaments, the flagellar fraction was suspended in acidic solution (glycine-HCl, 0.1% Triton X-100, pH 3.0) for 1 h, and HBB complexes were collected by centrifugation at 100,000 × *g* for 1 h. HBBs were resuspended in TET buffer and analyzed by mass spectrometry. Results were searched against the *Bacillus subtilis* Mascot database (FingerPrints Proteomics and Mass Spectrometry Facility, University of Dundee). The top 12 proteins as identified by their Mascot scores are listed in Table S4 in the supplemental material.

RESULTS

YvyG of *B. subtilis* shares secondary-structure homology with the *Salmonella* protein FlgN. Previous bioinformatic analysis postulated that YvyG of *B. subtilis* was an orthologue of FlgN (27). FlgN is an essential component of the flagellar type III secretion machinery (26, 36, 53). FlgN has been most extensively studied in

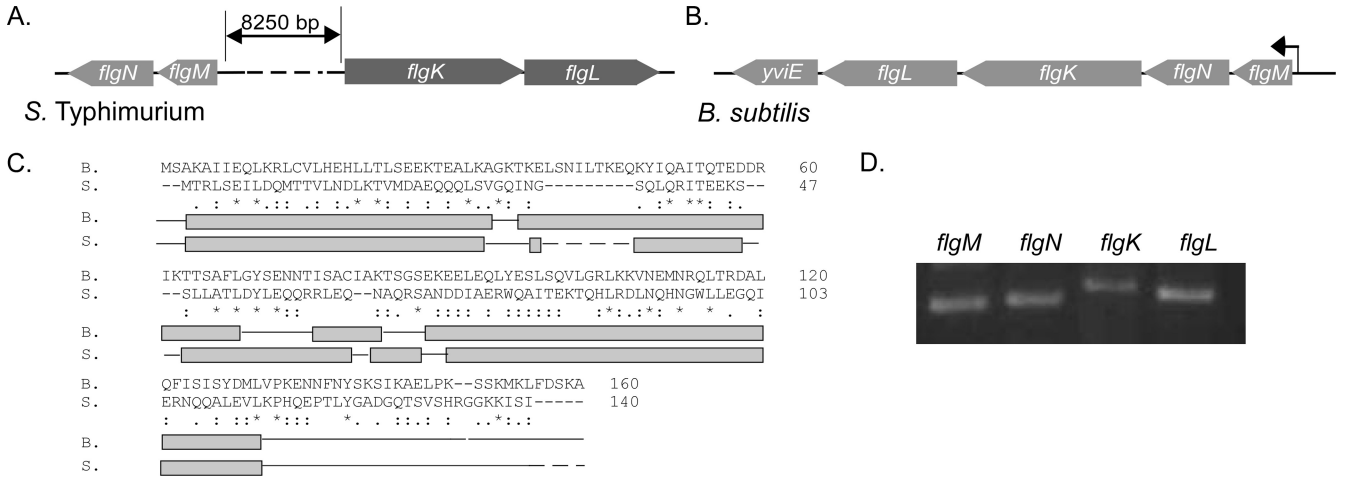

FIG 1 Primary-sequence and secondary-structure comparison of *B. subtilis* FlgN with *S.* Typhimurium FlgN. Schematic representations of the chromosomal regions surrounding *S.* Typhimurium *flgN* (A) and *B. subtilis flgN* (B) are shown. Arrows represent open reading frames, with the direction of the arrow indicating the direction of the open reading frame. The bent arrow represents the promoter located before the *flgM* coding region. (C) Primary-sequence alignment and secondary-structure comparison of *Bs-flgN* and *ST-flgN*. The primary amino acid sequence of FlgN from *B. subtilis* 168 (B) was aligned with that of *flgN* from *S.* Typhimurium (S). For primary-sequence alignments, an asterisk indicates a fully conserved amino acid, a colon indicates a highly conserved amino acid, and a period indicates a weakly conserved amino acid. Gaps indicate no homology. Dashed lines indicate a break in the sequence. For secondary-structure alignments light gray boxes indicate α-helices, solid lines indicate coiled coils, and dashed lines indicate a break in the sequence alignment. (D) RT-PCR analysis of cotranscription of *flgM*, *flgN*, *flgL*, and *flgK*. Regions of DNA internal to *flgM*, *flgN*, *flgK*, and *flgL* were amplified from cDNA generated using a primer specific to the gene 3′ proximal to *flgL*, using RNA from the wild-type strain (NCIB3610).

S. Typhimurium (26, 36), but homologues have been recognized in a number of different bacterial species (27, 53). Three criteria were employed by Pallen et al. (27) to identify FlgN homologues in a broad range of bacterial species: (i) the protein must be encoded by a gene adjacent to an *flgM* homologue (Fig. 1A and B), (ii) the gene should be of a similar length to *flgN* of *Salmonella* (Fig. 1C), and (iii) the protein must be recognizable (however distantly) by PSI-BLAST analysis as "FlgN-like." These criteria were set as the primary amino acid sequence of FlgN is highly variable (27). To confirm that YvyG is likely to be an orthologue of FlgN, the amino acid sequence of YvyG was compared with that of *S.* Typhimurium FlgN. As expected, there was little primary-sequence homology (Fig. 1C). However, upon comparison of the predicted secondary structures of YvyG and FlgN, a high degree of similarity was clearly apparent (Fig. 1C). Thus, YvyG was renamed FlgN, and its function in motility in *B. subtilis* was further investigated.

On the *B. subtilis* chromosome, the *flgM*, *flgN*, *flgK*, and *flgL* coding regions are adjacent. To ascertain whether all four genes were part of the same operon in the NCIB3610 strain, reverse transcription-PCR analysis was used. RNA was extracted from wild-type *B. subtilis*, and cDNA was synthesized using a primer specific to *yviE*, the gene proximal to *flgL* at the 3′ end (Fig. 1B). The cDNA generated was used as a template for PCR with primer pairs specific to the internal coding regions of *flgM*, *flgN*, *flgK*, and *flgL*. Regions of DNA internal to the coding regions of *flgM*, *flgN*, *flgK*, and *flgL* could each be amplified from cDNA generated using a primer at the 3′ end of *flgL* (just beyond the termination codon) (Fig. 1D), demonstrating that all four genes are cotranscribed.

FlgN is essential for swarming and swimming motility of *B. subtilis*. The *flgN* gene is located in a region of the chromosome known to be required for motility (9). To test if *flgN* is required for motility, a *B. subtilis* strain carrying an in-frame deletion of *flgN* was constructed, and its phenotype was assessed in swimming and swarming assays. A strain containing a deletion in the *hag* gene (DS1677) was used as a nonmotile control. While the wild-type strain was able both to swim and swarm efficiently (Fig. 2A, C, and E), this behavior was lost in the Δ*flgN* strain (NRS3570) (Fig. 2A, C, and E). Using reverse transcription-PCR analysis, we confirmed that transcription of the other genes in the operon was not impacted by the *flgN* deletion (Fig. 2F). To further ensure that this loss of motility was specific to the deletion of *flgN*, the motility of a strain where the coding region of *flgN* was reintroduced at the *amyE* locus under the control of an IPTG-inducible promoter ($P_{hy\text{-}spank}$) was tested. Both the swimming (Fig. 2B) and swarming (Fig. 2D and E) phenotypes of the Δ*flgN* strain could be restored by the reintroduction of *flgN* on the chromosome upon induction with IPTG. These data demonstrate for the first time *in vivo* that the protein product of the *flgN* gene is required for both swimming and swarming motility in *B. subtilis*. It is notable that higher levels of *flgN* transcription are required to complement the swarming defect presented by the Δ*flgN* strain than are needed for the swimming defect (compare Fig. 2B and D). This is most likely attributable to a higher demand for flagellum biosynthesis in swarming than swimming motility (54).

Deletion of *flgN* results in a loss of bimodal transcription of *hag*. To dissect the role of *flgN* in motility, the effect of deletion of *flgN* on the transcription of the flagellar filament gene *hag* was tested. Due to the heterogeneity in *sigD* transcription, transcription of *hag* is bimodal, and thus single-cell techniques are ideally suited for analysis (11, 12). To this end, a P_{hag}-*yfp* transcriptional reporter was integrated at a heterologous location on the chromosome. Flow cytometry and single-cell microscopy were used to assess the transcription profile using the fluorescence generated by YFP as a reporter. In the wild-type strain, the bimodality of *hag* transcription in the cell population is clearly evident (Fig. 3A and C). Strikingly, upon deletion of *flgN* bimodality is lost as *hag* transcription was observed for all cells within the population, albeit at a slightly lower level than in the wild type (Fig. 3A and C). The

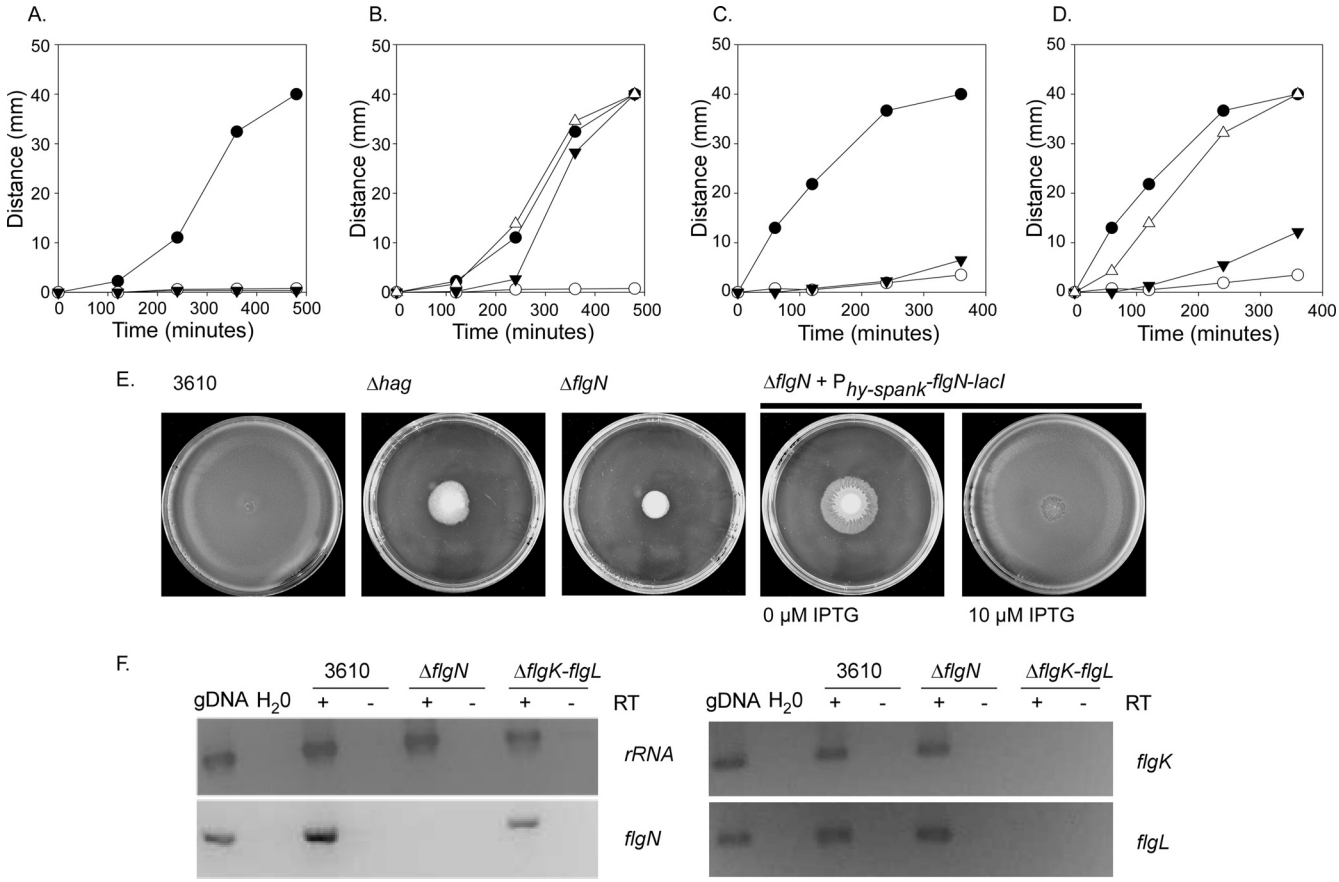

FIG 2 Δ*flgN* strains are nonmotile. Swim expansion assays (A and B) and swarm expansion assays (C and D) were performed. Wild-type (3610; filled circle), Δ*hag* (DS1677; filled triangle), and Δ*flgN* (NRS3570; open circle) strains were used for the experiments shown in panels A and C. Wild-type (3610; filled circle) and Δ*flgN* (NRS3570; open circle) strains along with the Δ*flgN amyE*::$P_{hy\text{-}spank}$-*flgN-lacI* (NRS3578) strain without (filled triangle) and with (open triangle) 10 μM IPTG induction were used for the experiments shown in panels B and D. Each graph is representative of three independent biological replicates. (E) Photographs of swarm expansion plates taken at the end of the assay, after 6 h of incubation at 37°C. (F) RT-PCR analysis of transcription of rRNA, *flgN*, *flgK*, and *flgL* in wild-type (NCIB3610), Δ*flgN* (NRS3570), and Δ*flgK-flgL* (NRS4060) strains. Genomic DNA (gDNA) and H_2O are shown as positive and negative controls for amplification, respectively. Reaction mixtures were incubated with (+) or without (−) reverse transcriptase (RT).

alteration in the *hag* transcription profile can be complemented upon reintroduction of *flgN* under the control of an IPTG-inducible promoter at the heterologous *amyE* locus, confirming the requirement of *flgN* for bimodal *hag* transcription (Fig. 3B). However, as the *hag* gene is still transcribed in the absence of *flgN*, these findings indicate that lack of motility in the Δ*flgN* strain is not due to a lack of *hag* transcription.

Loss of *flgN* is associated with a defect in flagellar biosynthesis. Given that the *hag* coding region is transcribed (Fig. 3), a lack of motility in the absence of *flgN* could arise from lack of translation of the *hag* transcript. To assess *hag* translation, a P*hag'-'lacZ* translational reporter fusion (under the control of the *hag* promoter, the *hag* leader region, Shine-Dalgarno sequence, and start codon) was constructed and introduced into *B. subtilis* at the *amyE* locus. When the β-galactosidase activity levels in the *flgN* mutant were compared with the wild-type levels, Hag translation was found to be 2-fold lower (Fig. 4A). However, a strain carrying an in-frame deletion of *flgE*, which encodes the main protein component of the flagellar hook, showed a 100-fold decrease in Hag translation (Fig. 4A) (55). It is likely that the observed decrease in the translation of *hag* in the Δ*flgN* mutant strain is a result of *hag* being transcribed at a slightly lower level in all cells than in the wild-type strain (Fig. 3). Alternatively, it is technically possible that translation itself may be regulated, as occurs in the absence of *flgE* (see Discussion) (55). While there is a statistically significant ($P = 0.01$) decrease in Hag translation in the absence of *flgN*, it did not appear to be sufficient to account for the complete lack of motility demonstrated in Fig. 2 (i.e., the severity of the motility defect does not match the small decrease in translation of Hag). A lack of motility in the presence of *hag* transcription and translation could be due to a lack of Hag polymerization. To test if Hag was secreted but not assembled into a flagellar filament in the Δ*flgN* strain, proteins were extracted from the cellular and supernatant fractions of cells grown to mid-exponential phase. The presence or absence of Hag was detected by Western blotting, with the cytoplasmic sigma factor, σ^A, used as a loading and fractionation control. For the wild-type strain Hag is detected in the cellular fraction (which includes assembled flagella) and in the supernatant fraction (including unassembled and sheared flagella) (Fig. 4B). However, for the Δ*flgN* strain Hag is present only in the supernatant fraction at a lower molecular weight (Fig. 4B). This is likely to be unpolymerized Hag or the products of proteolytic degradation resulting from the action of the extracellular proteases (13). As a positive control for Hag secretion, a strain carry-

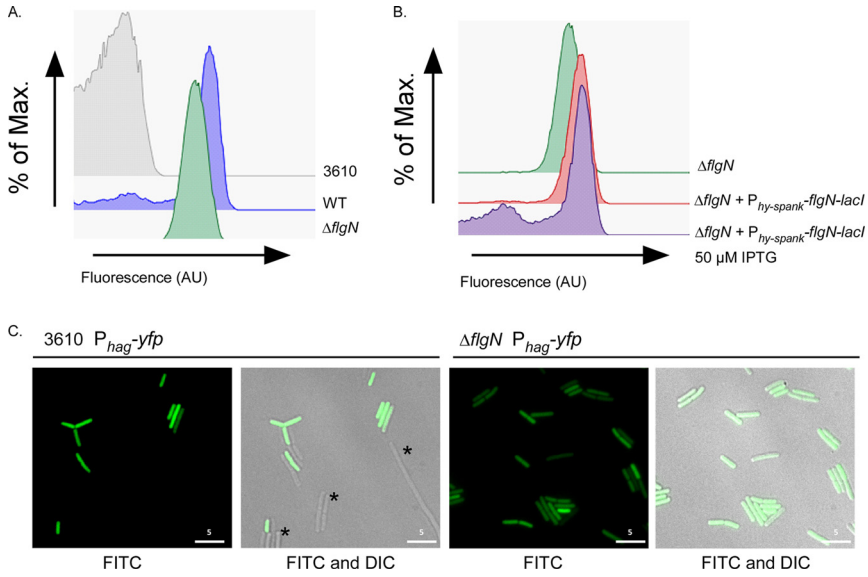

FIG 3 Deletion of *flgN* results in a loss of bimodal *hag* transcription. (A and B) Flow cytometry analysis of *hag* transcription in strains carrying the P_{hag}-*yfp* transcriptional reporter fusion. Strain 3610 was used as a nonfluorescent control. Shown are the wild-type (WT; NRS3076), Δ*flgN* (NRS3570), and Δ*flgN amyE*::$P_{hy\text{-}spank}$-*flgN-lacI* (NRS3713) strains without and with induction with 50 μM IPTG. (C) Fluorescence microscopy analysis of the wild-type (NRS3076) and Δ*flgN* (NRS3708) strains carrying the P_{hag}-*yfp* transcriptional reporter (false-colored green). Scale bar, 5 μm. Asterisks indicate examples of cells that do not transcribe *hag*. Max, maximum; AU, arbitrary units.

ing an in-frame deletion of *fliD*, which encodes the filament cap protein, was also assessed. As shown previously (13), this strain phenocopies the Hag secretion profile seen in the Δ*flgN* strain, thus supporting our conclusions.

Loss of filament polymerization in the Δ*flgN* strain was confirmed by single-cell fluorescence microscopy of strains where the codon for threonine at position 209 of the *hag* gene was mutated to cysteine to enable labeling with an Alexa Fluor 488 C_5 maleim-

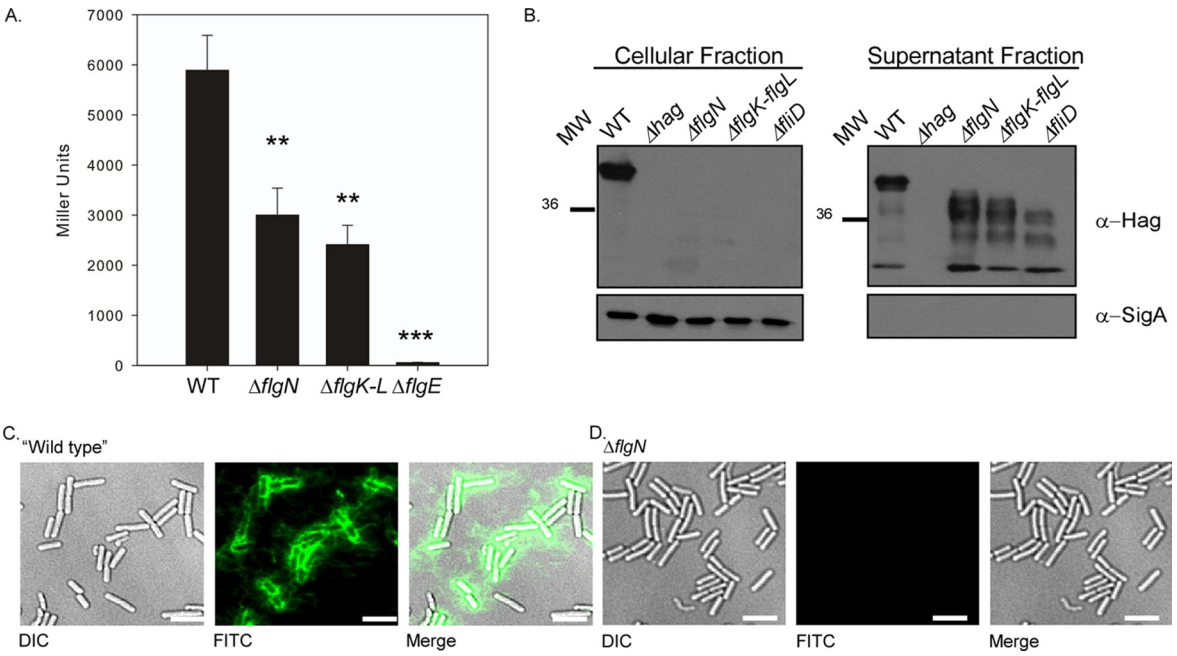

FIG 4 Deletion of *flgN* is associated with a decrease in *hag* translation and a block in filament assembly. (A) β-Galactosidase assays of strains carrying the P*hag*′-′*lacZ* translational reporter fusion. Shown are the wild-type (WT; NRS4795), Δ*flgN* (NRS4796), Δ*flgK-flgL* (NRS4799), and Δ*flgE* (NRS4798) strains. Data are plotted as the averages of at least three independent replicates. Error bars represent standard errors of the means. Asterisks denote significance as calculated by a Student *t* test: *, $P < 0.05$; **, $P < 0.01$; ***, $P < 0.001$. (B) Western blot analysis of cellular (including assembled flagella) and supernatant (including sheared and unassembled flagella) fractions of the wild-type (3610), Δ*hag* (DS1677), Δ*flgN* (NRS3570), Δ*flgK-flgL* (NRS4060), and Δ*fliD* (NRS4041) strains, separately probed with anti-Hag and anti-σ^A primary antibodies. MW, molecular weight in thousands; α, anti. (C and D) Fluorescence micrographs of strains carrying the Hag $T^{209}C$ point mutation labeled with Alexa Fluor 488 C_5 maleimide (false-colored green). Shown are the wild-type (NRS3719) (C) and Δ*flgN* (NRS3718) (D) strains. Scale bar, 5 μm.

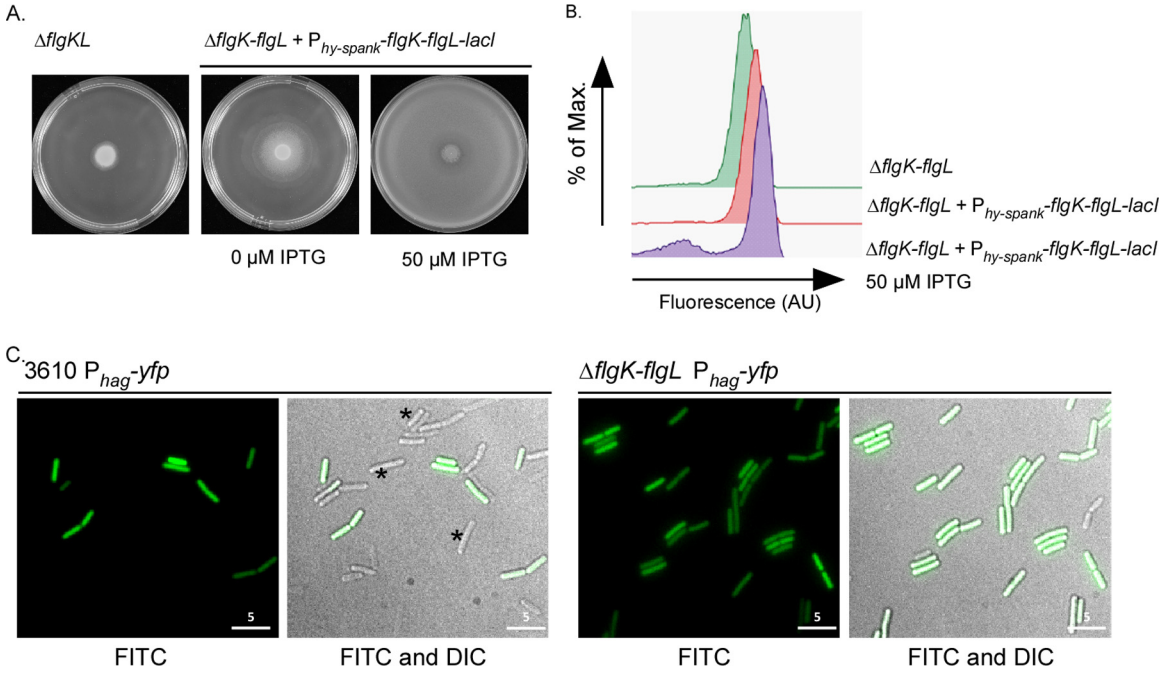

FIG 5 The Δ*flgN* strain phenocopies the Δ*flgK-flgL* strain. (A) Photographs of swarm expansion plates taken after 6 h of incubation at 37°C. Shown are the wild-type (3610), Δ*flgK-flgL* (NRS4060), and Δ*flgK-flgL amyE*::$P_{hy\text{-}spank}$-*flgK-flgL-lacI* (NRS 4064) strains without and with induction with 50 μM IPTG. (B) Flow cytometry analysis of *hag* transcription in strains carrying the P_{hag}-*yfp* transcriptional reporter fusion. Shown are the Δ*flgK-flgL* (NRS4071) and Δ*flgK-flgL amyE*::$P_{hy\text{-}spank}$-*flgK-flgL-lacI* (NRS4078) strains without and with induction with 50 μM IPTG. (C) Fluorescence microscopy analysis of the wild-type (NRS3076) and Δ*flgK-flgL* (NRS4071) strains carrying the P_{hag}-*yfp* transcriptional reporter (false-colored green). Scale bar, 5 μm. Asterisks indicate examples of cells that do not transcribe *hag*.

ide dye (45). In the wild-type background (NRS3719) the flagellar filaments are clearly visible (Fig. 4C). However, upon deletion of *flgN*, no signal was detected (Fig. 4D). Collectively, these data show that the Δ*flgN* strain is nonmotile due to both a small decrease in translation of Hag and a block in filament assembly, which results in the accumulation of unpolymerized Hag in the extracellular milieu. Together, these data prove that the lack of motility exhibited by the *flgN* mutant is due to a lack of flagellar filament assembly.

Deletion of the hook junction genes generates a strain which phenocopies the *flgN* mutant. A lack of filament polymerization in the absence of *flgN* is consistent with the hypothesis that *Bs*-FlgN is an orthologue of *St*-FlgN; i.e., if FlgK and FlgL are not properly localized to the hook-filament junction, the flagellar filament cannot be assembled (26, 53). We proposed that if *Bs*-FlgN were indeed an orthologue of *St*-FlgN, then a *B. subtilis* strain lacking *flgK* and *flgL* might phenocopy the Δ*flgN* strain. A strain carrying an in-frame deletion of *flgK-flgL* was constructed and found to be unable to swarm (Fig. 5A). In addition, flow cytometry and microscopy analyses revealed that, like deletion of *flgN*, deletion of *flgK-flgL* resulted in a loss of bimodality with respect to transcription of the σ^D-regulated gene *hag* (Fig. 5B and C) and a 2-fold decrease in Hag translation compared with the wild-type strain (Fig. 4A). Furthermore, upon deletion of *flgK-flgL*, Hag could not be detected in the cellular fraction but was instead found in the extracellular milieu (Fig. 4B). Using reverse transcription-PCR analysis, we confirmed that transcription of the other genes in the operon was not impacted by the *flgK-flgL* deletion (Fig. 2F). All of the phenotypes were proven to be specific to deletion of the *flgK-flgL* coding region as the mutant strain could be complemented by replacement of the *flgK-flgL* coding region at a heterologous location on the chromosome under the control of the $P_{hy\text{-}spank}$ promoter (Fig. 5A and B). In conclusion, a double deletion of *flgK* and *flgL* generates a strain that phenocopies the *flgN* mutant, as demonstrated by physiological, biochemical, and single-cell analyses. This is consistent with *Bs*-FlgN functioning as an orthologue of *St*-FlgN.

Overexpression of *flgK-flgL* cannot compensate for the absence of *flgN*. In *Salmonella* deletion of *flgN* can be compensated for by overexpression of *flgK* and *flgL* (16). This is because FlgN is not exclusively required for the secretion of its substrates but rather protects FlgK and FlgL from proteolysis and ensures that the substrates are efficiently transported to the export machinery (16, 17). To test if this was the case for the *B. subtilis flgN* deletion, the coding regions of *flgK* and *flgL* were integrated in the Δ*flgN* strain at a heterologous site on the chromosome under the control of an IPTG-inducible promoter. Induction of the *flgK-flgL* coding region was unable to restore motility to the Δ*flgN* strain, as determined by assaying swarming motility (Fig. 6A). To confirm that the flagellar filament was not polymerized upon overexpression of *flgK-flgL*, cellular protein samples (which include assembled flagella) were separated by SDS-PAGE and stained with Coomassie brilliant blue. Hag appears as a dominant protein band at ~36 kDa (Fig. 6B) and can be easily identified by comparison with proteins harvested from the Δ*hag* and wild-type strains (56). Moreover, the identity of the Hag protein was confirmed by mass spectrometry (see Fig. S1 in the supplemental material). Compared with the wild type, analysis of the cellular proteins for the Δ*flgN* strain indicated that Hag was not associated with the cell fraction (Fig. 6B). This is entirely consistent with the data pre-

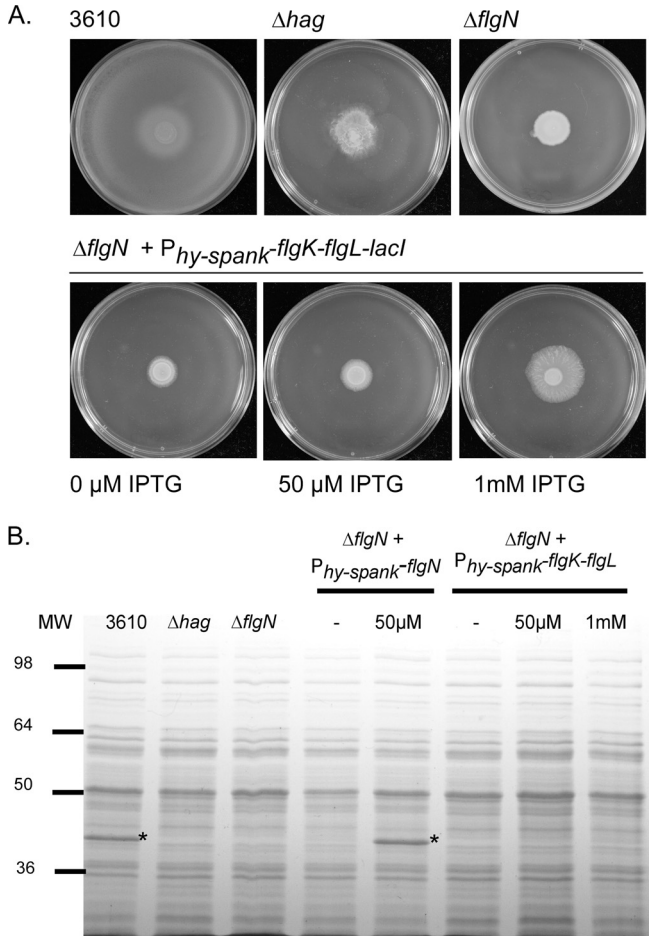

FIG 6 Overexpression of *flgK-flgL* cannot complement a Δ*flgN* mutant. (A) Photographs of swarm expansion plates taken after 6 h of incubation at 37°C. Shown are the wild-type (3610), Δ*hag* (DS1677), Δ*flgN* (NRS3570), and Δ*flgN amyE*::$P_{hy\text{-}spank}$-*flgK-flgL-lacI* (NRS4043) strains without and with induction with 50 μM IPTG or 1 mM IPTG. (B) Coomassie gel analysis of cellular fractions of the 3610, Δ*hag* (DS1677), Δ*flgN* (NRS3570), Δ*flgN amyE*::$P_{hy\text{-}spank}$-*flgN-lacI* (NRS3578), and Δ*flgN amyE*::$P_{hy\text{-}spank}$-*flgK-flgL-lacI* (NRS4043) strains without and with induction with 50 μM IPTG or 1 mM IPTG. The Hag protein was subsequently identified by mass spectrometry analysis and is marked with asterisks. MW, molecular weight in thousands.

sented above (Fig. 4 and 6A). As expected, the presence of the Hag band could be restored by the reintroduction of *flgN* on the chromosome upon induction with 50 μM IPTG (Fig. 6B). However, introduction of *flgK-flgL* in the Δ*flgN* background at a heterologous site could not complement the Δ*flgN* mutant with respect to Hag polymerization, even in the presence of 1 mM IPTG. The inability of *flgK-flgL* overexpression to compensate for deletion of *flgN* could be due to disruption of flagellar biosynthesis at an earlier stage. However, this possibility was ruled out as we demonstrated by Western blotting that the flagellar hook protein, FlgE, was detected in whole-cell lysates (which include assembled flagella) for both the wild-type and Δ*flgN* strains (see Fig. S2 in the supplemental material).

The inability of heterologous *flgK-flgL* expression to complement the *flgN* mutant strain is suggestive of a strict dependence on FlgN for FlgK-FlgL protein stability or secretion in *B. subtilis*. In an attempt to test if FlgK was unstable in the absence of *flgN*, strains were constructed to enable detection of FlgK by fusing FlgK to a poly histidine epitope tag. However, the presence of such an epitope tag at either the N or C terminus of the protein rendered FlgK nonfunctional, as determined by a nonmotile phenotype (see Fig. S3A in the supplemental material). As a method of attempting to assess FlgK assembly at the flagellar hook junction, we aimed to purify flagellar hook-basal bodies from both the wild-type and Δ*flgN* strains and to analyze the protein components of the complex by mass spectrometry. While we were successfully able to enrich the flagellar fraction of the wild-type strain (see Fig. S3B and Table S4 in the supplemental material), we were unable to do so for the Δ*flgN* strain. This is most likely because this methodology is dependent on an intact flagellar filament for isolation of the complex, and the *flgN* mutant does not form a flagellar filament (Fig. 4). Finally, in *S.* Typhimurium, FlgN interacts directly with FlgK and FlgL to protect the proteins from proteolytic cleavage (25). To test if FlgN could interact with either FlgK or FlgL to perform a similar role in *B. subtilis*, bacterial two-hybrid experiments were undertaken. However, an interaction could not be detected (data not shown), which could be due to inactivity of the fusion protein. Thus, despite extensive efforts, we were unable to determine the stability of FlgK in the absence of *flgN* or if there was an interaction between the proteins.

***In vivo* analysis of the role of phosphorylation in controlling motility.** Global proteomic strategies have identified a plethora of targets for both tyrosine and arginine kinases in *B. subtilis* (28–30). One such target is FlgN, which can be tyrosine phosphorylated on amino acid 49 (29) and arginine phosphorylated on amino acid 60 (30). Having demonstrated that FlgN is required for flagellar biosynthesis, we were presented with the ideal system to assess the role of tyrosine and arginine phosphorylation in controlling protein function *in vivo*. Site-directed mutagenesis was used to mutate the chromosomal copy of *flgN* tyrosine 49 to alanine ($Y^{49}A$) to assess the effects of preventing phosphorylation. As shown in Fig. 7, swarming motility was not affected. We next tested the impact of replacing tyrosine 49 with glutamic acid ($Y^{49}E$) to mimic the negative charge associated with phosphorylation. Once more, the strain containing the mutant allele of FlgN ($Y^{49}E$) exhibited a motility phenotype that was indistinguishable from that of the wild type (Fig. 7A). Subsequently, strains were constructed where the coding region of *flgN* on the chromosome was mutated such that the arginine at position 60 was replaced with either alanine or glutamic acid. The motility phenotypes of these strains were tested, and they were found to swarm at the same rate as the wild-type strain (Fig. 7A). SDS-PAGE analysis of whole-cell lysates also showed that Hag was synthesized and that the cellular localization was directly comparable to that of the wild type for each of the point mutation strains (Fig. 7B). These data demonstrate that mutation of the previously defined tyrosine or arginine phosphorylation site has no discernible impact on the function of FlgN in *B. subtilis* NCIB3610.

DISCUSSION

In this work we report that *yvyG* is required for the motility of *B. subtilis*. We demonstrate that the main role for YvyG is to enable flagellar filament polymerization. The data presented allow us to conclude that YvyG is indeed an orthologue of FlgN from *S.* Typhimurium, but in *B. subtilis* it would appear that there is a strict reliance on YvyG for the secretion and placement of FlgK and FlgL

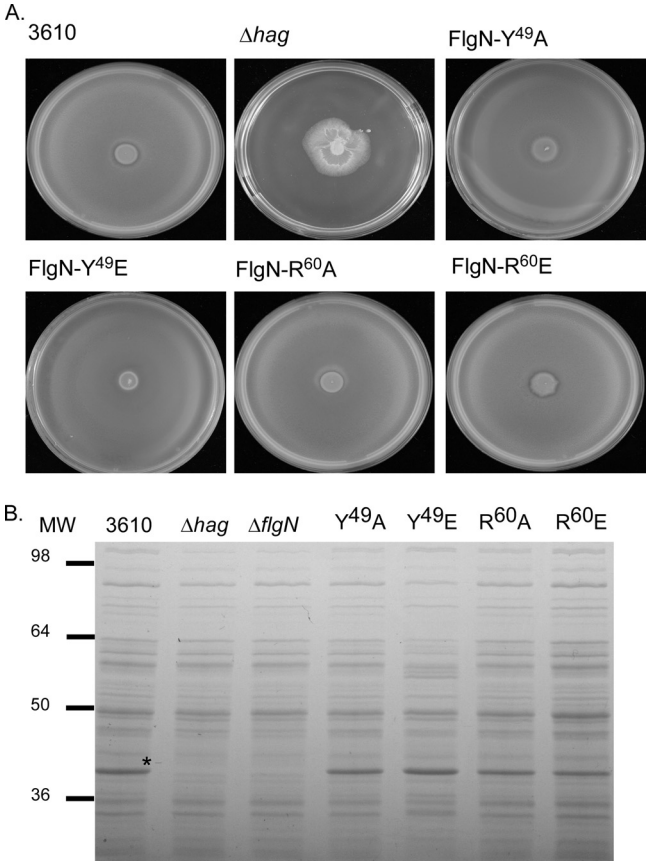

FIG 7 Mutation of identified FlgN phosphorylation sites does not affect motility. (A) Photographs of swarm expansion plates taken after 6 h of incubation at 37°C. Shown are the wild-type (3610), Δ*hag* (DS1677), *flgN*-Y^{49}A (NRS3571), *flgN*-Y^{49}E (NRS3724), *flgN*-R^{60}A (NRS4063), and *flgN*-R^{60}E (NRS4017) strains. (B) Coomassie gel analysis of cellular fractions of the 3610, Δ*hag* (DS1677), *flgN*-Y^{49}A (NRS3571), *flgN*-Y^{49}E (NRS3724), *flgN*-R^{60}A (NRS4063), and *flgN*-R^{60}E (NRS4017) strains. The Hag protein is marked with asterisks. MW, molecular weight in thousands.

at the hook-filament junction. In light of these data, we suggest that YvyG be referred to as FlgN.

The role of FlgN in the regulation of flagellum biosynthesis. This work suggests that in *B. subtilis* FlgN partially mediates flagellum biosynthesis through its ability to regulate *hag* transcription and translation. In wild-type *B. subtilis* the sigma factor σ^D (*sigD*) needed for *hag* transcription is transcribed only in a subpopulation of cells, resulting in bimodal expression of *hag* (11, 12). Deletion of *flgN* results is *hag* being transcribed in every cell, albeit at a lower level (Fig. 3), indicating that σ^D is active in every cell in this genetic background. Consistent with this, we did not observe any cell chaining in the absence of *flgN*, indicating that the σ^D-dependent autolysins (10) are also transcribed in all cells. It is known that σ^D can be regulated by transcription of the *sigD* gene and by interaction with the anti-sigma factor, FlgM (11). Therefore, the change in *hag* transcription observed upon deletion of *flgN* could be explained by a change in regulation by the anti-sigma factor, FlgM. In *S.* Typhimurium FlgM regulates the transcription of late-class σ^{28}-regulated flagellar genes by both sequestering free σ^{28} and destabilizing the σ^{28} RNA polymerase holoenzyme complex (57). Upon completion of HBB assembly, FlgM is secreted, and σ^{28} is able to activate target promoters (58). It has been previously reported that FlgN is able to regulate the translation of FlgM in *S.* Typhimurium (59), therefore raising the possibility that in the *B. subtilis* Δ*flgN* strain translation of FlgM is decreased, allowing σ^D to trigger transcription of *hag* in all cells. The regulation of FlgM in *B. subtilis* is poorly understood, and so whether this is the case has yet to be determined.

Deletion of *flgN* in *B. subtilis* also results in a 2-fold decrease in *hag* translation (Fig. 4A). This effect could technically be due to translational regulation, as is seen for the Δ*flgE* strain (Fig. 4A) (55). Indeed, recent studies in *B. subtilis* have identified the RNA binding protein CsrA, the CsrA regulatory protein FliW, and the molecular chaperone FliS as having roles in controlling Hag translation or secretion (13, 55, 60). When cellular levels of Hag are depleted, FliW binds to CsrA, leaving it unable to occlude the *hag* Shine-Dalgarno sequence, allowing translation to proceed. However, when Hag protein accumulates in the cytoplasm, it is able to interact with and sequester FliW, resulting in CsrA-mediated repression of translation (55). Therefore, inhibition of translation by CsrA relies on accumulation of Hag within the cell. However, the data presented in Fig. 4B show that in the absence of *flgN*, Hag accumulates not in the cytoplasm but in the extracellular milieu. This not only suggests that CsrA is not responsible for the observed decrease in Hag translation but also is in keeping with the hypothesis that FlgN is required for the assembly of FlgK and FlgL; in the absence of the hook-filament junction, flagellin cannot be properly assembled and so accumulates in the extracellular milieu (53). For this reason we favor the hypothesis that the change in the transcriptional profile of *hag* is responsible for the decrease in translation observed.

The role of FlgN phosphorylation. Tyrosine and arginine phosphorylation events have been implicated in the control of diverse biological processes in *B. subtilis*, including biofilm formation (38, 61), DNA replication (62), exopolysaccharide synthesis (63), the heat shock response (64), and potentially the regulation and/or assembly of the flagellar filament (30). The motility protein FlgN has been shown to be both tyrosine and arginine phosphorylated (29–31). Moreover, the subcellular localization of FlgN was reported to be impacted by deletion of the tyrosine kinase PtkA (31). However, site-directed mutagenesis of the reported FlgN tyrosine and arginine phosphorylation sites *in vivo* failed to impact the motility of *B. subtilis* (Fig. 7). These findings led us to conclude that a dominant role for phosphorylation of these residues does not exist. When these findings are considered in a wider context of the function of posttranslational modifications, they may not be surprising. For instance, in eukaryotes, it has been suggested that many phosphorylation events are nonfunctional or may occur at a very low stoichiometry such that they do not impact the function of the protein (65, 66). Indeed, two tyrosine kinases (61, 63) and one arginine kinase (30) have been identified in *B. subtilis*, but many more proteins have been identified as being phosphorylated, thereby suggesting that each kinase is promiscuous. This may imply that random encounters between kinases and phosphorylatable sites on different proteins might result in nonspecific and nonfunctional phosphorylation events. Alternatively, FlgN might act as a phosphate sink or store to remove free phosphate from the system (67).

Concluding remarks. The regulation and biosynthesis of the bacterial flagellum are best understood for Gram-negative bacterial species such as *S.* Typhimurium. However, recent work on *B.*

subtilis has begun to illuminate how Gram-positive bacterial species are able to coordinate flagellar assembly. These studies have uncovered key differences between Gram-negative and Gram-positive bacterial flagella as well as having highlighted many conserved mechanisms. The data presented here illustrate that FlgN from *B. subtilis* is essential for flagellar filament polymerization and therefore motility. We propose that *Bs*-FlgN is an orthologue of the *S.* Typhimurium chaperone protein FlgN and is required for the export and assembly of FlgK and FlgL at the hook-filament junction. By way of contrast, in a *B. subtilis* strain lacking *flgN* flagella are not detectable, and overexpression of *flgK-flgL* is not sufficient to overcome the motility defect exhibited by the Δ*flgN* strain. Therefore, while *Bs*-FlgN bears great functional similarity to *S*T-FlgN, there are crucial differences which suggest that there is a stricter dependence on FlgN for the export of FlgK and FlgL in *B. subtilis*. Overall, this work further emphasizes the previously underappreciated differences in flagellar gene regulation between Gram-positive and Gram-negative bacterial species.

ACKNOWLEDGMENTS

L.S.C. is the recipient of a Wellcome Trust Ph.D. studentship (093714/Z/10/Z). V.L.M. was funded by a Biotechnology and Biological Sciences Research Council grant (BB/I006915/1). A.O. was the recipient of a Biotechnology and Biological Sciences Research Council Doctoral Training Account grant (BB/D526161/1). The microscopy facilities are supported by a Wellcome Trust Strategic Award grant (083524/Z/07/Z).

The funders had no role in study design, data collection and analysis, decision to publish, or preparation of the manuscript.

We thank Kürsad Turgay for the kind gift of the anti-Hag antibody, Daniel Kearns for the kind gift of the anti-FlgE antibody and helpful discussions, Rosemary Clarke for assistance with flow cytometry, FingerPrints Proteomics and Mass Spectrometry Facility, University of Dundee, and Shin-Ichi Aizawa for his helpful (and repeated) advice regarding the purification of flagellar hook-basal bodies.

REFERENCES

1. **Chevance FF, Hughes KT.** 2008. Coordinating assembly of a bacterial macromolecular machine. Nat. Rev. Microbiol. **6:**455–465. http://dx.doi.org/10.1038/nrmicro1887.
2. **O'Toole GA, Kaplan HB, Kolter R.** 2000. Biofilm formation as microbial development. Annu. Rev. Microbiol. **54:**49–79. http://dx.doi.org/10.1146/annurev.micro.54.1.49.
3. **Cairns LS, Marlow VL, Bissett E, Ostrowski A, Stanley-Wall NR.** 2013. A mechanical signal transmitted by the flagellum controls signalling in *Bacillus subtilis*. Mol. Microbiol. **90:**6–21. http://dx.doi.org/10.1111/mmi.12342.
4. **Serra DO, Richter AM, Klauck G, Mika F, Hengge R.** 2013. Microanatomy at cellular resolution and spatial order of physiological differentiation in a bacterial biofilm. mBio. **4:**e00103–13. http://dx.doi.org/10.1128/mBio.00103-13.
5. **Marquez-Magana LM, Chamberlin MJ.** 1994. Characterization of the *sigD* transcription unit of *Bacillus subtilis*. J. Bacteriol. **176:**2427–2434.
6. **West JT, Estacio W, Marquez-Magana L.** 2000. Relative roles of the *fla/che* P_A, P_{D-3}, and P_{sigD} promoters in regulating motility and *sigD* expression in *Bacillus subtilis*. J. Bacteriol. **182:**4841–4848. http://dx.doi.org/10.1128/JB.182.17.4841-4848.2000.
7. **Helmann JD, Marquez LM, Chamberlin MJ.** 1988. Cloning, sequencing, and disruption of the *Bacillus subtilis* sigma 28 gene. J. Bacteriol. **170:**1568–1574.
8. **Chen YF, Helmann JD.** 1992. Restoration of motility to an *Escherichia coli fliA* flagellar mutant by a *Bacillus subtilis* sigma factor. Proc. Natl. Acad. Sci. U. S. A. **89:**5123–5127. http://dx.doi.org/10.1073/pnas.89.11.5123.
9. **Mirel DB, Lauer P, Chamberlin MJ.** 1994. Identification of flagellar synthesis regulatory and structural genes in a sigma D-dependent operon of *Bacillus subtilis*. J. Bacteriol. **176:**4492–4500.
10. **Marquez LM, Helmann JD, Ferrari E, Parker HM, Ordal GW, Chamberlin MJ.** 1990. Studies of sigma D-dependent functions in *Bacillus subtilis*. J. Bacteriol. **172:**3435–3443.
11. **Cozy LM, Kearns DB.** 2010. Gene position in a long operon governs motility development in *Bacillus subtilis*. Mol. Microbiol. **76:**273–285. http://dx.doi.org/10.1111/j.1365-2958.2010.07112.x.
12. **Kearns DB, Losick R.** 2005. Cell population heterogeneity during growth of *Bacillus subtilis*. Genes Dev. **19:**3083–3094. http://dx.doi.org/10.1101/gad.1373905.
13. **Mukherjee S, Babitzke P, Kearns DB.** 2013. FliW and FliS function independently to control cytoplasmic flagellin levels in *Bacillus subtilis*. J. Bacteriol. **195:**297–306. http://dx.doi.org/10.1128/JB.01654-12.
14. **Titz B, Rajagopala SV, Ester C, Hauser R, Uetz P.** 2006. Novel conserved assembly factor of the bacterial flagellum. J. Bacteriol. **188:**7700–7706. http://dx.doi.org/10.1128/JB.00820-06.
15. **Bennett JC, Hughes C.** 2000. From flagellum assembly to virulence: the extended family of type III export chaperones. Trends Microbiol. **8:**202–204. http://dx.doi.org/10.1016/S0966-842X(00)01751-0.
16. **Aldridge P, Karlinsey J, Hughes KT.** 2003. The type III secretion chaperone FlgN regulates flagellar assembly via a negative feedback loop containing its chaperone substrates FlgK and FlgL. Mol. Microbiol. **49:**1333–1345. http://dx.doi.org/10.1046/j.1365-2958.2003.03637.x.
17. **Thomas J, Stafford GP, Hughes C.** 2004. Docking of cytosolic chaperone-substrate complexes at the membrane ATPase during flagellar type III protein export. Proc. Natl. Acad. Sci. U. S. A. **101:**3945–3950. http://dx.doi.org/10.1073/pnas.0307223101.
18. **Evans LD, Stafford GP, Ahmed S, Fraser GM, Hughes C.** 2006. An escort mechanism for cycling of export chaperones during flagellum assembly. Proc. Natl. Acad. Sci. U. S. A. **103:**17474–17479. http://dx.doi.org/10.1073/pnas.0605197103.
19. **Minamino T, MacNab RM.** 2000. Interactions among components of the *Salmonella* flagellar export apparatus and its substrates. Mol. Microbiol. **35:**1052–1064. http://dx.doi.org/10.1046/j.1365-2958.2000.01771.x.
20. **Minamino T, Shimada M, Okabe M, Saijo-Hamano Y, Imada K, Kihara M, Namba K.** 2010. Role of the C-terminal cytoplasmic domain of FlhA in bacterial flagellar type III protein export. J. Bacteriol. **192:**1929–1936. http://dx.doi.org/10.1128/JB.01328-09.
21. **Bange G, Kummerer N, Engel C, Bozkurt G, Wild K, Sinning I.** 2010. FlhA provides the adaptor for coordinated delivery of late flagella building blocks to the type III secretion system. Proc. Natl. Acad. Sci. U. S. A. **107:**11295–11300. http://dx.doi.org/10.1073/pnas.1001383107.
22. **Minamino T, Namba K.** 2008. Distinct roles of the FliI ATPase and proton motive force in bacterial flagellar protein export. Nature **451:**485–488. http://dx.doi.org/10.1038/nature06449.
23. **Paul K, Erhardt M, Hirano T, Blair DF, Hughes KT.** 2008. Energy source of flagellar type III secretion. Nature **451:**489–492. http://dx.doi.org/10.1038/nature06497.
24. **Ozin AJ, Claret L, Auvray F, Hughes C.** 2003. The FliS chaperone selectively binds the disordered flagellin C-terminal D0 domain central to polymerisation. FEMS Microbiol. Lett. **219:**219–224. http://dx.doi.org/10.1016/S0378-1097(02)01208-9.
25. **Bennett JC, Thomas J, Fraser GM, Hughes C.** 2001. Substrate complexes and domain organization of the *Salmonella* flagellar export chaperones FlgN and FliT. Mol. Microbiol. **39:**781–791. http://dx.doi.org/10.1046/j.1365-2958.2001.02268.x.
26. **Fraser GM, Bennett JC, Hughes C.** 1999. Substrate-specific binding of hook-associated proteins by FlgN and FliT, putative chaperones for flagellum assembly. Mol. Microbiol. **32:**569–580. http://dx.doi.org/10.1046/j.1365-2958.1999.01372.x.
27. **Pallen MJ, Penn CW, Chaudhuri RR.** 2005. Bacterial flagellar diversity in the post-genomic era. Trends Microbiol. **13:**143–149. http://dx.doi.org/10.1016/j.tim.2005.02.008.
28. **Levine A, Vannier F, Absalon C, Kuhn L, Jackson P, Scrivener E, Labas V, Vinh J, Courtney P, Garin J, Seror SJ.** 2006. Analysis of the dynamic *Bacillus subtilis* Ser/Thr/Tyr phosphoproteome implicated in a wide variety of cellular processes. Proteomics **6:**2157–2173. http://dx.doi.org/10.1002/pmic.200500352.
29. **Macek B, Mijakovic I, Olsen JV, Gnad F, Kumar C, Jensen PR, Mann M.** 2007. The serine/threonine/tyrosine phosphoproteome of the model bacterium *Bacillus subtilis*. Mol. Cell. Proteomics **6:**697–707. http://dx.doi.org/10.1074/mcp.M600464-MCP200.
30. **Elsholz AK, Turgay K, Michalik S, Hessling B, Gronau K, Oertel D, Mader U, Bernhardt J, Becher D, Hecker M, Gerth U.** 2012. Global impact of protein arginine phosphorylation on the physiology of *Bacillus*

subtilis. Proc. Natl. Acad. Sci. U. S. A. **109:**7451–7456. http://dx.doi.org/10.1073/pnas.1117483109.
31. **Jers C, Pedersen MM, Paspaliari DK, Schutz W, Johnsson C, Soufi B, Macek B, Jensen PR, Mijakovic I.** 2010. *Bacillus subtilis* BY-kinase PtkA controls enzyme activity and localization of its protein substrates. Mol. Microbiol. **77:**287–299. http://dx.doi.org/10.1111/j.1365-2958.2010.07227.x.
32. **Garnak M, Reeves HC.** 1979. Phosphorylation of Isocitrate dehydrogenase of *Escherichia coli*. Science **203:**1111–1112. http://dx.doi.org/10.1126/science.34215.
33. **Deutscher J, Kuster E, Bergstedt U, Charrier V, Hillen W.** 1995. Protein kinase-dependent HPr-CcpA interaction links glycolytic activity to carbon catabolite repression in Gram-positive bacteria. Mol. Microbiol. **15:**1049–1053. http://dx.doi.org/10.1111/j.1365-2958.1995.tb02280.x.
34. **Cozy LM, Phillips AM, Calvo RA, Bate AR, Hsueh YH, Bonneau R, Eichenberger P, Kearns DB.** 2012. SlrA/SinR/SlrR inhibits motility gene expression upstream of a hypersensitive and hysteretic switch at the level of sD in *Bacillus subtilis*. Mol. Microbiol. **83:**1210–1228. http://dx.doi.org/10.1111/j.1365-2958.2012.08003.x.
35. **Hsueh YH, Cozy LM, Sham LT, Calvo RA, Gutu AD, Winkler ME, Kearns DB.** 2011. DegU-phosphate activates expression of the anti-sigma factor FlgM in *Bacillus subtilis*. Mol. Microbiol. **81:**1092–1108. http://dx.doi.org/10.1111/j.1365-2958.2011.07755.x.
36. **Kutsukake K, Okada T, Yokoseki T, Iino T.** 1994. Sequence analysis of the *flgA* gene and its adjacent region in *Salmonella* Typhimurium, and identification of another flagellar gene, *flgN*. Gene **143:**49–54. http://dx.doi.org/10.1016/0378-1119(94)90603-3.
37. **Verhamme DT, Kiley TB, Stanley-Wall NR.** 2007. DegU co-ordinates multicellular behaviour exhibited by *Bacillus subtilis*. Mol. Microbiol. **65:**554–568. http://dx.doi.org/10.1111/j.1365-2958.2007.05810.x.
38. **Kiley TB, Stanley-Wall NR.** 2010. Post-translational control of *Bacillus subtilis* biofilm formation mediated by tyrosine phosphorylation. Mol. Microbiol. **78:**947–963. http://dx.doi.org/10.1111/j.1365-2958.2010.07382.x.
39. **Arnaud M, Chastanet A, Debarbouille M.** 2004. New vector for efficient allelic replacement in naturally nontransformable, low-GC-content, gram-positive bacteria. Appl. Environ. Microbiol. **70:**6887–6891. http://dx.doi.org/10.1128/AEM.70.11.6887-6891.2004.
40. **Liu H, Naismith JH.** 2009. A simple and efficient expression and purification system using two newly constructed vectors. Protein Expr. Purif. **63:**102–111. http://dx.doi.org/10.1016/j.pep.2008.09.008.
41. **Ostrowski A, Mehert A, Prescott A, Kiley TB, Stanley-Wall NR.** 2011. YuaB functions synergistically with the exopolysaccharide and TasA amyloid fibers to allow biofilm formation by *Bacillus subtilis*. J. Bacteriol. **193:**4821–4831. http://dx.doi.org/10.1128/JB.00223-11.
42. **Sievers F, Wilm A, Dineen D, Gibson TJ, Karplus K, Li W, Lopez R, McWilliam H, Remmert M, Soding J, Thompson JD, Higgins DG.** 2011. Fast, scalable generation of high-quality protein multiple sequence alignments using Clustal Omega. Mol. Syst. Biol. **7:**539. http://dx.doi.org/10.1038/msb.2011.75.
43. **Jones DT.** 1999. Protein secondary structure prediction based on position-specific scoring matrices. J. Mol. Biol. **292:**195–202. http://dx.doi.org/10.1006/jmbi.1999.3091.
44. **Buchan DW, Minneci F, Nugent TC, Bryson K, Jones DT.** 2013. Scalable web services for the PSIPRED protein Analysis Workbench. Nucleic Acids Res. **41:**W349–357. http://dx.doi.org/10.1093/nar/gkt381.
45. **Blair KM, Turner L, Winkelman JT, Berg HC, Kearns DB.** 2008. A molecular clutch disables flagella in the *Bacillus subtilis* biofilm. Science **320:**1636–1638. http://dx.doi.org/10.1126/science.1157877.
46. **Allan C, Burel JM, Moore J, Blackburn C, Linkert M, Loynton S, Macdonald D, Moore WJ, Neves C, Patterson A, Porter M, Tarkowska A, Loranger B, Avondo J, Lagerstedt I, Lianas L, Leo S, Hands K, Hay RT, Patwardhan A, Best C, Kleywegt GJ, Zanetti G, Swedlow JR.** 2012. OMERO: flexible, model-driven data management for experimental biology. Nat. Methods **9:**245–253. http://dx.doi.org/10.1038/nmeth.1896.
47. **Murray EJ, Strauch MA, Stanley-Wall NR.** 2009. σX is involved in controlling *Bacillus subtilis* biofilm architecture through the AbrB homologue Abh. J. Bacteriol. **191:**6822–6832. http://dx.doi.org/10.1128/JB.00618-09.
48. **Karlinsey JE, Tanaka S, Bettenworth V, Yamaguchi S, Boos W, Aizawa SI, Hughes KT.** 2000. Completion of the hook-basal body complex of the *Salmonella* Typhimurium flagellum is coupled to FlgM secretion and *fliC* transcription. Mol. Microbiol. **37:**1220–1231. http://dx.doi.org/10.1046/j.1365-2958.2000.02081.x.
49. **Murray EJ, Kiley TB, Stanley-Wall NR.** 2009. A pivotal role for the response regulator DegU in controlling multicellular behaviour. Microbiology **155:**1–8. http://dx.doi.org/10.1099/mic.0.023903-0.
50. **Miller J.** 1972. Experiments in molecular genetics. Cold Spring Harbor Laboratory Press, Cold Spring Harbor, NY.
51. **Aizawa SI, Dean GE, Jones CJ, Macnab RM, Yamaguchi S.** 1985. Purification and characterization of the flagellar hook-basal body complex of *Salmonella* Typhimurium. J. Bacteriol. **161:**836–849.
52. **Kubori T, Okumura M, Kobayashi N, Nakamura D, Iwakura M, Aizawa SI.** 1997. Purification and characterization of the flagellar hook-basal body complex of *Bacillus subtilis*. Mol. Microbiol. **24:**399–410. http://dx.doi.org/10.1046/j.1365-2958.1997.3341714.x.
53. **Gygi D, Fraser G, Dufour A, Hughes C.** 1997. A motile but non-swarming mutant of *Proteus mirabilis* lacks FlgN, a facilitator of flagella filament assembly. Mol. Microbiol. **25:**597–604. http://dx.doi.org/10.1046/j.1365-2958.1997.5021862.x.
54. **Fraser GM, Hughes C.** 1999. Swarming motility. Curr. Opin. Microbiol. **2:**630–635. http://dx.doi.org/10.1016/S1369-5274(99)00033-8.
55. **Mukherjee S, Yakhnin H, Kysela D, Sokoloski J, Babitzke P, Kearns DB.** 2011. CsrA-FliW interaction governs flagellin homeostasis and a checkpoint on flagellar morphogenesis in *Bacillus subtilis*. Mol. Microbiol. **82:**447–461. http://dx.doi.org/10.1111/j.1365-2958.2011.07822.x.
56. **Diethmaier C, Pietack N, Gunka K, Wrede C, Lehnik-Habrink M, Herzberg C, Hubner S, Stulke J.** 2011. A novel factor controlling bistability in *Bacillus subtilis*: the YmdB protein affects flagellin expression and biofilm formation. J. Bacteriol. **193:**5997–6007. http://dx.doi.org/10.1128/JB.05360-11.
57. **Chadsey MS, Karlinsey JE, Hughes KT.** 1998. The flagellar anti-sigma factor FlgM actively dissociates *Salmonella* Typhimurium sigma28 RNA polymerase holoenzyme. Genes Dev. **12:**3123–3136. http://dx.doi.org/10.1101/gad.12.19.3123.
58. **Kutsukake K.** 1994. Excretion of the anti-sigma factor through a flagellar substructure couples flagellar gene expression with flagellar assembly in *Salmonella* Typhimurium. Mol. Gen. Genet. **243:**605–612.
59. **Karlinsey JE, Lonner J, Brown KL, Hughes KT.** 2000. Translation/secretion coupling by type III secretion systems. Cell **102:**487–497. http://dx.doi.org/10.1016/S0092-8674(00)00053-2.
60. **Yakhnin H, Pandit P, Petty TJ, Baker CS, Romeo T, Babitzke P.** 2007. CsrA of *Bacillus subtilis* regulates translation initiation of the gene encoding the flagellin protein (*hag*) by blocking ribosome binding. Mol. Microbiol. **64:**1605–1620. http://dx.doi.org/10.1111/j.1365-2958.2007.05765.x.
61. **Gerwig J, Kiley TB, Gunka K, Stanley-Wall N, Stulke J.** 2014. The protein tyrosine kinases EpsB and PtkA differentially affect biofilm formation in *Bacillus subtilis*. Microbiology **160:**682–691. http://dx.doi.org/10.1099/mic.0.074971-0.
62. **Petranovic D, Michelsen O, Zahradka K, Silva C, Petranovic M, Jensen PR, Mijakovic I.** 2007. *Bacillus subtilis* strain deficient for the protein-tyrosine kinase PtkA exhibits impaired DNA replication. Mol. Microbiol. **63:**1797–1805. http://dx.doi.org/10.1111/j.1365-2958.2007.05625.x.
63. **Mijakovic I, Poncet S, Boel G, Maze A, Gillet S, Jamet E, Decottignies P, Grangeasse C, Doublet P, Le Marechal P, Deutscher J.** 2003. Transmembrane modulator-dependent bacterial tyrosine kinase activates UDP-glucose dehydrogenases. EMBO J. **22:**4709–4718. http://dx.doi.org/10.1093/emboj/cdg458.
64. **Fuhrmann J, Schmidt A, Spiess S, Lehner A, Turgay K, Mechtler K, Charpentier E, Clausen T.** 2009. McsB is a protein arginine kinase that phosphorylates and inhibits the heat-shock regulator CtsR. Science **324:**1323–1327. http://dx.doi.org/10.1126/science.1170088.
65. **Landry CR, Levy ED, Michnick SW.** 2009. Weak functional constraints on phosphoproteomes. Trends Genet. **25:**193–197. http://dx.doi.org/10.1016/j.tig.2009.03.003.
66. **Beltrao P, Albanese V, Kenner LR, Swaney DL, Burlingame A, Villen J, Lim WA, Fraser JS, Frydman J, Krogan NJ.** 2012. Systematic functional prioritization of protein posttranslational modifications. Cell **150:**413–425. http://dx.doi.org/10.1016/j.cell.2012.05.036.
67. **Sourjik V, Schmitt R.** 1998. Phosphotransfer between CheA, CheY1, and CheY2 in the chemotaxis signal transduction chain of *Rhizobium meliloti*. Biochemistry **37:**2327–2335. http://dx.doi.org/10.1021/bi972330a.

Microbiology (2014), **160**, 56–66 DOI 10.1099/mic.0.072389-0

The prevalence and origin of exoprotease-producing cells in the *Bacillus subtilis* biofilm

Victoria L. Marlow,[1] Francesca R. Cianfanelli,[1] Michael Porter,[2] Lynne S. Cairns,[1] J. Kim Dale[3] and Nicola R. Stanley-Wall[1]

Correspondence
Nicola R. Stanley-Wall
n.r.stanleywall@dundee.ac.uk

[1]Division of Molecular Microbiology, College of Life Sciences, University of Dundee, Dundee DD1 5EH, UK

[2]Centre for Gene Regulation and Expression, College of Life Sciences, University of Dundee, Dundee DD1 5EH, UK

[3]Division of Cell and Developmental Biology, College of Life Sciences, University of Dundee, Dundee DD1 5EH, UK

Biofilm formation by the Gram-positive bacterium *Bacillus subtilis* is tightly controlled at the level of transcription. The biofilm contains specialized cell types that arise from controlled differentiation of the resident isogenic bacteria. DegU is a response regulator that controls several social behaviours exhibited by *B. subtilis* including swarming motility, biofilm formation and extracellular protease (exoprotease) production. Here, for the first time, we examine the prevalence and origin of exoprotease-producing cells within the biofilm. This was accomplished using single-cell analysis techniques including flow cytometry and fluorescence microscopy. We established that the number of exoprotease-producing cells increases as the biofilm matures. This is reflected by both an increase at the level of transcription and an increase in exoprotease activity over time. We go on to demonstrate that exoprotease-producing cells arise from more than one cell type, namely matrix-producing and non-matrix-producing cells. *In toto* these findings allow us to add exoprotease-producing cells to the list of specialized cell types that are derived during *B. subtilis* biofilm formation and furthermore the data highlight the plasticity in the origin of differentiated cells.

Received 12 August 2013
Accepted 22 October 2013

INTRODUCTION

The formation of sessile communities of microbial cells called biofilms is a process common to many bacterial strains (Costerton *et al.*, 1995). The resultant biofilm communities can have both beneficial and detrimental impacts on human society and are linked with processes as diverse as bioremediation and chronic infections (Costerton *et al.*, 1987). Biofilm formation is underpinned by the production of an extracellular matrix that is commonly composed of DNA, proteins and exopolysaccharides (Flemming & Wingender, 2010). The extracellular matrix generates and stabilizes the 3D structure and provides protection to the resident bacteria (Branda *et al.*, 2005).

Bacillus subtilis is a Gram-positive soil-dwelling bacterium used as a model for biofilm formation (Vlamakis *et al.*, 2013). The biofilm matrix is composed of TasA amyloid-like fibres (Branda *et al.*, 2006; Romero *et al.*, 2010), a secreted exopolysaccharide (Branda *et al.*, 2001; Chai *et al.*, 2012) and a bacterial hydrophobin called BslA that forms a hydrophobic coat over the biofilm (Hobley *et al.*, 2013; Kobayashi & Iwano, 2012; Ostrowski *et al.*, 2011). Synthesis of the components within the biofilm extracellular matrix is tightly regulated at the level of transcription (Vlamakis *et al.*, 2013). In *B. subtilis*, one key regulator that is required for biofilm formation, due to its role in controlling the biosynthesis of the BslA coat protein, is DegU (Kobayashi, 2007; Ostrowski *et al.*, 2011). DegU is the response regulator of the DegS–DegU two-component regulatory system (Dahl *et al.*, 1991). Phosphorylated DegU (hereafter DegU-P)-regulated processes are upregulated in response to several environmental signals (for a review see Murray *et al.*, 2009a) but of particular relevance to biofilm formation the system is activated when rotation of the flagella is impeded (Cairns *et al.*, 2013).

B. subtilis biofilm formation is hallmarked by the differentiation of genetically identical cells within the population into specialist subtypes (Branda *et al.*, 2001; Vlamakis *et al.*, 2008). To date, cells specialized towards motility, biofilm matrix production and sporulation have been identified (Vlamakis *et al.*, 2008). However, the occurrence and origin of cells that produce extracellular proteases (hereafter exoproteases) within the biofilm have not been examined. The production of exoproteases by *B. subtilis*

Abbreviations: DegU-P, phosphorylated DegU; DIC, differential interference contrast.

occurs heterogeneously in planktonic culture (Veening *et al.*, 2008) and transcription is dependent on DegU-P (Dahl *et al.*, 1992; Tsukahara & Ogura, 2008). Moreover, exoprotease activity has been shown to be required for pellicle formation in laboratory isolates of *B. subtilis* (Connelly *et al.*, 2004). Therefore, given this knowledge, and the known role for DegU-P in controlling biofilm formation (Kobayashi, 2007; Stanley & Lazazzera, 2005; Verhamme *et al.*, 2007), here we define the impact of changing DegU-P levels on the proportion of cells in the biofilm population that transcribe the genes required for exoprotease synthesis. We identify that as biofilm formation progresses, exoprotease production increases at the level of both transcription and activity. Using live cell microscopy analysis of microcolony formation, we assess the origin of the exoprotease-producing cells and identify that they arise from both matrix-producing cells and non-matrix-producing cells. These findings shed light on the diversity of specialized cell types contained within the biofilm and highlight plasticity in their origin.

METHODS

Growth conditions. The *Escherichia coli* and *B. subtilis* strains used and constructed in this study are detailed in Table 1. Both *E. coli* and *B. subtilis* strains were routinely grown in Luria–Bertani (LB) medium (per litre: 10 g NaCl, 5 g yeast extract and 10 g tryptone). Biofilm pellicles were grown in 10 ml MSgg medium (5 mM potassium phosphate and 100 mM MOPS at pH 7.0 supplemented with 2 mM $MgCl_2$, 700 μM $CaCl_2$, 50 μM $MnCl_2$, 50 μM $FeCl_3$, 1 μM $ZnCl_2$, 2 μM thiamine, 0.5 % glycerol and 0.5 % glutamate) (Branda *et al.*, 2001) at 23 or 25 °C as defined, for up to 96 h. Complex colony biofilms were grown on MSgg solidified with 1.5 % Select Agar (Invitrogen) at 30 or 37 °C for the times indicated. Ectopic gene expression was induced with IPTG at the concentrations detailed. When appropriate, antibiotics were used at the following concentrations: ampicillin 100 μg ml^{-1}, chloramphenicol 5 μg ml^{-1}, kanamycin 25 μg ml^{-1}, lincomycin 25 μg ml^{-1} with erythromycin 5 μg ml^{-1} and spectinomycin 100 μg ml^{-1}.

Strain construction. *E. coli* strain MC1061 [F′*lacI*q *lacZ*M15 Tn*10* (*tet*)] was used for the construction and maintenance of plasmids. *B. subtilis* 168 derivatives were generated by transformation of competent cells with plasmids using standard protocols (Harwood & Cutting, 1990). SPP1 phage transductions, for introduction of DNA into *B. subtilis* strain NCIB3610 (hereafter 3610), were conducted as described previously (Verhamme *et al.*, 2007).

Plasmid construction

pNW700. *mCherry* (711 bp) was amplified from pRSET-mCherry (kindly provided by Roger Y. Tsien, University of California, San Diego) using primers NSW1000 (5′-GGCCAAGCTTAAGGAGGTGATCATTAAAAATGGTGAGCAAGGGCGAGGAG-3′) and NSW1001 (5′-CGTAGGATCCTTACTTGTACAGCTCGTCCAT-3′). The resulting PCR product was digested with *Bam*HI and *Hin*dIII and inserted into pNW600 (Murray *et al.*, 2009b), digested the same way to replace the *gfp* coding region with the *mCherry* coding region yielding a P*tapA–mCherry* fusion in a vector that allows for integration at the non-essential *amyE* locus.

pNW702. pNW700 was digested with *Eco*RI and *Bam*HI to release the P*tapA–mCherry* coding region, which was ligated into the *lacA* integration vector pDR183 which was digested the same way. This would enable integration at the non-essential *lacA* locus.

pNW725. *mKate2* (746 bp) was amplified by PCR using the pTMN387 (kind gift of Professor Richard Losick, Harvard University) as the template and primers mKate-for (NRS1026) (5′-GTACAAGCTTAAGGAGGAACTACTATGGATTCAATAGAAAAGGTAAG-3′) and mKate-rev (NRS1027) (5-GTACGGATCCTTATCTGTGCCCCAGTTTGCT-3) (Chen *et al.*, 2013). The PCR product was digested with *Hin*dIII and *Bam*HI and ligated into plasmid pNW600 (Murray *et al.*, 2009b), which was cut the same way to yield the P*tapA–mKate2* reporter fusion in a vector that allows for integration at the non-essential *amyE* locus.

pNW726. The P*tapA–mKate2* coding region was released from pNW725 by *Eco*RI and *Bam*HI digestion. The fragment was ligated into the *lacA* integration vector pDR183, which was digested the same way. This would enable integration at the non-essential *lacA* locus.

Biofilm formation assays. Analysis of biofilm formation was performed as previously described (Branda *et al.*, 2001; Verhamme *et al.*, 2007).

Secreted protease activity assay. Each 10 ml pellicle sample was collected by centrifugation (17 000 ***g*** for 10 min), after which the supernatant was removed and stored at −20 °C until use. The remaining cell pellet was used to determine the wet pellet weight. From 48 h onwards the cell pellet was resuspended in 10 ml double-distilled water (ddH_2O) and subjected to gentle sonication (such that the cells did not lyse (Ostrowski *et al.*, 2011)), and the cell pellet was collected by centrifugation for 20 min, at 9000 ***g*** at 4 °C, prior to wet pellet weight analysis. To determine extracellular protease activity, the azocasein assay (Braun & Schmitz, 1980) was performed. A 150 μl aliquot of thawed supernatant was mixed with 500 μl of 2 % (w/v) azocasein (Sigma), along with 100 μl Tris-HCl (pH 8.0) and 650 μl ddH_2O. A blank sample was prepared containing ddH_2O in place of the supernatant and a medium-only control sample containing LB in place of the supernatant was also prepared. The samples were incubated for 1 h at 30 °C, after which 375 μl of 14 % (v/v) perchloric acid was added to stop each reaction. The samples were centrifuged (17 000 ***g*** for 5 min) and 750 μl of the supernatant was mixed directly in a cuvette with 75 μl of 10 M NaOH and the absorbance at 436 nm was measured using a spectrophotometer. The background activity of the medium-only control was subtracted and activity was calculated as ΔA_{436}/h/ml/mg protein (Cairns *et al.*, 2013).

Flow cytometry. The fluorescence of strains harbouring *gfp* promoter fusions was measured in single cells extracted from biofilm-forming conditions after incubation at either 30 or 37 °C as described previously (Murray *et al.*, 2009b; Vlamakis *et al.*, 2008).

Time-lapse microscopy. Single colonies of *B. subtilis* were inoculated into 5 ml of MSgg medium and grown overnight at 30 °C and 220 r.p.m. The next morning cells were diluted 25-fold into 3 ml of 15 % MSgg medium. After approximately 4 h of incubation at 30 °C and 220 r.p.m., or when the cells had reached mid-exponential phase of growth, the sample was diluted to an OD_{600} of 0.007 in fresh 15 % MSgg medium. This enabled the visualization of single cells with the appropriate spacing for the start of the time-lapse acquisition. Then, 2 μl of this cell suspension was inoculated onto a thin matrix of 15 % MSgg supplemented with 1.5 % agarose (Invitrogen ultrapure agarose) on a microscope slide. Each slide was prepared as follows. A 125 μl Gene Frame (AB-0578; ABgene House) was attached to a standard microscope slide (VWR superpremium). The Gene Frame was next filled with molten 15 % MSgg supplemented with 1.5 % agarose (hereafter 15 % MSgg-agarose) with the addition of IPTG at the defined concentrations and covered firmly with a standard microscope slide to flatten the agarose surface.

Table 1. Strains and plasmids used in this study

Strain	Relevant genotype/description*	Reference, source or construction†
168	*trpC2*	BGSC
DS1993	NCIB3610 *degU*::Tn*10* (MLS)	D. Kearns
NCIB3610	Wild-type (prototroph)	BGSC
NRS1314	NCIB3610 *degU*::pBL204 (*cml*)	Verhamme *et al.* (2007)
NRS1325	NCIB3610 *amyE*::P*hy-spank-degU hy 32* (*spc*) *degU*::pBL204 *(cml)*	Verhamme *et al.* (2007)
NRS2313	168 P*bpr–gfp* (*cml*)	Veening *et al.* (2008)
NRS2315	NCIB3610 P*bpr–gfp* (*cml*)	NRS2313→NCIB3610
NRS2769	NCIB3610 *degU*::Tn*10* (MLS) P*bpr–gfp* (*cml*)	DS1993→NRS2313
NRS2771	NCIB3610 *amyE*::P*hy-spank-degU hy 32* (*spc*) *degU*::Tn*10* (MLS) (*cml*) P*bpr–gfp* (*cml*)	NRS1311→NRS2769
NRS3372	168 *lacA*::P*tapA–mCherry* (*erm*)	pNW702→168
NRS3373	NCIB3610 *lacA*::P*tapA–mCherry* (*erm*)	NRS3372→NCIB3610
NRS3378	NCIB3610 P*bpr–gfp* (*cml*) *lacA*::P*tapA–mCherry* (*erm*)	NRS2313→NRS3373
NRS3921	NCIB3610 P*bpr–gfp* (*cml*) *lacA*::P*tapA–mKate2* (*erm*)	NRS3925→NRS2315
NRS3922	NCIB3610 *lacA*::P*tapA–mKate2* (*erm*)	NRS3925→NCIB3610
NRS3925	168 *lacA*::P*tapA–mKate2* (*erm*)	pNW726→NCIB3610

*Drug resistance cassettes are indicated as follows: *cml*, chloramphenicol resistance; *kan*, kanamycin resistance; *tet*, tetracycline resistance; MLS, lincomycin and erythromycin resistance; *spc*, spectinomycin resistance.
†The direction of strain construction is indicated with DNA or phage (SPP1) (→) recipient strain. BGSC, *Bacillus* Genetic Stock Center.

When the 15 % MSgg-agarose had sufficiently cooled and solidified the upper slide was carefully removed and the 15 % MSgg-agarose was carefully removed with a surgical scalpel blade (Swann Morton number 11) leaving behind either one or two strips of MSgg-agarose (~1.5 mm wide) in the centre of the Gene Frame. For experiments where two or more strips were required the strips were spaced at least 4 mm apart. de Jong *et al.* (2011) established that these conditions provide air cavities that are essential for efficient growth of *B. subtilis*. After inoculation the cell suspension was allowed to dry after which the Gene Frame was sealed with a coverslip (22 × 22 mm; VWR) 1.5 mm thick. The microscope slides were incubated at 30 °C in a temperature-controlled environmental chamber (Weather Station; Applied Precision). Prior to the start of acquisition the cells were allowed to equilibrate on the agarose pads for 3 h. Time-lapse imaging of microcolony development and P*tapA–mKate* and P*bpr–gfp* expression was performed using a DeltaVision Core wide field microscope (Applied Precision) mounted on an Olympus IX71 inverted stand with an Olympus ×60, 1.4 NA lens and CoolSNAPHQ camera (Photometrics) with differential interference contrast (DIC) and fluorescence optics. For each experiment 12 independent fields were manually identified and their *XYZ*-positions were stored in the microscope control software (SoftWorx; Applied Precision). Images (512 × 512 pixels with 2 × 2 binning and 12 *Z* sections spaced at 1 µm) were acquired every 15 min for up to 12 h. GFP was imaged using a 100 W mercury lamp and an FITC filter set (excitation 490/20; emission 528/38) with an exposure time of 200 ms. mKate2 was imaged using a 100 W mercury lamp and a TRITC filter set (excitation 555/28; emission 617/73) with an exposure time of 300 ms. DIC images were acquired with an LED transmitted light source (Applied Precision) at 32 % intensity and exposure times between 25 and 50 ms. Post-acquisition images were rendered and analysed using OMERO software (http://openmicroscopy.org) (Allan *et al.*, 2012). The threshold used to define activation of the transcriptional reporter was set as a fluorescence intensity value greater than two standard deviations above the mean background fluorescence.

Microscopy of cells harvested from complex colonies

DIC microscopy and fluorescence microscopy. Colony biofilms were grown as before (Branda *et al.*, 2001; Verhamme *et al.*, 2007) and harvested as previously described for flow cytometry (Murray *et al.*, 2009b; Vlamakis *et al.*, 2008) with the exception that the cells were not fixed. After washing in 1× PBS the cells were diluted 10-fold into GTE buffer (50 mM glucose, 10 mM EDTA at pH 8, 20 mM Tris/HCl at pH 8), 2 µl of the cell suspension was spotted onto a 1.5 % agarose pad and images were acquired using a DeltaVision Core wide field microscope (Applied Precision) mounted on an Olympus IX71 inverted stand with an Olympus ×100, 1.4 NA lens and Cascade2 512 EMCCD camera (Photometrics). Images (512 × 512 pixels with 13 *Z* sections spaced at 0.2 µm) were acquired with DIC and fluorescence optics. GFP and mCherry were detected using a 100 W mercury lamp and an FITC filter set (excitation 490/20; emission 528/38) and a TRITC filter set (excitation 555/28; emission 617/73), respectively. DIC images were acquired with an LED transmitted light source (Applied Precision) at 32 % intensity and exposure times between 25 and 50 ms. Post-acquisition images were rendered and analysed using OMERO software (http://openmicroscopy.org) (Allan *et al.*, 2012). All figures were assembled in Canvas 12 (ACD Systems).

Phase-contrast and fluorescence microscopy. Colony biofilms were grown and harvested as for DIC and fluorescence microscopy and prepared for imaging as described above. Microscopy was performed using a ×100 Plan-NEOFLUAR 1.30 oil immersion lens on an Axio Imager M1 microscope mounted with an Axiocam MRm camera (Zeiss). GFP fluorescence was visualized using an FITC filter set (excitation 490/40; emission 525/50) and images were rendered and analysed using the AxioVision Rel. 4.8 (Zeiss) software. All figures were assembled in Canvas 12 (ACD Systems).

Biofilm sectioning and confocal microscopy. Complex colonies formed by strain NRS3921 were grown on MSgg solidified with 1.5 % agar as described above. A quarter section of the colony (after 48 h growth) was excised with a no. 10 surgical scalpel and placed into

O.C.T. compound (Agar Scientific) and frozen in iso-pentene chilled with liquid nitrogen. Cross-sections (9 μm) of the colony were cut using a Leica CM3050S cryomicrotome. The sections were transferred onto SuperFrost Ultra Plus adhesion microscope slides (VWR). Each section was fixed with 150 μl of 4 % para-formaldehyde in PBS for 10 min. The sections were then washed three times with Tris-buffered saline. A drop of mounting medium was applied onto the slide containing the colony sections (modified from Hobley *et al.*, 2013), onto which a 1.5 mm thick coverslip was placed. After removal of excess mounting medium the cover glass was sealed with nail varnish. The slides were stored at −20 °C prior to analysis. Samples were imaged using a Zeiss LSM710 confocal scanning laser microscope fitted with 488 and 594 nm lasers and a planApo ×25/0.8 NA oil objective. During each experiment the laser settings, scanning speed, photomultiplier gains and pinhole settings were kept constant for all acquired images. Images were captured using Zen2011 software and image analysis was conducted using the OMERO platform (www.openmicroscopy.org) (Allan *et al.*, 2012). All figures were assembled in Canvas 12 (ACD Systems).

RESULTS AND DISCUSSION

An increase in transcription of the exoprotease-encoding *bpr* gene is observed at the single-cell level in the presence of high DegU-P

The two major exoproteases synthesized by *B. subtilis* are subtilisin and bacillopeptidase, which are encoded by the *aprE* and *bpr* genes, respectively (Msadek, 1999). We followed exoprotease production using a P*bpr–gfp* reporter construct that was integrated at the native location on the chromosome (Veening *et al.*, 2008). The P*bpr–gfp* construct was introduced into NCIB3610 wild-type and *degU* mutant strains (Table 1) and transcription was monitored using flow cytometry and single-cell microscopy based on detection of GFP. Transcription from the *bpr* reporter fusion in the wild-type biofilm colony was assessed after 17 h of incubation. All the cells exhibited a low and homogeneous level of expression (Fig. 1a). Analysis confirmed that expression from the *bpr* promoter was DegU-dependent as the level of fluorescence decreased to the background basal level in the presence of a mutation in *degU* (Fig. 1b). These findings demonstrate that the transcriptional reporter behaved as expected during biofilm formation and in the NCIB3610 isolate of *B. subtilis* used here.

We next investigated the impact of increasing levels of DegU-P on transcription from the *bpr* promoter element to establish if this would promote heterogeneity in *bpr* transcription. To control the level of DegU-P in the cell, the *degU32 hy* mutant allele of the *degU* coding region was introduced into the chromosome under control of the IPTG-inducible promoter (P*hy-spank* using pDR111) at the heterologous *amyE* locus (Verhamme *et al.*, 2007). This variant of DegU carries a histidine to leucine mutation in amino acid 12 and exhibits a lower level of dephosphorylation than wild-type DegU (Dahl *et al.*, 1991). The strain additionally contained a deletion of the native copy of *degU* and carried a P*bpr–gfp* reporter fusion at the native *bpr* locus on the chromosome (Table 1). Note that as transcription of *degU32 hy* is increased, biofilm formation itself is inhibited (Verhamme *et al.*, 2007). Both flow cytometry and fluorescence microscopy analysis demonstrated that consistent with DegU-P activating transcription from the *bpr* promoter region the number of GFP-positive cells increased with the addition of up to 25 μM IPTG to the growth medium (Fig. 2). The number of GFP-positive cells increased from 7 % in the absence of IPTG (Fig. 2a, f, k) to 84 % in the presence of 7.5 μM IPTG (Fig. 2e, j, o). The GFP-positive cells could be divided into low expression (10^1–10^2 AU) and high expression (10^2–10^4 AU) cells with the number of cells within the high expression category increasing alongside the level of DegU-P. Thus, it is evident that transcription from the *bpr* promoter can be highly heterogeneous in the biofilm population and that this is correlated with increases in the level of DegU-P.

The level of exoprotease production increases during biofilm formation

We next assessed if changes in the frequency of exoprotease transcription occurred over time during biofilm formation. Increases in exoprotease production would indicate an increase in the level of DegU-P during biofilm formation. To test this, transcription from the P*bpr–gfp* reporter construct in the wild-type strain was assessed at the single-cell level from samples isolated from complex colony and pellicle biofilms over a time-course of development, namely 17, 24, 48 and 72 h for colony biofilms (Fig. 3) and 24, 36, 48, 60, 72 and 96 h for pellicle biofilms (Fig. 4). Representative pellicle biofilm images at the point of collection are presented as inserts within Fig. 4. Flow cytometry and single-cell microscopy analysis of the disrupted biofilms revealed that transcription from the *bpr* promoter region increased during biofilm development for both biofilm types (Figs 3 and 4); moreover, transcription became highly heterogeneous as the biofilm matured [compare Fig. 3a(i) with 3a(iv) and Fig. 4c with 4d, e and f]. As reported above (Fig. 2), the GFP-positive cells in the biofilm could be subdivided into low (10^1–10^2 AU) and high (10^2–10^3 AU) expressing cells with the number of individual cells within the high expression category increasing over time. In fact, the peak in exoprotease transcription occurred at 72 h for the colony biofilm and 96 h for the pellicle biofilm. These findings demonstrate that transcription from the *bpr* promoter increases over time during biofilm formation.

To correlate *bpr* transcription with exoprotease production, the level of active extracellular proteases in the pellicle biofilm supernatant was quantified biochemically (Fig. 5). Consistent with the increase in *bpr* transcription that was observed in more mature biofilms, the level of extracellular proteases in the pellicle supernatant fraction increased during biofilm formation as measured using caesin digestion assays (see Methods; compare Fig. 3 with Fig.

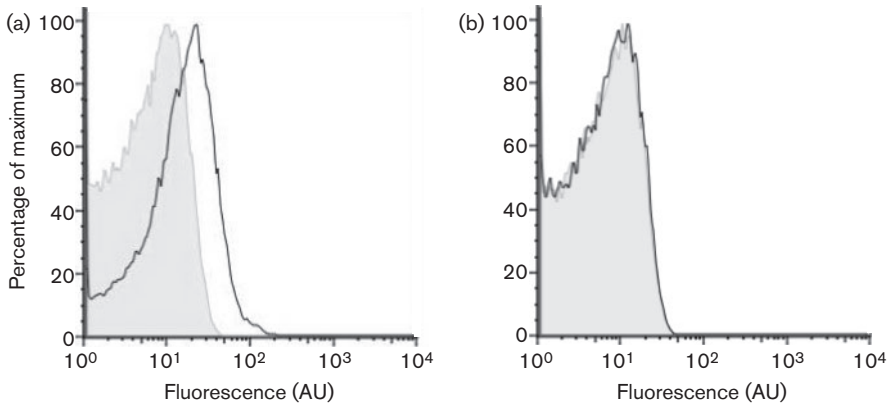

Fig. 1. Transcription of the exoprotease-encoding *bpr* gene observed at the single cell level is dependent on DegU-P. Flow cytometry analysis of 3610 P*bpr–gfp* (NRS2315) (black line) (a) and 3610 P*bpr–gfp degU* (NRS2769) (black line) (b) using the parental 3610 strain as a negative control (grey-shaded area). Cells were grown under biofilm formation conditions for 17 h at 37 °C. A representative example is shown from three independent experiments.

5). At 96 h, exoprotease activity in the extracellular environment was four fold higher than that quantified for the 24 h biofilm (Fig. 5). These biochemical analyses link increases in transcription from the P*bpr–gfp* reporter with increased exoprotease activity levels in the biofilm community.

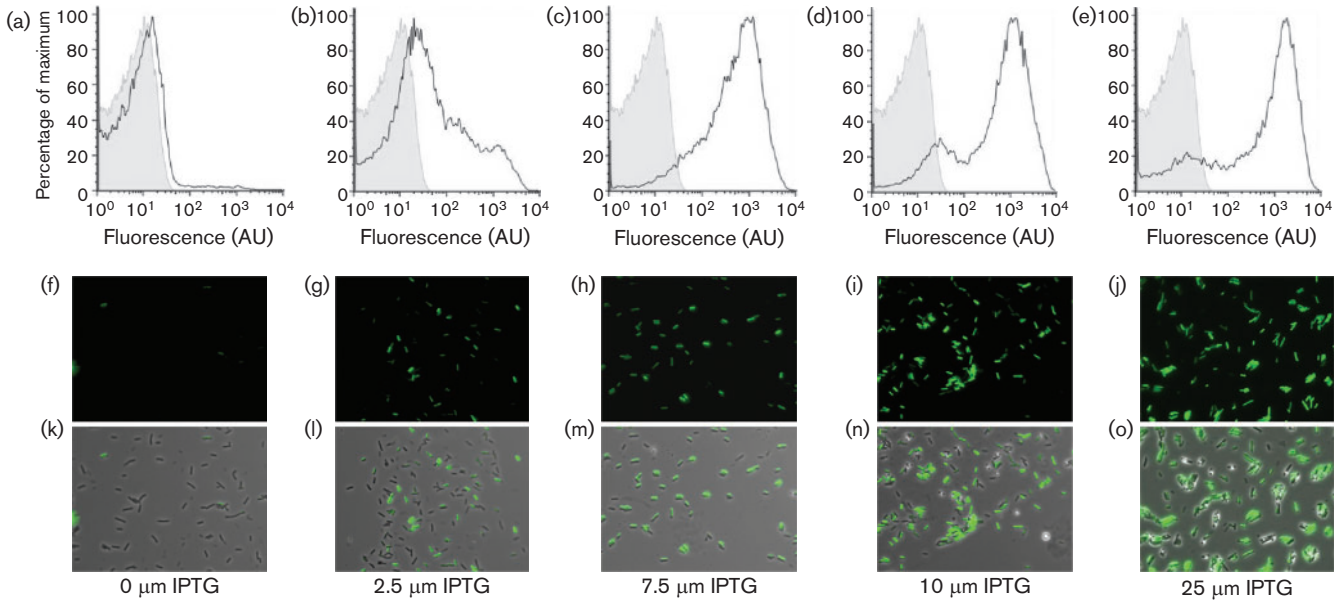

Fig. 2. An increase in transcription of the exoprotease-encoding *bpr* gene is observed at the single-cell level in the presence of high DegU-P. (a–e) Flow cytometry analysis. The grey-shaded area represents the parental 3610 strain as a negative control and the black lines the experimental sample. (f–o) Microscopy of P*bpr–gfp degU*, *amyE*::P*hy-spank-degU32 hy* cells (NRS2771). (f–j) Fluorescence was imaged in the FITC channel to detect GFP production. (k–o) The same cells analysed by phase-contrast fluorescence microscopy showing the overlay with the GFP expression with the cells. The cells were grown under biofilm formation conditions for 17 h at 37 °C in the presence of 0 μM IPTG (a, f, k), 2.5 μM IPTG (b, g, l), 7.5 μM IPTG (c, h, m), 10 μM IPTG (d, i, n) and 25 μM IPTG (e, j, o) prior to collection. In each case, one representative example is presented from three independent experiments.

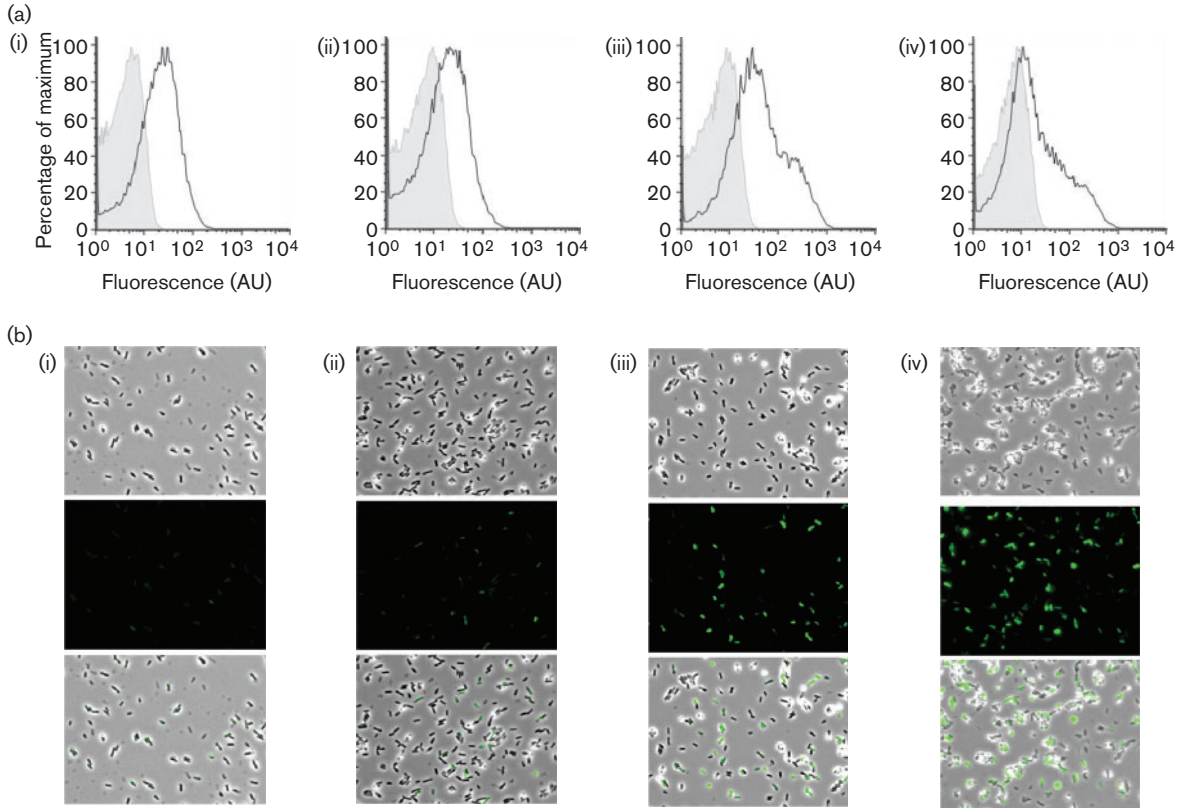

Fig. 3. Transcription of *bpr* increases over time during biofilm formation. (a) Transcription of *bpr* from cells extracted from complex colonies was monitored over a 72 h period using a *bpr–gfp* transcriptional fusion strain (NRS2315). Colonies were grown at 30 °C and collected for flow cytometry analysis (grey-shaded area, non-fluorescent control 3610 strain; black line, *bpr–gfp*) after 17 h (i), 24 h (ii), 48 h (iii) and 72 h (iv). (b) The same cells were then analysed by phase-contrast fluorescence microscopy after 17 h (i), 24 h (ii), 48 h (iii) and 72 h (iv). Shown are the phase-contrast (top) and FITC (GFP) channel (middle) and an overlay of both channels (bottom). A representative example is presented from three independent experiments.

Exoprotease-producing cells are located at the surface of the mature biofilm

Flow cytometry and single-cell microscopy analysis of disrupted biofilms allow quantification of the population that express the P*bpr–gfp* reporter (Figs 1–4). However, these techniques do not allow analysis of the spatial localization of transcription in the biofilm (Vlamakis *et al.*, 2008). To determine the spatial localization of the exoprotease-producing cells in the biofilm, 48 h colony biofilms formed by strain NRS3921 were cryosectioned as described previously [see Methods and Vlamakis *et al.* (2008)]. Following fixation, the thin layer cross-sections of the biofilm were imaged by confocal microscopy and expression from the P*bpr–gfp* reporter was detected. These microscopy analyses confirmed the flow cytometry analysis presented in Figs 3 and 4, which demonstrated that a subpopulation of the cells was highly fluorescent (indicative of high levels of P*bpr–gfp* transcription). Retention of the biofilm structure allowed us to determine that this group of cells was found towards the top of the colony biofilm near the air–biofilm interface (Fig. 6). The subpopulation of cells with low levels of GFP was found towards the centre of the biofilm section. It was highly apparent that transcription of the reporter fusion was heterogeneous within the biofilm and that there was structure in the transcription profile with respect to the organization of the mature biofilm.

The protease-producing cell population overlaps with the matrix-producing cell population

The analysis reported above allows us to add exoprotease-producing cells to the list of specialized cell types that are found in the developing *B. subtilis* biofilm (Branda *et al.*, 2001; Vlamakis *et al.*, 2008). Previously characterized cell types include cells that are motile, cells that transcribe the *eps* and *tapA* operons needed for biofilm matrix assembly (hereafter matrix-producing cells), and cells that are sporulating (Vlamakis *et al.*, 2008). It has previously been established that motile cells transition into matrix cells and that the matrix-producing cells progress to form endospores

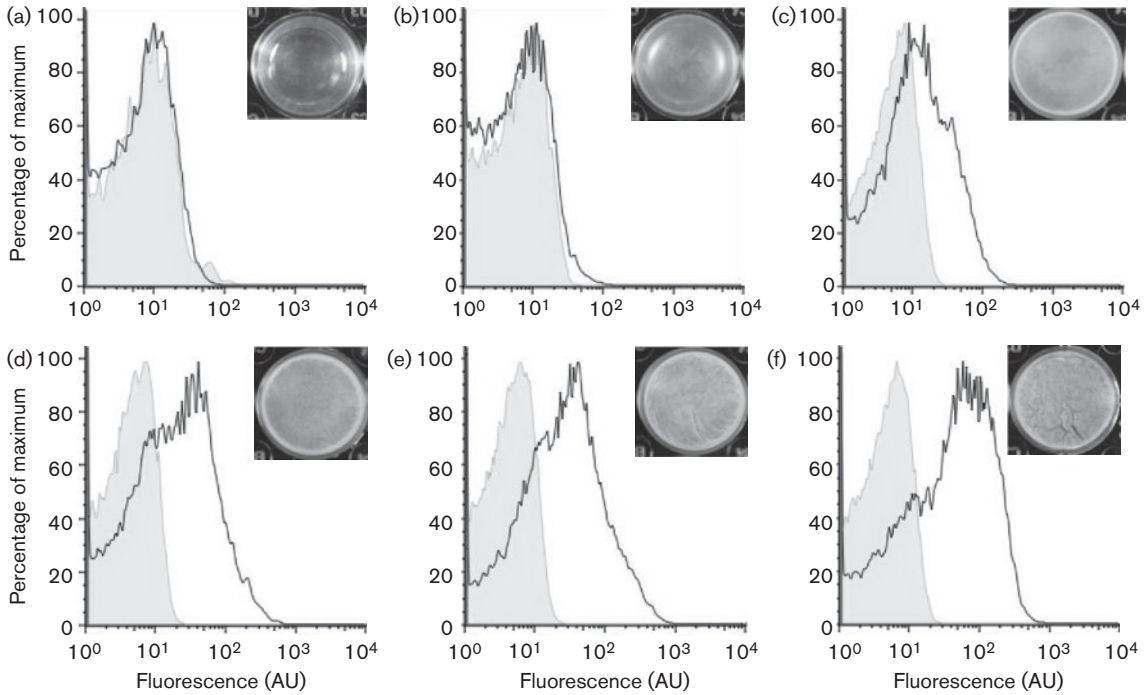

Fig. 4. An increase in transcription of the exoprotease-encoding *bpr* gene occurs during pellicle formation. Transcription of *bpr* from cells extracted from pellicle biofilms was monitored over a 96 h period using a *bpr–gfp* transcriptional fusion strain (NRS2315). Transcription of *bpr* from cells extracted from pellicles grown at 23 °C was monitored over a 96 h period using a *bpr–gfp* transcriptional fusion. Flow cytometry data are shown from cells extracted from pellicles at 24 h (a), 36 h (b), 48 h (c), 60 h (d), 72 h (e) and 96 h (f). The non-fluorescent NCIB3610 control line is shown as the grey-shaded area and the experimental sample as a black line. A representative example of both the expression analysis and pellicle formation is presented from three independent experiments.

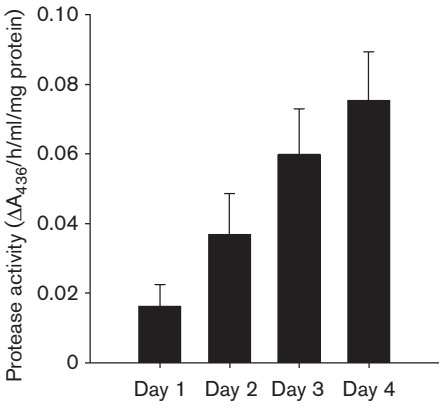

Fig. 5. Protease secretion was analysed from supernatant collected from pellicles during biofilm formation. Protease secretion was assessed using an azocasein assay from pellicle supernatants. Pellicles were grown at 25 °C for up to 96 h and samples were collected at 24 h (day 1), 48 h (day 2), 72 h (day 3) and 96 h (day 4). Enzyme activity was normalized against wet pellet weight of the pellicle. Data are presented as the mean of four independent experiments and the error bars represent SEM.

at late biofilm stages (Vlamakis *et al.*, 2008). In addition, it has been proposed that matrix production and protease production are mutually exclusive events and that both cell types arise directly from motile cells in response to different environmental signals (Lopez *et al.*, 2009). This has not been tested experimentally and is somewhat at odds with the knowledge that matrix production decreases during biofilm formation (Vlamakis *et al.*, 2008) while exoprotease production increases (Figs 3 and 4) at a time during biofilm formation when motile cells are absent from the biofilm (Vlamakis *et al.*, 2008). Therefore, to define the origin of the exoprotease-producing cells and investigate the relationship between exoprotease production and matrix production, we constructed a dual reporter strain which carried the P*bpr–gfp* fusion at the native locus and a P*tapA–mCherry* transcriptional fusion at the heterologous *lacA* locus (NRS3378). We examined the prevalence of cells that co-expressed both fusions as indicated by fluorescence in both the FITC (P*bpr–gfp*) and TRITC (P*tapA–mCherry*) channels in cells extracted from 24 h pellicle biofilms. As indicated in Fig. 7(a) (asterisks), co-expression from the *tapA* and *bpr* promoter regions was clearly observed within the cells that are false coloured yellow. We next examined expression from each promoter by fluorescence

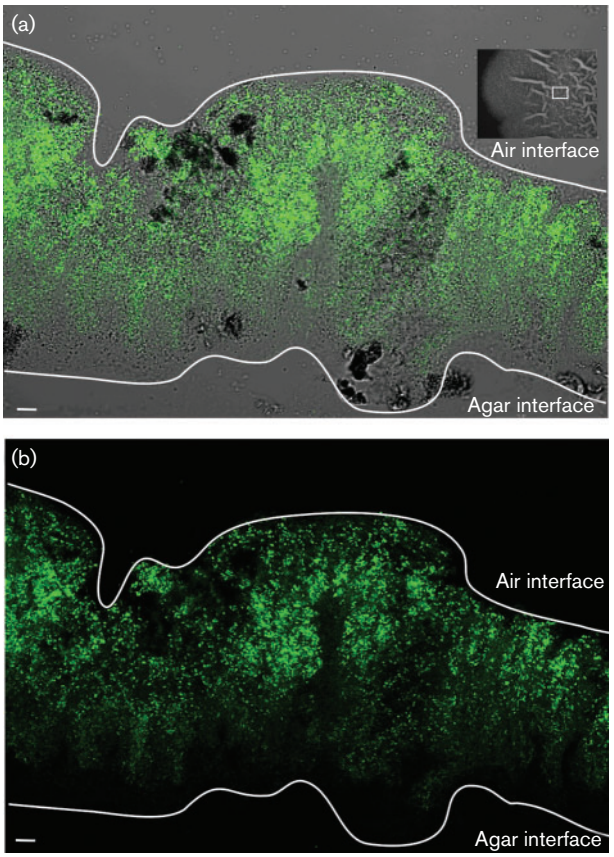

Fig. 6. Spatial analysis of *bpr* transcription within the mature biofilm. (a) Bright-field and FITC merged image and (b) FITC image of a 9 μm vertical cross-section of a 48 h colony biofilm harbouring the P*bpr–gfp* reporter fusion (NRS3921) detected by confocal microscopy. The top (air interface) and bottom (agar interface) of the colony biofilm are indicated for reference purposes and shown as white lines. In (a), a 48 h colony biofilm is shown and the white box represents the approximate region of the biofilm that was imaged in cross-section. Bars, 10 μm. The images shown are representative of at least three independent experiments during which multiple fields of view were examined.

microscopy over a time-course of biofilm formation using cell samples that were extracted from complex colonies (Fig. 7b). The parental strain NCIB3610 was used as a control for microscopy (data not shown). Our analysis demonstrated, as expected, that the proportion of matrix-producing cells was high at early time points of biofilm formation and was lower in the later stages of biofilm development (Fig. 7b, compare 14 h with 72 h) (Vlamakis *et al.*, 2008). Moreover, as described above, the proportion of cells in the biofilm that had transcribed the P*bpr–gfp* reporter fusion increased over time (Fig. 7b). Thus, each transcriptional fusion behaved as expected in the dual reporter fusion strain NRS3378 and the findings suggest that matrix production and exoprotease production are not necessarily mutually exclusive cell states. However, note that the co-expressing cells could represent a transition between one cell state and another or possibly apparent co-expression that is a reflection of the stability of the fluorescent reporter fusions.

Matrix-producing cells can transition into exoprotease-producing cells

To trace the origin of exoprotease-producing cells and to investigate the relationship between exoprotease production and matrix production in greater detail, we performed real-time fluorescence single-cell microscopy analysis in developing microcolonies (de Jong *et al.*, 2011; Young *et al.*, 2012). Our initial analysis highlighted that the mCherry fluorescent protein was not a suitable reporter protein for the live cell microscopy analysis. Live cell microscopy demands multiple images to be taken and the fluorescence from mCherry was found to be susceptible to rapid photobleaching (data not shown). Therefore, strain NRS3921 was constructed where the mCherry reporter was replaced with mKate2, yielding a strain that carried the P*tapA–mKate2* and P*bpr–gfp* reporter fusions (Table 1). The strain was grown in microscope chambers for up to 13 h, with images acquired every 15 min (see Methods). As expected, P*tapA–mKate2* matrix gene expression was bimodal in the developing microcolony and P*bpr–gfp* exoprotease gene expression was heterogeneous in the population (Fig. 7c). Moreover, consistent with microscopy and flow cytometry analysis from the time-course of biofilm formation (Figs 3 and 4), transcription from the P*bpr–gfp* reporter fusion was observed more frequently at later time points in microcolony development (compare 570 with 750 min time points in Fig. 7c).

The data collected from the live cell imaging were used to trace the origin of matrix-positive cells over several cell cycles. To achieve this we followed multiple cells during division, noting the phenotype as indicated by expression from the reporter fusions. We established that the majority of exoprotease-producing cells arose from cells that had persisted in a non-matrix-expressing state for more than one generation (Figs 7c and 8, cell highlighted by the green arrowheads, and data not shown). However, we established that exoprotease-producing cells were not precluded from arising directly from matrix-producing cells as the transition of a matrix-producing cell into an exoprotease producer was frequently detected (Fig. 8). This is exemplified in Fig. 8 where the white and yellow arrowheads on the micrographs highlight two cells that transition directly from matrix production to exoprotease production over time. In addition, it was observed that exoprotease-producing cells were (infrequently) capable of transitioning back to matrix-transcribing cells. This is demonstrated in Fig. 8 by the blue arrowheads. These findings demonstrate that exoprotease production and *tapA* matrix gene expression are not incompatible events and can exist for a sustained period of time within one cell.

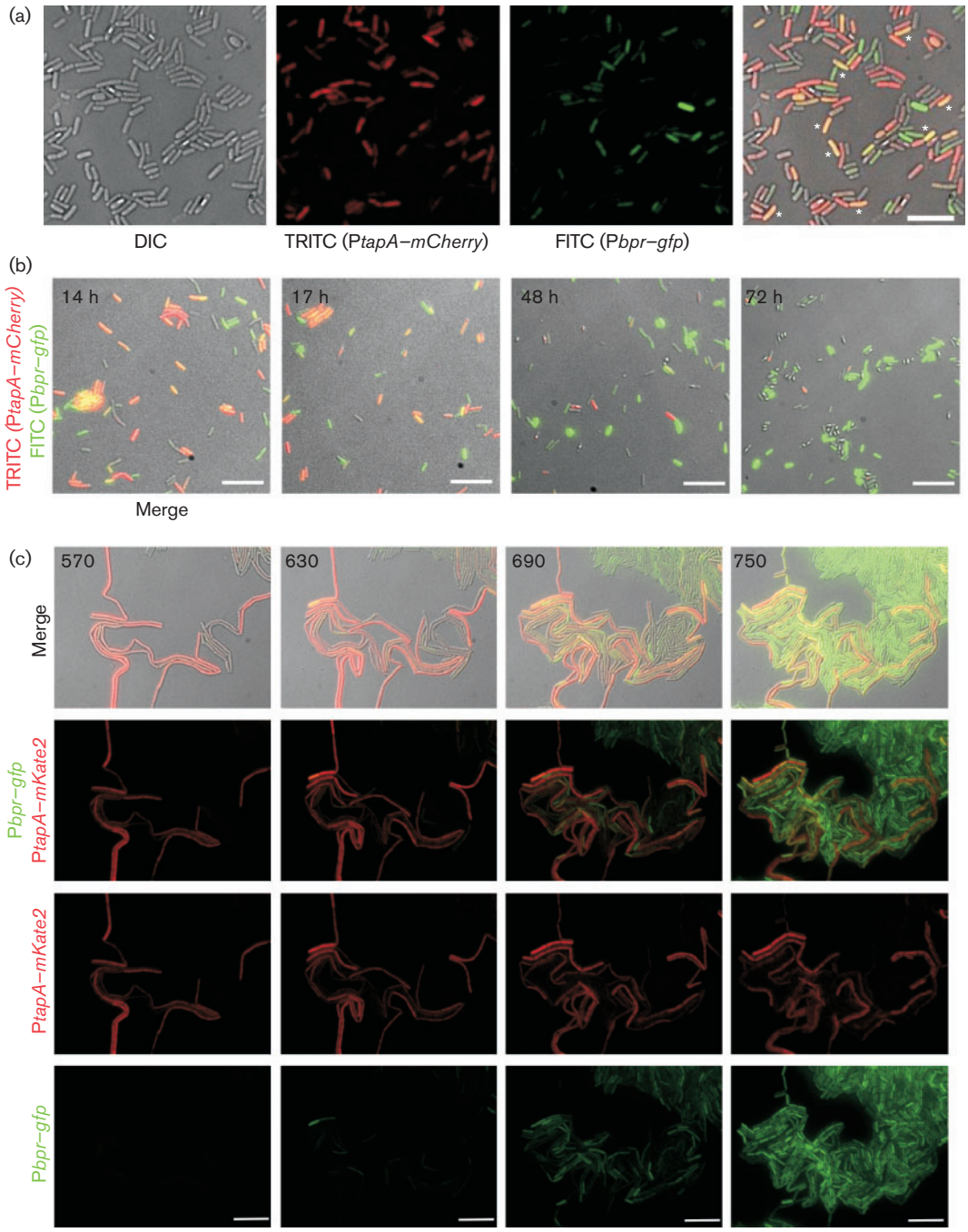

Fig. 7. Co-expression of the *bpr* and *tapA* genes. (a, b) Static microscopy of NRS3378 cells harbouring the P*tapA–mCherry* and P*bpr–gfp* transcriptional reporter fusions extracted from a pellicle biofilm after 24 h growth at 37 °C (a), where the asterisks indicate selected cells for which fluorescence was detected in both the TRITC (false coloured red) and the FITC (false coloured green) channels, for colony biofilms grown at 37 °C for the time (hours) indicated in the upper left-hand corner (b). Bars, 5 μm; the images are representative of multiple fields of view. (c) Microscopy analysis of NRS3921 harbouring P*tapA–mKate2* and P*bpr–gfp* transcriptional reporter constructs in real-time during microcolony development at 30 °C. Strain NRS3921 was imaged every 15 min. Images from the DIC, FITC (false coloured green) and TRITC (false coloured red) channels are shown above. The time (minutes) is indicated in the upper left-hand corner. Bars, 10 μm.

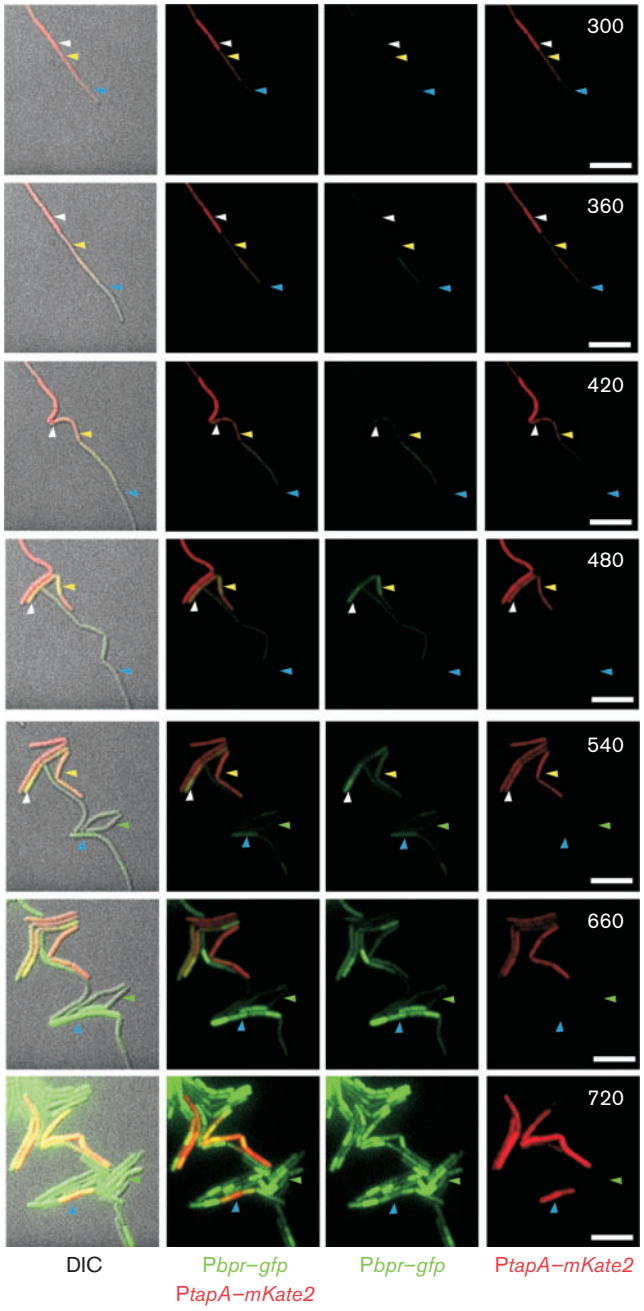

Fig. 8. Origin of exoprotease-producing cells. Microscopy analysis of NRS3921 harbouring P*tapA–mKate2* and P*bpr–gfp* transcriptional reporter constructs during microcolony development at 30 °C. Strain NRS3921 was imaged every 15 min. Images from the DIC, FITC (false coloured green) and TRITC (false coloured red) channels are shown. The white and yellow arrowheads indicate cells that have transitioned directly from matrix production to exoprotease production. The green arrowheads indicate cells that have transitioned directly from a non-fluorescent state to exoprotease production. The blue arrowheads indicate cells that have transitioned from matrix-producing cells to exoprotease production and back to matrix production. The time (minutes) is indicated in the upper right-hand corners. Bars, 5 μm.

Concluding Remarks

Here we have studied the prevalence and origin of exoprotease-producing cells in the developing *B. subtilis* biofilm. We have determined that the production of extracellular proteases is correlated with later stages of biofilm formation. This is perhaps due to a role in biofilm dispersal or nutrient acquisition and is consistent with the *in situ* localization of the exoprotease-producing cells at the biofilm–air interface. Note that this is the same region of the mature biofilm where developing spores are located and are therefore perhaps dispersed into the environment (Branda *et al.*, 2001; Vlamakis *et al.*, 2008). Through the use of live single-cell fluorescence microscopy we have defined the origin of exoprotease-producing cells and established that there is not a strict dependence on the phenotype of the parental cell. We noted the development of the exoprotease-producing state from both a matrix OFF state and matrix ON state. Indeed, a matrix- and exoprotease-producing cell state can exist for an extended period of time, demonstrating that they are not mutually exclusive cell states (Fig. 8). The biological significance of having a group of cells that can contribute to the production of the biofilm extracellular matrix and extracellular proteases remains to be elucidated. However, co-production of these molecules may indicate a need to increase nutrient acquisition from the extracellular environment when a sessile lifestyle is adopted. The single-cell analyses techniques used in this study clearly demonstrate the diversity of cell differentiation processes in the biofilm and indicate that, unlike matrix-producing cells that arise only from motile cells (Vlamakis *et al.*, 2008), the origin of exoprotease-producing cells in the population is more flexible. In addition, as matrix-producing cells can transition into exoprotease-producing cells, it will be of interest in the future to determine if exoprotease-positive cells subsequently transition into spore formers. If correct, this would add an additional step to the cell fate lineage previously observed during biofilm development (Vlamakis *et al.*, 2008).

ACKNOWLEDGEMENTS

V. L. M. was funded by a BBSRC-funded research grant (BB/C520404/1). F. R. C. and L. S. C. were supported by Wellcome Trust grants (100149/Z/12/Z, 093714/Z/10/Z, respectively). Microscopy facilities were supported by a Wellcome Trust Strategic Award grant (083524/Z/07/Z). We are very grateful to Drs Swift and Appleton and other members of the light microscopy team for their assistance and to Dr Clarke for help with flow cytometry.

REFERENCES

Allan, C., Burel, J. M., Moore, J., Blackburn, C., Linkert, M., Loynton, S., Macdonald, D., Moore, W. J., Neves, C. & other authors (2012). OMERO: flexible, model-driven data management for experimental biology. *Nat Methods* **9**, 245–253.

Branda, S. S., González-Pastor, J. E., Ben-Yehuda, S., Losick, R. & Kolter, R. (2001). Fruiting body formation by *Bacillus subtilis*. *Proc Natl Acad Sci U S A* **98**, 11621–11626.

Branda, S. S., Vik, S., Friedman, L. & Kolter, R. (2005). Biofilms: the matrix revisited. *Trends Microbiol* **13**, 20–26.

Branda, S. S., Chu, F., Kearns, D. B., Losick, R. & Kolter, R. (2006). A major protein component of the *Bacillus subtilis* biofilm matrix. *Mol Microbiol* **59**, 1229–1238.

Braun, V. & Schmitz, G. (1980). Excretion of a protease by *Serratia marcescens*. *Arch Microbiol* **124**, 55–61.

Cairns, L. S., Marlow, V. L., Bissett, E., Ostrowski, A. & Stanley-Wall, N. R. (2013). A mechanical signal transmitted by the flagellum controls signalling in *Bacillus subtilis*. *Mol Microbiol* **90**, 6–21.

Chai, Y., Beauregard, P. B., Vlamakis, H., Losick, R. & Kolter, R. (2012). Galactose metabolism plays a crucial role in biofilm formation by *Bacillus subtilis*. *MBio* **3**, e00184-12.

Chen, Y., Yan, F., Chai, Y., Liu, H., Kolter, R., Losick, R. & Guo, J. H. (2013). Biocontrol of tomato wilt disease by *Bacillus subtilis* isolates from natural environments depends on conserved genes mediating biofilm formation. *Environ Microbiol* **15**, 848–864.

Connelly, M. B., Young, G. M. & Sloma, A. (2004). Extracellular proteolytic activity plays a central role in swarming motility in *Bacillus subtilis*. *J Bacteriol* **186**, 4159–4167.

Costerton, J. W., Cheng, K. J., Geesey, G. G., Ladd, T. I., Nickel, J. C., Dasgupta, M. & Marrie, T. J. (1987). Bacterial biofilms in nature and disease. *Annu Rev Microbiol* **41**, 435–464.

Costerton, J. W., Lewandowski, Z., Caldwell, D. E., Korber, D. R. & Lappin-Scott, H. M. (1995). Microbial biofilms. *Annu Rev Microbiol* **49**, 711–745.

Dahl, M. K., Msadek, T., Kunst, F. & Rapoport, G. (1991). Mutational analysis of the *Bacillus subtilis* DegU regulator and its phosphorylation by the DegS protein kinase. *J Bacteriol* **173**, 2539–2547.

Dahl, M. K., Msadek, T., Kunst, F. & Rapoport, G. (1992). The phosphorylation state of the DegU response regulator acts as a molecular switch allowing either degradative enzyme synthesis or expression of genetic competence in *Bacillus subtilis*. *J Biol Chem* **267**, 14509–14514.

de Jong, I. G., Beilharz, K., Kuipers, O. P. & Veening, J. W. (2011). Live cell imaging of *Bacillus subtilis* and *Streptococcus pneumoniae* using automated time-lapse microscopy. *J Vis Exp* **53**, 3145.

Flemming, H. C. & Wingender, J. (2010). The biofilm matrix. *Nat Rev Microbiol* **8**, 623–633.

Harwood, C. R. & Cutting, S. M. (1990). *Molecular Biological Methods for Bacillus*. Chichester: Wiley.

Hobley, L., Ostrowski, A., Rao, F. V., Bromley, K. M., Porter, M., Prescott, A. R., MacPhee, C. E., van Aalten, D. M. & Stanley-Wall, N. R. (2013). BslA is a self-assembling bacterial hydrophobin that coats the *Bacillus subtilis* biofilm. *Proc Natl Acad Sci U S A* **110**, 13600–13605.

Kobayashi, K. (2007). Gradual activation of the response regulator DegU controls serial expression of genes for flagellum formation and biofilm formation in *Bacillus subtilis*. *Mol Microbiol* **66**, 395–409.

Kobayashi, K. & Iwano, M. (2012). BslA (YuaB) forms a hydrophobic layer on the surface of *Bacillus subtilis* biofilms. *Mol Microbiol* **85**, 51–66.

Lopez, D., Vlamakis, H. & Kolter, R. (2009). Generation of multiple cell types in *Bacillus subtilis*. *FEMS Microbiol Rev* **33**, 152–163.

Msadek, T. (1999). When the going gets tough: survival strategies and environmental signaling networks in *Bacillus subtilis*. *Trends Microbiol* **7**, 201–207.

Murray, E. J., Kiley, T. B. & Stanley-Wall, N. R. (2009a). A pivotal role for the response regulator DegU in controlling multicellular behaviour. *Microbiology* **155**, 1–8.

Murray, E. J., Strauch, M. A. & Stanley-Wall, N. R. (2009b). σ^X is involved in controlling *Bacillus subtilis* biofilm architecture through the AbrB homologue Abh. *J Bacteriol* **191**, 6822–6832.

Ostrowski, A., Mehert, A., Prescott, A., Kiley, T. B. & Stanley-Wall, N. R. (2011). YuaB functions synergistically with the exopolysaccharide and TasA amyloid fibers to allow biofilm formation by *Bacillus subtilis*. *J Bacteriol* **193**, 4821–4831.

Romero, D., Aguilar, C., Losick, R. & Kolter, R. (2010). Amyloid fibers provide structural integrity to *Bacillus subtilis* biofilms. *Proc Natl Acad Sci U S A* **107**, 2230–2234.

Stanley, N. R. & Lazazzera, B. A. (2005). Defining the genetic differences between wild and domestic strains of *Bacillus subtilis* that affect poly-γ-DL-glutamic acid production and biofilm formation. *Mol Microbiol* **57**, 1143–1158.

Tsukahara, K. & Ogura, M. (2008). Characterization of DegU-dependent expression of *bpr* in *Bacillus subtilis*. *FEMS Microbiol Lett* **280**, 8–13.

Veening, J. W., Igoshin, O. A., Eijlander, R. T., Nijland, R., Hamoen, L. W. & Kuipers, O. P. (2008). Transient heterogeneity in extracellular protease production by *Bacillus subtilis*. *Mol Syst Biol* **4**, 184.

Verhamme, D. T., Kiley, T. B. & Stanley-Wall, N. R. (2007). DegU co-ordinates multicellular behaviour exhibited by *Bacillus subtilis*. *Mol Microbiol* **65**, 554–568.

Vlamakis, H., Aguilar, C., Losick, R. & Kolter, R. (2008). Control of cell fate by the formation of an architecturally complex bacterial community. *Genes Dev* **22**, 945–953.

Vlamakis, H., Chai, Y., Beauregard, P., Losick, R. & Kolter, R. (2013). Sticking together: building a biofilm the *Bacillus subtilis* way. *Nat Rev Microbiol* **11**, 157–168.

Young, J. W., Locke, J. C., Altinok, A., Rosenfeld, N., Bacarian, T., Swain, P. S., Mjolsness, E. & Elowitz, M. B. (2012). Measuring single-cell gene expression dynamics in bacteria using fluorescence time-lapse microscopy. *Nat Protoc* **7**, 80–88.

Edited by: W. Meijer

 doi:10.1111/mmi.12342

A mechanical signal transmitted by the flagellum controls signalling in *Bacillus subtilis*

Lynne S. Cairns, Victoria L. Marlow, Emma Bissett, Adam Ostrowski and Nicola R. Stanley-Wall*
Division of Molecular Microbiology, College of Life Sciences, University of Dundee, Dundee DD1 5EH, UK.

Summary

In the natural environment bacteria predominantly live adhered to a surface as part of a biofilm. While many of the components needed for biofilm assembly are known, the mechanism by which microbes sense and respond to contact with a surface is poorly understood. *Bacillus subtilis* is a Gram-positive model for biofilm formation. The DegS–DegU two-component system controls several multicellular behaviours in *B. subtilis*, including biofilm formation. Here we identify the *B. subtilis* flagellum as a mechanosensor that activates the DegS–DegU regulatory pathway. Inhibition of flagellar rotation by deletion or mutation of the flagellar stator gene, *motB*, results in an increase in both *degU* transcription and DegU~P driven processes, namely exoprotease production and poly-γ-DL-glutamic acid biosynthesis. Similarly, inhibition of flagellar rotation by engaging the flagellar clutch or by tethering the flagella with antibodies also promotes an increase in *degU* transcription that is reflective of increased DegU~P levels in the cell. Collectively, these findings strongly indicate that inhibition of flagellar rotation acts as a mechanical trigger to activate the DegS–DegU two-component signal transduction system. We postulate that inhibition of flagellar rotation could function as a mechanical trigger to activate bacterial signal transduction cascades in many motile bacteria upon contact with a surface.

Introduction

Persistent adhesion of bacterial cells to a surface is the first step in the formation of a biofilm – a complex community of bacteria encased in a self-produced exopolymeric matrix (Flemming and Wingender, 2010). The settlement of microbes on a surface within the confines of a biofilm can confer many advantages to the population, including increased access to nutrients and protection from environmental stress (Costerton *et al.*, 1995). Despite significant recent advances in our understanding of the regulatory pathways and key building blocks required for the nucleation and growth of biofilms for many species of bacteria (Flemming and Wingender, 2010; Lopez *et al.*, 2010; Vlamakis *et al.*, 2013), it is not fully understood how a motile cell senses and responds to a surface.

The bacterial flagellum is a complex molecular machine comprised of over 30 different proteins and is organized into three main structural domains: the basal body, hook and filament (Chevance and Hughes, 2008). The filament acts as a propeller to drive movement and is powered by a rotary motor that comprises stator and rotor protein complexes and can be driven by proton-motive or sodium-motive force (Manson *et al.*, 1977; Chernyak *et al.*, 1983). Torque is generated by specific interactions between the rotor and stator components (Zhou *et al.*, 1998a). The stator complex, which in *Escherichia coli* comprises a complex of four MotA proteins and two MotB proteins, forms two proton channels (Braun *et al.*, 1999; Kojima and Blair, 2004). It is thought that proton flux through the channels triggers a conformational change that alters the electrostatic interactions between MotA and the rotor protein FliG, resulting in torque generation (Zhou *et al.*, 1998a). As well as being required as a mechanical device for propulsion, the flagellum is also crucial for biofilm development in many bacterial species due to its role in the initial stages of surface adhesion (O'Toole *et al.*, 2000).

Bacillus subtilis is a Gram-positive, non-pathogenic, soil-dwelling bacterium that has emerged as a model organism for the study of biofilm formation (Vlamakis *et al.*, 2013). The development of the *B. subtilis* biofilm is tightly controlled and requires the activation of three transcriptional regulators: ComA (Lopez *et al.*, 2009c), Spo0A (Branda *et al.*, 2001; Hamon and Lazazzera, 2001) and DegU (Stanley and Lazazzera, 2005). Previous studies have delineated many of the signals required to activate both ComA and Spo0A. At high cell density the quorum sensing transcription factor, ComA is phosphorylated, resulting in production of the lipopeptide, surfactin (Nakano *et al.*, 1991). The production of surfactin, along with other signals that induce potassium leakage (Lopez *et al.*, 2009a; Shank and Kolter, 2011) and osmotic stress (Rubinstein *et al.*, 2012), triggers activation of a multicomponent phosphorelay which begins with the phosphorylation of one or more

Accepted 22 July, 2013. *For correspondence. E-mail n.r.stanleywall@dundee.ac.uk; Tel. (+44) (0)1382 386335; Fax (+44)(0)1382 388216.

sensor histidine kinases (namely KinA to KinE, each of which has a unique role in signal perception) (see Vlamakis *et al*., 2013) and culminates in phosphorylation of Spo0A (Burbulys *et al*., 1991). The level of phosphorylated Spo0A (hereafter Spo0A~P) within the cell dictates which bacterial behaviour will be stimulated or repressed (Fujita *et al*., 2005; Lopez *et al*., 2009b). Biofilm formation by *B. subtilis* requires a low level of Spo0A~P to indirectly promote the transcription of the *tapA-sipW-tasA* and *epsA-O* operons (Fujita *et al*., 2005; Chai *et al*., 2011), which encode the extracellular biofilm matrix amyloid protein, TasA and proteins required for the synthesis of the biofilm matrix exopolysaccharide (EPS) respectively (Vlamakis *et al*., 2013). The third component required for *B. subtilis* biofilm formation is the hydrophobic coat protein, BslA (formerly YuaB) (Kobayashi and Iwano, 2012; Hobley *et al*., 2013). Transcription of the *bslA* gene is indirectly activated by phosphorylated DegU (hereafter DegU~P) (Kobayashi, 2007; Ostrowski *et al*., 2011).

DegU is a response regulator that is phosphorylated by its cytoplasmic cognate sensor histidine kinase, DegS (Dahl *et al*., 1991). DegU~P is a pleiotropic regulator that controls a myriad of processes, including flagella-based motility (Amati *et al*., 2004; Verhamme *et al*., 2007; Hsueh *et al*., 2011; Patrick and Kearns, 2012), biofilm formation (Kobayashi, 2007; Verhamme *et al*., 2007), exoprotease production (Dahl *et al*., 1992) and biosynthesis of the exopolymer poly-γ-DL-glutamic acid (hereafter γ-PGA) (Stanley and Lazazzera, 2005). The ability of DegU~P to promote both motility and γ-PGA production is dependent on the small protein SwrA (Kearns *et al*., 2004; Stanley and Lazazzera, 2005; Calvio *et al*., 2008; Osera *et al*., 2009). The main role of SwrA is to regulate the number of flagellar hook-basal bodies in the cell (Kearns and Losick, 2005; Guttenplan *et al*., 2013). It is thought that the ability of DegU~P to regulate several different processes is underpinned by variation in promoter affinities (Kobayashi, 2007; Murray *et al*., 2009). A small protein, DegQ, aids the transfer of the phosphoryl moiety from DegS to DegU (Kobayashi, 2007) with recent work suggesting that this is due to the ability of DegQ to stabilize the phosphorylated form of DegS in the presence of DegU (Do *et al*., 2011). Transcription of *degQ* is positively regulated by ComA and thus increases in response to cell density, thereby ensuring that DegU~P levels also rise as growth approaches stationary phase (Msadek *et al*., 1991).

While many aspects of DegU activation and regulation are understood (for a review see Murray *et al*., 2009), the signal sensed by DegS to trigger phosphorylation of DegU has remained somewhat elusive. Previous studies have identified a link between the activity of the DegS–DegU system and osmolarity (Ruzal and Sanchez-Rivas, 1998), the structural maintenance of the chromosome (SMC)–ScpA–ScpB complex (Dervyn *et al*., 2004), ClpCP mediated proteolytic degradation (Ogura and Tsukahara, 2010), the RapG-PhrG quorum sensing system (Ogura *et al*., 2003) and, more recently, the completion status of the flagellar basal body (Hsueh *et al*., 2011). The aim of this work was to investigate the link between flagellar assembly and phosphorylation of DegU. We hypothesized that inhibition of flagellar rotation might trigger activation of the DegS–DegU two-component system. This would provide a mechanism to allow motile cells to detect and respond to the presence of a surface during the initial stages of biofilm formation. The data presented here identifies the *B. subtilis* flagellum as a mechanosensor. Deletion of the flagellar stator gene, *motB*, triggered an increase in DegU~P levels, exemplified by an upregulation of *degU* transcription and two distinct DegU~P driven processes, namely exoprotease production and γ-PGA biosynthesis. Further experiments designed to perturb flagellar rotation by genetic and non-genetic methods also resulted in elevated DegU~P levels within the cell. We conclude that the DegS–DegU two-component regulatory system is activated by the lack of flagellar rotation. As the flagellar structure is highly conserved between microbial species, the arrest of flagellar rotation may present a mechanism by which many flagellated organisms detect and respond to a surface.

Results

Deletion of motB is associated with increased γ-PGA biosynthesis

To test if flagellar rotation was linked to the activity of the DegS–DegU two-component system, an in-frame non-polar deletion in the flagellar stator gene, *motB* was constructed (NRS3494). Disruption of the flagellar stator genes perturbs motility but has no effect on biosynthesis of the flagellum itself (Chevance and Hughes, 2008). Consistent with this, the Δ*motB* strain synthesized flagella but displayed a non-motile phenotype (Fig. S1A and C). The observed motility defect was complemented upon re-introduction of the *motB* coding sequence on the chromosome under the control of an IPTG-inducible promoter (Phy-spank) at the non-essential *amyE* locus (NRS3775) verifying the specificity in the deletion (Fig. S1B). Strikingly, as shown in Fig. 1A, the Δ*motB* strain displayed a mucoid colony phenotype on LB plates after growth overnight. The mucoid colony morphology was specific to deletion of *motB* as the colony morphology reverted to the flat dry phenotype exhibited by the wild-type strain upon heterologous expression of *motB* (Fig. 1A). Production of the exopolymer γ-PGA has been linked with mucoid colony morphology in *B. subtilis* (Stanley and Lazazzera, 2005). The relationship between the mucoid colony morphology of the *motB* deletion strain and γ-PGA production was confirmed as γ-PGA could be biochemically extracted from the culture

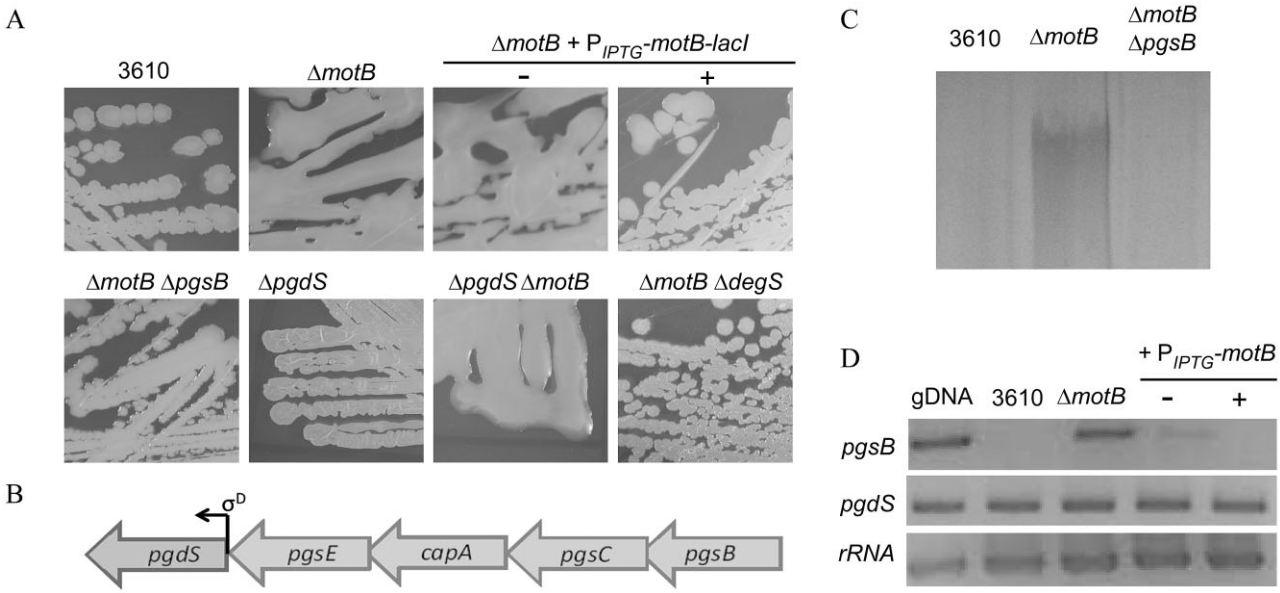

Fig. 1. Deletion of *motB* from the chromosome is associated with γ-PGA production.
A. Colony morphology of 3610 (wild-type), Δ*motB* (NRS3494), Δ*motB* + *amyE*::P_{IPTG}-*motB-lacI* (NRS3775) grown on LB agar plate in the absence or presence of 50 μM IPTG, Δ*motB* + *pgsB::spc* (NRS3434), Δ*pgdS* (NRS3347), Δ*pgdS*Δ*motB* (NRS3348) and Δ*motB* + *degS::cml* (NRS3398).
B. Schematic diagram of the γ-PGA synthesis operon and γ-PGA hydrolase gene. Arrows represent open reading frames (ORF), with the direction of the arrow indicating the direction of the ORF. The bent arrow represents the promoter located before the *pgdS* gene, which is driven by the alternative sigma factor, σ^D, as indicated.
C. SDS-PAGE of γ-PGA collected from cultures of NCIB3610, Δ*motB* (NRS3494) and Δ*motB* + *pgsB::spc* (NRS3434) grown to the onset of stationary phase.
D. Reverse-transcription-PCR analysis of *pgsB* and *pgdS*. Regions of DNA internal to *pgsB* and *pgdS* were amplified from cDNA generated from the wild-type (NCIB3610), Δ*motB* (NRS3494) and Δ*motB* + *amyE*::P_{IPTG}-*motB-lacI* (NRS3775) grown in the absence and presence of 50 μM IPTG. Genomic DNA (gDNA) was used as a positive control for the PCR reaction and the ribosomal 16S rRNA was amplified as an internal control.

supernatant collected at the onset of stationary phase upon deletion of *motB* (Fig. 1C and Fig. S1D).

Increased γ-PGA biosynthesis in the absence of *motB* was predicted to be the consequence of: (i) decreased hydrolysis of γ-PGA and/or (ii) increased biosynthesis of γ-PGA. γ-PGA biosynthesis is driven by the protein products of the *pgsB* operon, while turnover is catalysed by the endo-γ-glutamyl peptidase, PgdS (Fig. 1B) (Candela and Fouet, 2006). Consistent with deletion of *motB* triggering increased γ-PGA biosynthesis, reverse-transcription (RT)-PCR analysis showed that transcription of the *pgsB* coding region could not be detected in NCIB3610, but was detectable upon deletion of *motB* (Fig. 1D). Furthermore, the mucoid phenotype of the Δ*motB* strain was abolished upon disruption of *pgsB* (Fig. 1A). In contrast, the *pgdS* coding region was transcribed in NCIB3610, Δ*motB* and the complemented strain (Fig. 1D). Consistent with these data, deletion of *pgdS* did not result in a mucoid colony morphology on LB agar plates indicating that the *pgdS* deletion strain did not phenocopy the *motB* strain (Fig. 1A). Collectively, these data demonstrate that deletion of *motB* triggers increased biosynthesis of the exopolymer γ-PGA.

Biosynthesis of γ-PGA is triggered by high levels of DegU~P in B. subtilis *NCIB3610*

Consistent with our hypothesis that flagellar rotation might control the activity of the DegS–DegU two-component system, production of γ-PGA is linked with high levels of DegU~P (Stanley and Lazazzera, 2005; Osera *et al.*, 2009). Transcription of the γ-PGA synthetase gene, *pgsB* is directly regulated by DegU~P (Ohsawa *et al.*, 2009), supporting the hypothesis that γ-PGA biosynthesis is increased in the Δ*motB* strain due to an increase in the level of DegU~P. It is worth noting that in certain *B. subtilis* isolates, such as R0-FF-1, γ-PGA is a component of the biofilm matrix (Stanley and Lazazzera, 2005; Morikawa *et al.*, 2006). However, in NCIB3610 this is not the case as γ-PGA is not synthesized, despite the presence of an intact γ-PGA biosynthetic operon on the chromosome (Branda *et al.*, 2006; Srivatsan *et al.*, 2008; Earl *et al.*, 2012). We therefore hypothesized that in NCIB3610 the DegU~P levels are suppressed and that this suppression was alleviated upon deletion of *motB*. To test if directly increasing the level of DegU~P was sufficient to allow biosynthesis

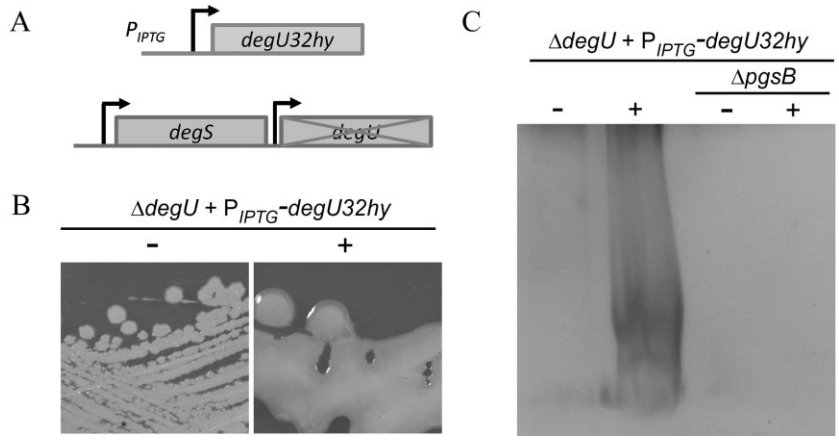

Fig. 2. Increasing DegU~P levels allows γ-PGA production in NCIB3610.
A. Schematic diagram of the construction of the Δ*degU* + *amyE*::P_{IPTG}-*degU32hy-lacI* strain (NRS1325). Bent arrows represent the promoters located before each gene.
B. Colony morphology of the Δ*degU* + *amyE*::P_{IPTG}-*degU32hy-lacI* (NRS1325) strain without and with induction with 25 μM IPTG.
C. SDS-PAGE of γ-PGA collected from cultures of Δ*degU* + *amyE*::P_{IPTG}-*degU32hy-lacI* (NRS1325) and Δ*degU* + *amyE*::P_{IPTG}-*degU32hy-lacI* + *pgsB::spc* (NRS3770) grown to the onset of stationary phase in the absence or presence of 25 μM IPTG.

of γ-PGA by NCIB3610, we used a synthetic strain of NCIB3610 that contained a disruption in the native *degU* gene and carried an allele of *degU* containing an $H^{12}L$ amino acid mutation (*degU32hy*) under the control of an IPTG-inducible promoter at the non-essential *amyE* locus (NRS1325) (Verhamme *et al*., 2007) (Fig. 2A). The *degU32 hy* gene encodes a DegU variant that is described as exhibiting a slower rate of dephosphorylation by comparison with the wild-type protein, thus increasing the level of DegU~P in the cell (Dahl *et al*., 1992). As shown in Fig. 2B, induction of *degU32hy* expression with 25 μM IPTG resulted in a highly mucoid colony phenotype. The relationship between the mucoid colony morphology and γ-PGA production was confirmed as γ-PGA could be biochemically extracted from culture supernatant collected at the onset of stationary phase upon induction of *degU32 hy* expression (Fig. 2C). Moreover, disruption of the γ-PGA synthetase gene, *pgsB*, in this background abolished γ-PGA production as assessed by the presence of flat dry colonies (data not shown) and a lack of exopolymer extraction from the culture supernatant (Fig. 2C). Intriguingly, a strain carrying the *degU32 hy* allele retained γ-PGA biosynthesis in the absence of *degS* as defined by a mucoid colony morphology (data not shown). These findings indicate that DegU $H^{12}L$ can be phosphorylated by another kinase or by acetyl phosphate (Wolfe *et al*., 2003; 2008) as has been suggested previously for the accumulation of low levels of native DegU~P in the absence of *degS* (Kobayashi, 2007; Verhamme *et al*., 2007). These data highlight that increasing the level of DegU~P in NCIB3610 results in γ-PGA production. This is replicated upon deletion of *motB*, suggesting that upon inhibition of flagellar rotation DegU~P levels are increased.

The ΔmotB strain shows increased degU transcription and protease production

To determine if DegU~P levels were increased in the Δ*motB* strain two approaches were taken. First, transcription of *degU* was quantified upon deletion of *motB* and second, protease production was quantified as an indirect measure of DegU~P levels. DegU~P positively autoregulates transcription of *degU*, therefore measuring the level of activity from the *degU* promoter provides an indirect measurement of DegU~P in the cell (Kobayashi, 2007; Veening *et al*., 2008). To this end, a P*degU–lacZ* transcriptional reporter fusion was constructed and integrated into the wild-type, Δ*motB* and Δ*motB* complemented strains. Cells were harvested from cultures grown to the onset of stationary phase, and β-galactosidase assays performed. As shown in Fig. 3A, in Δ*motB* transcription of *degU* is increased approximately fourfold when compared with the wild-type ($P < 0.01$). This effect is specific to deletion of *motB* as transcription of *degU* can be restored to wild-type levels by expression of *motB* from an IPTG-inducible promoter integrated at a non-essential locus (Fig. 3A).

To test the effect of deletion of both stator components a Δ*motAB* (NRS3744) strain was constructed. Consistent with inhibition of flagellar rotation promoting an increase in DegU~P levels, the phenotypes reported for Δ*motB* were replicated in the double mutant strain. We first established that the non-polar *motAB* deletion strain synthesized flagella and exhibited a motility defect that could be specifically complemented by heterologous induction of *motAB* transcription using an IPTG-dependent promoter (Fig. S1A and C). Next, we examined the phenotype when grown on LB agar plates. The Δ*motAB* deletion strain exhibited a mucoid colony phenotype that could be complemented upon heterologous expression of *motAB* (Fig. S1B). Consistent with these findings, transcriptional analysis demonstrated that the *motAB* strain showed an increase in the level of *degU* expression (Fig. 3A). These data suggest that DegU~P levels are elevated in the both Δ*motB* and Δ*motAB* strains.

High levels of DegU~P are closely associated with exoprotease biosynthesis (Dahl *et al*., 1992; Kobayashi, 2007; Verhamme *et al*., 2007). DegU~P positively regulates transcription of the *aprE* gene, which encodes the alkaline

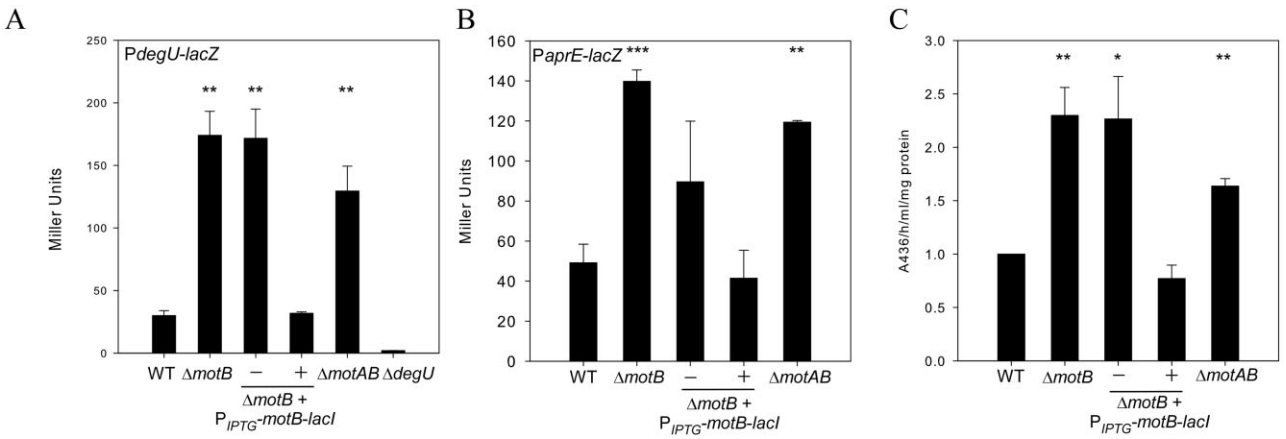

Fig. 3. Transcription of *degU* and *aprE* is increased alongside total protease activity in Δ*motB*.
A. β-Galactosidase assays of strains carrying the P*degU–lacZ* transcriptional reporter fusion. Strains shown are WT (wild-type NRS4351), Δ*motB* (NRS4345), *motB* + *amyE*::P_{IPTG}-*motB-lacI* (NRS4396) grown in the absence or presence of 50 μM IPTG, Δ*motAB* (NRS4354) and Δ*degU* (NRS4373). All cells were collected at the onset of stationary phase.
B. β-Galactosidase assays of strains carrying the P*aprE–lacZ* transcriptional reporter fusion. Strains shown are WT (wild-type NRS1561), Δ*motB* (NRS3440), Δ*motB* + *amyE*::P_{IPTG}-*motB-lacI* (NRS3858) grown in the absence or presence of 50 μM IPTG and Δ*motAB* (NRS4093). All cells were collected at the onset of stationary phase.
C. Total protease activity assays performed with the supernatant collected from cells grown in (B).
Data in parts (A), (B) and (C) are plotted as the average of at least three independent replicates; in (C) data are represented as a fold change relative to the wild-type strain which was assigned value of 1. Error bars represent standard error of the mean. An asterisk denotes significance as calculated by the Student's *t*-test where * represents $P < 0.05$, ** $P < 0.01$ and *** $P < 0.001$.

protease subtilisin (Mukai *et al*., 1990). We therefore hypothesized that if DegU~P levels were high in the absence of *motB* this would correlate with an increase in *aprE* transcription and, moreover, an increase in the total protease activity in the extracellular environment. To establish if *aprE* transcription was altered in the Δ*motB* and Δ*motAB* strains, a P*aprE–lacZ* transcriptional reporter fusion was integrated at the non-essential *thrC* locus. Cells were harvested for β-galactosidase activity assays and the culture supernatant collected for measurement of extracellular protease activity (see *Experimental procedures*). Transcription of *aprE* was increased approximately threefold in the Δ*motB* ($P < 0.001$) and twofold in the Δ*motAB* ($P < 0.01$) strains when compared with the wild-type (Fig. 3B). The increase in transcription was specific as induction of *motB* transcription in the *motB* deletion strain reduced *aprE* transcription levels back to wild-type levels (Fig. 3B). In accordance with these data, total protease activity was increased by twofold upon deletion of *motB* and 1.6-fold in the Δ*motAB* strain (Fig. 3C) ($P < 0.01$).

Previous work has indicated that DegU can be phosphorylated in the absence of DegS (Kobayashi, 2007; Verhamme *et al*., 2007). To demonstrate that the upregulation in DegU~P processes seen in the Δ*motB* strain was transmitted through DegS, the *degS* gene was disrupted in the Δ*motB* background and γ-PGA production assessed by colony morphology. As seen in Fig. 1A, the colony morphology of the Δ*motB* Δ*degS* strain reverted to that of the wild-type. Collectively these findings demonstrate that deletion of the flagellar stator gene, *motB*, causes an increase in the DegU~P level within the population, leading to an upregulation of at least two distinct DegU~P regulated processes. This is reliant on the presence of DegS.

Mutation of motB to disturb proton flux phenocopies the ΔmotB strain

Given the importance of MotB in the generation of torque, we hypothesized that the increase in DegU~P regulated processes in the Δ*motB* background might be linked with the inhibition of flagellar rotation. Although the precise mechanisms by which torque is generated are not yet fully understood, it has been shown that protonation of a conserved aspartate in the MotB transmembrane domain is essential (Sharp *et al*., 1995; Zhou *et al*., 1998b). To test if disruption of proton flux through the MotAB complex, and therefore inhibition of flagellar rotation, were key to triggering an increase in DegU~P levels, the conserved aspartate residue of *motB* (aspartate 24 in *B. subtilis*; Fig. S2A) was mutated to alanine (*motB* $D^{24}A$) by site-directed mutagenesis. This construct was first integrated into the wild-type strain at a non-essential site on the chromosome under the control of an IPTG-inducible promoter. Upon induction of expression with 1 mM IPTG, the mutated *motB* allele conferred a dominant-negative phenotype with respect to both swarming motility (Fig. S2B) and γ-PGA production (Fig. S2D). These findings demonstrate that the MotB-$D^{24}A$ protein is synthesized and is functional as it has a dominant phenotype over the native MotB. Next, the construct was integrated into the Δ*motB*

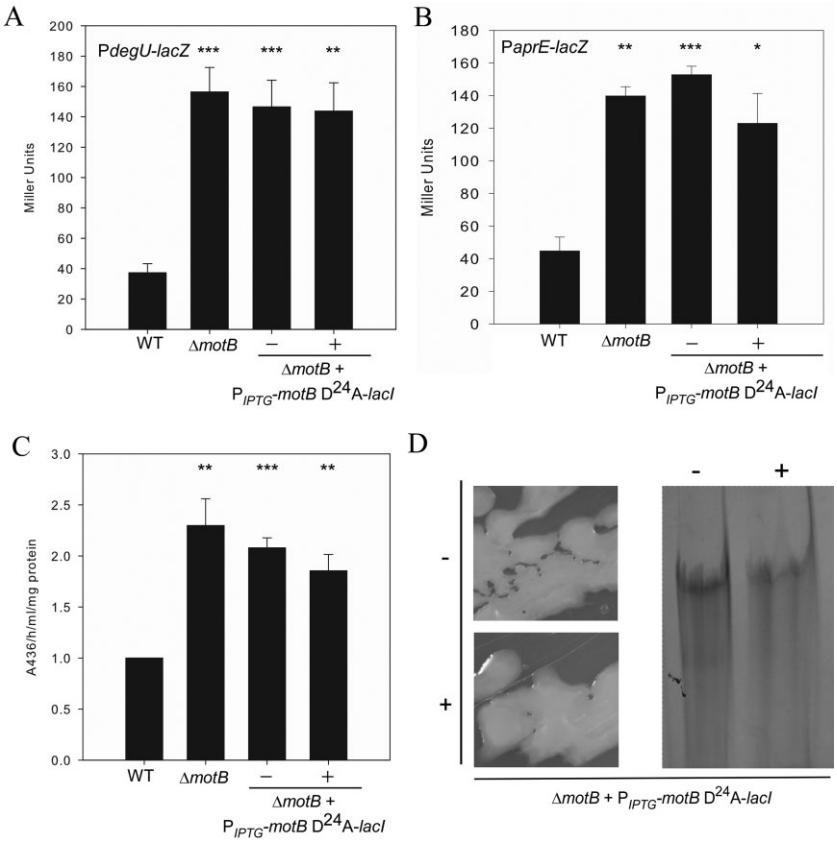

Fig. 4. The *motB* D[24]A allele cannot complement Δ*motB*.
A and B. β-Galactosidase assays of strains carrying the (A) P*degU–lacZ* or (B) P*aprE–lacZ* transcriptional reporter fusion. Strains shown are WT (wild-type NRS4351), Δ*motB* (NRS4345), *motB* + *amyE*::P$_{IPTG}$-*motB*-D[24]A-*lacI* (NRS4397) grown in the absence or presence of 50 μM IPTG and Δ*degU* (NRS4373).
B. β-Galactosidase assays of strains carrying the P*aprE–lacZ* transcriptional reporter fusion. Strains shown are WT (wild-type NRS1561), Δ*motB* (NRS3440), Δ*motB* + *amyE*::P$_{IPTG}$-*motB*-D[24]A-*lacI* (NRS3870) grown in the absence or presence of 50 μM IPTG. All cells in (A) and (B) were collected at the onset of stationary phase.
C. Total protease activity assays performed with supernatants collected from cells grown in (B).
Data in (A), (B) and (C) are plotted as the average of at least three independent replicates. In (C) data are represented as a fold change relative to the wild-type strain which was assigned value of 1. Error bars represent standard error of the mean. An asterisk denotes significance as calculated by the Student's *t*-test where * represents $P < 0.05$; ** $P < 0.01$; and *** $P < 0.001$.
D. Colony morphology of Δ*motB* + *amyE*::P$_{IPTG}$-*motB*-D[24]A-*lacI* (NRS3870) grown on LB agar in the absence and presence of 50 μM IPTG. SDS-PAGE analysis of γ-PGA collected from cultures of Δ*motB* + *amyE*::P$_{IPTG}$-*motB*-D[24]A-*lacI* (NRS3870) grown in the absence or presence of 50 μM IPTG.

strain background. As expected, in contrast to complementation of the *motB* strain with the wild-type allele of *motB*, induction of *motB* D[24]A transcription did not restore motility to the *motB* deletion strain (Fig. S2C). Next the effect of the *motB* D[24]A mutation with regard to *degU* and *aprE* transcription, protease activity and γ-PGA biosynthesis was assessed.

It was determined that induction of *motB* D[24]A expression was unable to complement Δ*motB* with respect to both *degU* and *aprE* transcription, which remained fivefold and threefold higher than in the wild-type respectively (Fig. 4A and B). Similarly protease activity was maintained at a higher level in the presence of *motB* D[24]A (Fig. 4C). γ-PGA production was confirmed based on the mucoid colony morphology and analysis of exopolymers extracted from culture supernatant (Fig. 4D). These data support the hypothesis that perturbation of proton flux, and therefore flagellar rotation, is necessary to trigger an increase in DegU~P activity.

Engaging the flagellar clutch causes an increase in degU transcription

To assess if the increase in DegU~P regulated processes was specific to deletion or mutation of the flagellar stator genes the effect of perturbing flagellar rotation by an alternative genetic means was tested. The *epsE* gene encodes a bi-functional protein, EpsE, that can act as (i) a flagellar clutch to disable flagellar rotation and (ii) a glycosyltransferase enzyme required for the formation of

robust biofilms (Blair *et al*., 2008; Guttenplan *et al*., 2010). Overexpression of *epsE* under the control of an IPTG-inducible promoter inhibits motility by interaction with FliG, thereby disengaging the rotor from the stator (Blair *et al*., 2008; Guttenplan *et al*., 2010). To test if inhibition of flagellar rotation by overexpression of *epsE* would also trigger an increase in DegU~P levels, the coding region of *epsE* was integrated at a non-essential locus on the chromosome under the control of an IPTG-inducible promoter. To ensure that any effect on DegU~P was specific to the clutch activity of *epsE* and not due to the glycosyltransferase function, site-directed mutagenesis was used to mutate aspartate 94 to alanine (*epsE* $D^{94}A$) to yield a protein variant that retained clutch activity but lost glycosyltransferase functionality. Simultaneously, lysine 106 was mutated to glutamic acid (*epsE* $K^{106}E$) to yield a protein variant that lost clutch activity but possessed glycosyltransferase activity. Both single amino acid mutations have been previously characterized by Guttenplan *et al*. (2010).

First, the motility phenotypes of these strains were assessed to ensure that the point mutations introduced functioned as expected. As shown in Fig. S3A, induction of either the *epsE* WT or *epsE* $D^{94}A$ coding regions inhibited swarming motility, while induction of the *epsE* $K^{106}E$ coding region in the otherwise wild-type strain had no impact on swarming motility as compared with NCIB3610. As these phenotypes are entirely in line with the previous report (Guttenplan *et al*., 2010), we proceeded to assess the effect of these mutations on *degU* transcription. The strains were grown to mid-exponential phase, at which point expression of *epsE* (or the mutant alleles) was induced by the addition of IPTG. Samples were collected over time to assess β-galactosidase activity. Induction of *epsE* WT or *epsE* $D^{94}A$ expression resulted in a fourfold increase in *degU* transcription by comparison with the wild-type, while induction of *epsE* $K^{106}E$ phenocopied the wild-type (Fig. 5A and Fig. S3B).

Engaging the flagellar clutch causes an increase in DegU~P regulated processes

To test if the upregulation of *degU* transcription observed upon induction of *epsE* translated to an increase in DegU~P-regulated processes, transcription of the *bslA* gene was measured. The *bslA* promoter is the main target of DegU~P during biofilm formation by *B. subtilis* (Kobayashi, 2007; Verhamme *et al*., 2009; Ostrowski *et al*., 2011). Therefore, it was hypothesized that an increase in DegU~P levels by inhibition of flagellar rotation would result in increased *bslA* transcription. A P*bslA–lacZ* transcriptional reporter fusion was integrated into the *epsE* WT, $D^{94}A$ and $K^{106}E$ strains and activity measured over time by β-galactosidase assays. A similar trend to that reported for *degU* transcription was observed. Induction of expression of *epsE* WT or *epsE* $D^{94}A$ resulted in a threefold increase in transcription by comparison with the wild-type (Fig. 5B and Fig. S3C). As predicted from the *degU* transcription analysis results, induction of *epsE* $K^{106}E$ phenocopied the wild-type strain.

The effect of overexpression of *epsE* on *aprE* transcription and total protease activity was then tested. As seen for *degU* and *bslA* transcription, *aprE* transcription was increased threefold upon inhibition of flagellar rotation (Fig. 5C and Fig. S3D). In accordance with the *aprE* transcription analysis data, 120 min after induction of *epsE* or *epsE* $D^{94}A$, total protease activity was twofold higher than the wild-type levels, while the protease activity of the *epsE* $K^{106}E$ strain was not significantly different from the wild-type (Fig. 5C). Consistent with DegU~P directing both *bslA* transcription (Kobayashi, 2007; Verhamme *et al*., 2009) and exoprotease production (Mukai *et al*., 1990), we noted that the level of *degU* transcription started to increase 20 min after IPTG induction of *epsE* transcription, whereas both *bslA* and *aprE* transcription began to rise 40 min post induction (compare Fig. 5A with Fig. 5B and C). These data demonstrate that *bslA* and *aprE* are only transcribed after the level of DegU~P increases. It is important to note that at this point the transcriptional repressor AbrB will have been removed from the promoter elements (Olmos *et al*., 1996; Verhamme *et al*., 2009).

γ-PGA production was then assessed. Induction of either *epsE* WT or *epsE* $D^{94}A$ expression overnight on LB-agar plates containing 1 mM IPTG yielded a mucoid colony phenotype (Fig. 6A). The mucoid phenotype was not seen when IPTG was lacking or when either the wild-type or *epsE* $K^{106}E$ expression strain was examined (Fig. 6A). Consistent with the colony phenotypes, γ-PGA was extracted from the culture supernatant and analysed by SDS-PAGE for both the *epsE* WT and *epsE* $D^{94}A$ expression strains (Fig. 6C). To determine if the γ-PGA production, and hence DegU~P levels, was reliant on input from DegS, the *degS* gene was disrupted in the *epsE* WT, *epsE* $D^{94}A$ and *epsE* $K^{106}E$ expression strains and γ-PGA production monitored using colony phenotype in the absence and presence of IPTG. A dry, flat colony morphology was observed for all strains carrying the *degS* disruption upon heterologous expression of *epsE* and the mutant *epsE* alleles with IPTG (Fig. 6B). Taken together, these data indicate that inhibition of flagellar rotation by EpsE results in an increase in DegU~P levels, which is reflected by an upregulation of *bslA* transcription, exoprotease activity and γ-PGA production. As proven for the *motB* strain (Fig. 1), DegS is responsible for increasing the levels of DegU~P upon induction of EpsE. Thus the signal generated by inhibition of flagellar rotation when EpsE is present is likely to be the same as when flagellar rotation is inhibited due to mutation or disruption of MotB.

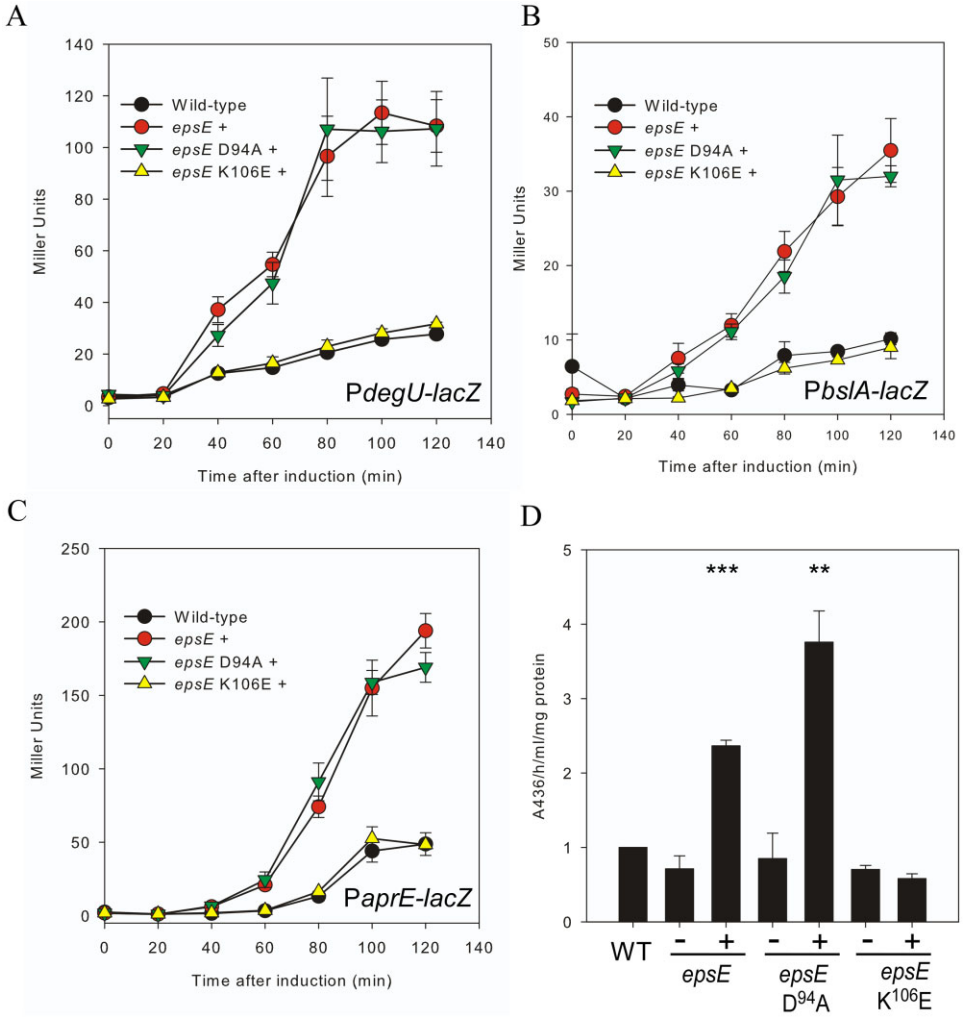

Fig. 5. Engaging the flagellar clutch causes an increase in DegU~P levels.
A–C. β-Galactosidase assays of strains carrying the (A) P*degU–lacZ*, (B) P*bslA–lacZ* or (C) P*aprE–lacZ* transcriptional reporter fusion. Cells were grown to 0.5 OD_{600} and induced with 1 mM IPTG (final concentration). Strains shown are: (A) wild-type (NRS4351), *epsE* + (P_{IPTG}-*epsE*-*lacI* (NRS4374)), *epsE* $D^{94}A$ + (P_{IPTG}-*epsE*-$D^{94}A$-*lacI* (NRS4392)) and *epsE* $K^{106}E$ (P_{IPTG}-*epsE*-$K^{106}E$-*lacI* (NRS4394)); (B) Wild-type (NRS2052), P_{IPTG}-*epsE*-*lacI* (NRS4405), P_{IPTG}-*epsE*-$D^{94}A$-*lacI* (NRS4406) and P_{IPTG}-*epsE*-$K^{106}E$-*lacI* (NRS4407); (C) Wild-type (NRS1561), P_{IPTG}-*epsE*-*lacI* (NRS4345), P_{IPTG}-*epsE*-$D^{94}A$-*lacI* (NRS4393) and P_{IPTG}-*epsE*-$K^{106}E$-*lacI* (NRS4395). Data shown in (A), (B) and (C) are plotted as the average of at least three independent replicates. Error bars represent standard error of the mean.
D. Total protease activity assays performed with supernatants collected from cells grown in (C) after 120 min of induction in the absence or presence of 1 mM IPTG. Data are plotted as the average of at least three independent replicates and are represented as a fold change relative to the wild-type strain (WT) which was assigned value of 1. Error bars represent standard error of the mean. An asterisk denotes significance as calculated by the Student's *t*-test, where ** represents $P < 0.01$; and *** $P < 0.001$.

Tangling of flagella increases DegU~P activity

Data presented thus far indicate that inhibition of flagellar rotation by genetic manipulation activates the DegS–DegU two-component signal transduction system. We next used a non-genetic method to block flagellar rotation (Meister *et al*., 1987). An antibody raised against the flagellar filament protein, Hag, was used to tangle flagella (see Fig. 7A and Movies S1–S4) and the impact on *degU* transcription measured. Prior to this we used Western blot analysis to check the specificity of the Hag antibody (Fig. S4). To ensure that any effects seen were specific to the Hag antibody, and not due to off-target effects of the serum, three independent pre-immune sera were used as controls. The wild-type strain carrying the P*degU–lacZ* transcriptional reporter fusion was grown in liquid culture to mid-exponential phase at which point either pre-immune sera or the Hag antibody in sera was added (1:20 dilution). Swimming motility was immediately checked by real-time live single cell microscopy (see Fig. 7A and Movies S1–S4) and samples were collected over time for β-galactosidase assays. Analysis demonstrated that transcription from the

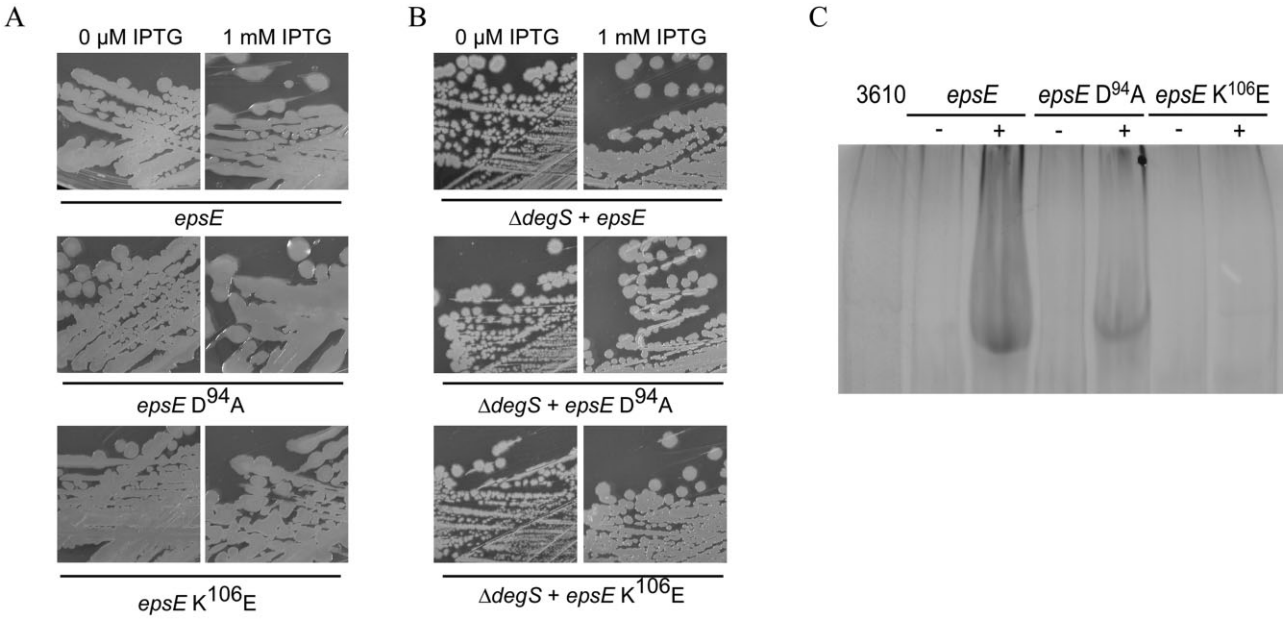

Fig. 6. Engaging the flagellar clutch triggers an increase in γ-PGA production that requires DegS.
A. Colony morphology of P_{IPTG}-*epsE-lacI* (NRS4085), P_{IPTG}-*epsE*-$D^{94}A$-*lacI* (NRS4388) and P_{IPTG}-*epsE*-$K^{106}E$-*lacI* (NRS4389) in the absence and presence of 1 mM IPTG after growth overnight at 37°C.
B. Colony morphology of P_{IPTG}-*epsE-lacI* + *degS::cml* (NRS4399), P_{IPTG}-*epsE*-$D^{94}A$-*lacI* + *degS::cml* (NRS4400) and P_{IPTG}-*epsE*-$K^{106}E$-*lacI* + *degS::cml* (NRS4401) in the absence and presence of 1 mM IPTG after growth overnight at 37°C.
C. SDS-PAGE of γ-PGA collected from cultures of 3610 (wild-type NRS1561), P_{IPTG}-*epsE-lacI* (NRS4345) and P_{IPTG}-*epsE*-$D^{94}A$-*lacI* (NRS4393) and P_{IPTG}-*epsE*-$K^{106}E$-*lacI* (NRS4395), grown in the absence or presence of 1 mM IPTG, at the onset of stationary phase.

degU promoter was upregulated only 15 min after addition of the antibody, and increased fourfold by comparison with the pre-immune sera controls after 30 min (Fig. 7B) ($P < 0.001$). This trend of increased transcription was maintained over the course of the experiment (Fig. 7B). To further validate these data, exoprotease activity assays were undertaken with samples collected at the end of each time-course. The mean level of exoprotease activity for the

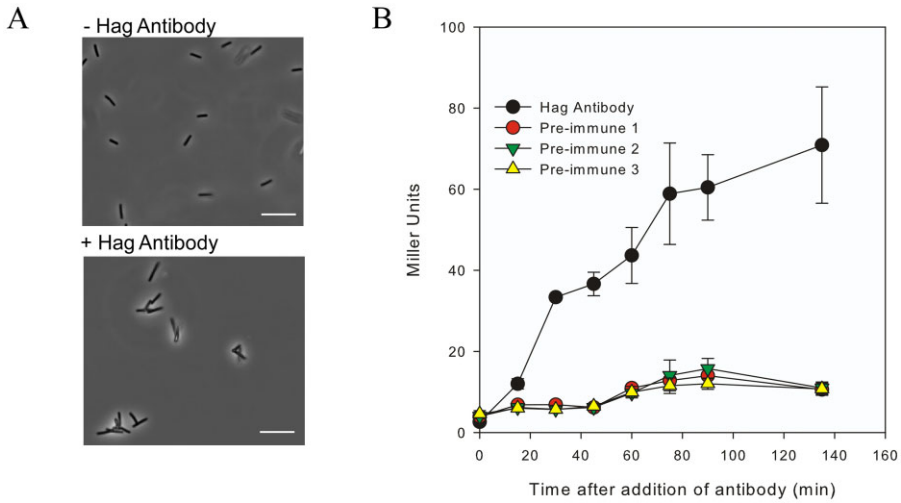

Fig. 7. Tethering the flagella triggers an increase in *degU* transcription.
A. Micrographs of cells containing the P*degU–lacZ* transcriptional reporter fusion (NRS4351) grown presence or absence of Hag antibody in sera. Micrographs are static images taken from movies filmed 5 min after the addition of antibody to the culture (see Movies S1 and S2). Scale bars represent 100 pixels.
B. β-Galactosidase assays of the wild-type strain carrying the P*degU–lacZ* transcriptional reporter fusion (NRS4351) grown in the presence of a 1:20 dilution of either pre-immune sera or the Hag-specific antibody. Three independent pre-immune sera were used as controls. Data are plotted as the average of at least three independent replicates. Error bars represent standard error of the mean.

three pre-immune sera controls was calculated and compared with that of the experimental sample incubated with Hag anti-sera. Analysis demonstrated a statistically significant ($P = 0.01$) 13-fold increase in exoprotease activity upon inhibition of flagellar rotation by tangling of the flagella. The mean level of protease activity in the presence of sera alone was 0.004 ± 0.001 ΔA_{436} h^{-1} ml^{-1} per mg of total protein compared with 0.05 ± 0.001 ΔA_{436} h^{-1} ml^{-1} per mg of total protein in the presence of the sera containing the anti-hag antibody. Collectively, these data unequivocally demonstrate that inhibition of rotation of the *B. subtilis* flagellum either genetically or mechanically results in an increase in *degU* transcription and DegU~P regulated processes, findings that are consistent with the activation of the sensor kinase, DegS.

Discussion

In the natural environment bacteria predominantly live adhered to a surface as part of a biofilm (Costerton *et al.*, 1995; Vlamakis *et al.*, 2013). However, how a motile cell is able to sense and respond to the presence of a surface is poorly understood. Here, we show that inhibition of flagellar rotation acts as a signal to trigger an increase in the level of DegU~P via the sensor kinase DegS. This is a regulatory pathway that is needed for biofilm formation by the Gram-positive bacterium *B. subtilis* (Stanley and Lazazzera, 2005; Kobayashi, 2007; Verhamme *et al.*, 2007). These findings clearly demonstrate that *B. subtilis* can effectively use the flagellum for both signal transduction purposes as well as a mechanical device for propulsion. These findings add to the small but growing body of evidence indicating that the flagellum is utilized by the cell to explore and respond to external stimuli in diverse bacterial species (Belas and Suvanasuthi, 2005; Wang *et al.*, 2005; Gode-Potratz *et al.*, 2011; Friedlander *et al.*, 2013). We propose that inhibition of flagellar rotation would occur due to physical contacts with a surface, and that the consequential activation of a signal transduction pathway may present a mechanism by which flagellated organisms detect and respond to a surface.

Activation of the DegS–DegU two-component regulatory system

Previous work has highlighted a role of DegU~P in controlling flagellar assembly (Amati *et al.*, 2004; Hsueh *et al.*, 2011). Indeed it has been shown that DegU is preferentially activated in genetic backgrounds that promote cell chaining, with further experiments tentatively suggesting that DegU might play a role in sensing the status of flagellar assembly (Hsueh *et al.*, 2011). The data presented herein demonstrate that the DegS–DegU two-component regulatory system is activated when the flagellum stops rotating. Therefore DegU~P has a role both in flagellar biosynthesis and in responding to signals inputted by the flagellum. Data demonstrating that inhibition of flagellar rotation acts as a trigger to activate the DegS–DegU two-component system allows the *B. subtilis* flagellum to be classified as a mechanosensor that controls bacterial cell behaviour. To the best of our knowledge this is the first example of a classical two-component system being activated in response to a mechanical signal: namely inhibition of flagellar rotation. We suggest that repression of flagellar rotation occurs when the flagellum encounters a surface; a process that is mimicked in our study by flagella tangling experiments (Fig. 7).

Surface sensing by the flagellum

Our findings add *B. subtilis* to the small list of microorganisms for which surface sensing has been linked with downstream alterations in gene transcription and protein synthesis (McCarter *et al.*, 1988; Kawagishi *et al.*, 1996). For example, transcriptomic and proteomic screens have shown that genes and proteins are differentially regulated between liquid and surface grown bacteria (Kim and Surette, 2004; Wang *et al.*, 2004). Moreover, in *Vibrio parahaemolyticus*, which possesses a dual flagellar system, it has been shown that slowing the rotational speed of the polar flagellum triggers gene expression changes that result in the transcription of genes essential for the synthesis of lateral flagella (McCarter *et al.*, 1988; Kawagishi *et al.*, 1996). Furthermore, inhibition of rotation of the polar flagellum also impacts genes associated with cyclic-di-GMP signalling and virulence, thereby suggestive of a global role for flagellar mediated surface sensing in controlling bacterial cell physiology (Gode-Potratz *et al.*, 2011).

The transition from motility to attachment

The attachment of bacteria to a surface is the first step in the formation of a biofilm, where the initial stage of adhesion is often mediated by flagella- or pili-based motility (O'Toole *et al.*, 2000). Indeed, several studies have identified flagella, or flagellar motility, as a key aspect of biofilm development and biofilm 'microanatomy' (O'Toole and Kolter, 1998; Pratt and Kolter, 1998; Watnick and Kolter, 1999; Lemon *et al.*, 2007; Friedlander *et al.*, 2013; Serra *et al.*, 2013). The subsequent transition to persistent adhesion is often mediated by polysaccharides (Watnick and Kolter, 2000). In *Caulobacter crescentus* a direct link between surface-sensing by the flagellum and irreversible adhesion has been shown, where upon reaching the surface, pili-dependent inhibition of flagellum rotation stimulates concomitant synthesis of the holdfast, promoting permanent attachment (Li *et al.*, 2012). Moreover,

exopolysaccharides have been shown to 'wheel-lock' flagellar rotation resulting in co-ordination of motility inhibition and stimulation of biofilm formation (Zorraquino *et al.*, 2013). Alternatively, or indeed additionally, flagellar brake or clutch activity can play a role in the transition between motility and biofilm formation to ensure separation of these mutually exclusive cell behaviours (Blair *et al.*, 2008; Pilizota *et al.*, 2009; Boehm *et al.*, 2010; Paul *et al.*, 2010). This can be exemplified by the *B. subtilis* flagellar clutch, EpsE that was utilized in this study. It is of interest to note that EpsE is encoded within the *epsA-O* operon that is required for the synthesis of one of the major structural components of the biofilm, the exopolysaccharide. EpsE therefore links inhibition of motility to exopolysaccharide production and biofilm formation (Blair *et al.*, 2008; Guttenplan *et al.*, 2010; Guttenplan and Kearns, 2013). Here we provide evidence that induction of EpsE will reinforce biofilm formation through increased biosynthesis of BslA (Fig. 5B), a bacterial hydrophobin that coats the *B. subtilis* biofilm (Kobayashi and Iwano, 2012; Hobley *et al.*, 2013) and functions synergistically with the exopolysaccharide and TasA amyloid fibres to facilitate assembly of the biofilm matrix (Ostrowski *et al.*, 2011). Proteins functionally similar to EpsE have been classed as flagellar 'brakes' in *E. coli* (Boehm *et al.*, 2010; Paul *et al.*, 2010) and *Rhodobacter sphaeroides* (Pilizota *et al.*, 2009). Therefore, the ability of a single protein to inhibit flagellar rotation appears to be a general mechanism used by bacteria to facilitate the transition to a sessile state.

Concluding remarks

There are, of course, outstanding questions that follow our discovery; the first being how a slowing or lack of flagellar rotation is sensed. There are several mechanisms by which this might occur. One possibility is that DegS, as a cytoplasmic sensor kinase, interacts with components of the flagellar motor when rotation is stopped. This postulated mechanism is similar to that proposed for the cyclic-di-GMP (c-di-GMP)-binding protein, YcgR, which interacts with the flagellar motor proteins FliG, FliM (Paul *et al.*, 2010) and MotA (Boehm *et al.*, 2010), when c-di-GMP levels are high resulting in the inhibition of motility. Consistent with this, in *Pseudomonas aeruginosa* the chemotaxis-like Wsp signal transduction system, which is essential for biofilm formation, has been shown to produce c-di-GMP in response to surface growth (Guvener and Harwood, 2007; O'Connor *et al.*, 2012). A second possible mechanism may involve the stator-associated transmembrane protein, FliL. Previous studies have identified FliL as a possible intermediary between the inhibition of rotation and signal transduction (Belas and Suvanasuthi, 2005; Cusick *et al.*, 2012). Moreover, recent studies in different bacterial species have identified several roles for FliL in bacterial motility and surface-sensing (Lee *et al.*, 2013). For example, FliL has been shown to be associated with (Motaleb *et al.*, 2011) and enhance the function of the flagellar stator (Suaste-Olmos *et al.*, 2010), with evidence now suggesting that overexpression of FliL alongside MotAB is sufficient to overcome surface friction associated with swarming on hard agar (Partridge and Harshey, 2013). Therefore, given that the function of FliL does not appear to be strictly conserved between bacterial species it will be of interest to determine if FliL is also a key player in surface-sensing and flagellar rotation in *B. subtilis*. Alternatively, we cannot exclude the possibility that DegS might directly sense changes in the intracellular environment that are triggered by a lack of flagellar rotation, such as ion flux (Kawagishi *et al.*, 1996) or potentially energy status (Watson and Fedor, 2012). Intriguingly, recent work in *E. coli* has identified the flagellar stator, not the flagellar filament, as a mechanosensor that is able to remodel itself in a load-dependent manner (Lele *et al.*, 2013). It is therefore possible that the increase in the number of stators required to drive flagellar torque under high loads might itself act as a signal to impact downstream signalling pathways. It will be of interest in the future to determine the underlying molecular detail of DegS activation, and moreover to clarify if our hypothesis that the flagellum acts as a mechanosensor to allow a sessile lifestyle to be adopted by other flagellated bacterial species holds true.

Experimental procedures

Growth conditions and strain construction

Escherichia coli and *B. subtilis* strains were routinely grown in Luria–Bertani (LB) broth (10 g NaCl, 5 g yeast extract, 10 g tryptone per litre) or on LB plates supplemented with 1.5% select agar (Invitrogen) at 37°C unless otherwise stated. When appropriate, isopropyl β-D-1-thiogalactopyranoside (IPTG) was added at the indicated concentrations. *E. coli* strain MC1061 [*F' lacIQ lacZM15 Tn10* (*tet*)] was used for the routine construction and maintenance of plasmids. When required, antibiotics were used at the following concentrations: 100 μg ml^{-1} ampicillin, 100 μg ml^{-1} spectinomycin, 1 μg ml^{-1} erythromycin and 25 μg ml^{-1} lincomycin. Strains were constructed using standard protocols. Phage transductions were carried out as previously described (Verhamme *et al.*, 2007). A full list of strains used in this study is provided in Table S1.

Construction of deletion strains

To construct the in-frame deletion of *motB* an approach similar to that previously described was used (Kiley and Stanley-Wall, 2010). The upstream region of *motB* was amplified from genomic DNA using primers NSW874 and NSW875, purified and digested with BamHI and XbaI, using the restriction sites engineered into the primers and ligated into pUC19 (Vieira and Messing, 1982) cut the same to yield pNW651. The downstream region of *motB* was amplified using primers NSW876

and NSW877, purified, and digested with XbaI and BamHI, using the restriction sites engineered into the primers and ligated into pUC19 cut the same to yield pNW652. The upstream and downstream regions of *motB* were released from pNW651 and pNW652 with BamHI and XbaI and XbaI and EcoRI, respectively, and ligated into pUC19 cut with BamHI and EcoRI to produce plasmid pNW653. The Δ*motB* region was then cut from pNW653 with BamHI and EcoRI and ligated into pMAD cut the same (Arnaud *et al*., 2004). Strain NRS3494 (NCIB3610 Δ*motB*) was generated by integration and curing of the region contained in pNW654 in strain NCIB3610. An in-frame deletion of *motAB* was constructed in a similar manner. The upstream region of *motA* was amplified from genomic DNA using primers NSW965 and NSW966, purified and digested with BamHI and XbaI, using restriction sites engineered into the primers. The downstream region of *motB* was excised from pNW652 with XbaI and EcoRI. The upstream region of *motA* and downstream region of *motB* were ligated into pUC19 cut with BamHI and EcoRI to yield pNW1019. The Δ*motAB* region was then cloned into pMAD cut with BamHI and EcoRI to yield pNW1021. Strain NRS3744 (NCIB3610 Δ*motAB*) was generated by integration and curing of the region contained in pNW1021 in strain NCIB3610. All primers and plasmids used in this study are listed in Tables S2 and S3.

Reverse transcription (RT)-PCR

RNA was isolated from the following strains grown to mid-exponential phase: NCIB3610 (wild-type), NRS3494 (Δ*motB*) and NRS3775 (Δ*motB* + $P_{spankhy}$-*motB-lacI*) with or without 50 μM IPTG. RNA isolation was carried out as described previously (Kiley and Stanley-Wall, 2010) using the RiboPure Bacteria RNA Isolation Kit (Ambion), according to manufacturer's instructions. cDNA was synthesized using random hexamers and subsequently treated with Rnase H for 20 min at 37°C. To amplify internal gene products the following primer pairs were used: NSW1474 and NSW1475 (*pgsB*), NSW1604 and NSW1605 (*pgdS*) and DEN5 and DEN7 (16S rRNA).

Motility assays

Swimming and swarming analyses were performed as described before (Verhamme *et al*., 2007) using low-salt LB (5 g NaCl, 5 g yeast extract, 10 g tryptone per litre) supplemented with 0.4% or 0.7% Bacto agar (Invitrogen) respectively. Plates were incubated at 37°C and the extent of swimming or swarming noted at defined intervals.

Whole-cell analysis of Hag

Proteins were collected from planktonic cultures grown to mid-exponential phase. Briefly, cells were harvested by centrifugation at 4700 *g*. Cells were suspended in 1× Bugbuster Master Mix (Novagen) and lysed according to manufacturer's instructions. Seven micrograms of proteins were resolved by SDS-PAGE and stained with Coomassie Brilliant Blue. Hag protein was identified by 1D SDS-PAGE analysis of the total cellular proteins by comparison with the Δ*hag* strain (DS1677). The protein identity was confirmed by mass spectrometry (FingerPrints Proteomics and Mass Spectrometry Facility, University of Dundee) (Diethmaier *et al*., 2011).

Inhibition of flagellar rotation with an anti-Hag antibody

A wild-type strain carrying the P*degU–lacZ* transcriptional reporter fusion (NRS4351) was grown to OD_{600} of 0.4 in LB prior to addition of a 1 in 20 dilution of Hag antibody (Prof. Kursad Turgay) or pre-immune sera. To check the motility of the cells, a small sample of each culture was imaged by microscopy at each time point. A thin channel was generated between a glass slide and the coverslip using double sided sticky tape. Cells were injected into the viewing chamber and visualized using a Zeiss Axio10 Imager.M10 under a Zeiss 40× EC Plan-NEO FLUAR objective and recorded using the high speed digital recorder function in the Zen lite software (Zeiss). Samples (0.5 ml) were collected by centrifugation over the course of the experiment, frozen at –20°C and later analysed by β-galactosidase assay.

β-Galactosidase assays

The β-galactosidase activity of strains harbouring *lacZ* promoter reporter fusions was measured as previously described (Verhamme *et al*., 2007; 2009). The values presented are the average β-galactosidase activities in Miller Units (Miller, 1972) determined from at least three independent samples. Error bars represent the standard error of the mean.

Protease plate assays

Analysis of protease production was carried out as previously described (Verhamme *et al*., 2007). Briefly, secreted protease production was analysed using LB agar plates supplemented with 1.5% (w/v) milk. *B. subtilis* cultures were grown to mid-late exponential phase in LB and 10 μl of culture spotted on to each plate (containing IPTG as required) and incubated at 37°C for 18 h prior to being photographed.

Secreted protease activity assay

Culture samples were collected by centrifugation (17 000 *g* for 5 min) after which the supernatant was removed and stored at –20°C until use. To determine extracellular protease activity the azocasein assay (Braun and Schmitz, 1980) was performed. A 150 μl aliquot of thawed supernatant was mixed with 500 μl of 2% w/v azocasein (Sigma), along with 100 μl of Tris-HCl (pH 8.0) and 650 μl of ddH_2O. A blank sample was prepared containing ddH_2O in the place of the supernatant and a media only control sample containing LB in the place of the supernatant was also prepared. The samples were incubated for 1 h at 30°C, after which 375 μl of 14% v/v perchloric acid was added to stop each reaction. The samples were centrifuged (17 000 *g* for 5 min) and 750 μl of the supernatant was mixed directly in a cuvette with 75 μl of 10 M NaOH and the absorbance at 436 nm was measured using a spectrophotometer. The background activity of the medium-only

control was subtracted and activity was calculated as ΔA_{436} h^{-1} ml^{-1} per mg of total protein.

γ-PGA isolation

The method used for γ-PGA isolation was adapted from Stanley and Lazazzera, (2005). Briefly, cells were grown overnight on LB lawn plates, collected in 5 ml LB and diluted to an OD_{600} of 0.01. Cells were grown to stationary phase in 25 ml LB and harvested by centrifugation. A total of 10 ml of the culture supernatant was retained and the cell pellet suspended in 2.5 ml of 0.14 mM NaCl. The cells were again harvested by centrifugation and the supernatant from the wash added to the previously collected supernatant. The combined supernatants were brought to pH 2.0 with concentrated sulphuric acid and incubated at 4°C overnight. To precipitate γ-PGA, 40 ml 100% ethanol was added to the supernatant and the sample incubated at –20°C for a minimum of 10 min. The γ-PGA was harvested by centrifugation and the resulting pellet suspended in 1 ml 10 mM Tris-HCl pH 8.0 and concentrated in a vacuum concentrator. The resulting γ-PGA pellet was suspended in 200 µl 10 mM Tris-HCl pH 8.0 and analysed by SDS-PAGE. Gels were stained with 0.5% methylene blue in 3% acetic acid for 30 min and de-stained in H_2O.

Acknowledgements

L.S.C. is the recipient of a Wellcome Trust PhD studentship (093714/Z/10/Z). V.L.M. was funded by Biotechnology and Biological Sciences Research Council grant number (BB/I006915/1). E.B. was funded by a College of Life Sciences James Black Scholarship, through the Wellcome Trust ISSF grant (097818/Z/11/A). A.O. was the recipient of a Biotechnology and Biological Sciences Research Council Doctoral Training Account grant (BB/D526161/1). The proteomic facilities in the College of Life Sciences are supported by a Wellcome Trust Strategic Award (097945/B/11/Z). The funders had no role in study design, data collection and analysis, decision to publish or preparation of the manuscript. We thank Zoe Landsborough for construction of pNW1060, Prof. Kürsad Turgay for the kind gift of the anti-Hag antibodies, and Dr Robert Ryan and members of the NSW laboratory for critical review of the manuscript. Finally, we thank Prof. Judy Armitage for many helpful and informative discussions.

References

Amati, G., Bisicchia, P., and Galizzi, A. (2004) DegU-P represses expression of the motility *fla-che* operon in *Bacillus subtilis*. *J Bacteriol* **186:** 6003–6014.

Arnaud, M., Chastanet, A., and Debarbouille, M. (2004) New vector for efficient allelic replacement in naturally nontransformable, low-GC-content, gram-positive bacteria. *Appl Environ Microbiol* **70:** 6887–6891.

Belas, R., and Suvanasuthi, R. (2005) The ability of *Proteus mirabilis* to sense surfaces and regulate virulence gene expression involves FliL, a flagellar basal body protein. *J Bacteriol* **187:** 6789–6803.

Blair, K.M., Turner, L., Winkelman, J.T., Berg, H.C., and Kearns, D.B. (2008) A molecular clutch disables flagella in the *Bacillus subtilis* biofilm. *Science* **320:** 1636–1638.

Boehm, A., Kaiser, M., Li, H., Spangler, C., Kasper, C.A., Ackermann, M., *et al*. (2010) Second messenger-mediated adjustment of bacterial swimming velocity. *Cell* **141:** 107–116.

Branda, S.S., Gonzalez-Pastor, J.E., Ben-Yehuda, S., Losick, R., and Kolter, R. (2001) Fruiting body formation by *Bacillus subtilis*. *Proc Natl Acad Sci USA* **98:** 11621–11626.

Branda, S.S., Chu, F., Kearns, D.B., Losick, R., and Kolter, R. (2006) A major protein component of the *Bacillus subtilis* biofilm matrix. *Mol Microbiol* **59:** 1229–1238.

Braun, T.F., Poulson, S., Gully, J.B., Empey, J.C., Van Way, S., Putnam, A., and Blair, D.F. (1999) Function of proline residues of MotA in torque generation by the flagellar motor of *Escherichia coli*. *J Bacteriol* **181:** 3542–3551.

Braun, V., and Schmitz, G. (1980) Excretion of a protease by *Serratia marcescens*. *Arch Microbiol* **124:** 55–61.

Burbulys, D., Trach, K.A., and Hoch, J.A. (1991) Initiation of sporulation in *B. subtilis* is controlled by a multicomponent phosphorelay. *Cell* **64:** 545–552.

Calvio, C., Osera, C., Amati, G., and Galizzi, A. (2008) Autoregulation of *swrAA* and motility in *Bacillus subtilis*. *J Bacteriol* **190:** 5720–5728.

Candela, T., and Fouet, A. (2006) Poly-gamma-glutamate in bacteria. *Mol Microbiol* **60:** 1091–1098.

Chai, Y., Norman, T., Kolter, R., and Losick, R. (2011) Evidence that metabolism and chromosome copy number control mutually exclusive cell fates in *Bacillus subtilis*. *EMBO J* **30:** 1402–1413.

Chernyak, B.V., Dibrov, P.A., Glagolev, A.N., Sherman, M.Y., and Skulachev, V.P. (1983) A novel type of energetics in a marine alkali-tolerant bacterium delta-muna-driven motility and sodium cycle. *FEBS Lett* **164:** 38–42.

Chevance, F.F., and Hughes, K.T. (2008) Coordinating assembly of a bacterial macromolecular machine. *Nat Rev Microbiol* **6:** 455–465.

Costerton, J.W., Lewandowski, Z., Caldwell, D.E., Korber, D.R., and Lappin-Scott, H.M. (1995) Microbial biofilms. *Annu Rev Microbiol* **49:** 711–745.

Cusick, K., Lee, Y.Y., Youchak, B., and Belas, R. (2012) Perturbation of FliL interferes with *Proteus mirabilis* swarmer cell gene expression and differentiation. *J Bacteriol* **194:** 437–447.

Dahl, M.K., Msadek, T., Kunst, F., and Rapoport, G. (1991) Mutational analysis of the *Bacillus subtilis* DegU regulator and its phosphorylation by the DegS protein kinase. *J Bacteriol* **173:** 2539–2547.

Dahl, M.K., Msadek, T., Kunst, F., and Rapoport, G. (1992) The phosphorylation state of the DegU response regulator acts as a molecular switch allowing either degradative enzyme synthesis or expression of genetic competence in *Bacillus subtilis*. *J Biol Chem* **267:** 14509–14514.

Dervyn, E., Noirot-Gros, M.F., Mervelet, P., McGovern, S., Ehrlich, S.D., Polard, P., and Noirot, P. (2004) The bacterial condensin/cohesin-like protein complex acts in DNA repair and regulation of gene expression. *Mol Microbiol* **51:** 1629–1640.

Diethmaier, C., Pietack, N., Gunka, K., Wrede, C., Lehnik-Habrink, M., Herzberg, C., *et al*. (2011) A novel factor controlling bistability in *Bacillus subtilis*: the YmdB protein affects flagellin expression and biofilm formation. *J Bacteriol* **193:** 5997–6007.

Do, T.H., Suzuki, Y., Abe, N., Kaneko, J., Itoh, Y., and Kimura, K. (2011) Mutations suppressing the loss of DegQ function in *Bacillus subtilis* (natto) poly-gamma-glutamate synthesis. *Appl Environ Microbiol* **77:** 8249–8258.

Earl, A.M., Eppinger, M., Fricke, W.F., Rosovitz, M.J., Rasko, D.A., Daugherty, S., *et al*. (2012) Whole-genome sequences of *Bacillus subtilis* and close relatives. *J Bacteriol* **194:** 2378–2379.

Flemming, H.C., and Wingender, J. (2010) The biofilm matrix. *Nat Rev Microbiol* **8:** 623–633.

Friedlander, R.S., Vlamakis, H., Kim, P., Khan, M., Kolter, R., and Aizenberg, J. (2013) Bacterial flagella explore microscale hummocks and hollows to increase adhesion. *Proc Natl Acad Sci USA* **110:** 5624–5629.

Fujita, M., Gonzalez-Pastor, J.E., and Losick, R. (2005) High- and low-threshold genes in the Spo0A regulon of *Bacillus subtilis*. *J Bacteriol* **187:** 1357–1368.

Gode-Potratz, C.J., Kustusch, R.J., Breheny, P.J., Weiss, D.S., and McCarter, L.L. (2011) Surface sensing in *Vibrio parahaemolyticus* triggers a programme of gene expression that promotes colonization and virulence. *Mol Microbiol* **79:** 240–263.

Guttenplan, S.B., and Kearns, D.B. (2013) Regulation of flagellar motility during biofilm formation. *FEMS Microbiol Rev* doi:10.1111/1574-6976.12018 [Epub ahead of print].

Guttenplan, S.B., Blair, K.M., and Kearns, D.B. (2010) The EpsE flagellar clutch is bifunctional and synergizes with EPS biosynthesis to promote *Bacillus subtilis* biofilm formation. *PLoS Genet* **6:** e1001243.

Guttenplan, S.B., Shaw, S., and Kearns, D.B. (2013) The cell biology of peritrichous flagella in *Bacillus subtilis*. *Mol Microbiol* **87:** 211–229.

Guvener, Z.T., and Harwood, C.S. (2007) Subcellular location characteristics of the *Pseudomonas aeruginosa* GGDEF protein, WspR, indicate that it produces cyclic-di-GMP in response to growth on surfaces. *Mol Microbiol* **66:** 1459–1473.

Hamon, M.A., and Lazazzera, B.A. (2001) The sporulation transcription factor Spo0A is required for biofilm development in *Bacillus subtilis*. *Mol Microbiol* **42:** 1199–1209.

Hobley, L., Ostrowski, A., Rao, F., Bromley, K., Porter, M., Prescott, A., *et al*. (2013) BslA is a self-assembling bacterial hydrophobin that coats the *Bacillus subtilis* biofilm. *Proc Natl Acad Sci USA* doi:10.1073/pnas.130639110.

Hsueh, Y.H., Cozy, L.M., Sham, L.T., Calvo, R.A., Gutu, A.D., Winkler, M.E., and Kearns, D.B. (2011) DegU-phosphate activates expression of the anti-sigma factor FlgM in *Bacillus subtilis*. *Mol Microbiol* **81:** 1092–1108.

Kawagishi, I., Imagawa, M., Imae, Y., McCarter, L., and Homma, M. (1996) The sodium-driven polar flagellar motor of marine *Vibrio* as the mechanosensor that regulates lateral flagellar expression. *Mol Microbiol* **20:** 693–699.

Kearns, D.B., and Losick, R. (2005) Cell population heterogeneity during growth of *Bacillus subtilis*. *Genes Dev* **19:** 3083–3094.

Kearns, D.B., Chu, F., Rudner, R., and Losick, R. (2004) Genes governing swarming in *Bacillus subtilis* and evidence for a phase variation mechanism controlling surface motility. *Mol Microbiol* **52:** 357–369.

Kiley, T.B., and Stanley-Wall, N.R. (2010) Post-translational control of *Bacillus subtilis* biofilm formation mediated by tyrosine phosphorylation. *Mol Microbiol* **78:** 947–963.

Kim, W., and Surette, M.G. (2004) Metabolic differentiation in actively swarming *Salmonella*. *Mol Microbiol* **54:** 702–714.

Kobayashi, K. (2007) Gradual activation of the response regulator DegU controls serial expression of genes for flagellum formation and biofilm formation in *Bacillus subtilis*. *Mol Microbiol* **66:** 395–409.

Kobayashi, K., and Iwano, M. (2012) BslA (YuaB) forms a hydrophobic layer on the surface of *Bacillus subtilis* biofilms. *Mol Microbiol* **85:** 51–66.

Kojima, S., and Blair, D.F. (2004) Solubilization and purification of the MotA/MotB complex of *Escherichia coli*. *Biochemistry* **43:** 26–34.

Lee, Y.Y., Patellis, J., and Belas, R. (2013) Activity of *Proteus mirabilis* FliL is viscosity dependent and requires extragenic DNA. *J Bacteriol* **195:** 823–832.

Lele, P.P., Hosu, B.G., and Berg, H.C. (2013) Dynamics of mechanosensing in the bacterial flagellar motor. *Proc Natl Acad Sci USA* **110:** 11839–11844.

Lemon, K.P., Higgins, D.E., and Kolter, R. (2007) Flagellar motility is critical for *Listeria monocytogenes* biofilm formation. *J Bacteriol* **189:** 4418–4424.

Li, G., Brown, P.J., Tang, J.X., Xu, J., Quardokus, E.M., Fuqua, C., and Brun, Y.V. (2012) Surface contact stimulates the just-in-time deployment of bacterial adhesins. *Mol Microbiol* **83:** 41–51.

Lopez, D., Fischbach, M.A., Chu, F., Losick, R., and Kolter, R. (2009a) Structurally diverse natural products that cause potassium leakage trigger multicellularity in *Bacillus subtilis*. *Proc Natl Acad Sci USA* **106:** 280–285.

Lopez, D., Vlamakis, H., and Kolter, R. (2009b) Generation of multiple cell types in *Bacillus subtilis*. *FEMS Microbiol Rev* **33:** 152–163.

Lopez, D., Vlamakis, H., Losick, R., and Kolter, R. (2009c) Paracrine signaling in a bacterium. *Genes Dev* **23:** 1631–1638.

Lopez, D., Vlamakis, H., and Kolter, R. (2010) Biofilms. *Cold Spring Harb Perspect Biol* **2:** a000398.

McCarter, L., Hilmen, M., and Silverman, M. (1988) Flagellar dynamometer controls swarmer cell differentiation of *V. parahaemolyticus*. *Cell* **54:** 345–351.

Manson, M.D., Tedesco, P., Berg, H.C., Harold, F.M., and Van der Drift, C. (1977) A protonmotive force drives bacterial flagella. *Proc Natl Acad Sci USA* **74:** 3060–3064.

Meister, M., Lowe, G., and Berg, H.C. (1987) The proton flux through the bacterial flagellar motor. *Cell* **49:** 643–650.

Miller, J. (1972) *Experiments in Molecular Genetics*. Cold Spring Harbor, NY: Cold Spring Harbor Laboratory.

Morikawa, M., Kagihiro, S., Haruki, M., Takano, K., Branda, S., Kolter, R., and Kanaya, S. (2006) Biofilm formation by a *Bacillus subtilis* strain that produces gamma-polyglutamate. *Microbiology* **152:** 2801–2807.

Motaleb, M.A., Pitzer, J.E., Sultan, S.Z., and Liu, J. (2011) A novel gene inactivation system reveals altered periplasmic flagellar orientation in a *Borrelia burgdorferi fliL* mutant. *J Bacteriol* **193:** 3324–3331.

Msadek, T., Kunst, F., Klier, A., and Rapoport, G. (1991) DegS–DegU and ComP–ComA modulator-effector pairs control expression of the *Bacillus subtilis* pleiotropic regulatory gene *degQ*. *J Bacteriol* **173:** 2366–2377.

Mukai, K., Kawata, M., and Tanaka, T. (1990) Isolation and phosphorylation of the *Bacillus subtilis degS* and *degU* gene products. *J Biol Chem* **265:** 20000–20006.

Murray, E.J., Kiley, T.B., and Stanley-Wall, N.R. (2009) A pivotal role for the response regulator DegU in controlling multicellular behaviour. *Microbiology* **155:** 1–8.

Nakano, M.M., Xia, L.A., and Zuber, P. (1991) Transcription initiation region of the *srfA* operon, which is controlled by the comP–comA signal transduction system in *Bacillus subtilis*. *J Bacteriol* **173:** 5487–5493.

O'Connor, J.R., Kuwada, N.J., Huangyutitham, V., Wiggins, P.A., and Harwood, C.S. (2012) Surface sensing and lateral subcellular localization of WspA, the receptor in a chemosensory-like system leading to c-di-GMP production. *Mol Microbiol* **86:** 720–729.

O'Toole, G., and Kolter, R. (1998) Flagellar and twitching motility are necessary for *Pseudomonas aeruginosa* biofilm development. *Mol Microbiol* **30:** 295–304.

O'Toole, G.A., Kaplan, H.B., and Kolter, R. (2000) Biofilm formation as microbial development. *Annu Rev Microbiol* **54:** 49–79.

Ogura, M., and Tsukahara, K. (2010) Autoregulation of the *Bacillus subtilis* response regulator gene *degU* is coupled with the proteolysis of DegU-P by ClpCP. *Mol Microbiol* **75:** 1244–1259.

Ogura, M., Shimane, K., Asai, K., Ogasawara, N., and Tanaka, T. (2003) Binding of response regulator DegU to the *aprE* promoter is inhibited by RapG, which is counteracted by extracellular PhrG in *Bacillus subtilis*. *Mol Microbiol* **49:** 1685–1697.

Ohsawa, T., Tsukahara, K., and Ogura, M. (2009) *Bacillus subtilis* response regulator DegU is a direct activator of *pgsB* transcription involved in gamma-poly-glutamic acid synthesis. *Biosci Biotechnol Biochem* **73:** 2096–2102.

Olmos, J., Bolanos, V., Causey, S., Ferrari, E., Bollvar, F., and Valle, F. (1996) A functional Spo0A is required for maximal *aprE* expression in *Bacillus subtilis*. *FEBS Lett* **381:** 29–31.

Osera, C., Amati, G., Calvio, C., and Galizzi, A. (2009) SwrAA activates poly-gamma-glutamate synthesis in addition to swarming in *Bacillus subtilis*. *Microbiology* **155:** 2282–2287.

Ostrowski, A., Mehert, A., Prescott, A., Kiley, T.B., and Stanley-Wall, N.R. (2011) YuaB functions synergistically with the exopolysaccharide and TasA amyloid fibers to allow biofilm formation by *Bacillus subtilis*. *J Bacteriol* **193:** 4821–4831.

Partridge, J.D., and Harshey, R.M. (2013) More than motility: *Salmonella* flagella contribute to overriding friction and facilitating colony hydration during swarming. *J Bacteriol* **195:** 919–929.

Patrick, J.E., and Kearns, D.B. (2012) Swarming motility and the control of master regulators of flagellar biosynthesis. *Mol Microbiol* **83:** 14–23.

Paul, K., Nieto, V., Carlquist, W.C., Blair, D.F., and Harshey, R.M. (2010) The c-di-GMP binding protein YcgR controls flagellar motor direction and speed to affect chemotaxis by a 'backstop brake' mechanism. *Mol Cell* **38:** 128–139.

Pilizota, T., Brown, M.T., Leake, M.C., Branch, R.W., Berry, R.M., and Armitage, J.P. (2009) A molecular brake, not a clutch, stops the *Rhodobacter sphaeroides* flagellar motor. *Proc Natl Acad Sci USA* **106:** 11582–11587.

Pratt, L.A., and Kolter, R. (1998) Genetic analysis of *Escherichia coli* biofilm formation: roles of flagella, motility, chemotaxis and type I pili. *Mol Microbiol* **30:** 285–293.

Rubinstein, S.M., Kolodkin-Gal, I., McLoon, A., Chai, L., Kolter, R., Losick, R., and Weitz, D.A. (2012) Osmotic pressure can regulate matrix gene expression in *Bacillus subtilis*. *Mol Microbiol* **86:** 426–436.

Ruzal, S.M., and Sanchez-Rivas, C. (1998) In *Bacillus subtilis* DegU-P is a positive regulator of the osmotic response. *Curr Microbiol* **37:** 368–372.

Serra, D.O., Richter, A.M., Klauck, G., Mika, F., and Hengge, R. (2013) Microanatomy at cellular resolution and spatial order of physiological differentiation in a bacterial biofilm. *mBio* **4:** e00103–e00113.

Shank, E.A., and Kolter, R. (2011) Extracellular signaling and multicellularity in *Bacillus subtilis*. *Curr Opin Microbiol* **14:** 741–747.

Sharp, L.L., Zhou, J., and Blair, D.F. (1995) Tryptophan-scanning mutagenesis of MotB, an integral membrane protein essential for flagellar rotation in *Escherichia coli*. *Biochemistry* **34:** 9166–9171.

Srivatsan, A., Han, Y., Peng, J., Tehranchi, A.K., Gibbs, R., Wang, J.D., and Chen, R. (2008) High-precision, whole-genome sequencing of laboratory strains facilitates genetic studies. *PLoS Genet* **4:** e1000139.

Stanley, N.R., and Lazazzera, B.A. (2005) Defining the genetic differences between wild and domestic strains of *Bacillus subtilis* that affect poly-gamma-dl-glutamic acid production and biofilm formation. *Mol Microbiol* **57:** 1143–1158.

Suaste-Olmos, F., Domenzain, C., Mireles-Rodriguez, J.C., Poggio, S., Osorio, A., Dreyfus, G., and Camarena, L. (2010) The flagellar protein FliL is essential for swimming in *Rhodobacter sphaeroides*. *J Bacteriol* **192:** 6230–6239.

Veening, J.W., Igoshin, O.A., Eijlander, R.T., Nijland, R., Hamoen, L.W., and Kuipers, O.P. (2008) Transient heterogeneity in extracellular protease production by *Bacillus subtilis*. *Mol Syst Biol* **4:** 184.

Verhamme, D.T., Kiley, T.B., and Stanley-Wall, N.R. (2007) DegU co-ordinates multicellular behaviour exhibited by *Bacillus subtilis*. *Mol Microbiol* **65:** 554–568.

Verhamme, D.T., Murray, E.J., and Stanley-Wall, N.R. (2009) DegU and Spo0A jointly control transcription of two loci required for complex colony development by *Bacillus subtilis*. *J Bacteriol* **191:** 100–108.

Vieira, J., and Messing, J. (1982) The pUC plasmids, an M13mp7-derived system for insertion mutagenesis and sequencing with synthetic universal primers. *Gene* **19:** 259–268.

Vlamakis, H., Chai, Y., Beauregard, P., Losick, R., and Kolter, R. (2013) Sticking together: building a biofilm the *Bacillus subtilis* way. *Nat Rev Microbiol* **11:** 157–168.

Wang, Q., Frye, J.G., McClelland, M., and Harshey, R.M. (2004) Gene expression patterns during swarming in *Salmonella typhimurium*: genes specific to surface growth and putative new motility and pathogenicity genes. *Mol Microbiol* **52:** 169–187.

Wang, Q., Suzuki, A., Mariconda, S., Porwollik, S., and Harshey, R.M. (2005) Sensing wetness: a new role for the bacterial flagellum. *EMBO J* **24:** 2034–2042.

Watnick, P., and Kolter, R. (1999) Steps in the development of a *Vibrio cholerae* El Tor biofilm. *Mol Microbiol* **34:** 586–595.
Watnick, P., and Kolter, R. (2000) Biofilm, city of microbes. *J Bacteriol* **182:** 2675–2679.
Watson, P.Y., and Fedor, M.J. (2012) The *ydaO* motif is an ATP-sensing riboswitch in *Bacillus subtilis*. *Nat Chem Biol* **8:** 963–965.
Wolfe, A.J., Chang, D.E., Walker, J.D., Seitz-Partridge, J.E., Vidaurri, M.D., Lange, C.F., *et al*. (2003) Evidence that acetyl phosphate functions as a global signal during biofilm development. *Mol Microbiol* **48:** 977–988.
Wolfe, A.J., Parikh, N., Lima, B.P., and Zemaitaitis, B. (2008) Signal integration by the two-component signal transduction response regulator CpxR. *J Bacteriol* **190:** 2314–2322.
Zhou, J., Lloyd, S.A., and Blair, D.F. (1998a) Electrostatic interactions between rotor and stator in the bacterial flagellar motor. *Proc Natl Acad Sci USA* **95:** 6436–6441.
Zhou, J., Sharp, L.L., Tang, H.L., Lloyd, S.A., Billings, S., Braun, T.F., and Blair, D.F. (1998b) Function of protonatable residues in the flagellar motor of *Escherichia coli*: a critical role for Asp 32 of MotB. *J Bacteriol* **180:** 2729–2735.
Zorraquino, V., Garcia, B., Latasa, C., Echeverz, M., Toledo-Arana, A., Valle, J., *et al*. (2013) Coordinated cyclic-di-GMP repression of *Salmonella* motility through YcgR and cellulose. *J Bacteriol* **195:** 417–428.

Supporting information

Additional supporting information may be found in the online version of this article at the publisher's web-site.

Molecular Microbiology (2014) 93(4), 587–598 ■
doi:10.1111/mmi.12697
First published online 18 July 2014

MicroReview

Biofilm formation by *Bacillus subtilis*: new insights into regulatory strategies and assembly mechanisms

Lynne S. Cairns, Laura Hobley and Nicola R. Stanley-Wall*
Division of Molecular Microbiology, College of Life Sciences, University of Dundee, Dundee DD1 5EH, UK.

Summary

Biofilm formation is a social behaviour that generates favourable conditions for sustained survival in the natural environment. For the Gram-positive bacterium *Bacillus subtilis* the process involves the differentiation of cell fate within an isogenic population and the production of communal goods that form the biofilm matrix. Here we review recent progress in understanding the regulatory pathways that control biofilm formation and highlight developments in understanding the composition, function and structure of the biofilm matrix.

Introduction

It is now recognized that the majority of microbes live in complex sessile communities called biofilms. In the biofilm individual cells are held together by a self-produced extracellular polymeric matrix commonly comprised of polysaccharides, proteins and DNA (Branda *et al*., 2005). For microbes, the biofilm lifestyle confers several advantages. For example, inhabitants can access hard to reach nutrients and receive protection from fluctuations in environmental conditions (Costerton *et al*., 1995). Indeed, due to these properties, biofilms have been harnessed in industrial settings for bioremediation purposes (Halan *et al*., 2012) and additionally exhibit the potential to be used in agricultural settings as a biological alternative to petrochemical derived fertilizers (Bais *et al*., 2004). However, one corollary is that biofilms frequently present problems with regard to public health, particularly due to their ability to colonize both natural and artificial surfaces within the human body which can result in chronic infections (Hall *et al*., 2014). Likewise, biofilms are problematic in industrial settings where their formation in cooling towers and pipelines, for example, can have serious implications (Liu *et al*., 2009).

While most natural biofilms are polymicrobial in composition, a great deal has been learnt, and remains to be discovered, from the analysis of single-species biofilms. Studies to investigate the molecular basis of biofilm formation by the Gram-positive soil dwelling bacterium *Bacillus subtilis* have been extensive since the recognition of its capability to form biofilms (Branda *et al*., 2001; Hamon and Lazazzera, 2001). Undeniably, this research has revealed many fundamental principles that underpin biofilm assembly, including: how complex signalling networks are integrated during a complex multicellular process (Vlamakis *et al*., 2013), how bacteria are able to sense and respond to specific stimuli (Lopez and Kolter, 2010) and how isogenic bacterial cells differentiate to follow distinct cell lineages (Lopez *et al*., 2009). Furthermore, many details of the properties of the macromolecules that provide structure to the biofilm are now known (Romero *et al*., 2010; 2011; Kobayashi and Iwano, 2012; Hobley *et al*., 2013). Many of the concepts which stem from studies in the *B. subtilis* biofilm field have broad implications for a range of bacterial species.

B. subtilis biofilms are predominantly studied using an ancestral strain called NCIB3610 and three experimental systems, namely: pellicle formation, where the architecturally complex bacterial community forms at an air-liquid interface (Branda *et al*., 2001), rugose colony formation on semi-solid agar surfaces (Branda *et al*., 2001) (Fig. 1A) and finally, given the role of *B. subtilis* as a biocontrol agent in agricultural settings, an increasing number of studies have focussed on the formation of biofilms on plant roots (Bais *et al*., 2004; Chen *et al*., 2012; 2013; Beauregard *et al*., 2013). A fundamental principle linking these models is that *B. subtilis* functions as a cooperative community both by differentiation of the isogenic progenitor population into specialized cell types (Vlamakis *et al*., 2008) and by the production of shared macromolecules that form the

Accepted 26 June, 2014. *For correspondence. E-mail n.r.stanleywall@dundee.ac.uk; Tel. (+44) 1382 386335; Fax (+44) 1382 388216.

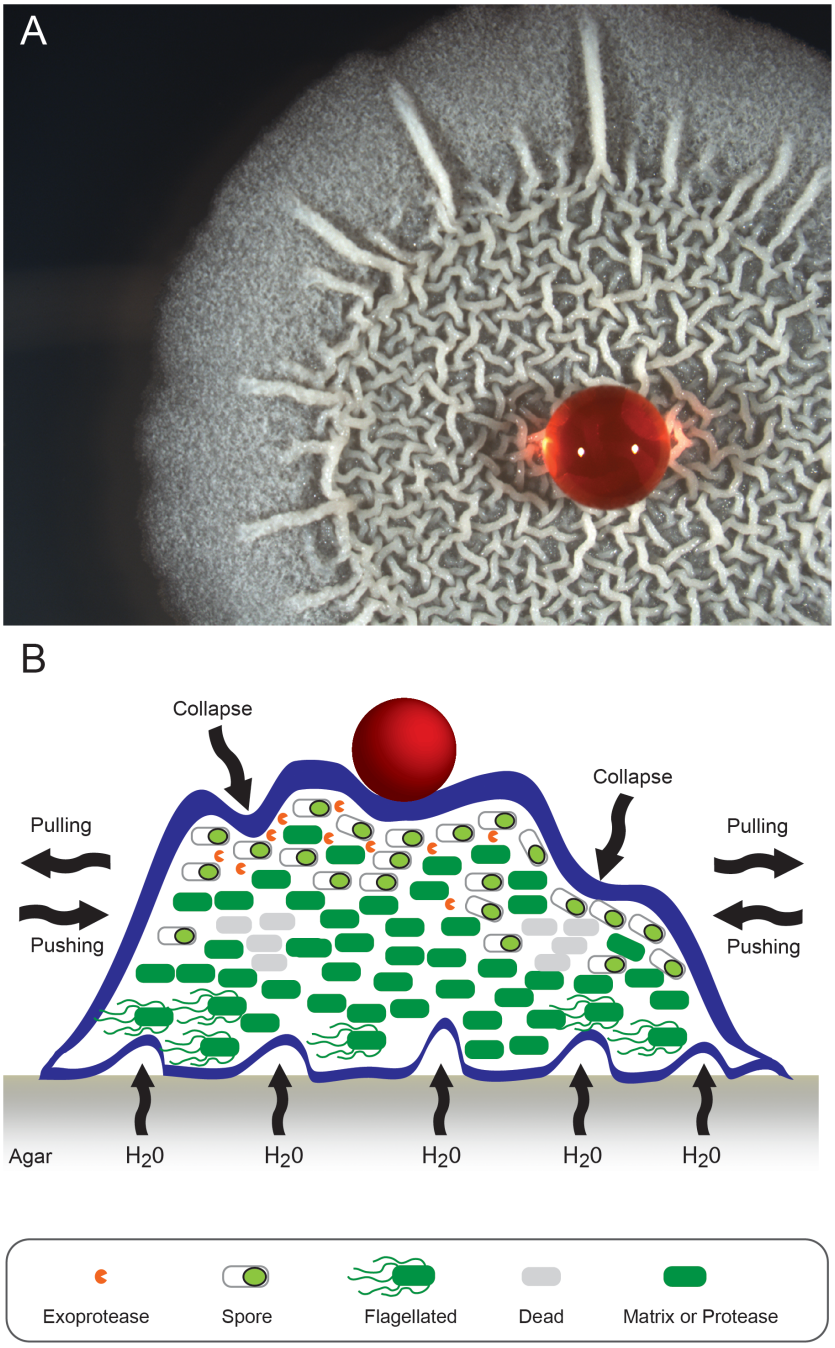

Fig. 1. *Bacillus subtilis* biofilm formation.
A. The mature biofilm exhibits a complex network of intertwined wrinkles and ridges and is highly hydrophobic. A 7 µl water droplet stained with red food colouring was placed on the biofilm.
B. The mature biofilm is generated as a consequence of many converging factors. This is represented schematically in cross-section in this figure. Contributing to biofilm formation is the differentiation of cell fate in the population, the death of cells at the base of wrinkles, the mechanical forces imparted by the biofilm matrix that both push or pull the community and the production of the extracellular matrix. The BslA coat is shown as a dark blue layer and the EPS and TasA fibres encased within this boundary but are not depicted. The red ball represents a water droplet and shows the hydrophobicity exhibited by the structure. Channels that allow fluids to flow into the biofilm are shown at the base of the structure.

communal biofilm matrix (Branda *et al*., 2006; Ostrowski *et al*., 2011). The *B. subtilis* biofilm matrix consists of proteins called TasA and TapA (Branda *et al*., 2006; Romero *et al*., 2011) and a large molecular weight secreted polysaccharide (Branda *et al*., 2001). Assembly of the mature biofilm also requires the presence of the biofilm coat protein called BslA (formerly YuaB) (Ostrowski *et al*., 2011; Kobayashi and Iwano, 2012; Hobley *et al*., 2013). Each of these extracellular molecules has the capacity to function as a 'communal good' in the community and production is subject to tight transcriptional control. Many aspects of the environmental signals and the regulatory pathways that influence *B. subtilis* biofilm formation have been extensively reviewed elsewhere (Lopez *et al*., 2009; Lopez and Kolter, 2010; Vlamakis *et al*., 2013). Therefore, here we will summarize the most recent insights into the regulatory networks that control biofilm formation, and will discuss the biosynthesis and function of the macromolecules that allow the mature three-dimensional biofilm to be constructed.

Regulating entry to biofilm formation

Biofilm formation is an energetically expensive process that requires the production of large macromolecules. Therefore, the decision to enter the biofilm state is tightly regulated and involves strict transcriptional control of the genes required to direct synthesis of matrix components. Phosphorylation, and thus activation, of the transcription factor Spo0A is central to biofilm initiation (Branda *et al*., 2001; Hamon and Lazazzera, 2001). Spo0A can be activated by various environmental signals that allow the cell to tune its behaviour to the local environment (Vlamakis *et al*., 2013) (Fig. 2). At threshold levels of Spo0A phosphate (Spo0A~P) two parallel pathways of anti-repression are triggered to allow transcription of operons critical for biofilm matrix production. The first anti-repression pathway ends with removal of the transition state regulator AbrB from DNA. AbrB directly binds to DNA to repress transcription from promoters involved in a plethora of cellular processes including those needed for biofilm formation (Hamon *et al*., 2004; Banse *et al*., 2008; Chu *et al*., 2008; Kobayashi, 2008; Verhamme *et al*., 2009; Chumsakul *et al*., 2011). AbrB itself is controlled by the Spo0A pathway by two distinct means: (i) Spo0A~P directly represses transcription of *abrB* (Strauch *et al*., 1990) and (ii) Spo0A~P promotes the expression of *abbA*, which encodes an AbrB anti-repressor (Banse *et al*., 2008). Structural studies have recently demonstrated that AbbA functions as a DNA mimetic for AbrB binding, and thus AbbA binds to AbrB to sequester the repressor away from target DNA (Tucker *et al*., 2014) (Fig. 2).

The second anti-repression pathway revolves around the transcriptional repressor SinR which directly inhibits transcription from the 15-gene *eps* operon (required for biosynthesis of the extracellular polysaccharide) and the *tapA-sipW-tasA* (hereafter *tapA*) operon (Kearns *et al*., 2005; Chu *et al*., 2008). The regulatory circuitry that underpins this pathway culminates in bimodal transcription of the *eps* and *tapA* operons (Chai *et al*., 2008). The repressive effect of SinR is alleviated by an anti-repressor protein named SinI. As with production of AbbA (Banse *et al*., 2008), transcription of the *sinI* coding region is triggered by threshold levels of Spo0A~P (Fujita *et al*., 2005). SinI binds to SinR in an essentially irreversible manner, forming a heterodimeric complex (Bai *et al*., 1993; Lewis *et al*., 1998; Scott *et al*., 1999; Newman *et al*., 2013). This leaves SinR unable to occlude target promoters, allowing transcription of target genes (Bai *et al*., 1993). Interestingly, while *sinR* is expressed in most cells, *sinI* is only transcribed by a small subpopulation (Chai *et al*., 2008). Given that a threshold level of SinI is needed to allow SinR inhibition, this leads to bimodal transcription of the *eps* and *tapA* operons (Chai *et al*., 2008). A second anti-repressor that binds to SinR, called SlrA, has also been discovered (Kobayashi, 2008; Chai *et al*., 2009). Crucially, the transcriptional regulation of *slrA* is distinct to that of *sinI*; *slrA* transcription is under the control of the transcriptional repressor YwcC, although the signal that relieves this repression is unknown (Kobayashi, 2008; Chai *et al*., 2009) (Fig. 2). However, this likely allows the integration of multiple upstream signals to repress SinR activity and activate biofilm matrix gene expression. Regulation of SinR is not restricted to transcriptional and post-translational mechanisms. Recent data link low serine levels in the cell with a decrease in the production of SinR (Subramaniam *et al*., 2013), which correspondingly triggers biofilm formation.

The action of SinR during biofilm formation is further complicated by SlrR. The *slrR* gene is under the transcriptional control of SinR and is thus expressed in the presence of high levels of SinI (Chai *et al*., 2010b). Induction of SlrR production stimulates transcription of the *tapA* and *eps* promoters (Chu *et al*., 2008; Kobayashi, 2008; Murray *et al*., 2009b), supporting the designation of SlrR as an activator of matrix production and biofilm formation (Kobayashi, 2008; Chai *et al*., 2010b). SlrR acts by binding to SinR with high affinity at equimolar stoichiometry (Chai *et al*., 2010c; Newman *et al*., 2013). This results in SinR being unable to bind to the *eps* and *tapA* promoter regions and also in the re-purposing of SinR function. The SlrR:SinR complex has unique DNA binding properties and represses transcription of genes required for motility and autolysins (Chai *et al*., 2010c). The net outcome is a concomitant repression of motility and autolysin genes with the activation of matrix genes, thereby promoting the transition from a motile state to biofilm formation (Chai *et al*., 2010c) (Fig. 2B). As SlrR re-purposes SinR activity, and prevents binding to target promoters (including that of *slrR*), it facilitates continued transcription of *slrR*. This means that cells accumulate high levels of SlrR in a self-reinforcing negative feedback loop (Chai *et al*., 2010c). In short, a cell can exist in an SlrR-low state where motility genes are expressed but matrix genes repressed, or in an SlrR-high state where cells exist as chains and are able to transcribe genes required for the synthesis of the biofilm matrix (Chai *et al*., 2010c). Fluorescent reporter fusion constructs coupled with microfluidic devices have allowed analysis of the complex network at the single cell level (Norman *et al*., 2013). Data revealed that the number of generations for which the 'memory' of the SlrR-high state was inherited was directly correlated with the initial level of SlrR in the cell. Basically, the higher the starting level of SlrR the greater the number of generations for which matrix gene expression was propagated (Norman *et al*., 2013).

However, removal of SinR from the *eps*, *tapA* and *slrR* promoter regions is not sufficient to allow transcription of these operons to proceed. RemA and RemB are also essential for biofilm formation (Winkelman *et al*., 2009; 2013). RemA has recently been identified as a DNA

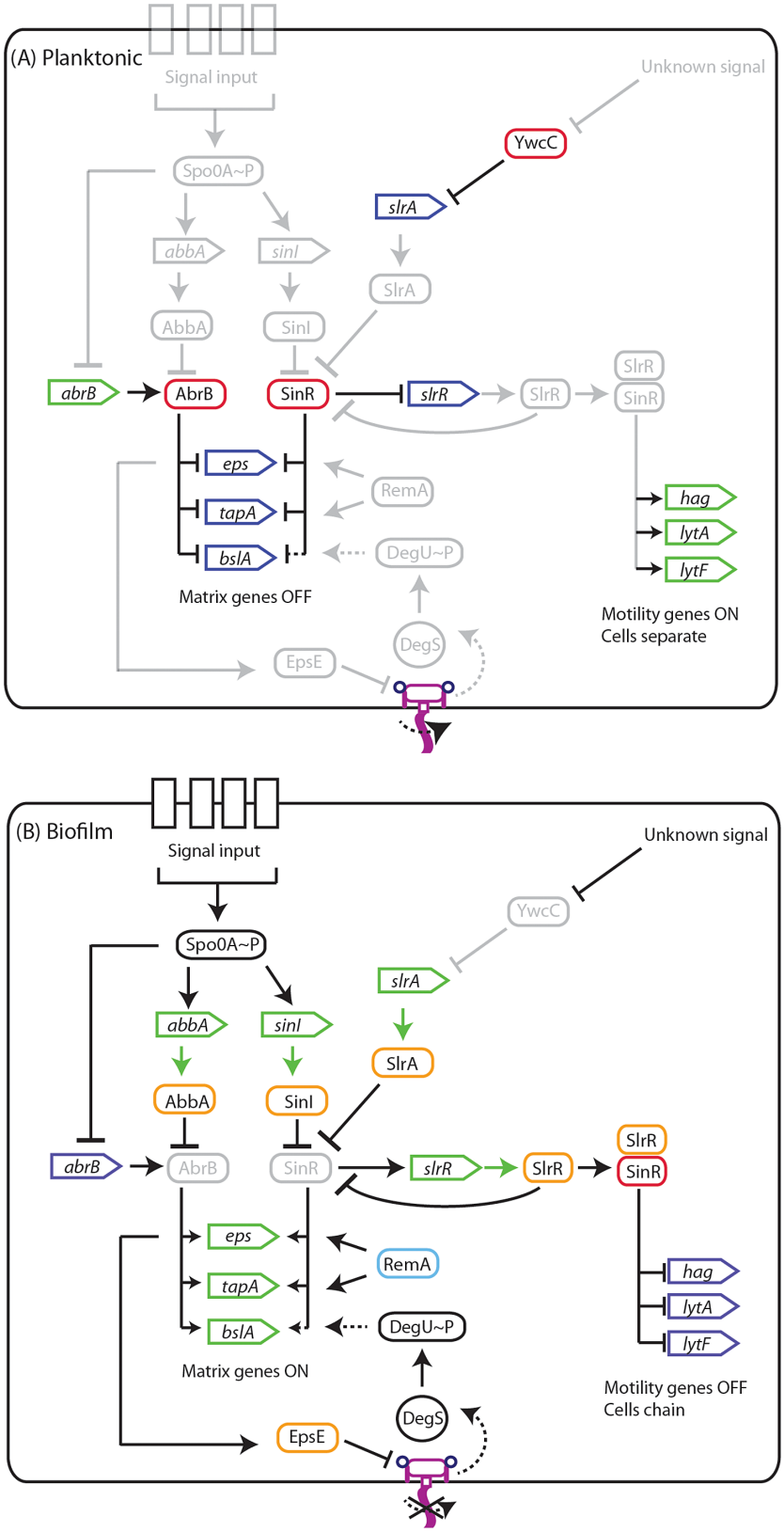

Fig. 2. Regulatory networks governing biofilm formation. Schematic of the complex regulatory pathways that control gene transcription during (A) planktonic growth and (B) growth as a biofilm. Rounded rectangles indicate proteins, triangles indicate open reading frames (ORFs), arrows indicate activation, T-bars indicate repression. Dashed arrows or T-bars indicate indirect activation and repression respectively. Green represents active gene transcription with a green arrow indicating translation, dark blue represents absence of gene transcription, red indicates a transcriptional repressor and orange indicates a protein–protein interaction. Light blue indicates a protein that is able to bind to DNA to activate transcription. Pink structure represents a flagellum, with the curved arrow indicating rotation and the cross indicating inhibition of flagellar rotation. Vertical rectangles labelled with "signal input" indicate sensor kinases for the Spo0A pathway, for more details see Vlamakis *et al.* (2013). Faded shading indicates parts of the pathway that are inactive.

binding protein that directly activates gene expression from the *eps* and *tapA* operons, and also promotes transcription of the *slrR* gene. RemA binds directly upstream from the *eps* promoter to sites that overlap with the SinR binding sites. Therefore, SinR acts as an anti-activator to occlude RemA binding to the promoter (Winkelman *et al*., 2013). RemA also binds upstream of the *tapA* promoter, but in this instance both SinR and RemA are able to bind simultaneously (Winkelman *et al*., 2013) (Fig. 2). These studies illustrate an additional pathway by which matrix gene expression can be controlled. How RemA itself is regulated is currently unknown but, intriguingly, on the chromosome *remA* is situated alongside genes connected to the stringent response, suggesting a link between *remA* and the nutrient status of the cell (Winkelman *et al*., 2009; 2013).

Inhibition of flagellar rotation triggers a signalling cascade

The transcription factor DegU is also intricately involved in regulating biofilm formation and exerts two opposing influences (Verhamme *et al*., 2007; Marlow *et al*., 2014b). DegU is phosphorylated by its cognate histidine kinase, DegS (Mukai *et al*., 1990). It is a pleiotropic regulator with roles in controlling many multicellular processes, including: swimming and swarming motility, biofilm formation, exoprotease production, γ-poly-D-L-glutamic acid production and sporulation (Murray *et al*., 2009a). The level of phosphorylated DegU (DegU~P) in the cell dictates which behaviour manifests. For example, activation of biofilm formation requires intermediate-levels of DegU~P and inhibition of biofilm formation requires high levels of DegU~P. Biofilm activation occurs when DegU~P indirectly promotes transcription of *bslA*, which encodes a hydrophobic biofilm coat protein (Kobayashi, 2007; Ostrowski *et al*., 2011; Hobley *et al*., 2013) (Figs 1B and 2). However, under conditions where DegU~P levels in the cell are high, biofilm formation is inhibited due to a lack of transcription from the *eps* and *tapA* operons (Verhamme *et al*., 2007; Marlow *et al*., 2014b). In this scenario a high percentage of the cells in the community enter the sporulation pathway (Marlow *et al*., 2014b). As sporulation is a developmental process that is triggered by high levels of Spo0A~P, these data suggest an as yet undefined link between high DegU~P levels and high Spo0A~P levels (Marlow *et al*., 2014b).

Several regulatory pathways have been identified as capable of controlling the level of DegU~P in the cell (Murray *et al*., 2009a); however, a definitive signalling molecule remains enigmatic. Recent work has indicated that the DegS-DegU pathway is activated by inhibition of flagellar rotation, as may conceivably occur when a cell senses a surface prior to adherence (Cairns *et al*., 2013; Chan *et al*., 2014). Indeed, perturbation of flagellar rotation by genetic or physical means triggered an increase in DegU~P levels. These findings suggest that upon sensing a surface DegS phosphorylates DegU to promote transcription of target genes, including *bslA*. In this way the arrest of flagellar rotation acts as an additional signal to initiate matrix synthesis (Cairns *et al*., 2013) (Fig. 2). Indeed, as will be described later, exopolysaccharide synthesis is intimately linked with a cessation of flagellar rotation, thus the cell has a mechanism to co-ordinate production of distinct components needed for biofilm assembly.

Cell differentiation during biofilm formation

Once biofilm formation has been initiated, the assembly and maturation process can begin. Biofilm formation begins with an isogenic population of progenitor cells. As the biofilm matures the resident cells differentiate to generate multiple cell types (Fig. 1B). Differentiation was first noted after macroscopic examination of the biofilm where a sporulation specific transcriptional reporter fusion was found to be expressed in aerial tips of the developing biofilm (Branda *et al*., 2001). Subsequent data derived from fluorescent cytological reporter fusions supported this conclusion (Veening *et al*., 2006). These initial findings were built upon and, using a combination of genetics and microscopy, individual cells were shown to follow a defined developmental programme that saw a motile cell become a matrix producer that terminally differentiated into a spore forming cell (Vlamakis *et al*., 2008). Consistent with this, all three cell types can be visualized within the biofilm at distinct locations and at distinct times, suggesting spatiotemporal regulation (Vlamakis *et al*., 2008). Further work has demonstrated that cells expressing genes required for extracellular protease production can also be found in the biofilm, and that they accumulate as the biofilm matures (Marlow *et al*., 2014a). Single cell time-lapse microscopy revealed that protease producing cells arise from cells that transcribe matrix genes and showed that both cell states can coexist over multiple generations (Marlow *et al*., 2014a). These findings infer that protease production may present an additional step in cell differentiation during biofilm maturation (Marlow *et al*., 2014a). It will be of interest to establish if protease producing cells transition into environmentally resistant spores or if they remain in the protease producing state and service the community in an altruistic manner through nutrient production and possibly by degradation of the extracellular biofilm matrix. It should be noted that highly comparable cellular differentiation events have been identified in the related entomopathogen *Bacillus thuringiensis* where defined cell fates have been observed during biofilm formation (Fagerlund *et al*., 2014). However, it

remains to be unequivocally established if the cell differentiation events observed constitute developmental processes *per se* or if they are a consequence of a regulatory response to environmental change and fluctuations in, for example, oxygen and nutrient levels, within the three dimensional structure of the biofilm (Fig. 1B).

Extracellular polysaccharides are needed for biofilm formation

The complex regulatory networks described above converge on the operons needed for biofilm matrix production. The dominant exopolysaccharide required for biofilm formation is synthesized by the protein products of the 15 gene *epsA-O* operon (referred to as the *eps* operon). To date, only a subset of proteins encoded by the *eps* operon has been studied in any detail. EpsA and EpsB act as a tyrosine kinase modulator and tyrosine kinase, respectively, and both are required for biofilm formation (Gerwig *et al*., 2014). The target proteins of EpsB remain uncharacterized and additionally there are no obvious targets that can be elucidated from examination of global phosphoproteomic datasets (Levine *et al*., 2006; Macek *et al*., 2007; Elsholz *et al*., 2012). However, in combination with previous work showing that the tyrosine kinase modulator, TkmA and tyrosine kinase, PtkA affect biofilm formation (Kiley and Stanley-Wall, 2010), a role for tyrosine phosphorylation in modulating biofilm formation is fully supported. Given that EpsB and PtkA appear to have differing effects on complex colony architecture, it may be reasonable to hypothesize that each has distinct protein targets (Gerwig *et al*., 2014). It is likely that global phosphoproteomic analyses performed under biofilm formation conditions will be needed to identify the targets of these kinases that are involved in biofilm formation.

The bi-functional protein, EpsE, is the best characterized protein encoded by the *eps* operon (Blair *et al*., 2008; Guttenplan *et al*., 2010). EpsE can inhibit flagellar rotation by interacting with the flagellar rotor protein FliG (Blair *et al*., 2008; Guttenplan *et al*., 2010). EpsE is thought to function by directly interacting with a number of surface exposed residues on FliG (Blair *et al*., 2008). This prohibits the generation of torque, resulting in a lack of flagellar motility. Further to its role as a flagellar clutch, EpsE also acts as a glycosyltransferase enzyme to promote the production of the extracellular polysaccharide (Blair *et al*., 2008; Guttenplan *et al*., 2010). The two functions of EpsE are genetically separable as mutations in residues required for interaction with FliG do not perturb biofilm morphology, while mutation of the glycosyltransferase active site does not interfere with the ability of EpsE to abrogate motility (Guttenplan *et al*., 2010). The clutch activity of EpsE likely allows the cell to inhibit motility quickly and efficiently and synergizes with glycosyltransferase activity to promote biofilm formation (Blair *et al*., 2008; Guttenplan *et al*., 2010). Additionally, induction of *epsE* transcription to perturb flagellar rotation increases the DegU~P level in the cell, leading to an increase in the transcription of *bslA* (Cairns *et al*., 2013) (Fig. 2). Consequently, EpsE provides a mechanism by which cells are able to inhibit flagellar motility and concurrently promote the synthesis of two distinct extracellular components needed for biofilm assembly.

The composition of the biofilm polysaccharide

The chemical composition of the polysaccharide synthesized by the products of the *eps* operon is elusive and currently two contrasting monosaccharide analyses are available. When *B. subtilis* strain NCIB3610 is grown in a defined medium containing glutamic acid and glycerol, the monosaccharides present in the carbohydrate biomass are galactose, glucose and *N*-acetyl-galactose (GalNAc). The prevalence of each sugar was largely dependent on the integrity of the *eps* operon (Chai *et al*., 2012) and these findings are largely supported by unpublished data from the NSW laboratory. Consistent with these data, genes involved in galactose metabolism are important for biofilm formation (Chai *et al*., 2012). Contrastingly, analysis of the polysaccharide biomass generated by strain NCIB3610 grown in TY broth (LB medium supplemented with magnesium sulphate and manganese sulphate) revealed an *eps* operon dependent mannose-dominated profile of monosaccharides (Jones *et al*., 2014). Therefore the molecular nature of the polysaccharide produced by the components of the *eps* operon remains to be established and may depend on the substrates available.

In addition to the EPS produced using the products of the *eps* operon, strains of *B. subtilis* commonly used for the analysis of biofilm formation have the genetic capability to synthesize the extracellular polysaccharide levan. Levan is a homopolymer of fructose and production is dependent on the levansucrase encoded by *sacB* (Benigar *et al*., 2014). During growth in the presence of sucrose, levan can be incorporated into the matrix of the pellicle (Dogsa *et al*., 2013) and can partially compensate for the absence of the *eps* gene cluster. While levan is not essential for biofilm formation *in vitro*, on the basis that sucrose is produced by plants, the presence of levan in the matrix may be relevant for biofilm formation by *B. subtilis* in its natural environment in the rhizosphere (Dogsa *et al*., 2013). Therefore it is logical to deduce that the exopolysaccharides made by *B. subtilis* that contribute to the biofilm matrix are likely to vary with growth conditions.

Extracellular proteins needed for biofilm formation

The main protein component of the biofilm matrix is TasA, which is encoded by the *tapA-sipW-tasA* operon (Branda

et al., 2006). TasA was first defined as a spore-associated protein with antimicrobial activity (also named CotN) (Stover and Driks, 1999). However, subsequent analysis showed that deletion of *tasA* was associated with a lack of biofilm formation when rugose colony and pellicle morphology were assessed (Branda *et al.*, 2006). The contribution of TasA to the matrix was found to be unique from that of the exopolysaccharide, as deletion of *tasA* produces a pellicle phenotype that is distinctive from that formed by an *eps* deletion strain (Branda *et al.*, 2006). Moreover, co-culture of the two single (otherwise isogenic) deletion strains results in a wild-type biofilm phenotype (Branda *et al.*, 2006), establishing that each product is a communal good that can be shared to benefit the entire population. TasA is localized to the biofilm matrix and its export from the cell is dependent on the SipW peptidase (Branda *et al.*, 2006). Electron microscopy coupled with immunogold-labelling detection techniques showed that TasA forms fibres that extend from the cells. These findings, in combination with further experiments showing that TasA could polymerize *in vitro* and was able to bind to an antibody specific for intermediates of amyloid aggregates, led to the description of TasA as an amyloid-like protein (Romero *et al.*, 2010). When TasA is purified from planktonic *B. subtilis* cells it is in an oligomeric state in solution. Fibre formation is stimulated by either a hydrophobic surface, such as electron microscopy grids (Romero *et al.*, 2010), or an acidic solution (Chai *et al.*, 2013). The secondary structure composition of TasA alters between its oligomeric and fibre states; in the oligomeric state the protein is α-helix rich, while during fibre formation a decrease in α-helices was observed along with a concurrent rise in β-sheet structure (Chai *et al.*, 2013). This is a phenomenon that has been previously reported for several eukaryotic amyloid-like proteins [Alzheimer amyloid peptide a-β (Fraser *et al.*, 1991), PI3 kinase (Zurdo *et al.*, 2001) and a Syrian hamster prion protein (Sokolowski *et al.*, 2003)].

The remaining protein encoded in the operon is TapA which forms a minor component of the TasA fibres and is required for their assembly (Romero *et al.*, 2011; 2014). In the absence of *tapA*, not only are the wild-type TasA decorated fibres unable to form, but the level of TasA protein is also reduced (Romero *et al.*, 2011). These data indicate that TapA is required for TasA stability and this may be due to the fibre form of TasA being more resistant to proteolytic cleavage than the unassembled oligomer. In agreement with these findings, phenotypically a *tapA* deletion strain is defective for pellicle formation (Romero *et al.*, 2011). Interestingly, it has been identified that SipW, the peptidase required for secretion of both TapA and TasA to the matrix, is a bi-functional protein that has a second, and specific, role in the development of submerged surface-adhered biofilm communities formed by a laboratory isolate (Terra *et al.*, 2012).

The bacterial hydrophobin

An additional extracellular component needed for biofilm formation is the bacterial hydrophobin BslA (Kobayashi and Iwano, 2012; Hobley *et al.*, 2013). BslA acts in a synergistic manner with both TasA and the EPS to allow biofilm assembly. This was concluded as deletion of *bslA* does not impact the synthesis of the high molecular weight polysaccharide or the generation of the TasA fibres synonymous with these matrix components, but does inhibit biofilm formation (Ostrowski *et al.*, 2011). BslA is essential for both the observed complexity and the extreme hydrophobicity displayed by the mature biofilm (Kobayashi and Iwano, 2012; Hobley *et al.*, 2013). While transcription of *bslA* is unimodal at the single cell level in the biofilm, BslA can be shared among non-producing members in a mixed strain biofilm (Hobley *et al.*, 2013). BslA is a surface-active protein that forms a hydrophobic layer surrounding the colony biofilm and a 'protein raft' below the floating pellicle (Kobayashi and Iwano, 2012; Hobley *et al.*, 2013). Consistent with these data, *in vitro* biophysical experiments demonstrated that BslA is capable of forming stable elastic films at hydrophilic to hydrophobic interfaces. Atomic level resolution of the BslA structure identified that BslA consists of two domains – an immunoglobulin-like domain and a unique highly hydrophobic 'cap' (Hobley *et al.*, 2013). The hydrophobic cap is essential both for *in vivo* hydrophobicity of the biofilm and the stability of the *in vitro* elastic films formed by recombinant protein (Hobley *et al.*, 2013). BslA has been termed a bacterial hydrophobin in homage to the fungal hydrophobins which form a hydrophobic protein coat on the surface of fungi (Elliot and Talbot, 2004), although, in actuality, similarities between BslA and the fungal hydrophobins are present at the physiochemical level and not the structural level. In short, BslA forms the third communal macromolecule made by *B. subtilis* during biofilm formation and further study is needed to elucidate the mechanisms underlying film formation and how BslA enables the assembly of the three dimensional biofilm.

The function of the biofilm matrix

The extracellular matrix confers several properties that promote survival of *B. subtilis* in the biofilm. It allows the erection of aerial structures containing sporulating cells (Branda *et al.*, 2001), confers extreme hydrophobicity (Epstein *et al.*, 2011) (Fig. 1A), provides pressure to spread resident cells across a surface (Seminara *et al.*, 2012) and is a source of mechanical stiffness (Asally *et al.*, 2012; Wilking *et al.*, 2013). The structure of the mature biofilm also serves a less obvious function and allows the formation of a network of liquid channels (Wilking *et al.*, 2013) (Fig. 1B). Such a system facilitates distribution of

nutrients to parts of the biofilm that would not be accessible using simple diffusion processes. The pressure within the channels is influenced by the rate of evaporation, driving liquid through the biofilm. The channels that form are interconnected and are maintained as the biofilm ages, indicating their physiological importance (Wilking *et al*., 2013). It is intriguing to speculate that the channels are lined by BslA to allow wicking of fluids into the deeper parts of the mature biofilm. Overall, the three dimensional architectural attributes that are imparted by the biofilm matrix are essential for the survival of its resident cells.

Putting the wrinkles in the biofilm

Despite growing knowledge of the function of the biofilm matrix and its complex structure it is still not entirely clear how the wrinkles and ridges in the mature biofilm are generated. One possibility is that inherent elasticity of the extracellular matrix is sufficient (Trejo *et al*., 2013). This has been supported by biophysical experimentation in combination with theoretical analyses. Data suggested that mechanical buckling instability was responsible for shaping the biofilm; i.e. when the cells in the biofilm push against a surface wrinkles are induced. The matrix is essential for this to occur as it confers elastic properties to the biofilm (Trejo *et al*., 2013). Additionally, it has been highlighted that localized cell death is involved in wrinkle formation (Asally *et al*., 2012). Indeed, cell death at the base of the biofilm was linked with buckling in the vertical plane and thus wrinkles. The mechanical strength of the matrix was needed for this to occur as deletion of genes associated with matrix production, including *epsH* and *tasA*, resulted in a more homogenous pattern of cell death that altered biofilm architecture to the extent that wrinkles were not formed. Interestingly, it was shown that wrinkles were formed in patterns that mirrored cell death zones when cell density was artificially increased in localized areas to increase cell death. This could indicate that wrinkling might allow the dissipation of mechanical forces that occur due to high cell density and subsequent cell death (Asally *et al*., 2012). It is highly likely that mechanical forces, potentiated by as yet undefined specific interactions between the extracellular molecules of the matrix, and localized cell death combine to allow the beautiful and intricate wrinkles to evolve over time.

Disassembly of the biofilm

The final stage of the biofilm cycle is that of disassembly. There are at least two mechanisms by which this could occur. First, transcription of the operons required for biofilm matrix production could be silenced and second the macromolecules in the biofilm matrix could be disrupted or degraded. We will first examine the potential for gene silencing. As discussed above matrix gene expression is bimodal in the population and is subject to hysteresis that locks cells into a state where the biofilm matrix is synthesized (Vlamakis *et al*., 2013). It has however been shown that some cells switch off matrix production and can return to a motile cell state (Vlamakis *et al*., 2008; Norman *et al*., 2013). At the level of gene expression this would involve reversing the SlrR-high state back to a SlrR-low state. In line with this, it has been noted that SlrR levels decline as the biofilm matures, a phenotype that was tied to instability of the protein (Chai *et al*., 2010a). The instability of SlrR was attributed to two underlying mechanisms: (i) cleavage by the ClpCP protease and (ii) autocleavage (Chai *et al*., 2010a). SlrR was identified as having a conserved motif usually found in LexA-type repressors, which undergo autocleavage upon the sensing of a cellular signal (Little, 1984). Indeed, site-directed mutation of amino acids in this motif resulted in increased stability of SlrR. However, while SlrR carries a LexA-type motif, it does not have the catalytic domain that would be essential for proteolytic activity (Newman and Lewis, 2013). Therefore, an alternative model has been presented where it is proposed that, due to the presence of two helical hooks, SlrR is able to aggregate which would result in its proteolytic cleavage by ClpCP (Newman and Lewis, 2013). The destruction of SlrR would allow SinR to engage with the matrix promoter regions thereby shutting down biosynthesis of TasA and the exopolysaccharide.

The second method of biofilm dispersal would involve degradation or disruption of the macromolecules in the extracellular environment. Consistent with this mechanism of dispersal, production of extracellular proteases has been correlated with late stages of biofilm formation (Marlow *et al*., 2014a). While it is important to keep in mind that a functional role for proteases in breaking down the protein components of the biofilm matrix has not yet been established, such activity is supported by the knowledge that the protease nattokinase of *B. subtilis* Natto has amyloid-degrading capabilities (Hsu *et al*., 2009). Therefore, it can be postulated that such an enzyme could have a role in disassembly of the TasA amyloid-like fibres in the matrix. Two further mechanisms of disassembly at the level of macromolecule hindrance have been proposed. The first was based on self-production of D-amino acids by late-stage biofilms (Kolodkin-Gal *et al*., 2010). D-amino acids were hypothesized to trigger disassembly by incorporating into the peptidoglycan cell wall and blocking TapA embedding into the wall, resulting in the release of the TasA fibres from the cell (Kolodkin-Gal *et al*., 2010; Romero *et al*., 2011). However, a recent study disputes this mechanism as it was elucidated that addition of D-amino acids resulted in misincorporation of D-amino acids into proteins, which reduced cellular growth (Leiman *et al*., 2013). Incorporation of D-amino acids into proteins can be prevented in the

presence of a functional D-aminoacyl-tRNA deacylase that removes D-amino acids from mischarged tRNAs (Soutourina *et al*., 2004). The *B. subtilis* strain used in the initial analysis contained a mutation in the D-aminoacyl-tRNA deacylase gene (namely *dtd*) that prevented expression of this enzyme (Leiman *et al*., 2013). When the mutation was repaired the D-amino acid inhibition of biofilm formation was not observed (Leiman *et al*., 2013). The second proposed mechanism of biofilm disassembly was self-production of the polyamine norspermidine (Kolodkin-Gal *et al*., 2012). It was postulated that within the extracellular environment norspermidine interacts with the exopolysaccharide component of the biofilm matrix, collapsing it and releasing the cells (Kolodkin-Gal *et al*., 2012). However, further studies have shown that *B. subtilis* completely lacks the biosynthetic pathway required for norspermidine synthesis and, consistent with this, detection of norspermidine within biofilm samples was not possible despite utilization of two separate detection methods (Hobley *et al*., 2014). Furthermore, analysis indicated that heterologous addition of low concentrations of norspermidine can replace the role of the related and natively produced polyamine, spermidine, during biofilm formation (Burrell *et al*., 2010; Hobley *et al*., 2014). It is therefore safe to say that the issue of biofilm disassembly by *B. subtilis* remains a much-debated topic within the field. Further investigation will be required to determine whether the reduction in biofilm biomass observed in late-stage biofilms is the result of an organized disassembly process or simply the result of the onset of sporulation by the majority of the population after exhaustion of the nutrient supply.

Looking forward

The environmental signals and regulatory pathways that control entry into biofilm formation have been well studied and it is known that they largely converge to control the production of the biofilm matrix components (Vlamakis *et al*., 2013). Regulation of transcription is critical to biofilm formation as it allows deployment of the matrix molecules at the correct time, and in the correct place. However, what is less understood is how the macromolecules interact in the extracellular environment to provide structure and rigidity, and moreover how they interact with surfaces in the host environment. It is likely that our understanding of this area of biofilm biology will require interdisciplinary collaborations as the techniques needed to illuminate this black box of biology will draw on carbohydrate chemistry, surface chemistry, and biophysics in combination with molecular biology. However enhanced knowledge in this arena is likely to be profitable as understanding the molecular nature of the biofilm matrix interactions will be a prelude to promoting or disrupting biofilm formation within healthcare, agricultural and industrial settings.

Acknowledgements

L.S.C. is funded by a Wellcome Trust PhD scholarship [093714/Z/10/Z]; L.H. is funded by a BBSRC grant [BB/I019464/1]. We thank members of the NSW laboratory for helpful comments and suggestions.

References

Asally, M., Kittisopikul, M., Rue, P., Du, Y., Hu, Z., Cagatay, T., *et al*. (2012) Localized cell death focuses mechanical forces during 3D patterning in a biofilm. *Proc Natl Acad Sci USA* **109:** 18891–18896.

Bai, U., Mandic-Mulec, I., and Smith, I. (1993) SinI modulates the activity of SinR, a developmental switch protein of *Bacillus subtilis*, by protein-protein interaction. *Genes Dev* **7:** 139–148.

Bais, H.P., Fall, R., and Vivanco, J.M. (2004) Biocontrol of *Bacillus subtilis* against infection of *Arabidopsis* roots by *Pseudomonas syringae* is facilitated by biofilm formation and surfactin production. *Plant Physiol* **134:** 307–319.

Banse, A.V., Chastanet, A., Rahn-Lee, L., Hobbs, E.C., and Losick, R. (2008) Parallel pathways of repression and antirepression governing the transition to stationary phase in *Bacillus subtilis*. *Proc Natl Acad Sci USA* **105:** 15547–15552.

Beauregard, P.B., Chai, Y., Vlamakis, H., Losick, R., and Kolter, R. (2013) *Bacillus subtilis* biofilm induction by plant polysaccharides. *Proc Natl Acad Sci USA* **110:** E1621–E1630.

Benigar, E., Dogsa, I., Stopar, D., Jamnik, A., Kralj Cigic, I., and Tomsic, M. (2014) Structure and dynamics of a polysaccharide matrix: aqueous solutions of bacterial levan. *Langmuir* **30:** 4172–4182.

Blair, K.M., Turner, L., Winkelman, J.T., Berg, H.C., and Kearns, D.B. (2008) A molecular clutch disables flagella in the *Bacillus subtilis* biofilm. *Science* **320:** 1636–1638.

Branda, S.S., Gonzalez-Pastor, J.E., Ben-Yehuda, S., Losick, R., and Kolter, R. (2001) Fruiting body formation by *Bacillus subtilis*. *Proc Natl Acad Sci USA* **98:** 11621–11626.

Branda, S.S., Vik, S., Friedman, L., and Kolter, R. (2005) Biofilms: the matrix revisited. *Trends Microbiol* **13:** 20–26.

Branda, S.S., Chu, F., Kearns, D.B., Losick, R., and Kolter, R. (2006) A major protein component of the *Bacillus subtilis* biofilm matrix. *Mol Microbiol* **59:** 1229–1238.

Burrell, M., Hanfrey, C.C., Murray, E.J., Stanley-Wall, N.R., and Michael, A.J. (2010) Evolution and multiplicity of arginine decarboxylases in polyamine biosynthesis and essential role in *Bacillus subtilis* biofilm formation. *J Biol Chem* **285:** 39224–39238.

Cairns, L.S., Marlow, V.L., Bissett, E., Ostrowski, A., and Stanley-Wall, N.R. (2013) A mechanical signal transmitted by the flagellum controls signalling in *Bacillus subtilis*. *Mol Microbiol* **90:** 6–21.

Chai, L., Romero, D., Kayatekin, C., Akabayov, B., Vlamakis, H., Losick, R., and Kolter, R. (2013) Isolation, characterization, and aggregation of a structured bacterial matrix precursor. *J Biol Chem* **288:** 17559–17568.

Chai, Y., Chu, F., Kolter, R., and Losick, R. (2008) Bistability and biofilm formation in *Bacillus subtilis*. *Mol Microbiol* **67:** 254–263.

Chai, Y., Kolter, R., and Losick, R. (2009) Paralogous antirepressors acting on the master regulator for biofilm formation in *Bacillus subtilis*. *Mol Microbiol* **74:** 876–887.

Chai, Y., Kolter, R., and Losick, R. (2010a) Reversal of an epigenetic switch governing cell chaining in *Bacillus subtilis* by protein instability. *Mol Microbiol* **78:** 218–229.

Chai, Y., Norman, T., Kolter, R., and Losick, R. (2010b) An epigenetic switch governing daughter cell separation in *Bacillus subtilis*. *Genes Dev* **24:** 754–765.

Chai, Y., Norman, T., Kolter, R., and Losick, R. (2010c) An epigenetic switch governing daughter cell separation in *Bacillus subtilis*. *Genes Dev* **24:** 754–765.

Chai, Y., Beauregard, P.B., Vlamakis, H., Losick, R., and Kolter, R. (2012) Galactose metabolism plays a crucial role in biofilm formation by *Bacillus subtilis*. *mBio* **3:** e184–e112.

Chan, J.M., Guttenplan, S.B., and Kearns, D.B. (2014) Defects in the flagellar motor increase synthesis of poly-gamma-glutamate in *Bacillus subtilis*. *J Bacteriol* **196:** 740–753.

Chen, Y., Cao, S., Chai, Y., Clardy, J., Kolter, R., Guo, J.H., and Losick, R. (2012) A *Bacillus subtilis* sensor kinase involved in triggering biofilm formation on the roots of tomato plants. *Mol Microbiol* **85:** 418–430.

Chen, Y., Yan, F., Chai, Y., Liu, H., Kolter, R., Losick, R., and Guo, J.H. (2013) Biocontrol of tomato wilt disease by *Bacillus subtilis* isolates from natural environments depends on conserved genes mediating biofilm formation. *Environ Microbiol* **15:** 848–864.

Chu, F., Kearns, D.B., McLoon, A., Chai, Y., Kolter, R., and Losick, R. (2008) A novel regulatory protein governing biofilm formation in *Bacillus subtilis*. *Mol Microbiol* **68:** 1117–1127.

Chumsakul, O., Takahashi, H., Oshima, T., Hishimoto, T., Kanaya, S., Ogasawara, N., and Ishikawa, S. (2011) Genome-wide binding profiles of the *Bacillus subtilis* transition state regulator AbrB and its homolog Abh reveals their interactive role in transcriptional regulation. *Nucleic Acids Res* **39:** 414–428.

Costerton, J.W., Lewandowski, Z., Caldwell, D.E., Korber, D.R., and Lappin-Scott, H.M. (1995) Microbial biofilms. *Annu Rev Microbiol* **49:** 711–745.

Dogsa, I., Brloznik, M., Stopar, D., and Mandic-Mulec, I. (2013) Exopolymer diversity and the role of levan in *Bacillus subtilis* biofilms. *PLoS ONE* **8:** e62044.

Elliot, M.A., and Talbot, N.J. (2004) Building filaments in the air: aerial morphogenesis in bacteria and fungi. *Curr Opin Microbiol* **7:** 594–601.

Elsholz, A.K., Turgay, K., Michalik, S., Hessling, B., Gronau, K., Oertel, D., *et al*. (2012) Global impact of protein arginine phosphorylation on the physiology of *Bacillus subtilis*. *Proc Natl Acad Sci USA* **109:** 7451–7456.

Epstein, A.K., Pokroy, B., Seminara, A., and Aizenberg, J. (2011) Bacterial biofilm shows persistent resistance to liquid wetting and gas penetration. *Proc Natl Acad Sci USA* **108:** 995–1000.

Fagerlund, A., Dubois, T., Okstad, O.A., Verplaetse, E., Gilois, N., Bennaceur, I., *et al*. (2014) SinR controls enterotoxin expression in *Bacillus thuringiensis* biofilms. *PLoS ONE* **9:** e87532.

Fraser, P.E., Nguyen, J.T., Surewicz, W.K., and Kirschner, D.A. (1991) pH-dependent structural transitions of Alzheimer amyloid peptides. *Biophys J* **60:** 1190–1201.

Fujita, M., Gonzalez-Pastor, J.E., and Losick, R. (2005) High- and low-threshold genes in the Spo0A regulon of *Bacillus subtilis*. *J Bacteriol* **187:** 1357–1368.

Gerwig, J., Kiley, T.B., Gunka, K., Stanley-Wall, N., and Stulke, J. (2014) The protein tyrosine kinases EpsB and PtkA differentially affect biofilm formation in *Bacillus subtilis*. *Microbiology* **160** (Pt 4): 682–691.

Guttenplan, S.B., Blair, K.M., and Kearns, D.B. (2010) The EpsE flagellar clutch is bifunctional and synergizes with EPS biosynthesis to promote *Bacillus subtilis* biofilm formation. *PLoS Genet* **6:** e1001243.

Halan, B., Buehler, K., and Schmid, A. (2012) Biofilms as living catalysts in continuous chemical syntheses. *Trends Biotechnol* **30:** 453–465.

Hall, M.R., McGillicuddy, E., and Kaplan, L.J. (2014) Biofilm: basic principles, pathophysiology, and implications for clinicians. *Surg Infect* **15:** 1–7.

Hamon, M.A., and Lazazzera, B.A. (2001) The sporulation transcription factor Spo0A is required for biofilm development in *Bacillus subtilis*. *Mol Microbiol* **42:** 1199–1209.

Hamon, M.A., Stanley, N.R., Britton, R.A., Grossman, A.D., and Lazazzera, B.A. (2004) Identification of AbrB-regulated genes involved in biofilm formation by *Bacillus subtilis*. *Mol Microbiol* **52:** 847–860.

Hobley, L., Ostrowski, A., Rao, F.V., Bromley, K.M., Porter, M., Prescott, A.R., *et al*. (2013) BslA is a self-assembling bacterial hydrophobin that coats the *Bacillus subtilis* biofilm. *Proc Natl Acad Sci USA* **110:** 13600–13605.

Hobley, L., Kim, S.H., Maezato, Y., Wyllie, S., Fairlamb, A.H., Stanley-Wall, N.R., and Michael, A.J. (2014) Norspermidine is not a self-produced trigger for biofilm disassembly. *Cell* **156:** 844–854.

Hsu, R.L., Lee, K.T., Wang, J.H., Lee, L.Y., and Chen, R.P. (2009) Amyloid-degrading ability of nattokinase from *Bacillus subtilis* natto. *J Agric Food Chem* **57:** 503–508.

Jones, S.E., Paynich, M.L., Kearns, D.B., and Knight, K.L. (2014) Protection from intestinal inflammation by bacterial exopolysaccharides. *J Immunol* **192:** 4813–4820.

Kearns, D.B., Chu, F., Branda, S.S., Kolter, R., and Losick, R. (2005) A master regulator for biofilm formation by *Bacillus subtilis*. *Mol Microbiol* **55:** 739–749.

Kiley, T.B., and Stanley-Wall, N.R. (2010) Post-translational control of *Bacillus subtilis* biofilm formation mediated by tyrosine phosphorylation. *Mol Microbiol* **78:** 947–963.

Kobayashi, K. (2007) Gradual activation of the response regulator DegU controls serial expression of genes for flagellum formation and biofilm formation in *Bacillus subtilis*. *Mol Microbiol* **66:** 395–409.

Kobayashi, K. (2008) SlrR/SlrA controls the initiation of biofilm formation in *Bacillus subtilis*. *Mol Microbiol* **69:** 1399–1410.

Kobayashi, K., and Iwano, M. (2012) BslA (YuaB) forms a hydrophobic layer on the surface of *Bacillus subtilis* biofilms. *Mol Microbiol* **85:** 51–66.

Kolodkin-Gal, I., Romero, D., Cao, S., Clardy, J., Kolter, R., and Losick, R. (2010) D-amino acids trigger biofilm disassembly. *Science* **328:** 627–629.

Kolodkin-Gal, I., Cao, S., Chai, L., Bottcher, T., Kolter, R., Clardy, J., and Losick, R. (2012) A self-produced trigger for

biofilm disassembly that targets exopolysaccharide. *Cell* **149:** 684–692.
Leiman, S.A., May, J.M., Lebar, M.D., Kahne, D., Kolter, R., and Losick, R. (2013) D-amino acids indirectly inhibit biofilm formation in *Bacillus subtilis* by interfering with protein synthesis. *J Bacteriol* **195:** 5391–5395.
Levine, A., Vannier, F., Absalon, C., Kuhn, L., Jackson, P., Scrivener, E., *et al*. (2006) Analysis of the dynamic *Bacillus subtilis* Ser/Thr/Tyr phosphoproteome implicated in a wide variety of cellular processes. *Proteomics* **6:** 2157–2173.
Lewis, R.J., Brannigan, J.A., Offen, W.A., Smith, I., and Wilkinson, A.J. (1998) An evolutionary link between sporulation and prophage induction in the structure of a repressor:anti-repressor complex. *J Mol Biol* **283:** 907–912.
Little, J.W. (1984) Autodigestion of lexA and phage lambda repressors. *Proc Natl Acad Sci USA* **81:** 1375–1379.
Liu, Y., Zhang, W., Sileika, T., Warta, R., Cianciotto, N.P., and Packman, A. (2009) Role of bacterial adhesion in the microbial ecology of biofilms in cooling tower systems. *Biofouling* **25:** 241–253.
Lopez, D., and Kolter, R. (2010) Extracellular signals that define distinct and coexisting cell fates in *Bacillus subtilis*. *FEMS Microbiol Rev* **34:** 134–149.
Lopez, D., Vlamakis, H., and Kolter, R. (2009) Generation of multiple cell types in *Bacillus subtilis*. *FEMS Microbiol Rev* **33:** 152–163.
Macek, B., Mijakovic, I., Olsen, J.V., Gnad, F., Kumar, C., Jensen, P.R., and Mann, M. (2007) The serine/threonine/tyrosine phosphoproteome of the model bacterium *Bacillus subtilis*. *Mol Cell Proteomics* **6:** 697–707.
Marlow, V.L., Cianfanelli, F.R., Porter, M., Cairns, L.S., Dale, J.K., and Stanley-Wall, N.R. (2014a) The prevalence and origin of exoprotease-producing cells in the *Bacillus subtilis* biofilm. *Microbiology* **160:** 56–66.
Marlow, V.L., Porter, M., Hobley, L., Kiley, T.B., Swedlow, J.R., Davidson, F.A., and Stanley-Wall, N.R. (2014b) Phosphorylated DegU manipulates cell fate differentiation in the *Bacillus subtilis* biofilm. *J Bacteriol* **196:** 16–27.
Mukai, K., Kawata, M., and Tanaka, T. (1990) Isolation and phosphorylation of the *Bacillus subtilis degS* and *degU* gene products. *J Biol Chem* **265:** 20000–20006.
Murray, E.J., Kiley, T.B., and Stanley-Wall, N.R. (2009a) A pivotal role for the response regulator DegU in controlling multicellular behaviour. *Microbiology* **155:** 1–8.
Murray, E.J., Strauch, M.A., and Stanley-Wall, N.R. (2009b) σX is involved in controlling *Bacillus subtilis* biofilm architecture through the AbrB homologue Abh. *J Bacteriol* **191:** 6822–6832.
Newman, J.A., and Lewis, R.J. (2013) Exploring the role of SlrR and SlrA in the SinR epigenetic switch. *Commun Integr Biol* **6:** e25658.
Newman, J.A., Rodrigues, C., and Lewis, R.J. (2013) Molecular basis of the activity of SinR protein, the master regulator of biofilm formation in *Bacillus subtilis*. *J Biol Chem* **288:** 10766–10778.
Norman, T.M., Lord, N.D., Paulsson, J., and Losick, R. (2013) Memory and modularity in cell-fate decision making. *Nature* **503:** 481–486.
Ostrowski, A., Mehert, A., Prescott, A., Kiley, T.B., and Stanley-Wall, N.R. (2011) YuaB functions synergistically with the exopolysaccharide and TasA amyloid fibers to allow biofilm formation by *Bacillus subtilis*. *J Bacteriol* **193:** 4821–4831.
Romero, D., Aguilar, C., Losick, R., and Kolter, R. (2010) Amyloid fibers provide structural integrity to *Bacillus subtilis* biofilms. *Proc Natl Acad Sci USA* **107:** 2230–2234.
Romero, D., Vlamakis, H., Losick, R., and Kolter, R. (2011) An accessory protein required for anchoring and assembly of amyloid fibres in *B. subtilis* biofilms. *Mol Microbiol* **80:** 1155–1168.
Romero, D., Vlamakis, H., Losick, R., and Kolter, R. (2014) Functional analysis of the accessory protein TapA in *Bacillus subtilis* amyloid fiber assembly. *J Bacteriol* **196:** 1505–1513.
Scott, D.J., Leejeerajumnean, S., Brannigan, J.A., Lewis, R.J., Wilkinson, A.J., and Hoggett, J.G. (1999) Quaternary re-arrangement analysed by spectral enhancement: the interaction of a sporulation repressor with its antagonist. *J Mol Biol* **293:** 997–1004.
Seminara, A., Angelini, T.E., Wilking, J.N., Vlamakis, H., Ebrahim, S., Kolter, R., *et al*. (2012) Osmotic spreading of *Bacillus subtilis* biofilms driven by an extracellular matrix. *Proc Natl Acad Sci USA* **109:** 1116–1121.
Sokolowski, F., Modler, A.J., Masuch, R., Zirwer, D., Baier, M., Lutsch, G., *et al*. (2003) Formation of critical oligomers is a key event during conformational transition of recombinant Syrian hamster prion protein. *J Biol Chem* **278:** 40481–40492.
Soutourina, O., Soutourina, J., Blanquet, S., and Plateau, P. (2004) Formation of D-tyrosyl-tRNATyr accounts for the toxicity of D-tyrosine toward Escherichia coli. *J Biol Chem* **279:** 42560–42565.
Stover, A.G., and Driks, A. (1999) Secretion. localization and antibacterial activity of tasA, a *Bacillus subtilis* spore-associated protein. *J Bacteriol* **181:** 1664–1672.
Strauch, M., Webb, V., Spiegelman, G., and Hoch, J.A. (1990) The SpoOA protein of *Bacillus subtilis* is a repressor of the *abrB* gene. *Proc Natl Acad Sci USA* **87:** 1801–1805.
Subramaniam, A.R., Deloughery, A., Bradshaw, N., Chen, Y., O'Shea, E., Losick, R., and Chai, Y. (2013) A serine sensor for multicellularity in a bacterium. *eLife* **2:** e01501.
Terra, R., Stanley-Wall, N.R., Cao, G., and Lazazzera, B.A. (2012) Identification of *Bacillus subtilis* SipW as a bifunctional signal peptidase that controls surface-adhered biofilm formation. *J Bacteriol* **194:** 2781–2790.
Trejo, M., Douarche, C., Bailleux, V., Poulard, C., Mariot, S., Regeard, C., and Raspaud, E. (2013) Elasticity and wrinkled morphology of *Bacillus subtilis* pellicles. *Proc Natl Acad Sci USA* **110:** 2011–2016.
Tucker, A.T., Bobay, B.G., Banse, A.V., Olson, A.L., Soderblom, E.J., Moseley, M.A., *et al*. (2014) A DNA mimic: the structure and mechanism of action for the anti-repressor protein AbbA. *J Mol Biol* **426:** 1911–1924.
Veening, J.W., Kuipers, O.P., Brul, S., Hellingwerf, K.J., and Kort, R. (2006) Effects of phosphorelay perturbations on architecture, sporulation, and spore resistance in biofilms of *Bacillus subtilis*. *J Bacteriol* **188:** 3099–3109.
Verhamme, D.T., Kiley, T.B., and Stanley-Wall, N.R. (2007) DegU co-ordinates multicellular behaviour exhibited by *Bacillus subtilis*. *Mol Microbiol* **65:** 554–568.
Verhamme, D.T., Murray, E.J., and Stanley-Wall, N.R. (2009) DegU and Spo0A jointly control transcription of two loci

required for complex colony development by *Bacillus subtilis*. *J Bacteriol* **191:** 100–108.
Vlamakis, H., Aguilar, C., Losick, R., and Kolter, R. (2008) Control of cell fate by the formation of an architecturally complex bacterial community. *Genes Dev* **22:** 945–953.
Vlamakis, H., Chai, Y., Beauregard, P., Losick, R., and Kolter, R. (2013) Sticking together: building a biofilm the *Bacillus subtilis* way. *Nat Rev Microbiol* **11:** 157–168.
Wilking, J.N., Zaburdaev, V., De Volder, M., Losick, R., Brenner, M.P., and Weitz, D.A. (2013) Liquid transport facilitated by channels in *Bacillus subtilis* biofilms. *Proc Natl Acad Sci USA* **110:** 848–852.
Winkelman, J.T., Blair, K.M., and Kearns, D.B. (2009) RemA (YlzA) and RemB (YaaB) regulate extracellular matrix operon expression and biofilm formation in *Bacillus subtilis*. *J Bacteriol* **191:** 3981–3991.
Winkelman, J.T., Bree, A.C., Bate, A.R., Eichenberger, P., Gourse, R.L., and Kearns, D.B. (2013) RemA is a DNA-binding protein that activates biofilm matrix gene expression in *Bacillus subtilis*. *Mol Microbiol* **88:** 984–997.
Zurdo, J., Guijarro, J.I., Jimenez, J.L., Saibil, H.R., and Dobson, C.M. (2001) Dependence on solution conditions of aggregation and amyloid formation by an SH3 domain. *J Mol Biol* **311:** 325–340.